

STATUS OF THESIS

Title of thesis

Performance of Self Compacting Concrete Containing Fly Ash and
MIRHA: Optimum Mix Design and Structural Behavior

I AGUS KURNIAWAN

hereby allow my thesis to be placed at the Information Resource Center (IRC) of Universiti Teknologi PETRONAS (UTP) with the following conditions:

1. The thesis becomes the property of UTP
2. The IRC of UTP may make copies of the thesis for academic purposes only.
3. This thesis is classified as

Confidential

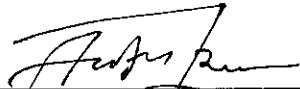
Non-confidential

If this thesis is confidential, please state the reason:

Some paper has been prepared during the mentioned period, the data result is kept confidential to protect originality

The contents of the thesis will remain confidential for one years.

Remarks on disclosure:




Signature of Author

Permanent address:
Blunyahrejo TR II/1106 D
Karangwaru, Yogyakarta, DIY
Indonesia 55241

Date : 2-6-2010

Endorsed by **Dr Nasir Shafiq**
Associate Professor
Civil Engineering Department
Universiti Teknologi PETRONAS



Signature of Supervisor

Assoc. Prof. Dr. Nasir Shafiq

Date : 2-6-2010

UNIVERSITI TEKNOLOGI PETRONAS

PERFORMANCE OF SELF COMPACTING CONCRETE CONTAINING FLY
ASH AND MIRHA: OPTIMUM MIX DESIGN AND STRUCTURAL
BEHAVIOR


by

AGUS KURNIAWAN

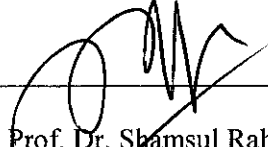
The undersigned certify that they have read, and recommend to the Postgraduate Studies Programme for acceptance this thesis for the fulfilment of the requirements for the degree stated.

Signature : 

Main Supervisor : Assoc. Prof. Dr. Nasir Shafiq

Signature : 

Co-Supervisor : Assoc. Prof. Ir. Dr. Muhd Fadhil Nuruddin

Signature : 

Head of Department : Assoc. Prof. Dr. Shamsul Rahman Mohamed Kutty

Date : 2 / 10 / 2010

PERFORMANCE OF SELF COMPACTING CONCRETE CONTAINING FLY
ASH AND MIRHA: OPTIMUM MIX DESIGN AND STRUCTURAL
BEHAVIOR

by

AGUS KURNIAWAN

A Thesis

Submitted to the Postgraduate Studies Programme

as a Requirement for the Degree of

DOCTOR OF PHILOSOPHY

CIVIL ENGINEERING

UNIVERSITI TEKNOLOGI PETRONAS

BANDAR SERI ISKANDAR,

PERAK

JUNE 2010

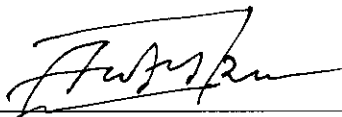
DECLARATION OF THESIS

Title of thesis Performance of Self Compacting Concrete Containing Fly Ash and
MIRHA: Optimum Mix Design and Structural Behavior

I AGUS KURNIAWAN

hereby declare that the thesis is based on my original work except for quotations and citations which have been duly acknowledged. I also declare that it has not been previously or concurrently submitted for any other degree at UTP or other institutions.


Witnessed by



Signature of Author

Permanent address:
Blunyahrejo TR II/1106 D
Karangwaru, Yogyakarta, DIY
Indonesia 55241

Date : 2-6-2010



Signature of Supervisor

Assoc. Prof. Dr. Nasir Shafiq

Date : 2.10.2010

ACKNOWLEDGEMENTS

I wish to express my most sincere gratitude to my supervisor AP. Dr.Nasir Shafiq and co-supervisor AP. Ir. Dr. Muhd Fadhil Nuruddin. I wish to also express my appreciation to the members of my advisory committee for their positive contribution towards my research funding graduate fellowship and research supplements from Universiti Teknologi PETRONAS are gratefully acknowledged. I would also like to thank Assoc. Prof. Dr. Mohd Noh Karsiti, Prof. Dr. Ibrahim Galal Shaaban and Assoc. Prof. Ir. Dr. Arazi Idrus for being in my examining committee which helped me complete my PhD Degree in Civil Engineering.

Special thanks to Aisyah binti Ahmad, Shahrman bin Idris, Ali, Ashraf, Suhaizi, Mazila, Anniza, Dominiq, Yusuf Iqbal, Fendi, Siti Aminah, Haikal, Raihan and Katlego Ngoepe as final year project graduate students for their help in the experiments.

Acknowledgements are also made to the Technical Staff for their assistance in the experimental program especially Johan Ariff, Meor Asniwan and Muhammad Hafiz for helping in conducting the static and dynamic beam test. My colleagues at Civil Engineering Department especially Ridho Bayuaji, Andri Kusbiantoro, Suwardo and Chin Siew Choo are very much appreciated.

Finally, and with all my heart, I wish to express my gratitude to my wife Erlina Sih Mahanani and all my children, for their continuous support throughout the course of this thesis.

ABSTRACT

Properties of hardened concrete are very important for load resistance, durability, stability and aesthetic point of view; its properties in fresh state are also very vital for good workmanship. In view of this, the self compacting concrete simply called SCC was initiated. The aim of producing of such was that it should be honey-like viscous material that contain low amount of water and high range water reducers to modify the viscosity of concrete. The principal aim of this research study was to develop the optimum mix design of SCC by addressing the issues highlighted in a number of research papers. Investigation of the rheology of the fresh concrete was made in order to satisfy the criteria of self compactibility.

Mechanical properties such as compressive strength, modulus of rupture and the tensile strength were determined. Durability properties that included total porosity, oxygen and water permeability and the corrosion potential of the selected mixes were investigated. Structural performance of the selected mixes was determined by conducting embedded steel bar pull-out test for bond behavior. Reinforced concrete beams were tested under monotonic loading for flexural/shear capacity with failure mechanism and dynamic loading for finding the fatigue endurance. A computer simulation using the software ATENA was performed in order to compare with respect to the static load test results of RC beams.

From the investigation of different results it was found that water-to-binder ratio (w/b) played a vital role in both fresh and hardened states of concrete. By maintaining the dosage of superplasticizers at optimum level as 3%; w/b can go as low as 0.25 with 10% fly ash self compacting concrete (FASCC) whereas it can go as low as 0.35 with 10% Microwave Incinerated Rice Husk Ash (MIRHA) self compacting concrete. It is worthy to note that if more than 80 MPa compressive strength of concrete is required at 28-days; fly ash based SCC will be the optimized solution. If concrete production at 28 days strength of 60 MPa and below is required, MIRHA SCC (MSCC) blended cement concrete would be feasible. A water-to-binder ratio between 0.25 to 0.37 and a superplasticizers of 3% were found as the optimum values for producing high performance SCC that satisfied the criteria of high strength, assurance of durability,

ABSTRAK

Ciri-ciri konkrit keras amat penting bagi ketahanan beban, ketahananlasakan, kestabilan dan nilai estetika; ia juga amat diperlukan bagi kerja-kerja mengkonkrit yang baik semasa konkrit baru dibancuh. Sehubungan dengan itu, konkrit mampat sendiri atau dipanggil SCC telah diperkenalkan. Tujuan penghasilan konkrit ini adalah supaya konkrit tersebut bersifat madu seperti bahan likat yang mengandungi jumlah air yang rendah dan tinggi dalam pengurang air untuk mengubahsuai kelikatan konkrit. Tujuan utama penyelidikan ini ialah untuk menghasilkan campuran konkrit SCC yang terbaik dengan mengambil kira masalah-masalah yang telah dikemukakan dalam pelbagai jurnal penyelidikan. Pengujian reologi terhadap konkrit baru bancuh telah dijalankan bagi memastikan konkrit mencapai kriteria kemampuan sendiri.

Sifat-sifat mekanikal seperti kekuatan mampatan, modulus kerosakan dan kekuatan tegangan telah dikenal pasti. Sifat ketahananlasakan yang mengandungi jumlah keporosan, ketelapan oksigen dan air dan potensi kekaratan bagi beberapa bancuhan terpilih telah diselidik. Prestasi struktur bagi bancuhan-bancuhan terpilih tersebut telah dikaji dengan menjalankan ujian tetulang tertanam pull-out untuk ciri ikatan. Rasuk-rasuk berkonkrit tertulang telah diuji di bawah beban berpusat satu untuk kapasiti lentur/regangan dengan mekanisma kerosakan dan bebanan dinamik untuk mendapatkan ketahan-rosakan. Simulasi komputer menggunakan perisian ATENA telah dijalankan untuk membandingkan keputusan-keputusan ujian beban pegun bagi rasuk-rasuk berkonkrit tertulang.

Daripada kajian terhadap keputusan yang berbeza, didapati bahawa nisbah air-kepada-pengikat (w/b) memainkan peranan yang sangat penting dalam kedua-dua konkrit baru bancuh dan konkrit keras. Dengan mengekalkan dos superplasticiser pada tahap optimum iaitu 3%, w/b boleh turun serendah 0.25 dengan 10% abu-terbang konkrit mampat sendiri (FASCC) dan boleh turun kepada 0.35 dengan 10% Microwave Incinerated Rice Husk Ash (MIRHA) konkrit mampat sendiri. Penemuan yang berguna untuk diketahui bahawa jika lebih daripada 80 MPa kekuatan mampatan konkrit diperlukan pada hari ke-28; SCC berabu-terbang adalah penyelesaian yang optimum. Jika penghasilan konkrit berkekuatan 60 MPa atau kurang pada 28 hari

diperlukan, MIRHA SCC (MSCC) konkrit simen-dikisar adalah sesuai. Nisbah air-kepada-pengikat di antara 0.25 hingga 0.37 dan kadar superplasticiser sebanyak 0.3% telah dikenal pasti sebagai nilai-nilai optimum untuk menghasilkan SCC berprestasi tinggi yang mencapai kriteria kekuatan tinggi, jaminan ketahanan, ikatan kuat antara konkrit dan keluli tertulang, kemuluran tinggi dan ketahan-rosakan yang lebih besar.

In compliance with the terms of the Copyright Act 1987 and the IP Policy of the university, the copyright of this thesis has been reassigned by the author to the legal entity of the university,

Institute of Technology PETRONAS Sdn Bhd.

Due acknowledgement shall always be made of the use of any material contained in, or derived from, this thesis.

© Agus Kurniawan, 2010
Institute of Technology PETRONAS Sdn Bhd
All rights reserved.

TABLE OF CONTENTS

STATUS OF THESIS	i
APPROVAL PAGE	i
TITLE PAGE.....	iii
DECLARATION OF THESIS	iii
ACKNOWLEDGEMENTS.....	v
ABSTRACT.....	vi
ABSTRAK.....	viii
COPYRIGHT PAGE.....	ix
TABLE OF CONTENTS	x
LIST OF TABLES	xiv
LIST OF FIGURES.....	xvi
PREFACE.....	xxii
1. INTRODUCTION	1
1. 1. General Remarks.....	1
1. 2. Development and Challenges of SCC.....	1
1. 3. Gaps in Current Research.....	3
1. 4. Objective and Scope.....	4
1. 5. Motivation	5
1. 6. Thesis Contributions	6
1. 7. Layout of the Thesis.....	6
2. LITERATURE REVIEW	8
2. 1. Introduction	8
2. 2. Pozzolan Waste Product in Malaysia.....	8
2. 3. Utilization of Fly Ash and MIRHA in Concrete.....	9
2.3.1. Fly ash and MIRHA Utilization in Vibrated Concrete	9
2.3.2. Fly ash and MIRHA Utilization in SCC	11
2. 4. Definition and Behavior of SCC.....	16
2.4.1. Mix Design Method of SCC.....	18
2.4.2. Rheological Properties of SCC	23
2.4.3. Pozzolan	31
2.4.4. Effect of Superplasticer	34
2. 5. Mechanical Properties of SCC.....	37
2.5.1. Compressive Strength of SCC.....	37
2.5.2. Tensile Strength of SCC.....	39
2. 6. Durability Properties of SCC.....	40
2.6.1. Porosity of Concrete.....	42
2.6.2. Permeability of Concrete.....	43

2.6.3.	Corrosion Resistance Properties of SCC.....	45
2. 7.	Structural Characteristic of SCC.....	48
2.7.1.	Bond Characteristic of SCC Structure	48
2.7.2.	Static Behavior of SCC Structure	49
2.7.3.	Dynamic Behavior of SCC structure.....	52
2. 8.	Summary and Concluding Remark.....	58
3.	RESEARCH METHODOLOGY	59
3. 1.	Introduction	59
3. 2.	Material Selection and Sample Preparation	61
3.2.1.	Aggregate Properties	61
3.2.2.	Cement Properties	63
3.2.3.	Microwave Incinerated Rice Husk Ash (MIRHA)	64
3.2.4.	Fly Ash	64
3.2.5.	Superplasticizers (Naphthalene Formaldehyde Sulphonate).....	65
3.2.6.	Mix Procedure.....	66
3. 3.	Rheological Properties	67
3.3.1.	V-funnel test	68
3.3.2.	L-box test.....	68
3.3.3.	T_{500} and Slump Flow Test.....	69
3. 4.	Mechanical Properties Test	70
3.4.1.	Compressive Strength Test.....	71
3.4.2.	Flexural Strength Test	71
3.4.3.	Split Cylinder test.....	72
3.4.4.	Porosity Test	73
3.4.5.	Permeability	74
3.4.6.	Corrosion Resistance Test	75
3. 5.	Structural Properties Test	77
3.5.1.	Bond Characteristic	77
3.5.2.	Testing of Reinforced Concrete Beam	78
4.	RHEOLOGICAL PROPERTIES OF SCC.....	83
4. 1.	Introduction	83
4. 2.	Trial Concrete Mix.....	83
4. 3.	Rheological properties.....	84
4. 4.	Effect of Water-binder Ratio on Rheological Properties	84
4.4.1.	Effect of Water-binder Ratio on V-funnel test	85
4.4.2.	Effect of Water-binder Ratio on L-box Test	92
4.4.3.	Effect of Water-binder Ratio on T_{500} Test.....	98
4.4.4.	Effects of Water-binder Ratio on Slump Flow Test	103
4. 5.	Effect of Superplasticizers to Rheological Properties.....	109
4.5.1.	Effect of Superplasticizers on V-funnel Test.....	110

4.5.2.	Effect of Superplasticizers on L-box Test	112
4.5.3.	Effect of Superplasticizers on T_{500} Test	114
4.5.4.	Effect of Superplasticizers on Slump Flow Test	115
4. 6.	Effect of Pozzolan Amount on Rheological Parameter	117
4. 7.	Summary.....	122
5.	MECHANICAL PROPERTIES OF SCC.....	125
5. 1.	Introduction	125
5. 2.	Compressive Strength of SCC.....	125
5.2.1.	Effects of Water-binder Ratio.....	125
5.2.2.	Effect of Superplasticizers on Compressive Strength of SCC.....	136
5.2.3.	Effect of Different fly ash Content	146
5. 3.	Flexural Strength Test.....	152
5. 4.	Split Tensile Test	153
5. 5.	Summary.....	155
6.	DURABILITY OF SCC	158
6. 1.	Introduction	158
6. 2.	Total Porosity Test of SCC.....	158
6.2.1.	Effect of Water-binder Ratio on Total Porosity.....	158
6.2.2.	Effects of Superplasticizers on Porosity.....	161
6.2.3.	Correlation Between Porosity and Compressive Strength	164
6. 3.	Permeability of Concrete.....	165
6.3.1.	Water Permeability.....	165
6.3.2.	Gas Permeability	168
6. 4.	Corrosion Characteristics	171
6. 5.	Summary.....	176
7.	STRUCTURAL BEHAVIOR OF SCC.....	177
7. 1.	Introduction	177
7. 2.	Bond Characteristic	177
7. 3.	Behavior of SCC Structure under Static Loading.....	184
7.3.1.	Computer Modeling	184
7.3.2.	Beam Testing under Static Load.....	189
7.3.3.	Crack Pattern of Static Test	194
7. 4.	Behavior of SCC Structure under Dynamic Loading	198
7.4.1.	Result of Dynamic Test	198
7.4.2.	S-N Curves of Dynamic Test.....	200
7.4.3.	Flexural Stiffness of a Specimen in a Dynamic Test.....	203
7.4.4.	Displacement and Load of Specimen in Dynamic Test.	204
7.4.5.	Crack Pattern of Dynamic Test.....	205
7. 5.	Summary.....	208
8.	CONCLUSIONS	211

8. 1.	Introduction	211
8. 2.	Fresh Concrete Properties.....	211
8. 3.	Mechanical Properties	212
8. 4.	Durability.....	213
8. 5.	Structural Behavior	214
8. 6.	Recommendations.....	215
	Reference	217
	Appendix A.....	231
A. 1.	Effects of Variation of FA Content with 3% SP and w/b of 0.25 and 0.32	231
A. 2.	Effects of Variation of Water Content with 3% SP.....	231
A. 3.	Effects of Variation of SP Content with 10% FA Content in Different w/b.....	231
A. 4.	Effects of Variation of SP Content with 10% MIRHA in Different w/b.....	232
A. 5.	Effects of Variation of Water Content with 3% SP in MSCC	232
A. 6.	Effects of Variation of Water Content with 3% SP in FMSCC	232
A. 6.	Effects of Variation of Water Content with 3% SP in NPSCC.....	233
A. 7.	Normal Concrete.....	233
	Appendix B. Compressive Strength.....	234
	Appendix C-1. ATENA Input.....	242
	Appendix C-2. ATENA Output	249
	Appendix D- LIST OF PUBLICATION	257

LIST OF TABLES

Table 2. 1. Details of concrete mixtures.....	12
Table 2. 2. Material proportion of RHA SCC.....	15
Table 2. 3. Mix design of RHA SCC	15
Table 2. 4. Specification of SCC proposed by JCSE	26
Table 2. 5. Rheology requirement of high-strength SCC	26
Table 2. 6. Rheological acceptance	27
Table 2. 7. Acceptance criteria for SCC.....	27
Table 2. 8. Slump Flow classes.....	28
Table 2. 9. Viscosity classes	28
Table 2. 10. Passing ability classes (L-box)	29
Table 2. 11. Rheological properties parameter determination.....	30
Table 2. 12. Exposure Conditions and Deterioration Mechanisms.....	41
Table 3. 1. Grading of the coarse and fine aggregate.....	63
Table 3. 2. Chemical composition of binder used in this study.....	65
Table 3. 3. Specific detail of oxygen and water permeability specimen.....	75
Table 4. 1. Rheological result of SCC.....	87
Table 4. 2. L-box ratio acceptable range	92
Table 4. 3. Mix proportion and rheological properties.....	119
Table 4. 4. SCC acceptance based on rheological properties	122
Table 5. 1. Mix proportion for various grade of SCC	130
Table 5. 2. Compressive strength of SCC	130
Table 5. 3. Compressive Strength Development of Concrete Samples.....	133
Table 5. 4. Mechanical properties of various mixtures	138
Table 5. 5. Tensile strength obtained by using the splitting test.....	154
Table 5. 6. Splitting tensile strength of SCC	155
Table 6. 1. Analyzed LPR of SCC	172
Table 6. 2. Corrosion risk from resistivity.....	173
Table 6. 3. Corrosion criteria	174
Table 6. 4. Corrosion rate of normal concrete and fly ash concrete	175
Table 7. 1. Calculation for embedded reinforcement for constant area.	178

Table 7. 2. Calculation for embedded reinforcement for 15 times of bar diameter...	178
Table 7. 3. Pull-out results and bond strength of constant area:.....	178
Table 7. 4. Pull-out results and bond strength of 15× of embedded length.....	179
Table 7. 5. Bond stress for SCC and NC pullout specimens	183
Table 7. 6. Mechanical properties and pull-out test results	184
Table 7. 7. Result of final test of static beam load.....	190
Table 7. 8. Load-deflection results of SCC and NC beams.....	194
Table 7. 9. Result of fatigue testing	198
Table 7. 10. Result of fatigue testing (continued).....	199
Table 7. 11. Cracking loads and crack characteristic of experimental SCC/NC beams	200

LIST OF FIGURES

Figure 2. 1. Bingham model for describing the deformation behavior of suspensions with the parameters of yield value τ_f and viscosity η	18
Figure 2. 2. Schematic composition of SCC.....	18
Figure 2. 3. Comparison of a typical mix design of SCC and conventional concrete .	19
Figure 2. 4. Aggregate proportion in concrete.....	21
Figure 2. 5. Mechanism of blocking	24
Figure 2. 6. Particle contact slant and particle contact angle.....	25
Figure 2. 7. Positions α and β of the sulfonic group	36
Figure 2. 8. Slump loss vs. time.....	37
Figure 2. 9. Strength of SCC versus w/b at different ages	38
Figure 2. 10. Correlation of w/c ratio and cube strength.....	39
Figure 2. 11. Corrosion and working electrode	46
Figure 2. 12. Relationship between concrete age, electrical resistivity and w/c ratio .	47
Figure 2. 13. Consolidation of voids under the reinforcement during pull-out test.....	49
Figure 2. 14. Analytical bond stress-slip relationship (monotonic loading)	51
Figure 2. 15. Idealization of beam load-deformation curves.....	51
Figure 2. 16. Failure type of reinforced concrete beam	52
Figure 2. 17. Range of number of cycles based on type of structure.....	53
Figure 2. 18. Load-displacement in dynamic load.....	55
Figure 2. 19. Typical S-N curve.....	56
Figure 2. 20. Variation of deflection and strain with applied number of cycles for specimen	57
Figure 3. 1. Flow chart for experimental program of this investigation	60
Figure 3. 2. Material, mixing and producing SCC.....	61
Figure 3. 3. (a) Coarse aggregate 20 – 8 mm, (b) Coarse aggregate 8 – 4 mm, (c). Fine aggregate (sand)	62
Figure 3. 4. MIRHA production.....	64
Figure 3. 5. Fly ash.....	65
Figure 3. 6. Superplasticizer	66
Figure 3. 7. Drum Mixer.....	67
Figure 3. 8. V-funnel.....	68
Figure 3. 9. L-Box apparatus	69
Figure 3. 10. Slump flow and T_{500} apparatus.....	70
Figure 3. 11. Pouring and measurement of slump flow and T_{500}	70
Figure 3. 12. Compression Machine (ELE ADR 3000).....	71
Figure 3. 13. Test setup profile for Flexural strength test	72
Figure 3. 14. Test setup profile split cylinder test.....	73
Figure 3. 15. Desiccators	74

Figure 3. 16. LPR Sweep Test and Configurations of electrodes;	75
Figure 3. 17. Sample and Data logger of corrosion testing	76
Figure 3. 18. Sample Dimensions of corrosion test	76
Figure 3. 19. Pull out test setup	78
Figure 3. 20. Beam Cross Section	79
Figure 3. 21. Loading setup and dimension of beam	79
Figure 3. 22. Layout of Test Frame for Static and Cyclic Loading	80
Figure 3. 23. Roell Amsler Dynamic Actuator with 500 kN capacity	80
Figure 3. 24. Installment of beam and computer control of machine	81
Figure 3. 25. Strain gauge location and data logger	81
Figure 3. 26. Typical crack of static and dynamic test of beam	82
Figure 4. 1. Effects of w/b on the V-funnel test values for 10% fly ash on FASCC with 3% SP	85
Figure 4. 2. Effects of w/b on the V-funnel test values for 10% MSCC with 3% SP	86
Figure 4. 3. V-funnel time with 3.5% SP, 10% RHA and 0.36 w/b	88
Figure 4. 4. Effects of water-binder ratio on the V-funnel test values for FMSCC with 20% FA and 10% MIRHA with 3% SP	88
Figure 4. 5. Effects of water-binder ratio on the V-funnel test values for FMSCC with 10% FA and 10% MIRHA	89
Figure 4. 6. Effect of water-binder ratio on V-funnel test of NPSCC	90
Figure 4. 7. Trend line of V-funnel time for 3% SP and 10% pozzolan and NPSCC	91
Figure 4. 8. Effect of w/b ratio and admixture dosage on slump flow and V-funnel	91
Figure 4. 9. Effects of w/b on the passing ratio, P_L for 10% fly ash with 3% SP	93
Figure 4. 10. Effects of w/b on the passing ratio for 10% MIRHA with 3% SP	94
Figure 4. 11. Effects of water-binder ratio on the passing ratio, for (a) 20% fly ash and 10% MIRHA with 3% SP ; (b) 10% fly ash and 10% MIRHA with 3% SP	95
Figure 4. 12. Effects of water-binder ratio on the passing ratio, for no pozzolan with 3% SP	96
Figure 4. 13. Trend line of passing ratio for 3% SP and 10% pozzolan	97
Figure 4. 14. Relationship between air content and w/b	98
Figure 4. 15. Effects of w/b on the T_{500} for 10% fly ash with 3% SP	98
Figure 4. 16. Effects of w/b on the T_{500} for 10% MIRHA with 3% SP	99
Figure 4. 17. Effects of water-binder ratio on the T_{500} , for 20% fly ash and 10% MIRHA with 3% SP	100
Figure 4. 18. Effects of water-binder ratio on the T_{500} , for 10% fly ash and 10% MIRHA with 3% SP	101
Figure 4. 19. Effects of water-binder ratio on T_{500} , for no pozzolan SCC with 3% SP	102
Figure 4. 20. Trend line of T_{500} for 3% SP and 10% pozzolan	103
Figure 4. 21. Effects of w/b on the slump flow values for 10% fly ash with 3% SP	104

Figure 4. 22. Effects of w/b on the slump flow values for 10% MIRHA with 3% SP	105
Figure 4. 23. Effects of w/b on the slump flow values for 20% fly ash and 10% MIRHA with 3% SP	106
Figure 4. 24. Slump flow with 3.5% SP, 10% RHA and 0.36 w/b.....	107
Figure 4. 25. Effects of w/b on the slump flow values for 10% fly ash and 10% MIRHA with 3% SP	107
Figure 4. 26. Effects of w/b on the slump flow values for no pozzolan SCC with 3% SP.....	108
Figure 4. 27. Trend line of slump flow for 3% SP and 10% pozzolan and NPSCC..	109
Figure 4. 28. Effects of superplasticizers content on the V-funnel test values for 10% fly ash with different w/b.....	110
Figure 4. 29. Effects of superplasticizers content on the V-funnel test values for 10% MIRHA with different w/b	111
Figure 4. 30. Correlation between w/c and workability of concrete.....	112
Figure 4. 31. Effects of superplasticizers content on the passing ratio for 10% fly ash with different w/b.....	113
Figure 4. 32. Effects of superplasticizers content on the passing ratio for 10% MIRHA with different w/b	113
Figure 4. 33. Effects of superplasticizers content on the T_{500} for 10% fly ash with different w/b.....	114
Figure 4. 34. Effects of superplasticizers content on the T_{500} for 10% MIRHA with different w/b.....	115
Figure 4. 35. Effects of superplasticizers content on the slump flow for 10% fly ash with different w/b.....	116
Figure 4. 36. Effects of superplasticizers content on the slump flow for 10% MIRHA with different w/b	116
Figure 4. 37. Effect of superplasticizers on slump flow.....	117
Figure 4. 38. Effects of different cement/fly ash content on the V-funnel test values of 3% SP mixes with different w/b.....	118
Figure 4. 39. Effects of different cement/fly ash content on the passing ratio, P_L of 3% SP mixes with different w/b.....	118
Figure 4. 40. Effects of different cement/fly ash content on the T_{500} test values of 3% SP mixes with different w/b.....	119
Figure 4. 41. Effects of different cement/fly ash content on the slump flow test values of 3% SP mixes with different w/b.....	120
Figure 4. 42. Influence of cement content and fly ash on slump flow	121
Figure 5. 1. Strength developments of FASCC with 10% fly ash and 3% SP in variation of w/b	126
Figure 5. 2. Strength performance of fly ash concrete with different w/b ratios.....	128
Figure 5. 3. FASCC compressive strength contain 3% SP at variation of water-binder ratio at 28 days	129

Figure 5. 4. Strength developments of MSCC with 10% MIRHA and 3% SP in variation of w/b	131
Figure 5. 5. MIRHA SCC compressive strength at 3% SP 10% MIRHA and at different water-binder ratio	132
Figure 5. 6. Strength development of SCC containing RHA	133
Figure 5. 7. Compressive strength of FMSCC with 3% SP at different water-binder ratio.....	134
Figure 5. 8. Compressive strength of NP SCC with OPC 500 kg/m ³	135
Figure 5. 9. NP SCC compressive strength with 3% SP and at different water-binder ratio.....	136
Figure 5. 10. Effect of superplasticizers on FASCC with water-binder ratio 0.25 and 10% fly ash.....	137
Figure 5. 11. Strength development of NC and high-strength SCC.....	138
Figure 5. 12. Effect of superplasticizers on FASCC with water-binder ratio 0.34 and 10% fly ash.....	139
Figure 5. 13. Compressive strength of FASCC with water-binder ratio 0.42 variation of superplasticizer.....	140
Figure 5. 14. Correlation of FASCC compressive strength and superplasticizers content.....	141
Figure 5. 15. Effect of superplasticizers content to the compressive strength.....	142
Figure 5. 16. Compressive strength of MSCC w/b 0.35 in variation of superplasticizer	143
Figure 5. 17. Compressive strength of MSCC with water-binder ratio 0.4 in variation of superplasticizer.....	143
Figure 5. 18. Compressive strength of MSCC with water-binder ratio 0.45 variation of superplasticizer.....	144
Figure 5. 19. Correlation of MSCC compressive strength and superplasticizers content	145
Figure 5. 20. Effects of different fly ash content on compressive strength.....	146
Figure 5. 21. Strength development of concrete with diatomite aspozzolan.....	147
Figure 5. 22. The influence of the content of fly ash on the amount of filling water	148
Figure 5. 23. Compressive strength of Portland cement–fly ash–silica fume concrete	149
Figure 5. 24. Water requirement of concrete containing fly ash and/or silica fume..	149
Figure 5. 25. Compressive strength vs. curing time for OPC and fly ash cement concretes	150
Figure 5. 26. Strength development 700°C and 600°C burning temperature of MIRHA	151
Figure 5. 27. Effect of fineness on strength gain at 28 days.....	151
Figure 5. 28. Optimum SCC mix design based on compressive strength	152
Figure 5. 29. Modulus of Rupture of SCC	153
Figure 5. 30. Split tensile of SCC	153

Figure 6. 1. Total porosity of concrete made of 5%, 10% and 15% FA content with a w/b of 0.25 and 0.32 at the age of 28 days	159
Figure 6. 2. Effect of water-binder ratio on porosity of 10% MSCC.....	160
Figure 6. 3. Effect of SP dosage on porosity in 10% FASCC with different water-binder ratio	161
Figure 6. 4. Effect of SP dosage on porosity in MIRHA SCC with different water-binder ratio	163
Figure 6. 5. Correlation between porosity and comp. strength in FASCC.....	164
Figure 6. 6. Correlation between porosity and compressive strength in MSCC.....	165
Figure 6. 7. Water permeability of FASCC.....	166
Figure 6. 8. Initial absorption values of the concretes investigated	167
Figure 6. 9. Variation of permeable voids with fly ash replacement	168
Figure 6. 10. Oxygen permeability of fly ash SCC in different ages.....	169
Figure 6. 11. Oxygen permeability of MSCC.....	170
Figure 6. 12. Water and mercury porosity of concrete.....	170
Figure 6. 13. Oxygen permeability of SCC	171
Figure 6. 14. LPR Testing Results for Sample Age 7 Days and 28 Days.....	172
Figure 6. 15. I corr (mA/cm ²) reading for different mixes in 7 days and 28 days. .	173
Figure 6. 16. Corrosion Rate (mm/year) reading for different mixes in 7 days and 28 days.....	175
Figure 7. 1. Effects of different fly ash content on bond strength with constant embedment area.....	180
Figure 7. 2. Effects of 5, 10 & 15% FA content bond strength 15 times diameter of embedment length	181
Figure 7. 3. Effect of superplasticizers on bond strength with w/b 0.35 and 0.4.....	181
Figure 7. 4. Effect of superplasticizers on bond strength with w/b 0.45.....	182
Figure 7. 5. Effect of water-binder ratio on bond strength in different sp content	182
Figure 7. 6. Finite Element mesh model of a beam	186
Figure 7. 7. Stress contour of σ_x in a beam in first increment load.....	186
Figure 7. 8. Stress contour of σ_x in a beam in final increment load.....	186
Figure 7. 9. Tensor of Principal stress of beam	187
Figure 7. 10. First crack in of beam	187
Figure 7. 11. Typical displacement vector of beam	188
Figure 7. 12. Typical displacement vector of steel reinforcement.....	188
Figure 7. 13. Typical stress on steel reinforcement in longitudinal axes	189
Figure 7. 14. Load-displacement diagram of SCC beam static load test	190
Figure 7. 15. Ultimate load and stiffness of SCC beam static load test.....	191
Figure 7. 16. Yield point load and ductility of SCC beam static load test.....	192
Figure 7. 17. Performance benchmark of static loading test	193
Figure 7. 18. Crack pattern of FASCC beam specimen (flexural failure).....	194

Figure 7. 19. Crack pattern of FMSCC beam specimen (flexural failure).....	195
Figure 7. 20. Crack pattern of MSCC beam specimen (shear failure).....	195
Figure 7. 21. Crack pattern of NPSCC beam specimen (bending failure)	196
Figure 7. 22. Crack pattern of Normal Concrete beam specimen (shear failure).....	196
Figure 7. 23. Cracking map of 70-80% of the ultimate length-all length in cm.....	197
Figure 7. 24. Crack pattern in SCC and normal concrete.....	198
Figure 7. 25. S-N curves of FASCC and MSCC	201
Figure 7. 26. S-N curves of FMSCC and NPSCC	201
Figure 7. 27. S-N curves of normal concrete.....	201
Figure 7. 28. Brittle failure of FASCC in dynamic test.....	202
Figure 7. 29. Number of cycle vs Flexural stiffness	203
Figure 7. 30. Displacement-load diagram for FASCC and MSCC.....	204
Figure 7. 31. Displacement-load diagram for FMSCC and diagram for NPSCC.....	205
Figure 7. 32. Displacement-load diagram for normal concrete	205
Figure 7. 33. FASCC crack pattern of dynamic test (number of cyclic in thousands)	206
Figure 7. 34. MSCC crack pattern of dynamic test.....	206
Figure 7. 35. FMSCC crack pattern of dynamic test.....	207
Figure 7. 36. NPSCC crack pattern of dynamic test	207
Figure 7. 37. Normal concrete crack pattern of dynamic test.....	208

PREFACE

This thesis has been prepared to extend the knowledge of self compacting concrete (SCC) when it mixed with fly ash and/or Microwave Incinerated Rice Husk Ash (MIRHA) as filler and also the role of these ashes as pozzolanic material in hydration process. Utilizations of such pozzolanic material are interesting due to the environmental issue caused by these pollutants in the air, especially in Malaysia that produce plenty of these abundant by-products. Self compacting concrete itself is well-known with its high workability, flowability, segregation resistance and homogeneity. Knowledge of this material has been already described on some journals published and other references and started to be used globally on construction industries. Yet, some characteristic of this relatively new material is less understood and the studies need to be widened to extend our understanding regarding this material. Structural element with applied self compacting concrete will behave differently due to its higher characteristic of mechanical properties and also behavior in micro element level compared to normal vibrated concrete.

Determination of accepted SCC mix design or ingredient proportion is very crucial and become the central of this study by reason of reliability of particular mixed whether it can be applied into the formwork without any vibration or not. Whereas this test so-called rheological properties test is fundamental to get the optimum mix design together with the result of mechanical properties test, while the durability properties will confirm all this optimum mix design. The optimum mix design then be applied into structural behavior test and observation of this behavior will determine of capability of particular mix proportion of SCC in real structure. The result showed very promising outcomes that fly ash and MIRHA were proven have ability to enhance to strength and sustain both monotonic and cyclic loading better than normal concrete.

It is hoped that readers will be able to use this thesis to know better of self compacting concrete incorporating fly ash and MIRHA, particularly how to produce better SCC with fly ash and MIRHA filler in optimum proportion and also understanding of behavior of this material both in fresh and hardened state especially the behavior when it applied into the structural element in building.

CHAPTER 1

INTRODUCTION

1. 1. General Remarks

Self compacting concrete (SCC) is a breakthrough invention in the advancement of concrete material. This material is distinguished by its special workability and the ability to compact itself, which is achieved without any mechanical vibration, whereas vibration is crucial in fresh concrete in order to achieve the highest possible density leading to stronger and less porous of hardened concrete. But the vibration, on the other hand, causes additional problems to the fresh concrete as well as other technical difficulties such as soundness of concrete, noise, segregation and bleeding. SCC eliminates the need of vibration which it has the ability to flow into the formwork and thoroughly fill the complex space due to its own weight without losing the resistance to aggregate segregation. It flows easily through every corner of the formwork and has the ability to flow through narrow openings without hindrance. This means the so-called blocking of coarse aggregates through bridging can be avoided.

Achievement of the above mentioned properties and behavior of SCC became possible due to development of high-range water reducer (HRWR), which are usually naphthalene-based superplasticizers and have the capability to modify the viscosity of the fresh mixes.

1. 2. Development and Challenges of SCC

Recently, the demand for concrete as structural material has become very high compared to steel material, which is expensive and needs more skill for construction as well as fabrication and requires more complex analysis to design. Concrete is commonly composed of cement and other cementitious materials such as fly ash, rice

husk ash or slag cement, coarse aggregate, fine aggregate or sand, water and chemical admixtures. Over the last two decades, many efforts have been made to achieve high strength concrete. High strength concrete promises better prospect in precast and construction industry. The minimum value of compressive strength of high strength concrete is supposed to be 50 MPa. Now concrete has been made with compressive strength more than 100 MPa, which made it possible to reduce the sizes of heavy structural members to a reasonable extent. High strength productions need low water consumption which leads to stiffer fresh concrete condition. In other words the high strength will give low workability, but in high water content the strength of concrete is significantly deteriorated. The discovery of self compacting concrete solves these problems.

The first mixes of SCC were developed at the University of Tokyo, Japan. The research activities started in late 1980's, and by 1990's Japan has developed and used SCC as stated by Okamura and Ouchi [1]. The new developments of self compacting concrete are focusing on high performance. This may be identified by its high workability, enhanced durability, reliable quality, uniform surface texture and higher strength. SCC has a variety of applications in civil engineering structures such as buildings, bridges, tunnels and other types of buildings. The developments of self compacting concrete are also mainly focused on the precast industry for manufacturing of large size bridge girders which are supposed to be subjected to harsh environment and cyclic nature of loading due to vehicular movement. These girders are usually composed of very congested steel reinforcement details, which are very suitable for self compacting concrete to be applied.

One of the characteristics of self compacting concrete was given by Poon and Ho [2] who stated that self compacting concrete (SCC) can be categorized as a high-performance material on the condition that it can flow under its own weight to achieve consolidation, which is determined by rheological properties and also has the high compressive strength. The rheological properties of SCC are targeted to have near zero yield stress, so that it behaves like a Newtonian fluid that possesses low but enough viscosity to minimize segregation potential. Whereas Djelal, et al. [3] stated that the other advantage of SCC is high transport ability. For the years to come, buildings have been getting taller and need to be stronger. To build such building, the concrete

should comprise very low viscosity able to be pumped through circular pipe that has high friction of its inner circle. Due to this circumstance, this material (SCC) has become increasingly needed.

The main challenges and issues of SCC are the achievement of high strength at competitive cost using highly efficient cement replacement materials, in order to insure long term durability, increase bond characteristics and improve the fatigue endurance under high cyclic load. The utilization of local resources such as waste product of fly ash and rice husk will be the urgent need, in order to save our environment caused by this material and at the same time extent the achievement of higher quality of concrete.

1.3. Gaps in Current Research

To date, the majority of research activities on SCC are focusing on rheological and basic engineering properties such as compressive strength, flexural strength, etc. Application of rice husk ash in producing high strength and high performance SCC is still lacking. Detailed structural behavior of SCC is still less known, so research activities are required to be extended to explore the structural characteristics such as effects of cyclic loading in beams, fatigue life prediction of SCC using cyclic loading experiments, modulus of elasticity, effects on bond between concrete, embedded steel bars, etc.

The study of Microwave Incinerated Rice Husk Ash (MIRHA) utilization in concrete has been investigated in almost the last three decades. However, application of rice husk ash in producing self compacting concrete is still limited. Recent activities on this material mostly work with vibrated concrete without looking into the self compactibility.

Very few research has been done on durability characteristics of SCC such as fluid permeability and corrosion resistance, as well as the investigation on bond behavior of embedded steel bars in SCC and development of empirical relationship.

1. 4. Objective and Scope

Filler is the essential component of SCC, and in most cases fly ash is usually used as filler for producing SCC. Fly ash is a by-product that is abundantly available in coal-fired power stations in Malaysia. Yet, there are many other waste materials such as rice husk available in large quantities in Malaysia. High quality ash after controlled burning of rice husk may be a good alternative to be used as filler or pozzolanic material in SCC. Based on the various issues and challenges as discussed for the development of SCC and various gaps as identified in the available research, the principal aim of this research was to develop comprehensive mix design for different strength levels by incorporating locally available waste materials such as rice husk ash and fly ash. The mix proportions were initially developed based on trials that were supposed to satisfy the workability requirement during the fresh state as well as the structural requirement such as compressive strength, bond characteristics, load-deflection behavior and fatigue endurance and the durability requirement.

This research was based on the following main objectives:

1. To develop the series of optimum mix design for 28 days target compressive strength from 50 to 80 MPa as requirement of high strength concrete by incorporating the fly ash and MIRHA as filler as well as pozzolanic material.
2. To measure the various parameters such as total porosity, gas permeability and corrosion potential in order to predict the durability of the SCC.
3. To determine the elastic properties such as flexural capacity using prism bending test and tensile strength using split cylinder test.
4. To estimate the bond characteristics of concrete with the embedded steel reinforcement by pull-out test.
5. To draw and analyze the different stages of load-deflection behavior of reinforced concrete beams until failure.
6. To evaluate the fatigue endurance of RC beams under cyclic loading subjected to a frequency of 5 Hz until failure or one million cycles.

1. 5. Motivation

A distinctive feature of self compacting concrete has been used in a wide range of applications which have been followed by extensive researches and developmental studies. Self compacting concrete is considered as the big breakthrough in concrete technology for many decades. The reason for the development of SCC is the need to advance the quality of concrete structures. Recent application of self compacting concrete is focused on high performance that is better and possesses more strength, less porous, improved durability, and faster construction. This type of concrete has ability to combine high workability and high strength together.

Utilization of fly ash in concrete has been extensively studied in some countries that produce this waste product material. Fly ashes have been increasingly used in almost all types of concrete to enhance durability and/or to reduce production cost as well.

Rice husk ash is the by-products of rice paddy milling industries in Malaysia. Rice husk has attracted more attention due to environmental issue. Rice husk has large dry volume due to its low bulk density and possesses rough and abrasive surfaces that are highly resistant to natural degradation that make disposal of rice husk become a challenging problem. It is recognized that concrete industries can consume large quantities of solid pozzolanic wastes.

Structural behavior of self compacting concrete containing fly ash and/or rice husk ash will behave differently as compared to the normal concrete due to its different mechanical properties and also in micro element level of those materials. Many concrete structural members are subjected to repeated loads with the magnitude which is below the maximum load under monotonic loading, while the self compacting concrete show the promising strength to sustain this type of load. Fatigue is one property of concrete that is not well understood, particularly in terms of the failure mechanism. The lack of this understanding, due to the difficulties in conducting and time-consuming experiments, has been the main motivation for this research.

1. 6. Thesis Contributions

The SCC performances on fresh and hardened concrete were investigated. The combination of experimental and finite element in structural behavior is presented in this thesis. From a scientific and practical point of view, the main contributions consist of:

1. To solve the Malaysia environmental issue by using pozzolan waste material product. Fly ash and rice husk have been duly used in this research. Self compacting concrete can be made cost effective by replacing the cement by pozzolan materials which is low-cost microfillers as it is waste material, which can compensate the high cost of chemical admixtures, such as superplasticizers. The results also confirm that it is possible to get high strength and high durability concrete economically using MIRHA by burning local available rice husk. The utilization of Microwave Incinerated Rice Husk Ash into the concrete mix proportions has given various effects to the concrete properties. The burning procedure adopted was able to extract the quality and quantity of amorphous SiO_2 at an optimum amount of MIRHA has significantly improved the compressive strength performance.
2. Knowledge of structural behavior of self compacting concrete containing fly ash and rice husk ash, especially brittle behavior of fly ash self compacting concrete due to high strength properties of this material. By reason of this finding, more confinement is needed to prevent early bursting in concrete cover of self compacting concrete structure and finally save the inner part of concrete element.

1. 7. Layout of the Thesis

The thesis is organized as follows:

Chapter 2 provides a review of available and related literature on the invention and an exploration in SCC, rheological properties in fresh concrete and some of the properties of hardened concrete, mix design of SCC and high performance concrete and also some structural behaviors of SCC in existing model. The research gaps in some areas in SCC are also described to determine the objectives of this thesis.

Chapter 3 describes the research methodology that contains the procedures of all experiment in this research. Experimental setup, test variables and procedure of preparation of all material are also described in detail in this chapter.

Chapter 4 provides the result of rheological tests to observe the fluidity of SCC, evaluate the deformability of SCC, filling ability of SCC through the formwork and passing through ability of SCC to the congested steel. The accepted mixes and unaccepted mixes of SCC are described, where the adjustment of the material proportion in mixed design is also considered necessary based on this acceptance.

Chapter 5 provides the results of all hardened concrete, including mechanical and physical properties of SCC and also analysis results in all aspects. The combination of result from Chapter 4 and Chapter 5 will determine the optimum mix design of SCC for the best material proportion and then applied into structural behavior test.

Chapter 6 presents the durability properties of self compacting concrete with several methods to measure durability parameters which cover porosity, permeability and corrosion characteristic. Since the durability properties is one aspect of high performances in concrete, the result of this chapter will support categorization of high performance concrete of tested SCC mixes.

Chapter 7 presents result and analysis of static and dynamic tests of beams including SN curved and fatigue analysis. The result will confirm all result in Chapter 5 and also illustrate the behavior of each beam with accordance to certain mix.

Chapter 8 concludes the results from the investigations which confirm and answer all objectives of this research. Some recommendations for future research to enhance the possibility of further investigation are given.

CHAPTER 2

LITERATURE REVIEW

2. 1. Introduction

This chapter was aimed to review through available literature, the various aspects of theory, data and results on the research of self compacting concrete. The literature reviewed in this chapter is divided into several parts. These include pozzolan waste issue in Malaysia and its utilization in both normal vibrated concrete and SCC. Definition and behavior of self compacting concrete, in addition the principal understanding of SCC, procedure of producing SCC and recent development in concrete industry are discussed. Description of mechanical properties of SCC, in order to give indications of quality control, and also a description of the procedure of mix proportion design. Finally, structural performance under monotonic and cyclic loading was reviewed.

2. 2. Pozzolan Waste Product in Malaysia

Ahmaruzzaman [4] stated that one of waste pozzolan is fly ash in Malaysia, which is generated during the combustion of coal for electricity production. Fly ash is an industrial by-product which is recognized as an environmental pollutant. Due to its environmental problems, fly ash research has been undertaken worldwide. While Norazlan [5] stated that Malaysian government promotes coal as a choice of fuel for power generation. The reason is that the main resource of fuel which was about 71% of total energy to generate power plant in 2002. Malaysia also has plans to reduce its dependency on natural gas by changing it to coal combustion; this decision certainly boosts up the fly ash production. The utilization of this waste product becomes so crucial to protect the environmental problem.

The other waste pozzolan product in Malaysia is rice husk. Omar [6] stated that Rice is the staple food in Malaysia. Most of the paddy in Malaysia is planted in Peninsula Malaysia and small portion in Sarawak and Sabah. A total of 296,000 paddy farmers exist in Malaysia, covering about 200,000 hectare of land. While Adam, et al. [7] stated that rice husk creates a major problem of disposal to the rice milling industry in Malaysia. To solve this problem efforts have been made in the past 20 years to use rice husk in various ways.

Adam [8] stated that the silica content found in Malaysian rice husk ash has a high specific surface area of 300 to 400 m²/g. The silica content was determined by x-ray fluorescence and it was shown to be 99.99% pure silica which plays main role in pozzolanic reaction in concrete to produce additional calcium silicate hydrate (C-S-H) binder. The following equations illustrate the pozzolanic reaction of fly ash with lime. Hydration cement reaction describe as: $C_3S + H \rightarrow C-S-H + Ca(OH)_2$. This lime product reacts with the silica from fly ash or rice husk ash with pozzolanic reaction: $CaOH + S \rightarrow C-S-H$.

2. 3. Utilization of Fly Ash and MIRHA in Concrete

2.3.1. Fly ash and MIRHA Utilization in Vibrated Concrete

Fly ash and MIRHA utilization in non-SCC were done by many researchers. Poon, et al. [9] studied on high strength concrete with large volumes of low calcium fly ash, and measured the parameters of compressive strength, heat of hydration, chloride diffusivity, degree of hydration, and pore structures of fly ash/ cement concrete and corresponding pastes. The investigation concluded that concrete with a 28-day compressive strength of 80 MPa could be obtained with a water-to-binder (w/b) ratio of 0.24 and fly ash content of 45%. With this proportion, concrete has lower heat of hydration and chloride diffusivity compared to the normal concrete or concrete with lower fly ash contents. The study was also confirmed by work of Lam, et al. [10] which quantified the reaction rates of cement and fly ash; the results demonstrated the dual effects of fly ash in concrete: act as a micro-aggregate and as a pozzolan. Almost the same investigation was also done by Zhang, et al. [11] by studying the hydration processes of high-volume fly ash cement paste by examining the non-evaporable

water content and investigation by Termkhajornkit, et al. [12] with the effect of water curing condition on hydration process.

Namagga and Atadero [13] utilized large volume of high calcium content fly ash as pozzolan in concrete. This high lime fly ash can be categorized as class C fly ash by ASTM because of its high calcium content. The percentage of 0 to 50% had been used in investigation with the result of 25 to 35% fly ash provided the optimum composition. The investigation of class C fly ash ASTM by Antiohos and Tsimas [14] with fly ash up to 30% of Greek high-calcium fly ashes, diversified both on their reactive silica content and silicon/calcium oxides ratio, were used to prepare mixes with Portland cement.

Singh and Garg [15] investigated the effect of temperature in hydration process by blending 60 to 70% fly ash with fluorogypsum, hydrated lime sludge, with and without Portland cement and chemical activator in different proportions. The hydration of these binders was studied by its performance in water and by accelerated aging at temperatures in the range of 27 to 50°C. The optimum temperature in compressive strength was noticed at 50°C. While Lee, et al. [16] investigated the effect of particle size distribution of fly ash–cement system on the fluidity of the cement pastes using class F fly ash.

McCarthy and Dhir [17] found that fly ash has a role in the development of high performance concretes by using multi-binder combinations. It is proven that the fly ash plays the role of post-production processing in ensuring fly ash suitability as a binder. On the other hand, in construction applications and cementitious binders are required; fly ash can be used and will give similar or improved properties compared to neat Portland cement binders.

Saraswathy, et al. [18] investigated wide range of fly ash content with concrete specimens prepared with 10%, 20%, 30% and 40% of activated fly ash replacement levels were evaluated for their compressive strength at 7, 14, 28 and 90 days and investigated the corrosion-resistance.

While utilization of MIRHA or Rice Husk Ash (RHA) in vibrated concrete was investigated by several researchers. Muhammad and Waliuddin [19] studied High

Strength Concrete (HSC) that was produced using RHA from Malaysian available materials. The effect of Rice Husk Ash (RHA) as a 10 to 30% replacement of cement on the strength of HSC was studied. RHA was obtained by burning rice husk, which is abundantly available in Malaysia. A total of 200 test specimens were cast and tested at 3, 7, 28 and 150 days with compressive and split tensile strengths of the test specimens were determined. The results showed that the strength of HSC decreased with RHA replacement while maintaining the same level of workability.

Nuruiddin, et al. [20] used RHA as cement replacement. They investigated the effect of burning procedure of RHA which contains high silica with micro porous structure inside RHA. Improper burning of rice husk cannot extract the maximum amount of amorphous silica that can contribute to the strength development and durability of concrete. MIRHA as cement replacement of 5%, 10%, and 15% of paste weight in the concrete mixture proportions was studied. Analysis with X-ray Diffraction (XRD) and X-ray Fluorescence (XRF) showed that MIRHA had 88.40% of silica content with partially crystalline structure. The Scanning Electron Microscope (SEM) also showed the promising effects of MIRHA to the Interfacial Transition Zone (ITZ) between aggregate and cement paste Mixture Proportions of Concrete. Similar investigation was done by Kamal, et al. [21]. They burnt rice husk at different burning temperatures and studied its effect to the compressive strength of concrete by compressive strength test at 3, 7 and 28 days. The results showed that 5% replacement of MIRHA with 800°C burning temperature provided good acceleration in compressive strength development in concrete, while the inclusion of 10% replacement of MIRHA with 700°C burning temperature improved the strength of concrete and MIRHA with a burning temperature of 600°C revealed that the optimum replacement of MIRHA was 10%.

2.3.2. Fly ash and MIRHA Utilization in SCC

Dinakar, et al. [22] studied the production and evaluation of SCC mixtures with high volumes of class F fly ash. Eight fly ash SCC mixtures of various strength grades (20 to 100 MPa) were deliberated at the desired fly ash percentages of 0, 10, 30, 50, 70 and 85% as shown in Table 2. 1. Tests were carried out on all mixtures to determine

the properties of fresh concretes in terms of rheology. The mechanical properties of hardened concretes that covered compressive strength, splitting tensile strength and elastic modulus were also determined. Test results showed that utilization of high volumes of class F fly ash in SCC mixtures decreases its 28-day compressive strength, and showed continuous and significant improvement at 90 and 180 days, which was most probably due to the pozzolanic reaction of fly ash. The similar investigation was also done by Sukumar, et al. [23] and Liu [24] with high volume of fly ash in self compacting concrete.

Table 2. 1. Details of concrete mixtures

No.	Concrete grade: MPa	Name	TCM: kg/m ³	Fly ash: %	Cement: kg/m ³	Fly ash: kg/m ³	Water: powder ratio	SP liquid weight: %
1	20	NC20	234	0	234	0	0.79	0
2		SCC558	550	85	83	468	0.41	2
3	30	NC30	319	0	319	0	0.58	0
4		SCC557	550	70	165	385	0.34	2
5		SCC757	750	70	225	525	0.33	2
6	60	NC60	500	0	500	0	0.37	0
7		SCC555	550	50	275	275	0.34	2.5
8		SCC655	650	50	325	325	0.34	2
9	90	NC90	552	0	552	0	0.29	1
10		SCC553	550	30	385	165	0.31	2.5
11		SCC530	500	30	350	150	0.36	1.75
12	100	NC100	659	0	659	0	0.22	1
13		SCC551	550	10	495	55	0.29	3

Note: TCM is total cementitious materials content. Superplasticiser (SP) dosage is percentage by weight of TCM.

Source: Dinakar, et al. [22]

Nehdi, et al. [25] stated that high-volume replacement SCC (including FA, GGBS and MIRHA) can help to achieve the workability and ease of construction benefits associated with conventional SCC as well as achieve much enhanced long-term durability. In other word it provides environmental benefits of using high-volume replacements of portland cement. This makes this material very appealing for future challenging construction projects.

Ravindrarajah, et al. [26] investigated the development of self compacting concrete with reduced segregation potential by increasing the fine particle content by replacing partially the fine and coarse aggregates by low-calcium fly ash. The experimental showed that partial replacement of coarse and fine aggregate could produce self compacting concrete with low segregation potential as assessed by the V-

funnel test. The results showed that fly ash was suitable to be used in producing self compacting high-strength concrete with reduced segregation potential. The similar research was also done by Bouzoubaâ and Lachemib [27]

Sonebi [28] investigated the development of medium strength SCC. The cost of materials will be decreased by reducing the cement content by using pulverised fuel ash (PFA) while minimizing the amount of superplasticizers (SP). The mixture mixes were made with w/b of 0.38 to 0.72 and 60 to 216 kg/m³ of cement content, 183 to 317 kg/m³ of PFA and 0% to 1% of SP, by mass of powder. The results showed that MS-SCC can achieve a 28-day compressive strength of 30 to 35 MPa by using up to 210 kg/m³ of PFA.

Nehdi, et al. [25] investigated the rapid chloride ion penetrability, sulfate expansion and deicing salt surface scaling resistance of SCC mixtures made with high-volume replacement binary, ternary, and quaternary cements using class F fly ash and also RHA. Results showed that SCC can be made with high-volume replacement composite cements and achieve good workability, high long-term strength, good deicing salt surface scaling resistance, low sulfate expansion and very low chloride ion penetrability.

Sahmaran and Yaman [29] investigated the effect of steel fibers with constant content at 60 kg/m³ in SCC. The results showed that high-volume coarse fly ash can be used to produce fiber reinforced self compacting concrete. However, there was some reduction of the concrete strength due to the use of high-volume coarse fly ash.

Utilization of rice husk as cement replacement in producing self compacting concrete were carried out by several researchers. Memon, et al. [30] explored the use of Rice Husk Ash (RHA) to increase the amount of fines; hence, achieve self-compactibility in an economical way with the mixture as shown in

Table 2. 2. The results indicated that the feasibility to develop low cost SCC using RHA, with cost analysis showed that the cost of ingredients of specific SCC mix is 42.47 percent less than the control concrete.

Table 2. 2. Material proportion of RHA SCC

Mix name	Water	Cement	RHA	Sikament NN (% by weight of binder)	Viscocrete-1 (% by weight of binder)	Water/Binder ratio
	(kg/m ³)	(kg/m ³)	(kg/m ³)			
CC3.5	200	500	0	3.5	2	0.4
CC4	200	500	0	4	2	0.4
CC4.5	200	500	0	4.5	2	0.4
5R3.5	200	500	25	3.5	-	0.38
5R4	200	500	25	4	-	0.38
5R4.5	200	500	25	4.5	-	0.38
10R3.5	200	500	50	3.5	-	0.36
10R4	200	500	50	4	-	0.36
10R4.5	200	500	50	4.5	-	0.36

Source: Memon, et al. [30]

The other investigation of SCC incorporating RHA, 10%, and 20%, and two different water/cementitious material ratios (0.40 and 0.35) as shown in Table 2. 3, were done by Ahmadi, et al. [31]. The result indicated the optimum content of RHA as cement replacement was 20%.

Table 2. 3. Mix design of RHA SCC

MIX DESIGN (KG/M ³)						
Mix	Gravel	Sand	Water	Cement	RHA	W/B
SCC(0%RHA)	770	970	184	460	0	0.4
SCC(10%RHA)	770	970	184	414	46	0.4
SCC(20%RHA)	770	970	184	368	92	0.4
OC(0%RHA)	1043	700	184	460	0	0.4
OC(10%RHA)	1043	700	184	414	46	0.4
OC(20%RHA)	1043	700	184	368	92	0.4
SCC(0%RHA)	770	1000	161	460	0	0.35
SCC(10%RHA)	770	1000	161	414	46	0.35
CC(20%RHA)	770	1000	161	368	92	0.35
OC(0%RHA)	1043	750	161	460	0	0.35
OC(10%RHA)	1043	750	161	414	46	0.35
OC(20%RHA)	1043	750	161	368	92	0.35

Source: Ahmadi, et al. [31]

2. 4. Definition and Behavior of SCC

Self compacting concrete is rather a new technique or procedure for producing concrete which tends to level-off in any kind of formwork without any energy. A lot of the extensive research and development work were so far dedicated to the achievement of fresh properties, many new assessment methods and procedures have been introduced for determining the right properties of fresh concrete.

Colleparidi [32] described the history of self compacting concrete that it was discovered in 1983 by Professor Okamura from University of Tokyo to investigate the growing durability problem related to concrete structure in Japan. The major concern of this finding was the poor durability performance due to improper consolidation of the fresh concrete. Professor Okamura started to publish his idea and concept in 1986 of a high durability concrete which has the ability to compact itself achieving full compaction. This idea was then followed by several investigations and also the utilization of pozzolan material such as fly ash and MIRHA or the other local raw materials.

Peter, et al. [33] stated that self compacting concrete eliminates the need for internal or external vibration due to its ability to freely flow in and around dense reinforcement and fills the mold completely without any blockages. SCC would be an ideal material for impossible pouring position of normal concrete. Generally the required flow properties of fresh concrete are achieved using new generation superplasticisers to reduce the water-binder ratio (w/b). In addition supplementary filler materials, that are usually inert in nature, such as lime stone powder, natural pozzolans, and fly ash are also introduced to increase the viscosity and reduce the cost of concrete.

Abhishek, et al. [34] and Celik and Stephen [35] noted that conventional concrete tends to have problems relating to consolidation in the area of congested reinforcement. The large numbers of air voids affect the performance and durability of concrete. Self compacting concrete can be used to minimize this problem, because it is designed to consolidate under its own weight.

A concrete can be categorized as SCC if it achieves some of the characteristic as described by Timo [36] and Ambedkar [37]:

1. Filling ability is ability to fill a formwork completely under its own weight.
2. Passing ability is ability to overcome obstacles under its own weight without hindrance. Obstacles could be reinforcement, small openings, etc.
3. Segregation resistance is homogeneous composition of concrete during and after transportation and placement.

Properly designed self-consolidating concrete can be highly flowable, yet it needs to be stable without separation or segregation. It can easily spread due to low viscosity of this concrete and fill the formwork without any consolidation and without undergoing a significant separation. Youjun, et al. [38] also stated that the development of self compacting concrete has made casting of dense reinforcement and mass concrete convenient, has minimized noise, and has improved the quality of in situ concrete.

As described by Stefan and Wolfgang [39] and D'Aloia, et al. [40], self compacting concrete is always recognized by its special workability. For this purpose, an optimum mix design should be established which exhibits flowability, self-compaction and homogeneity or stability. SCC should have all the requisite fresh concrete properties at the time of placement. The nature of the application determines the necessary of workability and workability retention period.

Flowing of SCC was described by Stefan and Wolfgang [39], Chidiac, et al. [41], Nicolas [42], Jacek and Janusz [43] and Coussot [44]. They stated that in the fresh state SCC corresponds the rheology to a Bingham flow law with the parameters of yield value and viscosity. The Bingham flow law describes the deformation behavior of a suspension under shear stress. It is composed of a constant factor, the yield value τ_b , and a variable component that depends on the ratio of the applied shear stress τ to the rate of the load application $\dot{\gamma}$ and is described by viscosity η . The yield value gives the energy that must be applied externally to make the suspension start to flow. The viscosity that describes the resistance to deformation during the flow is shown in Figure 2. 1.

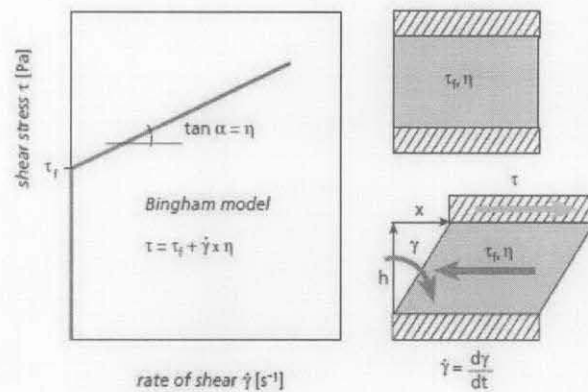


Figure 2. 1. Bingham model for describing the deformation behavior of suspensions with the parameters of yield value τ_f and viscosity η

Source: Stefan and Wolfgang [39]

2.4.1. Mix Design Method of SCC

A number of procedures have been proposed for designing SCC. Dinakar, et al. [22] detailed the schematic composition of SCC as shown in Figure 2. 2. However, this schematic requires specific adjustments to all the ingredients such as sand, coarse aggregates, superplasticisers and water, to arrive at an optimal mix proportion.

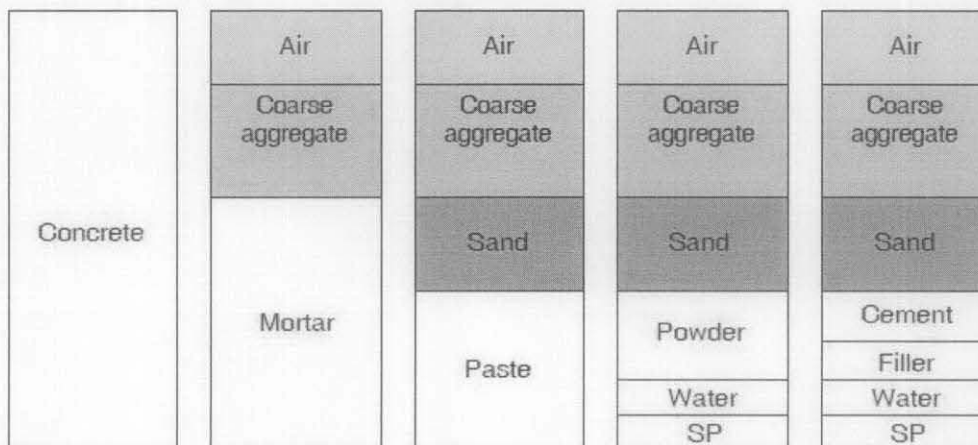


Figure 2. 2. Schematic composition of SCC

Source: Dinakar, et al. [22]

The amount of water in concrete mixes is usually represented by water-cement ratio (w/c), which is ratio of water over cement in weight, while for the mixes that use the filler material such as fly ash or MIRHA this ratio includes filler material known as binder. So ratio of cement together with filler is represented by water-binder ratio (w/b).

Ozkul and Dogan [45] stated that self compacting concrete provides high flowability. It should also have ability to high segregation resistance, which can be obtained by using high amount of fine material or by adding a viscosity modifying admixture, or both. Klaus and Klug [46] described a comparison of a typical mix design of SCC and conventional concrete as shown in Figure 2. 3.

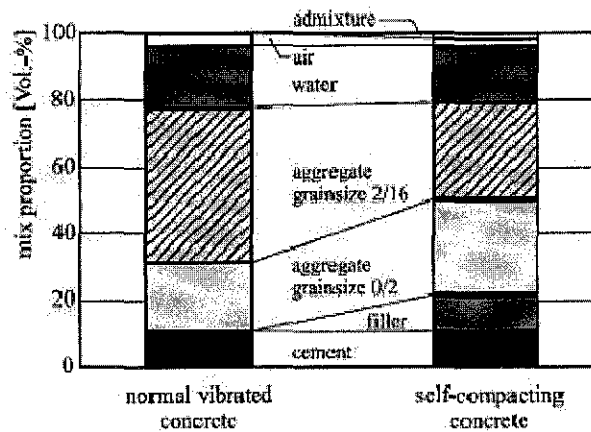


Figure 2. 3. Comparison of a typical mix design of SCC and conventional concrete

Source Klaus and Klug [46]

Sukumar, et al. [23] stated that SCC consists of five constituent materials that are cement, mineral admixture, coarse aggregate, fine aggregate and chemical admixture. The filler material such as fly ash facilitates better flow characteristics of SCC in the fresh state. The mix design procedure should follow these aspects:

1. For consistent with good flow ability and better segregation resistance, the powder content should be fixed at an optimum range between 400 and 600 kg/m³ of concrete as per the specifications for SCC.

2. Based on particle packing theory, the amount of each of these aggregates can be calculated for a given packing factor as determined experimentally.
3. The next important controlling factor is the w/b. Several trials should be conducted to determine the best w/b ratio for the given targeted design strength.

Brouwers and Radix [47] suggested that the gravel content in the concrete mix corresponds to 50% of its packed density, and sand content in the mortar corresponds to about 50% of its packed density, while Ozbay, et al. [48] proposed the mix design with Taguchi's method.

Nan, et al. [49] proposed a mix design for SCC that included fly ash and GGBS as pozzolan which were proven to increase durability characteristics, such as fluid permeability, ionic diffusion and corrosion resistance of self compacting concrete. Most of the SCC mixes as discussed in a number of research papers were mainly based on trial and error and the results show that the proposed method can produce high-quality SCC. Compared to the methods developed by Japanese Ready-Mixed Concrete Association (JRMCA), this method is simpler, easier to implement and less time consuming and requires a smaller number of trial mixes.

Grace and CoConn [50] stated that water-to-powder ratio and admixtures control the fluidity of the paste phase. If the aggregate particles have too much friction due to poor grading or shape, the paste will have to be very fluid to compensate and achieve the desired concrete flowability. The use of high paste fraction (high volume of cementitious material) increases space between the aggregate particles. The rheology is controlled by adjusting the water-to-powder ratio and using appropriate admixtures specifically designed for SCC production. Jianxin and Jörg [51] noted that properties of concrete are affected by cementitious matrix, aggregate, and the addition of pozzolanic admixtures. These materials are often to be used to modify the microstructure of the matrix and to optimize the transition zone. The reduction of the water-cement ratio will decrease the porosity and refine the capillary pores in matrix. High performance concrete uses w/c ranges which is usually between 0.28 and 0.38 and in ultra-high performance concrete the water to cement ratio is even lower than 0.2 Dhir, et al. [52] proposed a relationship between the amount of fine aggregates and coarse aggregate for the different cement contents as shown in Figure 2. 4.

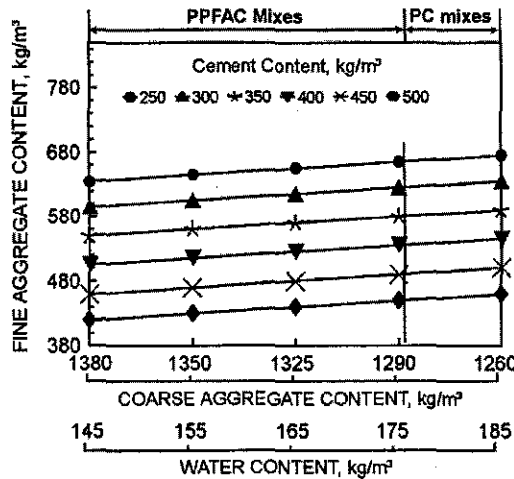


Figure 2. 4. Aggregate proportion in concrete

Source: Dhir, et al. [52]

Grace and CoConn [50] recommended that a nominal maximum size of the coarse aggregate must be chosen with respect to obtaining the desired passing ability and stability of the plastic concrete. When the use of a coarse aggregate larger than 12.5 mm ($\frac{1}{2}$ in.) is required, it will generally be beneficial to blend two or more different aggregate sizes to obtain an optimum gradation. Typical nominal maximum size of aggregate used in SCC is 19 mm ($\frac{3}{4}$ in.), although aggregates as large as 25 mm have been used. Aggregates with a nominal maximum size larger than 25 mm are not recommended for use in SCC.

Bilal [53] proposed some recommendation of producing SCC. Fine aggregates shall compose more than 55% of the total aggregate used. Powder content may be considered as part of sand. The maximum size of coarse aggregates of SCC mix is 20 mm. Bilal [53] also proposed proportion of materials used in SCC. The following proportion shall be used: Coarse Aggregate (>5 mm) $< 45\%$ by weight of total aggregate. Fine aggregate (< 4 mm) $> 55\%$ by weight of total aggregate. Paste $> 35\%$ of the mix volume.

Ping-Kun [54] stated that concrete without good workability is not High Performance Concrete (HPC). To achieve high strength and high performance in rheology and also reducing creep, shrinkage and low durability, Chang, et al. [55]

suggested the use of water-reducing agent, superplasticizers and pozzolanic materials in the mix designs.

Muhammad, et al. [56] with his experience stated that concrete mix design involves complicated issues, and the correct ways to perform this can be achieved with experts' advice and experience. Mix design of High Performance Concrete is complicated because this concrete includes more materials, like superplasticizers and pozzolan such as silica fume, fly ash, MIRHA, etc. Furthermore, keeping a low w/b with sufficient workability makes the design process more complicated. Ricardo and Marta [57] also stated that the increasing use of high-performance concrete in conventional structures has attracted more attention from researchers and engineers in order to establish the correct application of this material in structural construction. Using high-performance concrete in terms of increasing strength and stiffness will decrease significantly the dimension of the structure, in other words the cost of the building will be less than normal concrete building. Taylor, et al. [58] added that the use of HSC can provide clear economic advantages in reducing construction costs.

Mullick [59] mentioned that many attempts have been made to define high performance concrete. A quantitative definition is that it should have a maximum water-cement ratio of 0.35, a minimum durability factor of 80 percent in freeze-thaw resistance test as per ASTM C666, a minimum compressive strength of 21 MPa at 4 hours, 34 MPa at 1 day or 69 MPa at 28 days. However, such quantitative definitions may not be satisfactory in all situations. Generally, qualitative definitions are concrete which meets special performance requirements that cannot be always achieved routinely by using only conventional materials and normal mixing, placing and curing practices. The requirements may involve enhancement of characteristics such as strength, toughness, volume stability or service life in severe environments or the essential feature of this concrete is that its ingredients and proportions are specifically chosen to have particularly appropriate properties for the expected use of the structures. These properties are usually high strength or low permeability as stated by Neville [60].

The moisture problem in building structure is usually mitigated using high-performance concrete with water binder ratio less than 0.38. Like normal concrete

compaction, the SCC contains a small amount of superplasticizers. Furthermore, in order to avoid the separation of large particles in the SCC, additives that enhance viscosity or filler are used. Additives to improve viscosity are often used when concrete is cast under water and for tunnel lining. As the use of self compacting concrete is becoming common, the risk of exposing it to fire increases. It was found that SCC has the ability to decrease the risk of fire as investigated by Noumowé, et al. [61].

Poon and Ho [2] stated that segregation in flowing concrete is an important issue to be understood in SCC productions. To avoid this phenomenon, high powder content in the range of 500-600 kg/m³ concrete is needed. The replacement of cement and also cement itself should have the size less than 120 µm. The production of concrete generally has cementitious material of 350 to 450 kg/m³ so filler or replacement of 100 to 200 kg/m³ is needed to satisfy the powder requirement.

2.4.2. Rheological Properties of SCC

2.4.2.1. Description of Rheological Properties

Schwartzentruber, et al. [62] stated that rheological properties, which included viscosity and shear yield stress, are well correlated with empirical test results in the range of flowable mixes. Fresh SCC must be stable to ensure the homogeneity; however, several problems like bleeding, settlement or segregation can occur, sometimes simultaneously on construction sites. Segregation can appear during placing or afterwards due to sedimentation of the coarsest aggregates of the suspension under gravity forces.

Gene [63] mentioned some factors that affect the workability which are: quantity of cementitious materials, characteristics of materials, consistency, grading of fine aggregate, shape of sand grains, grading and shape of coarse aggregate, proportion of fine to coarse aggregate, percentage of air entrained, type and quantity of pozzolan or other supplementary cementitious material, quantity of water, mixture and ambient temperatures, amount and characteristic of admixtures used and time in transit.

SCC must have the ability to flow through narrow openings without hindrance. Furthermore, the blocking of coarse aggregates through bridging has to be avoided. Figure 2. 5 shows the mechanism of blocking of coarse aggregate by a two-dimensional illustrative model as described by Wüstholz [64].

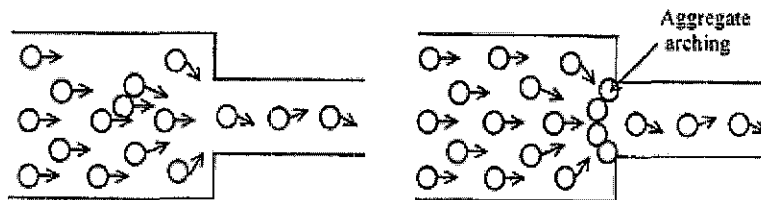


Figure 2. 5. Mechanism of blocking

Source: Wüstholz [64]

François and Sedran [65] stated that packing density of a concrete mix is from the knowledge of three types of parameters: packing density of monosize classes, size distribution of the mix and compaction energy.

The rheological properties of the powder suspension, consisting of cement, concrete additions, mixing water and plasticizer were investigated by Stefan and Horst [66], are determined by the water/solids ratio and the plasticizer content. The planned quantity of mixing water should be at least as high as the saturation water content. This is the water content that is necessary to wet the surfaces of the solid particles and to fill the voids in the particulate mass of powder. It characterizes the transition between a particulate mass and a suspension at which the apparent cohesion is lost and the particle mix begins to flow on application of energy. To do so the properties of the suspension can be controlled by water and plasticizer.

Zhuguo, et al. [67] stated that fresh concrete, which is often thought to have a viscoplastic effect is actually a type of particle assembly which contains water, cement grains, and aggregates grains. Almost all particles in the fresh concrete tend to make contact with their adjacent particles. The particles that are completely separated in the initial state push aside the surrounding water, and also come in contact with others when they move.

The slant contact of particles is not generally parallel to the plane of maximum shear stress. This is clearly illustrated in Figure 2. 6.

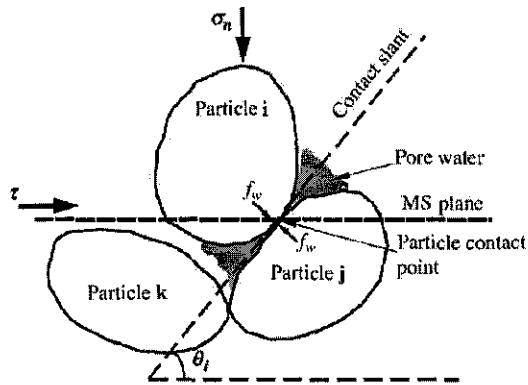


Figure 2. 6. Particle contact slant and particle contact angle

Source: Zhuguo, et al. [67]

2.4.2.2. Acceptable Range of Rheological Properties

Comprehensive guideline for measurement of rheological properties are discussed and presented by Schutter [68]. Workability in SCC or rheology in special term used in SCC is a crucial factor that affects the application and properties of SCC. It was found that many guidance and code give different acceptable range of self compactibility. This section describes several acceptable ranges in various papers and code. However, the British code (the code which is adopted in Malaysia) does not give any recommendation of producing SCC and all the assessment parameter.

Dinakar, et al. [22] stated that in recent practice, there are no universally accepted standards for testing SCC. Yet, several researchers have developed procedures for evaluating rheological properties and produced various range of acceptance. Yun, et al. [69] categorized the type of SCC based on rheological properties which were proposed by JSCE (Japan Society of Civil Engineers) as presented in Table 2. 4.

Table 2. 4. Specification of SCC proposed by JCSE

Rank	1	2	3
Construction condition			
Minimum gap between reinforcement (mm)	30-60	60-200	≥200
Amount of reinforcement (kg/m ³)	≥350	100-350	≤100
Filling height of U-box test (mm)	≥300	≥300	≥300
Absolute volume of coarse aggregates per unit volume of SCC (m ³ /m ³)	0.28-0.30	0.30-0.33	0.30-0.36
Flowability slump flow (mm)	650-750	600-700	500-650
Segregation resistance ability			
Time required to flow through V-funnel (s)	10-20	7-20	7-20
Time required to reach 500 mm of slump flow (s)	5-25	3-15	3-15

Source: Yun, et al. [69]

Masahiro, et al. [70] also give recommendation for requirement of high strength self compacting concrete as presented in Table 2. 5.

Table 2. 5. Rheology requirement of high-strength SCC

Testing Items	Unit	Spec.
Fresh concrete		
Slump Flow	(mm)	600 or 650
Flow time until 500mm	(sec.)	3 to 15
U type filling capacity	(mm)	min.300
V type Funnel flow time	(sec.)	8 to 15
Air content	(%)	4.5
Chloride ion content	(kg/m ³)	max.0.3
Hardened concrete		
Compressive strength	MPa	50

Source: Masahiro, et al. [70]

While Domone [71] stated that nearly 50% of the applications used values in the range of 650 to 700 mm, with nearly 90% in the range of 600 to 750 mm and recommended T_{500} times ranged from 1.8 to more than 12 s and V-funnel times from 3 to 15 s.

Ozbay, et al. [48] and Lachemi, et al. [72] recommended that slump flow range must be 500 to 700 mm for SCC and a funnel test flow time less than 6 seconds is recommended for a concrete to qualify for self compacting. While Bapat, et al. [73] recommended the acceptable range of self compactability as shown in Table 2. 6.

Table 2. 6. Rheological acceptance

No.	Test Methods	Unit	Minimum	Maximum
01	Slump flow	Mm	650	800
02	T ₅₀ cm slump flow	Sec	2	5
03	V- funnel	Sec	6	12
04	Time increase V- funnel T ₂ minute	Sec	0	+3
05	L- box	h ₂ /h ₁	0.8	1.0

Source: Bapat, et al. [73]

The other researcher Ravikumar, et al. [74] proposed the other acceptable range as shown in Table 2. 7.

Table 2. 7. Acceptance criteria for SCC

S. No.	Method	Unit	Typical range of values	
			Minimum	Maximum
1	Slump-flow	mm	650	800
2	T50 slump flow	Sec	2	5
3	V-funnel	Sec	6	12
4	L-Box	(h ₂ /h ₁)	0.8	1.0

Source: Ravikumar, et al. [74]

Mohammad, et al. [75] classified three classes of rheological properties:

1. Low flow ability, less than 500 mm, having a high V-time above 12 s.
2. Moderate slump flow lay between 500 and 600 mm, having V-time between 8 and 13 s. The mix achieved SCC V-time target but insufficient flow ability.
3. High slump flow should be above 600 mm, having V-time less than 8 s. The mixes have sufficient slump flow but very low V-time.

While Abhishek, et al. [34] based on their studies recommended that for a good SCC the slump flow should be in the range of 600 to 750 mm, V-funnel time with range of 3 to 8 seconds and J-ring value should be 10 to 15 mm.

EFNARC [76] the “European Federation of Producers and Contractors of Specialist Products for Structures” classified the self compactibility in several classes which are characterized as:

1. Flowability Slump-flow SF 3 classes:

Table 2. 8. Slump Flow classes

Class	Slump-flow in mm
SF1	550 to 650
SF2	660 to 750
SF3	760 to 850

Source: EFNARC [76]

a. SF1 (550 - 650 mm) is appropriate for:

- unreinforced or slightly reinforced concrete structures that are cast from the top with free displacement from the delivery point such as housing slabs
- casting by a pump injection system such as tunnel linings
- sections that are small enough to prevent long horizontal flow such as piles and some deep foundations).

b. SF2 (660 - 750 mm) is suitable for many normal applications such as walls, columns)

c. SF3 (760 – 850 mm) is typically produced with a small maximum size of aggregates (less than 16 mm) and is used for vertical applications in very congested structures, structures with complex shapes, or for filling under formwork. SF3 will often give better surface finish than SF 2 for normal vertical applications but segregation resistance is more difficult to control.

2. Viscosity, (measure of the speed of flow) Viscosity VS or VF 2 classes

Table 2. 9. Viscosity classes

Class	T ₅₀₀ , s	V-funnel time in s
VS1/ VF1	≤ 2	≤ 8
VS2/ VF2	> 2	9 to 25

Source: EFNARC [76]

- a. VS1/VF1 has good filling ability even with congested reinforcement. It is capable of self compacting concrete and generally has the best surface finish. However, it is more likely to suffer from bleeding and segregation.
 - b. VS2/VF2 has no upper class limit but with increasing flow time it is more likely to exhibit thixotropic effects, which may be helpful in limiting the formwork pressure or improving segregation resistance. Negative effects may be experienced regarding surface finish such as blow holes and sensitivity to stoppages or delays between successive lifts.
3. Passing ability that flow without any blocking, passing ability PA divided into 2 classes

Table 2. 10. Passing ability classes (L-box)

Class	Passing ability
PA1	≥ 0,80 with 2 rebars
PA2	≥ 0,80 with 3 rebars

Source: EFNARC [76]

Examples of passing ability specifications are given below:

- a. PA 1 structures with a gap of 80 mm to 100 mm, such as housing or vertical structures
- b. PA 2 structures with a gap of 60 mm to 80 mm, such as civil engineering structures

Daczko and Constantiner [77] proposed the guidance (which is adopted by “Precast/Prestressed Concrete Institute Interim SCC Guidelines FAST Team” as guideline to produce and asses SCC in United States) to identify the controlling parameters associated with the element specific ratings made for each of the seven elements characteristics as shown in Table 2. 11.

Table 2. 11. Rheological properties parameter determination

		Slump flow			T 50 time			L-Box			V-Funnel		
		<22"	22-26"	>26"	<3 sec	3-5 sec	>5 sec	<75	75-90	>90	<6 sec	6-10	>10
Member Characteristics	Reinforcement Level	Low											
		Medium											
		High											
	Element Shape Intricacy	Low											
		Medium											
		High											
	Element Depth	Low											
		Medium											
		High											
	Surface Finish Importance	Low											
		Medium											
		High											
	Element Length	Low											
		Medium											
		High											
Wall Thickness	Low												
	Medium												
	High												
Coarse Aggregate Content	Low												
	Medium												
	High												
Placement Energy	Low												
	Medium												
	High												

Note: Dark blocks represent potential problem areas.

Source: Daczko and Constantiner [77]

Table 2. 11 presents the slump flow, T-50, L-Box and V-funnel tests to assist in establishing the initial performance targets and measurement techniques and they are very useful to the practitioner to decide directly which rheological properties target will be chosen. The use of the parameter selection tables is one way of linking test methods to performance characteristics. However, it can be noticed that the use of all of these tables may not be appropriate for some SCC applications. In slump flow test,

the lowest slump flow will be the value applicable to the ranked member characteristics. This will reduce the potential for instability, as well as optimize the performance/cost relationship. The dark blocks indicate potential problem areas. For example, if the application has a high level of reinforcement, a slump flow of less than 22 inches (559 mm) is not recommended. In column of T-50, the lowest T-50 time will be applicable to the ranked member characteristics. The T-50 time will be affected by both the final fluidity level, as well as the plastic viscosity. For a given slump flow range, this test is a good measure of a mixtures plastic viscosity. The same way can be applicable to other columns.

2.4.3. Pozzolan

Akers [78] stated that all fly ashes have pozzolanic properties, which has the ability to react with calcium hydroxide to form compounds with cementitious properties. The product of hydration reaction is calcium silicate hydrate (CSH) and calcium hydroxide $[\text{Ca}(\text{OH})_2]$. Fly ashes have high percentages of silicon dioxide (SiO_2). The $\text{Ca}(\text{OH})_2$ will react with the SiO_2 to form another CSH.

Goni, et al. [79] studied the effect of hydrothermal treatment on the pozzolanic reaction of fly ashes from coal combustion (ASTM class F). C_2SH , and CSH gel, different solid solutions of katoites which are the cubic crystallographic variety of hydrogarnets series (C_3ASH_4) and a mixed oxide (CaFe_2O_4) are formed from the effect of fly ash. The hydrated compounds are originator of a new kind of low-energy cement called Fly Ash Belite Cement (FABC); besides, they have potential properties to intercalate toxic ions. Therefore, they can be used as immobilization systems of these ions.

Anne-Mieke and Geert [80] found that to achieve compactibility of concrete, high filler contents are often used, and in order to avoid problems with excessive heat development during hardening, inert filler materials can be used. Singh, et al. [81] also stated that the using of a variety of waste materials as supplementary cementing materials is rapidly growing. Blast furnace slag, fly ash, silica fume and rice husk ash, have already been recognized as mineral admixtures for blended cement production.

Shafiq, et al. [82] stated that the pozzolanic activity of fly ash is very useful for producing high performance concrete. Its major constituents of fly ash as pozzolan are SiO_2 , Al_2O_3 , Fe_2O_3 and CaO , where their percentage depends on the type of coal burned at the power plant. Fly ash comes from burning of bituminous coals like anthracite that contains low amounts of calcium oxide (CaO), therefore known as low calcium fly ash and be classified as class-F by ASTM. Fly ash is the by-product of coal-fired electric power station which lowers heat of hydration and improves the durability and also contributes to concrete strength by pozzolanic and filler effects as statement by Poon, et al. [83]

Ahmaruzzaman [4] stated fly ash and Microwave Incinerated Rice Husk Ash (MIRHA) have similar specification for calcium content, which is low in calcium, while high calcium content is not recommended since it can obstruct the polymerization process.

Muhammad and Waliuddin [19] investigated the role of RHA in concrete, indicated that the silica of soil migrates into the plant in the shape of monosilicic acid which concentrates the silica by evaporation. Electron microscope studies have shown dispersion of silica throughout the cellular structure of the husk. Jatuphon, et al. [84] stated that the water-binder ratio of mortar affects the pozzolanic reaction of rice husk ash. When the use of rice husk ash is increased, the compressive strength due to pozzolanic reaction is also increased.

An investigation of pozzolan is an activity in microstructure fraction that was done by Fernández-Jiménez and Palomo [85]. They presented the work in the relationship between the mineralogical and microstructural characteristics of alkaline activated fly ash mortars, which was activated with NaOH , Na_2CO_3 , and waterglass solutions and established their mechanical properties. The results showed that in all cases the main reaction product formed is an alkaline aluminosilicate gel, with low-ordered crystalline structure. This material has resulted in the excellent mechanical-cementitious properties of the activated fly ash. Microstructure of Si/Al and Na/Al ratios of the aluminosilicate gel changes as a function of the activator type used in the system. As a result of the secondary reaction, zeolites are formed.

Vagelis [86] mentioned that fly ash is the combustion residue (coal mineral impurities) in coal-fired electric power plants, which flies out with the flue gas stream and is removed by mechanical separators, electrostatic precipitators, or bag filters. Two general classes of fly ash can be defined: low-calcium fly ash (class-F) produced by burning anthracite or bituminous coal, and high-calcium fly ash (class-C) produced by burning lignite or sub-bituminous coal. Class-F is categorized as a normal pozzolan, a material consisting of silicate glass, modified with aluminum and iron and the CaO content is less than 10%. Class-F requires Ca(OH)_2 to form strength-developing products (pozzolanic activity), and therefore is used in combination with Portland cement, which produces Ca(OH)_2 during its hydration.

Papadakis, et al. [87] were the first to propose a general simplified scheme describing the pozzolanic activity in terms of chemical reactions, but without an extended experimental verification. Bertil [88] proposed to increase the viscosity in SCC by using the following fillers: fly ash, glass filler, limestone powder and silica fume (or silica fume slurry). The other researcher, Sari, et al. [89] used quartzite filler (fine sand) in high strength concrete.

Rice husk ash is a good pozzolan which can be used to create a special concrete mixture. The use of rice husk ash to replace cement becomes popular because of its high reactivity in the mix. According to Rodrigues de Sensale [90], at later ages more than 90 days, rice husk ash concrete has a strength higher than concrete without rice husk ash, and the highest values of strength were achieved in a concrete with 20% rice husk ash.

Rodrigues de Sensale [90] concluded that residual MIRHA provides a positive effect on the compressive strength at early ages, but the long term behavior of the concretes with MIRHA produced by controlled incineration was more significant. The rising in compressive strength of concretes with MIRHA formed by controlled incineration is primarily due to the pozzolanic effect.

Pipat [91] stated that for the mix containing fly ash, at the same dosage of polycarboxylate-based superplasticizers, the amount of absorption of water increased as the replacement percentage of fly ash is increased. So the repulsion between

particles increased with an increase in replacement ratio and then better fluidity of paste can be achieved.

2.4.4. Effect of Superplasticizer

Mohammad, et al. [75] stated that superplasticizers in concrete production affect highly flowable mixtures with enhanced viscosity. Bharatkumar, et al. [92] investigated the effect of superplasticizers on mix proportion. As a result of using superplasticizers, the water content in a mix can be reduced. While Leemann and Winnefeld [93] investigated the influence of different viscosity modifying agents (VMA) on the flow properties and the rheology of self compacting mortars. They used the inorganic VMA microsilica (MS), nanosilica slurry (NS) and organic VMA based on high molecular ethylenoxide derivate (EO), natural polysaccharide (PS) and starch derivate (ST). In addition, different VMA are combined with superplasticizers (SP). At constant w/b the addition of VMA causes a decrease of mortar flow and increase flow time (V-funnel test), yield stress and plastic viscosity. In constant dosage of superplasticizers (SP) mixtures with VMA require a higher w/b to keep the same rheology properties as the reference mixtures without VMA. Despite the higher w/b, flow time and plastic viscosity respectively are only slightly reduced.

Mullick [59] stated that the role of superplasticizers, long chain molecule organic compounds, is to get adsorbed into cement grains, impart a negative charge to them, which repel each other and get deflocculated and dispersed. The improvement in workability of concrete could be either to produce flowing concrete for the same cement and water contents as in the control mix. Alternately, it enables water content to be reduced by about 20 percent or more and results in high strength, because of low water-cement ratio.

Bjömström and Chandra [94] investigated the rheological properties of cement pastes made with different types of cement and superplasticizers. Experiments involved cement particles dispersion, fluidity, viscosity, yield stress and zeta potential. Obtained results showed that the chemical compositions of the cements such as C₃A and sulfate content, alkali and ground lime content are important features controlling the rheology of cement pastes. The results also revealed that the

mechanism by which these polymers disperse cement particles differs fundamentally. Sulfonated superplasticizers induced a negative charge on cement particles dispersing by electrostatic repulsion, whereas with the polycarboxylate-based polymer the dispersion mechanism is mainly controlled by steric hindrance.

Ravindrarajah, et al. [95] stated that SCC is currently produced with sufficient amount of superplasticizers. Drying shrinkage was influenced by the mix compositions and superplasticizers dosage. Pierre, et al. [96] stated that the use of superplasticizers in concrete making has extended in variety of applications. They are now included in all the essential high-performance concrete such as SCC, casting concrete under water, fiber reinforced concrete, fly ash concrete, reactive powder concrete, etc. With the use of superplasticizer, water is no longer the sole ingredient in concrete that control rheological properties; the gap between cement grains may be close to a considerable extent during mixing of the hydrated cement paste. By moving the cement grains closer to one another, it then becomes possible to produce concretes in which a highly dense and relatively non-porous cementitious matrix is generated that exhibit a far superior resistance to aggressive agent penetration than that of normal concretes.

Borsoi, et al. [97] stated that Viscosity Modifying Admixtures (VMA) can be advantageously used to the amount of water demand or to counteract the segregation effect caused by slight increase of superplasticizer. A combination of cementitious admixtures and superplasticizers also serves to incite more efficient and substantial use of hydraulic or mineral additives pozzolanic by reducing the amount required in developing the initial CSH deliver bond strength at the beginning of the formation of concrete. To some extent, it improves the performance of superplasticizers in ecological performance of Portland cement, hydraulic binders and concrete.

Pierre, et al. [96] and Jean, et al. [98] stated that majority of current superplasticizers used in concrete industry are polynaphthalene sulfonates (PNS) or polymelamine sulfonates (STDs), especially those acting in a way the electrostatic repulsion. The use of polycarboxylates, reverse acting by steric repulsion, also became more common. The necessary characteristics of polymer-based superplasticizers is now well known such as in the case polynaphthalene sulfonates.

Sulfonate groups should be in position β on benzene ring and not in a position of α as shown in Figure 2. 7. It has also been determined that the highest level is better sulfonation and that the average optimal rate of polymerization is between 9 and 10. In this case, the polymer chain does not show excessive cross linking. At this moment, the PNS and PMS polymerization process are identified and properly controlled, to the point where it can be stated that the basic molecule used to produce commercial superplasticizers is generally of high quality. In an effective PNS for example, sulfonation level is on the order of 90% and more than 85% sulfonate groups are found in the β position; still further, the percentage of monomers, dimers and trimers reached only 30% of the total mass. The control over the level of cross linking can also be provided in order to preserve maximum flexibility and power for the polymer cover. The general rule is unfortunately still raises a few exceptions.

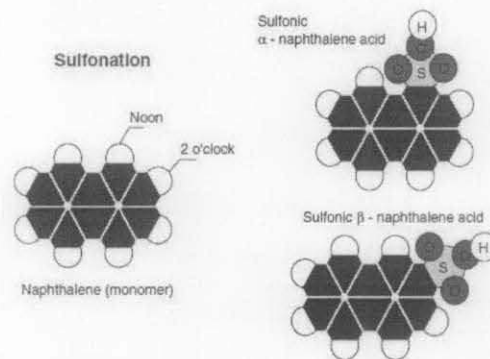


Figure 2. 7. Positions α and β of the sulfonic group

Source: Pierre, et al. [96]

Pierre, et al. [96] found that the range of superplasticizers dosage relatively has little influence to initial slump. But it can be noted that dosages of 1.1% and 1.2% made the concrete bleed slightly, while Rixom and Mailvaganam [99] found that at 4% SP the concrete still perform well without bleeding due to the using of lower w/b . At 60 minutes, the concrete with 1.0% superplasticizers had lost its slump, while at 90 minutes, concrete with 1.1% still had slump of 140 mm and 1.2% still had 230 mm as illustrated in Figure 2. 8.

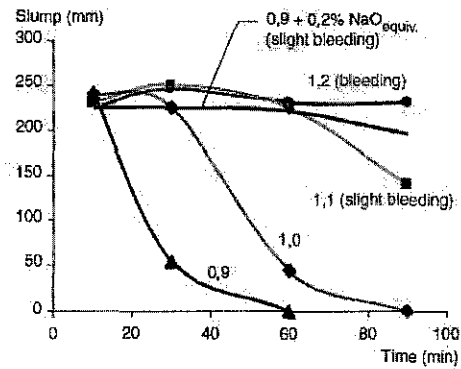


Figure 2. 8. Slump loss vs. time

Source: Pierre, et al. [96]

2. 5. Mechanical Properties of SCC

Mechanical properties are used to define the strength characteristic which is usually determined by the amount of stress or force which is needed to break the material. There are various types of stress and force in the concrete. Compression is a force in certain amount to crush concrete and this may be used to determine a concrete compressive strength. While tensile strength refers to concrete ability to withstand a tension force. And flexural strength refers to a concrete ability to remain intact when it is bent. Mechanical properties are measured with machines and devices which help to ensure accurate measurements to the slightest degree.

2.5.1. Compressive Strength of SCC

All investigation that involved SCC was always checking of its compressive strength as the major properties of almost all types of concrete. The following are some of the references which describe several factor that influence the compressive strength. Reinhardt and Stegmaier [100] investigated the mechanical properties of self compacting concrete and influence of a heat treatment on the SCC properties. To evaluate the influence on the compressive strength, different powder and viscosity-agent type were used and exposed to heat treatment with different maximum temperatures. It has been found that there is an influence of the composition of the concrete and the effect of w/c on the compressive strength after heat treatment. The

reason for the substantial loss of strength in concrete is a change of the pore size distribution due to heat treatment.

Corinaldesi and Moriconi [101] investigated the mechanical properties of self compacting concrete in thin precast elements containing homogeneously dispersed steel fibers at a dosage of 10% by mass of cement without using ordinary steel-reinforcing mesh with water to cement ratio of 0.40. Compression and flexure tests were carried out to investigate the mechanical performance.

Based on experiments done by Bertil [88] a correlation between strength of sealed SCC, f_{CB} and water-binder ratio (w/b) at different ages is given by this equation:

$$f_{CB} = 2.07[\ln(t) + 11.7] \times (w/b)^{-0.042[\ln(t)+29]} \quad (2.1)$$

The equation is based on the reported results shown in Figure 2. 9.

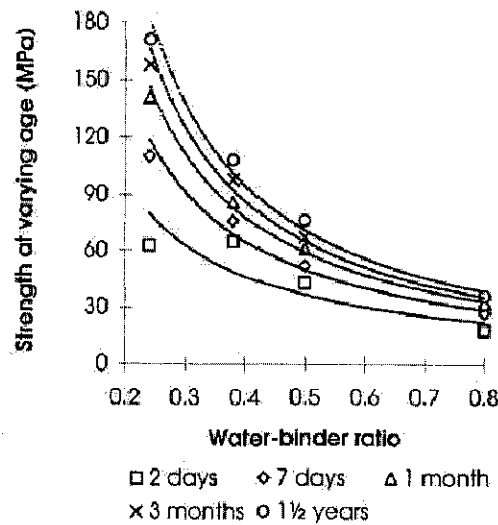


Figure 2. 9. Strength of SCC versus w/b at different ages

Source: Bertil [88]

Chidiac, et al. [41] investigated comparative evaluation between rheological of fresh concrete and properties of hardened self compacting concrete and also its correlation to the durability. Other researchers, McCarthy, et al. [102] developed relationships between required water cement ratio and PFA concrete compressive strength characteristics. This is shown in Figure 2. 10.

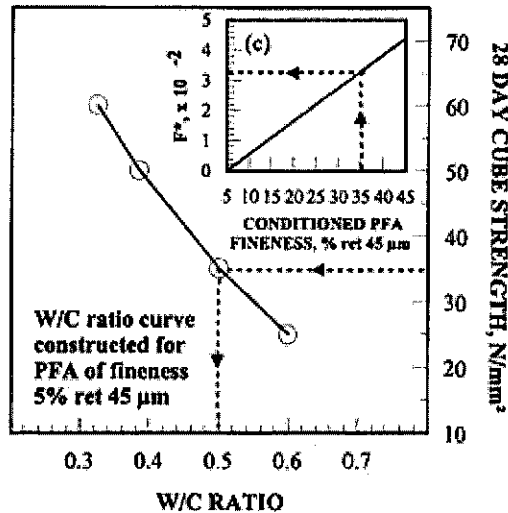


Figure 2. 10. Correlation of w/c ratio and cube strength

Source: McCarthy, et al. [102]

Celik and Carino [103] stated that the strength of the concrete will give a direct indication of its capacity to resist load. To test this capacity the test may include: strength compressive strength, tensile, shear and combination of these. Correlations can be developed which are related to concrete strength properties to certain other concrete properties that involve much more complicated tests, such as when durability aspects are concerned of the research.

2.5.2. Tensile Strength of SCC

Tensile strength of concrete is measured by applying a force that separates the sample by certain load at the point where it breaks. BS 1881: Part 117: 1983 suggested the split cylinder test for measuring the tensile strength of concrete. Castel, et al. [104] investigated the tensile properties of SCC with the result that there was no significant difference between SCC and normal concrete tensile strength which was observed by using the splitting test, the direct axial tension test and the beam test.

Druta [105] compared the splitting tensile strength and compressive strength values of self compacting and normal concrete specimens and to examine the bonding between the coarse aggregate and the cement paste using the Scanning Electron

Microscope. The result indicated an increasing strength and a better bonding between aggregate and cement paste in SCC compared to normal concrete.

Balendran, et al. [106] found that with lower water-binder ratio, it increases the split cylinder strength. Shannag [107] investigated the effect of pozzolan, the result indicated that the natural pozzolan-silica fume combinations can improve the compressive and splitting tensile strengths, workability, and elastic modulus of concretes, more than natural pozzolan and silica fume alone. Bhanjaa and Sengupta [108] investigated the influence of silica fume as pozzolan on tensile strength in concrete of high-performance concrete (HPC) from mix proportion with water-binder ratios ranging from 0.26 to 0.42 and silica fume-binder ratios from 0% to 30%.


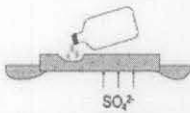
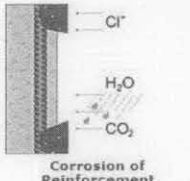
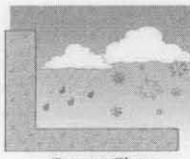

2. 6. Durability Properties of SCC

Durability is defined as the capability of the concrete to maintain its performance and all aspects of strength during long period of time under all exposure condition. Durability of concrete depends on several factors which affects significantly to its performance throughout the service condition.

Assié, et al. [109] qualified the potential durability of self compacting concrete and compared the result with vibrated concrete with similar grade of compressive strength. Durability properties such as water porosity, chloride diffusion, oxygen permeability and additional properties need to be studied for a better understanding. Mercury porosity, water absorption by capillarity, carbonation and ammonium nitrate leaching were examined. The result indicated that the durability of both concretes could be regarded as equivalent with the same level of compressive strength and self compacting concrete can be considered to be as durable as vibrated concrete.

Detwiler and Taylor [110] mentioned the important exposure conditions and deterioration mechanisms in concrete structures. In practice, several of these deterioration mechanisms could act simultaneously with possible synergistic effects. Their classification is shown in Table 2. 12.

Table 2. 12. Exposure Conditions and Deterioration Mechanisms

Durability Aspect/Exposure	Mechanism
 <p>Alkali-Aggregate Reaction</p>	Alkali-Silica Reaction Alkali-Carbonate Reaction
 <p>SO₄²⁻ Chemical Resistance</p>	Sulfates Seawater Acids
 <p>Cl⁻ H₂O CO₂ Corrosion of Reinforcement</p>	Corrosion Corrosion Resistance Carbonation
 <p>Freeze-Thaw</p>	Freezing and Thawing Deicer Scaling D-Cracking
 <p>Miscellaneous</p>	Abrasion Erosion Fire Resistance Efflorescence

Source: Detwiler and Taylor [110]

Corinaldesi and Moriconi [101] investigated the durability behavior of self compacting concrete in thin precast elements containing homogeneously dispersed steel. Drying shrinkage tests were carried out in order to evaluate the contribution of steel fibers in counteracting the high concrete strains due to a low aggregate-cement ratio. Freezing and thawing resistance cycles were investigated on concrete specimens treated with a hydrophobic agent and also carbonation and chloride.

Dinakar, et al. [111] studied the durability properties of self compacting concretes with high volume replacements of fly ash. Eight fly ash self compacting concretes mixes of various strength grades were designed at desired fly ash percentages of 0, 10, 30, 50, 70 and 85, in comparison with five different mixtures of normal vibrated concretes at equivalent strength grades. Permeable voids, water absorption, acid attack and chloride permeation were measured to assess the durability properties. Results indicated that the SCC showed higher permeable voids and water absorption than the vibrated normal concretes of the same strength grades. And in acid attack and chloride diffusion studies the high volume fly ash SCC had significantly decreased its weight losses.

Chandra [112] stated that durability characteristics of concrete principally depend upon its microstructure of pores size distribution and their connectivity. The microstructure controls the moisture movement, which is one of the major causes of concrete deterioration. The presence of moisture in large size pores can initiate the same type of chemical activity within the microstructure that may cause to lose strength, embedded steel bars to corrode and concrete to lose mass. Chao-Lung and Meng-Feng [113] stated that in terms of the durability, the percentage content of cement paste is crucial to both volume stability and long-term performance of self compacting concrete.

2.6.1. Porosity of Concrete

Porosity of concrete is formed by an incomplete compaction of the mixture, i.e. entrapped air or by entrained air. The mechanism of transport of liquid and gas into the pores takes place in various forms such as: in pores with radius (r) less than 100 nm; molecular diffusion takes place; when r is 100 to 10000 nm a molecular flux is observed and if $r > 10000$ nm the viscous flux is experienced. Also Brown, et al. [114] mentioned that the structure of the porosity in concrete strongly influences its performance.

Reinhardt and Stegmaier [100] investigated the influence of heat treatment on the pore size distribution and the compressive strength of different SCC. The heat curing of the SCC leads to a change of the pore size distribution to coarser pores but not to

increase total pore volume of the concrete. The change of the pore size distribution is correlated to the w/b, increasing w/b influence on the pore radius in the concretes.

Chang, et al. [115] discussed the influence of environmental factors such as relative humidity and ambient temperature on the performance of concrete structures. It is known that the porosity of concrete controls the permeability, which allows water and gases to penetrate into the concrete. Chandra [112] noted that the influence of environmental factors as the behavior of concrete structure particularly in long term is derived from its porosity. Mass losses due to chemical attacked and other durability issues were investigated by Al-Tamimi and Sonebi [116].

Hearn, et al. [117] stated that, in general durability is defined as the ability of material to withstand the intended exposure conditions. Durability concepts encompass both porosity and permeability properties of concrete. Porosity of concrete is complex, as it is not a static system and can simultaneously undergo evolution during the hydration process and deterioration during exposure to the environment. Mass transport measurement through this continually changing pore structure becomes a function of testing parameters and the type of transport that is being tested. Almost all engineering properties, such as strength, durability, shrinkage, creep, permeability and ionic diffusion are directly influenced or controlled by the relative amounts of the different type and sizes of pores. The initial porosity of concrete is determined by the sum of the volume of mixing water, intentionally entrained air, and accidental voids due to incomplete compaction. As the cement reacts with water, the new solids in cement hydrates and partly occupies space in the original water-filled space between cement grains and around aggregates. The porosity of concrete can be classified as follow: porosity of the aggregates, water and air filled voids after consolidation and final set; and water and air filled voids after partial hydration of the cement.

2.6.2. Permeability of Concrete

Zhu and Bartos [118] investigated the permeation properties, including oxygen permeability, capillary water absorption and chloride diffusivity, of different SCC mixes. SCC mixes showed significantly lower values of coefficient of permeability

and water absorption compared to the vibrated concretes of the same strength grade. The chloride diffusivity was very much dependent on the type of cement replacement, the SCC and the reference mixes using PFA showed much lower values of chloride migration coefficient than the other mixes.

Nehdi, et al. [25] investigated the rapid chloride ion penetrability measured at 28 and 91 days of SCC mixtures, including the ASTM C1202 rapid chloride ion penetrability classification ranges. The OPC SCC mixture achieved rapid chloride ion penetrability in the high range at 28 days ($>4000\text{C}$). At 28 days, binary mixtures incorporating 50% class F fly ash decreased the rapid chloride penetrability from a high to a moderate range. The most efficient mixtures in decreasing the 28-day chloride ion penetrability were quaternary mixtures incorporating either 6% silica fume or 6% RHA. SCC with high-volume replacement cements gives excellent workability at a competitive cost.

Cabrera and Hasan [119] evaluated the performance durability of repaired material with included data on the performance related properties, a commercial pre-packed cementitious material, a commercial pre-packed cementitious material modified with polymer, a pozzolanic cement containing 70% ordinary Portland cement and 30% pulverised fuel ash, an ordinary Portland cement containing a commercial organic corrosion inhibitor. The tests were for evaluation of the repaired materials with the following properties: compressive strength, bond strength, porosity and permeability.

Shafiq and Cabrera [120] stated that the knowledge of concrete durability needs to be extended especially behavior of concrete resistance against the transport of aggressive element into the pores. These aggressive elements can be liquid or gaseous, which are transported into concrete via the pore network in the cement paste matrix or via micro-cracks. The permeability of the concrete is governed by some factors: the substance flowing and its local concentration, the environmental conditions, the pore structure of concrete, the pore radius, the degree of saturation of the pore system and the temperature. The transport of fluid into concrete is not due to one single mechanism, but by several mechanisms which act simultaneously. This transportation occurred due to the wide range of pore sizes and a varying moisture

concentration in the concrete as a function of the climatic exposure conditions. The pore network which gives the path to transporting liquid and also its development depends on the properties and composition of the concrete constituent material, the initial curing condition and its duration, the testing age and climatic exposure during drying and finally the condition of the concrete.

2.6.3. Corrosion Resistance Properties of SCC

Hassan, et al. [121] investigated the structural performance and cracking behavior of corroded reinforced concrete beams made with SCC with respect to corrosion level and compared to those of normal concrete beams. The beams were partially immersed in sodium chloride solution, and subjected to an impressed current until they reached three levels of corrosion with 0%, 10%, and 30% theoretical mass loss. The beams were then tested under mid-span concentrated load until failure with the results indicated that at severe corrosion level, the failure mode for the SCC beam had changed from shear failure to anchorage slipping failure.

Saraswathy, et al. [18] investigated the corrosion with various activation techniques, such as physical, thermal and chemical. With these methods of activation, hydration of fly ash blended cement was accelerated and thereby improved the corrosion-resistance and strength of concrete. Concrete specimens were prepared with 10%, 20%, 30% and 40% of activated fly ash replacement levels were evaluated for their compressive strength at 7, 14, 28 and 90 days and the results were compared with ordinary Portland cement concrete. Corrosion-resistance of fly ash cement concrete was measured by using anodic polarization technique and electrical resistivity and ultrasonic pulse velocity measurements. The investigation confirmed that up to a critical level of 20 to 30% replacement; activated fly ash cement improved both the corrosion-resistance and strength of concrete.

Batis and Routoulas [122] studied the corrosion in steel bar in high pH values (greater than or equal to 12.5) of the concrete pore solution causes passivation of embedded rebars, because the creation of Fe_3O_4 or Fe_2O_3 is closely attached to very thin film. Passivation can be vanished by the diffusion of aggressive species of corrosion environment to the area of reinforcement bar. Penetration of the porous

concrete matrix with chloride ions, water and oxygen causes corrosion of the steel and form corrosion products, commonly known as rust. After the volume is significantly greater than the original iron, corrosion products can develop tension in steel/concrete interphase. Reinforcement corrosion can cause delamination and spalling of concrete cover, which can cause more corrosion and eventually failure of the reinforced structures. Early detection and monitoring the condition of reinforcing bars by a non-destructive technique is very important. Laboratory techniques to examine the corrosion of steel reinforcement included electrochemical methods such as polarization curves.

Gürten, et al. [123] described the Linear Polarisation Resistance (LPR) method; this can be determined from the slope of applied potential against measured current. Steel used in experiment is polarized to single cycle for each measurement to ± 20 mV of the corrosion potential at a scan rate of 1 mV/s utilizing EG&G Model 360 potentiostat/ galvanostat.. Corrosion state of the steel bar that embedded in concrete is studied by using the three electrode techniques. A saturated calomel electrode (SCE), platinum foil was used as reference and auxiliary electrodes are used as shown in Figure 2. 11.

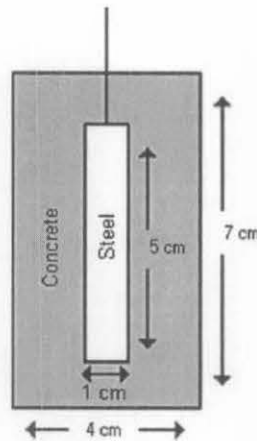


Figure 2. 11. Corrosion and working electrode

Source: Gürten, et al. [123]

Birbilis and Holloway [124] found that estimation of corrosion rate, i_{corr} , expressed as current density is determined by Stern–Geary equation:

$$i_{corr} = \frac{B}{R_p} \quad (2.2)$$

where B is a constant (26–52 mV) and R_p represents the (measured) polarization resistance per unit surface area of reinforcement with units of $\Omega \text{ cm}^2$. Measuring R_p per unit of surface area is difficult due to not roughness of the reinforced sections, and the use of a counter electrode that surface area is necessarily much smaller than that of the reinforced concrete structure to be tested

Chang, et al. [55] showed the relationships between w/c ratio and resistivity under any type of cement paste system. The lower w/c and also age will give higher electrical resistivity. This relationship is shown in Figure 2. 12.

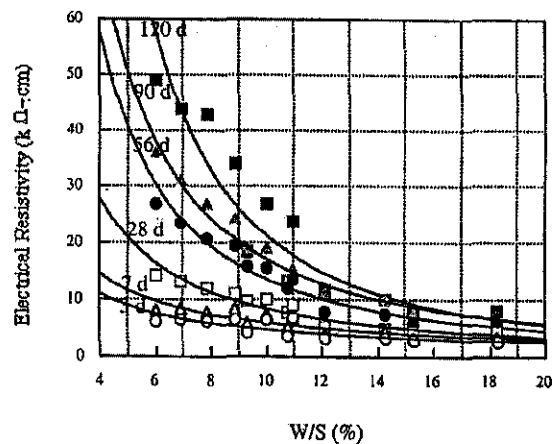


Figure 2. 12. Relationship between concrete age, electrical resistivity and w/c ratio

Source: Chang, et al. [55]

Miranda, et al. [125] investigated corrosion resistance of fly ash mortars. Corrosion potential (E_{corr}) and polarization resistance (R_p) values for steel electrodes embedded in Portland cement mortar and two fly ash mortars activated with NaOH and waterglass NaOH solutions. Chloride-free activated fly ash mortars were found to passivity steel reinforcement as speedily and effectively as Portland cement mortars, which gives protection for corrosion. The polarization curves and the response to short-term anodic current pulses (galvano static pulse technique) corroborate the full and stable passivation of the steel by the concrete manufactured with these binders.

Gürten, et al. [123] stated that embedded steel rebars in concrete are initially immune to corrosion because of the alkaline environment provided by concrete. Corrosion occurs by the loss of alkalinity due to carbonation and of the concrete and/or chlorides which prevent re-passivation reaction and that leads to pitting

corrosion. Prinya, et al. [126] mentioned that carbonation and chloride attacks are two main factors of corrosion of steel bar in concrete, so when carbon dioxide or chloride reaches the reinforced steel, the depassivation of the steel occurs and the steel reinforcement starts to corrode.

2. 7. Structural Characteristic of SCC

Boroni [127] stated that self compacting concrete has come out of the research laboratory and now becomes industrial product. Its application in variety of structures shows that it can be used as a reliable material with confidence. This material has good performance and now has become an extension to a standard solution for many structures, incorporating all the steps of the development process to achieve maximum results in performance and cost. Because of the application of SCC for structural purposes, bridges, etc, it is recommended that structural behavior with static and dynamic loading conditions must be fully understood.

2.7.1. Bond Characteristic of SCC Structure

SCC is recognized for its excellent deformability, high resistance to segregation, and use in congested reinforced concrete structures. The bond characteristics of such SCC are very important for their application in practical construction. While Hassan, et al. [128] with different investigation bond in SCC, found that bond stress has been described as the shear stress transferred from the concrete to the reinforcing bar. In the beginning bond stress is derived from the weak chemical bond between the steel and the hardened hydrated cement paste of concrete. When slip starts to occur, friction contributes to the bond and the bond resistance is derived principally from the bearing, or mechanical interlock of the ribs on the surface of the deformed bar with the concrete. Castel, et al. [104] investigated the possible differences between bond and cracking properties of self compacting concrete and vibrated concrete. Tension member tests did not show any significant difference between SCC and Vibrated Concrete (VC) in terms of transfer length irrespective of the compressive strength of the concrete. Bond properties of both types of concrete are similar.

Valcuende and Parra [129] investigated the bond characteristic of SCC. The result indicated that there is consolidation in the area of contact between the concrete and the ribs, giving a more effective support to the latter as shown in Figure 2. 13. Since the compression strength of the SCC is similar to that of the normal concrete, their respective bond behaviors come close. Tensile strength is mostly responsible for the ultimate bond strength and this value is slightly higher in normal concrete.

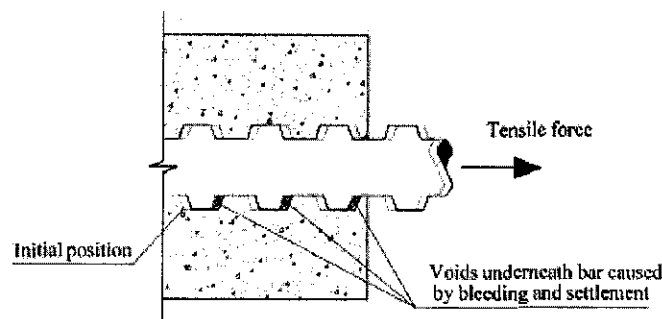


Figure 2. 13. Consolidation of voids under the reinforcement during pull-out test

Source: Valcuende and Parra [129]

Esfahani, et al. [130] investigated the local bond strength between self compacting concrete and steel reinforcing bars. Twelve concrete specimens grouped in two series made of normal concrete and SCC were tested. The result indicated that the local bond strength of top bars for SCC is about 20% less than that for NC. Similar investigation was done by Hassan, et al. [131] with the results indicated that the bond stress was slightly higher in the SCC pullout specimen compared to the NC, the difference was more pronounced in the top bars and at 28 days of testing.

2.7.2. Static Behavior of SCC Structure

Effendy [132] investigated the behavior of flexural self compacting concrete beams using palm oil fuel Ash (POFA) from Malaysia source, while Lambros [133] investigated the reinforced concrete beam to study the comparative shear resistance of SCC and NC which filled into steel columns with and without additional steel reinforcement. Han and Yao [134] attempted to study the possibility of using thin-walled HSS columns filled with SCC. Test data on 38 HSS columns were filled with SCC to investigate the influence of different concrete compaction methods on the

composite columns. Han and Yao [135] repeated their experiment with pre load column using hollow structural steel (HSS) columns filled with concrete. Peter, et al. [136] investigated the pilling of self compacting concrete. The experimental result clearly demonstrated that the SCC in situ piles had better control on geometry when cast against soil form work. Filho, et al. [137] analyzed the bond behavior of an innovative construction material, self compacting concrete , in comparison to vibrated concrete, using pull-out and beam tests.

Chabib, et al. [138] investigated SCC confined in FRP tubes. The experiment was laboratory investigation on the behavior of SCC confined in short GFRP tubes and subjected to axial and transverse load, including the effect of using expansive cement and shrinkage-reducing admixtures to enhance the GFRP tube-SCC interfacial contact. The result showed differences behavior between NC and SCC-filled GFRP specimens in the transition region of the response curves, in which the shift from a linear to a non-linear behavior in the load–deformation and stress–strain curves subsequent to the failure of the concrete core was more sudden for the tested SCC-filled GFRP specimens than NC.

Hassan, et al. [139] investigated the shear strength and cracking behavior of full scale beams made with self consolidating concrete as well as normal concrete. The ultimate shear strength of SCC beams was lower than that of NC.

Dehn, et al. [140] found that the load bearing capacity of a reinforced concrete structure is influenced by the bond behavior between the steel bars and the concrete. The other factors that affect this capacity are mentioned below:

1. anchorage of the reinforcing bars
2. crack width control
3. lapped reinforcing bars
4. rotation capacity of the concrete structures

Frank, et al. [141] mentioned that a systematic investigation of the bond behavior between the rebar and the SCC is necessary, especially considering the time development of the bond strength. The main parameters which influence on the bond behavior are the surface of the rebar, the number of load cycles, the mix design, the

direction of concreting, as well as the geometry of the test specimens in pull-out test. Figure 2. 14 shows the analytical bond stress-slip relationship for monotonic loading.

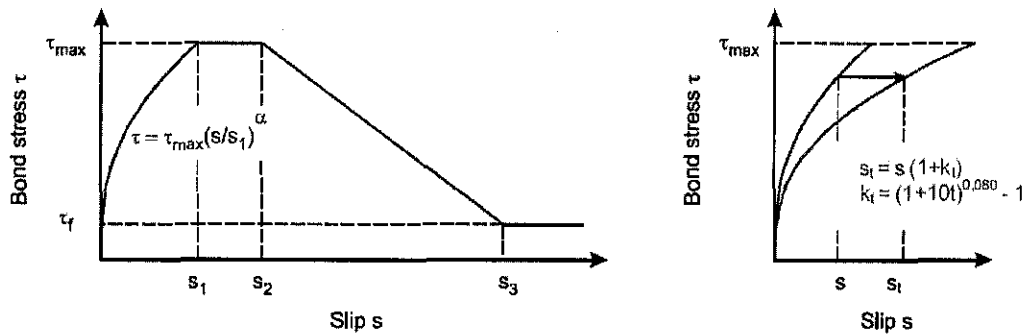


Figure 2. 14. Analytical bond stress-slip relationship (monotonic loading)

Source: Frank, et al. [141]

A beam is one of the most common structural elements. It bends when subjected to loads acting transversely to its centroidal axis. It can be assumed that all the loads and reactions lie in a simple plane that also contains the centroidal axis of the flexural member and the principal axis of every cross-section, and the beam will simply bend in the plane of loading without twisting. Idealization of static loading was described completely by Ghosh and Saatcioglu [142] as shown in Figure 2. 15.

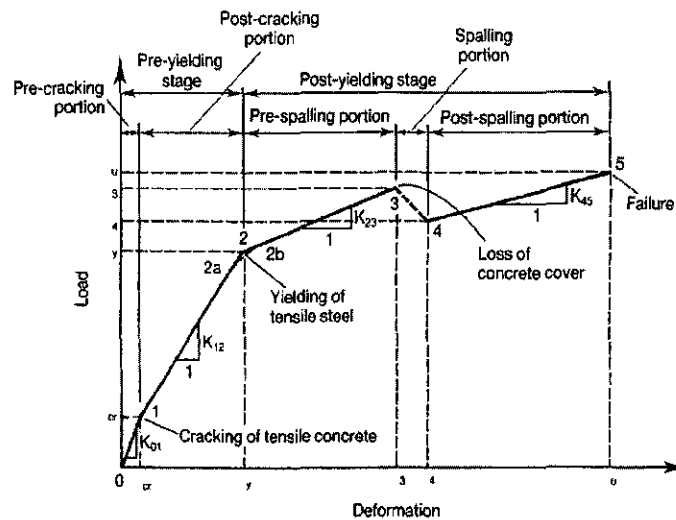


Figure 2. 15. Idealization of beam load-deformation curves

Source: Ghosh and Saatcioglu [142]

Ulrika [143] mentioned that the global behavior of failure in a reinforced concrete beam or slab can be generalized to membrane, flexural and shear failure. Membrane failure occurs due to tensile stress and in some cases compressive stress, in-plane forces in the element. Flexural failure in beam occurs after formation of plastic hinges, resulting in a mechanism or when the in-plane deformations are large enough to make the beam slip off the supports. Shear failure occurs due to diagonal tension and compression related to flexural behavior. However, direct shear response is typical for short-duration dynamic loads and is caused by the high shear inertia forces, which do not exist under static or slow dynamic loading. These types of failure can be seen in Figure 2. 16.

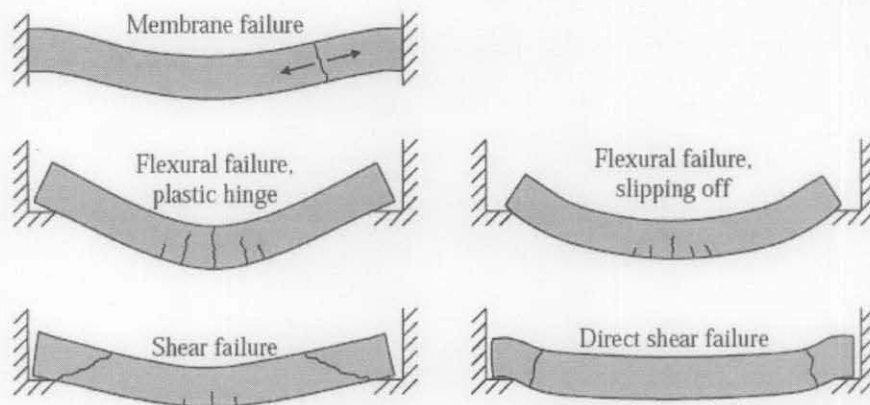


Figure 2. 16. Failure type of reinforced concrete beam

Source: Ulrika [143]

2.7.3. Dynamic Behavior of SCC structure

Hassan, et al. [128] investigated the strength, cracking and deflection performance of self compacting concrete beams subjected to shear failure in dynamic load test. However, the dynamic investigation in SCC is still rare, and needs further research to study this behavior. Some aspects of dynamic behavior are discussed in the following paragraphs.

Ezeldin and Balaguru [144], and Maekawa and Farouk [145] mentioned that fatigue is the process of cumulative damage which is caused by repeated fluctuating loads. Fatigue loading types can be either high-cycle low amplitude or low-cycle high

amplitude. The range of cyclic loading into a spectrum of cycles which classified the fatigue loads into three ranges, the low-cycle fatigue loading occurs with less than 1000 cycles, whereas the high-cycle fatigue loading is defined in the range of 10^3 to 10^7 cycles. This range of fatigue loading occurs in bridges, highways, airport runways and machine foundations and can be seen in Figure 2. 17. The super-high-cycle fatigue loading is characterized by even higher cycles of fatigue loads. This category was established in recent years for the newly developed sophisticated modern structures such as elevated sections on expressways and offshore structures.

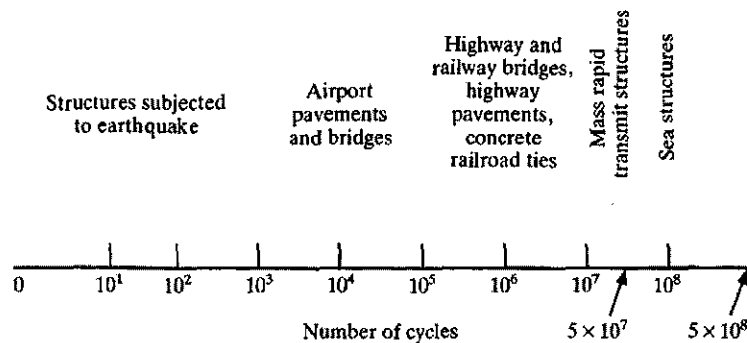


Figure 2. 17. Range of number of cycles based on type of structure

Source: Ezeldin and Balaguru [144]

Zihai and Masaki [146] noted that in solving various fatigue problems, the time-varying characteristics of cyclic loads on structures due to winds, waves, vehicles and so forth are often oversimplified by assuming the loading positions as fixed.

Houssam, et al. [147] mentioned that the fatigue strength can be defined as the load-carrying capacity of a structure under a certain number of cycles. The fatigue life of a structure is defined as the number of fatigue loading cycles until failure under a certain fatigue loading level. The fatigue strength of a concrete member corresponds to a life of ten million cycles which is assumed to be about 55% of the initial static strength of the member and the other researchers Khaled and Raymond [148] suggested 80% of ultimate strength. In recent years, considerable interest has developed to study the fatigue behavior of reinforced concrete members. The wide spread adoption of ultimate strength design procedures and the use of higher strength and more durable materials require structural concrete members to perform satisfactorily under high stress levels for a longer period of time. Repeated loading

may lead to internal cracking of a member that alters its stiffness and load-carrying capacity, the energy dissipated under cyclic loading decreases to a minimum at 10% of the lifetime, before increasing up to failure as mentioned by Minh-Tan, et al. [149]

Christos, et al. [150] stated that the fatigue strength of a concrete member corresponding to cyclic loading is assumed to be about 55% of the initial static strength of the member, and all factors should be considered in experiment, such as the range of loading, rate of loading, eccentricity of loading, loading history, material properties, and environmental conditions influence fatigue strength. Ben-Amoz. [151] stated that proceeding from single slip and opening mode damage curves, two-mode damage curves are derived that reflect the micro process of crack by the presence of a macro scale of both damage modes in each cycle.

Breitenbücher and Ibuk [152] stated that concrete structures fatigues can occur by a compounding of degradation processes. In addition a large scatter of such variations has to be considered. Concrete structures exposed to cyclic loads can fatigue and degradation processes take place extensively within the microstructure of this material. During few thousands of load cycles micro cracking already takes place to some extent, which can be mainly detected by changes in the dynamic of modulus Young.

Schläfli and Brühwiler [153] mentioned that fatigue loading is caused by repeated loading which may exceed 100 million over the service life of a bridge. Jun, et al. [154] said that fatigue is a process of progressive, permanent internal structural changes occurring in a material subjected to repetitive stress. Paulo, et al. [155] mentioned that during the past decades several attempts, by numerical and experimental investigation, have been carried out to improve the knowledge about the fatigue behavior. And this fatigue behavior can be represented by several methods. Nieto, et al. [156], Jun, et al. [154], Li and Takashi [157], and Miguel, et al. [158] stated that fatigue strength is commonly defined as a fraction of the static strength that can be supported repeatedly for a given number of cycles. It can be represented by stress-fatigue life curves, normally referred to as S-N curves. In the case of fatigue in bending, S refers to the flexural stress according to elastic theory. Singh and Kaushik [159] that that S can be stress levels. Peiyin, et al. [160] stated the

understanding of fatigue loading is obtained through establishing the relationship between cumulative damage and the onset of the energy release in a cycle, which simulates the degenerative process of the stiffness of concrete under cyclic loading. Zihai and Masaki [146] presented the results by correlating number of cycles and vertical displacement. Krige and Mahachi [161] correlated the number of cycles and stiffness of beam, while Jongsung and Hongseob [162] displayed the dynamic result by relating the load and displacement as shown in Figure 2. 18.

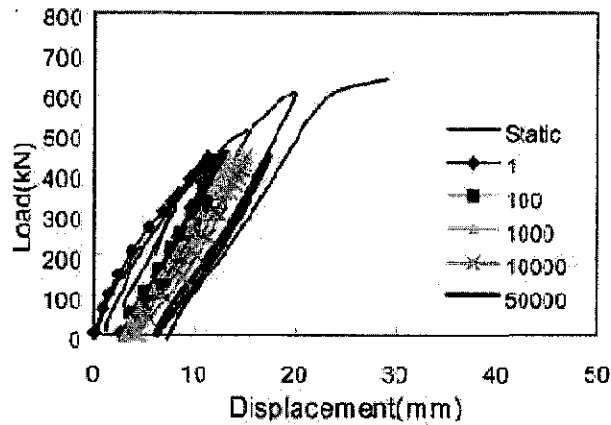


Figure 2. 18. Load-displacement in dynamic load

Source: Jongsung and Hongseob [162]

Lee and Barr [163], Christoph and Masoud [164], and Takashi and Victor [165] stated that fatigue can be defined as a process of progressive structural changes in a permanent internal material through repeated loading. This change is mainly related to the progressive growth of internal micro cracks, which result in a significant increase in irrecoverable strain. At the macro level, this manifests itself as changes in mechanical properties materials. Fatigue loading is usually divided into two categories such as low and high cycle loading. Low-cycle loading involves the application of several cycles of load at high stress levels. On the other hand, high cyclic load will be characterized by a large number of cycles at stress lower levels, with broad spectrum fatigue loads in inclusion of super-high-cycle loading. Andrea, et al. [166] stated that progressive crack growth under cyclic load in the dynamic test affected the behavior of beam, and caused significant changes in mechanical properties (strength, toughness, stiffness, hysteretic behavior, etc.) eventually leading

to failure. Several theoretical models have been proposed to describe such phenomena and to predict the fatigue life.

Hordijk and Reinhardt [167] stated that the main characteristic of fatigue behavior of concrete, and also of other materials, is that the number of load cycles, N , that can be performed before failure occurs, increases for a decreasing upper load level. When the relative upper load (or stress) level is plotted against the logarithm of the number of cycles to failure, then a linear relation will be found. These types of curves are Wohler curves or S-N curves. If the deformations are recorded during a fatigue test on concrete and plotted against the number of cycles performed then a curve will generally be obtained that is known as a cyclic creep curve. A typical curve is shown in Figure 2. 19.

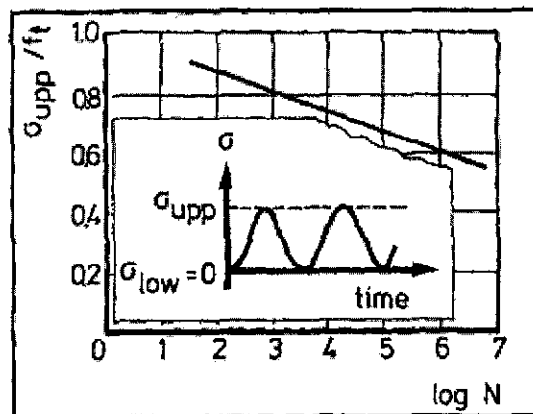


Figure 2. 19. Typical S-N curve

Source: Hordijk and Reinhardt [167]

Weena, et al. [168] studied the use of confining structural member that is subjected to cyclic loading. In the seismic design of reinforced concrete structures, sufficient level of ductility is important for energy absorption. This is a common practice to use confining reinforcement in both the earthquake resisting of structures and other structures, to improve the ductility of structural members.

Understanding of mechanism of the damage caused by repeated loading was discussed by Bin, et al. [169]. Mechanistic approach is based on applying the concept of a fracture or damage mechanics to model the material damage due to repeated loading. Paris law is generally used to describe the fatigue crack growth for members

subjected to tensile loads. Paris law relates the stress intensity factor to subjected crack growth under a fatigue stress regime. Following are the formula.

$$\frac{da}{dN} = C\Delta K^m \quad (2.3)$$

- where a = the crack length
- N = the number of load cycles
- C and m = material constants
- ΔK = the range of the stress intensity factor.

Typical hysteresis loops were recorded by Naaman and ammoud [170] at various stages of the fatigue life of each specimen. The area enclosed by the load versus deflection hysteresis loop describes the amount of damage done to the specimen during any recorded cycle of loading. The hysteresis loop allows us to extract the values of deflections at P_{max} and P_{min} , and the permanent deflection at any cycle and finally the variation of the deflection between the minimum and maximum loads gives a good indication of the loss of stiffness of the specimen due to fatigue loading. The other important result of the fatigue tests is the increase in the differential deflection between the minimum and maximum applied load levels (P_{max} and P_{min}) with the number of loading cycles. Typical results are illustrated in Figure 2. 20.

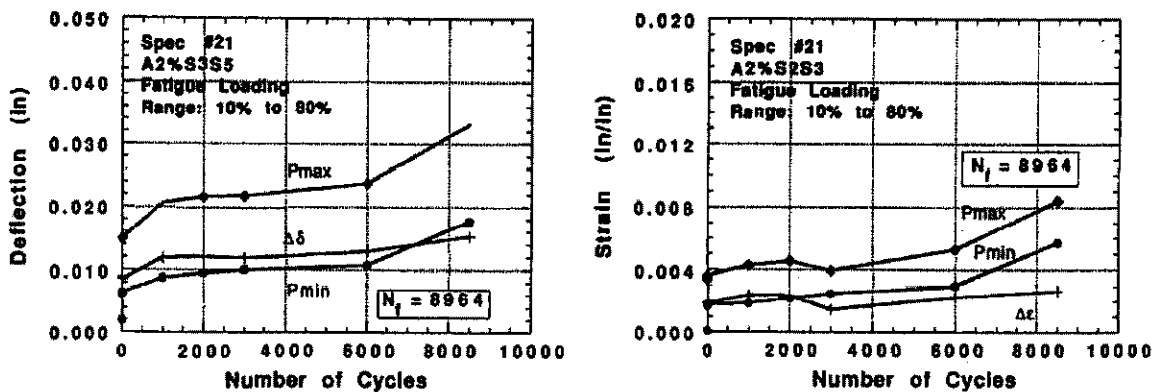


Figure 2. 20. Variation of deflection and strain with applied number of cycles for specimen

Source: Naaman and ammoud [170]

The research on reinforced concrete beams by Mallet [171] concluded that shear fatigue failure could occur in beams with or without stirrups, the fatigue life of reinforcement being much the same whether it is longitudinal tensile reinforcement or transverse stirrups. As the fatigue loading of a beam progresses, and the subsequent cracks propagate, there is a redistribution of stress; thus, fatigue failure is not always by the same mechanism as static failure as reported by Barnes and Mays [172].

2. 8. Summary and Concluding Remark

After detailed review of the available literature on self compacting concrete, it is understood that most of the research focused on developing the mix design for SCC, to establish models or standards for fresh properties of SCC. The literature showed some significant gaps in the area of research on self compacting concrete. Some of the prominent gaps are found as:

- a. Application of rice husk ash in producing high strength and high performance SCC and its structural behavior.
- b. Durability characteristics, such as fluid permeability and corrosion resistance of MIRHA self compacting concrete.
- c. Bond behavior of embedded steel bars in MIRHA SCC and development of empirical relationship.
- d. Fatigue life prediction and dynamic behavior of SCC both on fly ash self compacting concrete or MIRHA self compacting concrete using cyclic loading experiments.

These gaps derived from literature review were investigated in this research. The methodology of the research is explained consecutively.

CHAPTER 3

RESEARCH METHODOLOGY

3. 1. Introduction

To achieve the better understanding of capability of self compacting concrete containing fly ash and MIRHA and also to achieve the objective of this thesis which is to produce the optimum mix design and other objectives, some tests and several assessments need to be run to determine some properties and characteristic of this material.

To determine proper SCC mix design or ingredient proportion of self compacting concrete the so-called rheological properties test needs to be run. This test is very crucial and becomes the most important part of this study by reason of reliability of particular mixed whether it can be poured into the formwork with its ability to flow fluently without any vibration or not. On the other hand, this test is also essential to get the optimum mix design together with the result of mechanical properties test. Mechanical properties cover the compressive strength as the major properties of this material, flexural strength test as well as tensile strength as a compliment to determine its strength quality.

However, comprehensive understanding of the quality of self compacting concrete containing fly ash and MIRHA need to be extended with the durability properties test. Durability properties will convince us that this material is reliable enough to sustain environmental influence into the concrete. Porosity test is the most important property in concrete durability. Nevertheless, the other tests also necessitate to be run such as permeability and corrosion resistance test. All the result from rheological, mechanical and durability properties will determine the optimum mix design i.e. the best ingredient proportion of involved material.

The optimum mix design is then applied into structural behavior test and observation of this behavior will determine the capability of particular mix proportion of SCC in real structure. All these methodology can be illustrated in a flow chart in Figure 3. 1 which shows the experimental program that was adopted in this research.

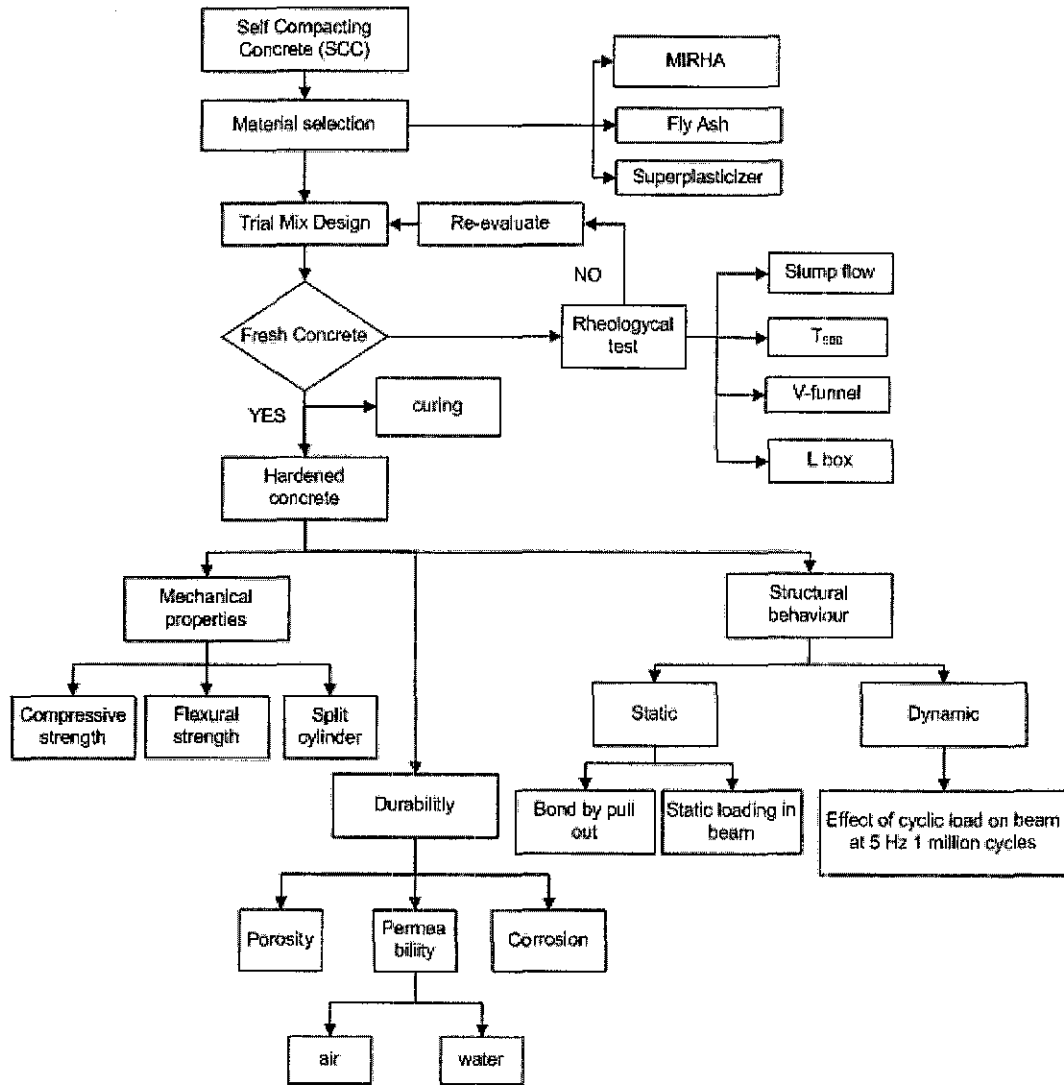


Figure 3. 1. Flow chart for experimental program of this investigation

The procedures detailed of each item in Figure 3. 1 are described in the next several sections.

3. 2. Material Selection and Sample Preparation

This section discusses the material selection, trial mix proportioning and mixing procedures, and production of self compacting concrete. This process was conducted on three stages are summarized in Figure 3. 2.

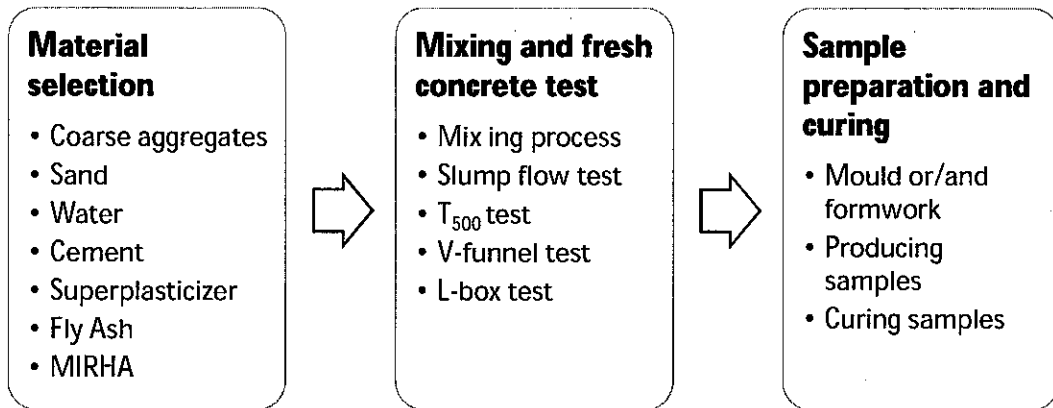


Figure 3. 2. Material, mixing and producing SCC

The materials used in this research project are aggregate, Ordinary Portland Cement (OPC), Microwave Incinerated Rice Husk Ash, Fly Ash, high range water reducer (HRWR) superplasticizer, water. Properties and characteristics of each material are given in the following sections.

3.2.1. Aggregate Properties

Aggregates fill almost 65 – 70% of total volume of hardened concrete. As such, the aggregates have a large impact on the behavior of concrete. Grace and CoConn [50] suggested that the nominal maximum size of coarse aggregate should be chosen with respect to the desired stability of the plastic concrete. When the size of coarse aggregate exceeds 12.5 mm, it will be beneficial to mix a combination of two or more different sizes to obtain an optimum grading. Typical nominal maximum aggregate size used in the SCC is 20 mm, although the aggregates as large as 25 mm can be used. However, the aggregates with a nominal maximum size greater than 25 mm is not recommended in the SCC. The aggregates should be clean, hard, strong and free of absorbed chemicals or coatings of clay and other fine materials that cause the

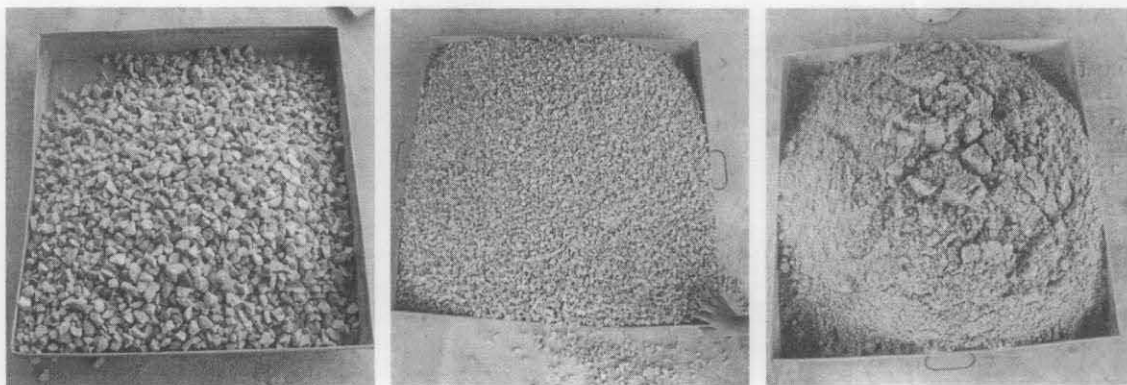
deterioration of concrete. To assess these characteristics several tests were conducted, such as:

- a. Aggregate Impact Value
- b. Sieve Analysis of Fine and Coarse Aggregate
- c. Silt Content Test

For preparation of coarse aggregates, first they were sieved and then immersed in water and followed by drying for one day at room temperature. The purpose of immersion was to remove dirt from the surface of the coarse aggregates that might decrease the strength or proportion of the concrete and as well to ensure that the coarse aggregates are fully saturated. Then the coarse aggregates must be dried for one day at room temperature to make sure the coarse aggregates condition was saturated surface dry. This ensures that the coarse aggregates will not absorb water during the mixing.

Two types of coarse aggregate and sand were used in this study (Figure 3.3):

- a. Coarse aggregate 20 – 8 mm
- b. Coarse aggregate 8 – 4 mm
- c. Fine aggregate or sand is typically composed of particles with diameters that range from 75 μ m to 5 mm,



(a)

(b)

(c)

Figure 3.3. (a) Coarse aggregate 20 – 8 mm, (b) Coarse aggregate 8 – 4 mm, (c).

Fine aggregate (sand)

The grading of aggregates is presented in Table 3. 1:

Table 3. 1. Grading of the coarse and fine aggregate

BS Sieve Size (mm)	Passing (%)		
	CA, 20 – 8 mm	CA, 8 – 4 mm	Fine aggregate
20.00	99.2	-	-
14.00	72.4	-	-
10.00	31.3	-	-
5.00	3.0	20.6	-
3.35	2.1	3.1	-
2.36	1.8	1.3	66.7
2.00	-	0.7	62.1
1.18	-	0.7	47.2
0.60	-	-	32.3
0.30	-	-	29.1
0.21	-	-	12.4
0.15	-	-	7.8
Pan	0	0	0

The determination of the Aggregate Impact Value (AIV) with using this equation:

$$AIV = \frac{B}{A} \times 100\% \quad (3.1)$$

From the test the Aggregate Impact Value (AIV) was 43.83%. While the silt content the result showed that the amount of dreg in sand was below 8% of water weighth.

3.2.2. Cement Properties

Ordinary Portland Cement which used throughout this study was complied with the requirement of Malaysia standard SIRIM MS 522: Part 1:2000, certificate no: PT 020301, which is loosely based on the British standard BS 12, this is superseded by EN 196 which is the European Union standard. The OPC is 50 kg weight product from Tasek Corporation Berhad, Ipoh. The chemical composition is presented in Table 3. 2.

The grading of aggregates is presented in Table 3. 1:

Table 3. 1. Grading of the coarse and fine aggregate

BS Sieve Size (mm)	Passing (%)		
	CA, 20 – 8 mm	CA, 8 – 4 mm	Fine aggregate
20.00	99.2	-	-
14.00	72.4	-	-
10.00	31.3	-	-
5.00	3.0	20.6	-
3.35	2.1	3.1	-
2.36	1.8	1.3	66.7
2.00	-	0.7	62.1
1.18	-	0.7	47.2
0.60	-	-	32.3
0.30	-	-	29.1
0.21	-	-	12.4
0.15	-	-	7.8
Pan	0	0	0

The determination of the Aggregate Impact Value (AIV) with using this equation:

$$AIV = \frac{B}{A} \times 100\% \quad (3. 1)$$

From the test the Aggregate Impact Value (AIV) was 43.83%. While the silt content the result showed that the amount of dreg in sand was below 8% of water weighth.

3.2.2. Cement Properties

Ordinary Portland Cement which used throughout this study was complied with the requirement of Malaysia standard SIRIM MS 522: Part 1:2000, certificate no: PT 020301, which is loosely based on the British standard BS 12, this is superseded by EN 196 which is the European Union standard. The OPC is 50 kg weight product from Tasek Corporation Berhad, Ipoh. The chemical composition is presented in Table 3. 2.

3.2.3. Microwave Incinerated Rice Husk Ash (MIRHA)

Rice husk is one of the bulky wastes that are readily available everywhere in the world without cost. Microwave combustion of rice husk turned it into highly amorphous silica rich pozzolanic material. For this study rice husk was obtained from BERNAS, Malaysia. The rice husk was burnt into a microwave oven at 800°C for 4 hours. The grayish ash was then ground using Los Angeles abrasion machine at 300 cycles in order to achieve 180 µm or lower size grain which is achieved by sieving process, all this process is illustrated in Figure 3. 4. The chemical composition result of MIRHA is presented in Table 3. 2.

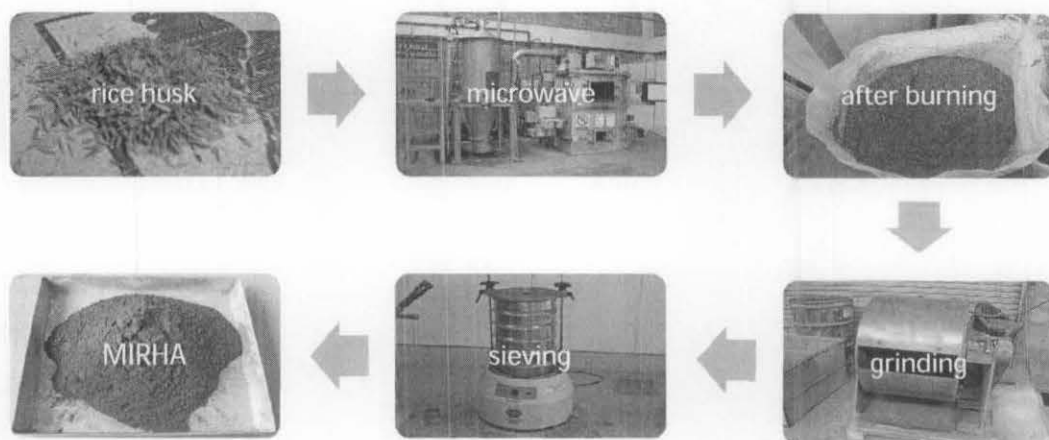


Figure 3. 4. MIRHA production

3.2.4. Fly Ash

For this study fly ash was supplied by YTL Cement Malaysia and was originally obtained from Manjung power station (Figure 3. 5). The fly ash was class F that complied by the BS EN 450:1995. The cement composition of the fly ash used is provided in Table 3. 2.

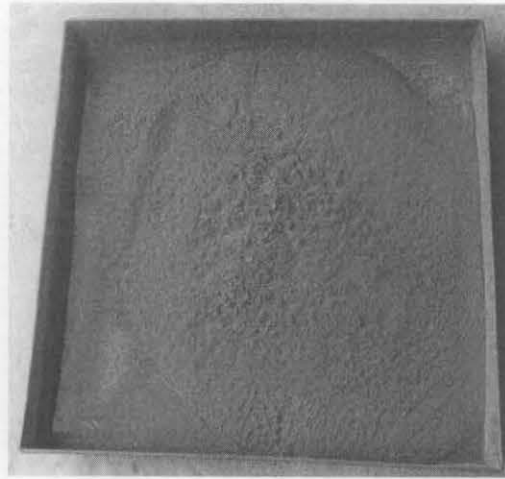


Figure 3. 5. Fly ash

Table 3. 2. Chemical composition of binder used in this study

Chemical composition	Percentage, %		
	OPC	Fly Ash ¹	MIRHA ²
SiO ₂	20.3	56.39	90.75
Al ₂ O ₃	4.2	17.57	0.75
Fe ₂ O ₃	3	9.07	0.28
CaO	62	11.47	0.87
MgO	2.8	0.98	0.63
SO ₃	3.5	0.55	0.33
K ₂ O	0.9	1.98	3.77
Na ₂ O	0.2	1.91	0.02

Note: ¹ Fly ash from Manjung, Malaysia, data provided by Shafiq, et al. [82]

² Test results obtained from XRF's Universiti Teknologi Petronas, Malaysia.

3.2.5. Superplasticizers (Naphthalene Formaldehyde Sulphonate)

Superplasticizers is a chemical admixtures that can be added to concrete mixtures to improve its workability. Strength of concrete will be inversely proportional to water content added. In order to produce stronger concrete, a lesser amount of water added, which makes the concrete mixture very much unworkable and difficult to mix. In such instances, superplasticizers are used. Superplasticizers are also often used when pozzolanic ash is added to improve the concrete strength. Addition of superplasticizers is almost essential when producing high strength concrete, fiber reinforced concrete and self compacting concrete. The superplasticizers used in this

study were Sikament-NI High Range Water-Reducing Concrete Admixture, Naphthalene Formaldehyde Sulphonate type, supplied by Sika Kimia Sdn Bhd, and complied with BS 5075. The method of dosing and container are shown in Figure 3. 6.



Figure 3. 6. Superplasticizer

3.2.6. Mix Procedure

Binder elements in mix proportion of self compacting concrete include Portland cement and fillers i.e. fly ash and MIRHA. For concrete mix proportioning (normal and SCC) compressive strength requirement is the main governing criteria. The replacement of a portion of cement with fly ash and/or MIRHA can improve the filling ability and stability, without affecting the one day compressive strength of the concrete.

To improve the slump flow of the SCC mixtures, water alone cannot serve the purpose; it also required to improve the content of the binder mixture that can prevent segregation. When the desired slump flow increases and also the filling ability, the adding of powder content is required to achieve adequate passing ability and stability. In this case, specifically designed high range water reducers (HRWR) or superplasticizers are used. To make all the ingredients mixed properly and uniformly, the drum mixer was used (Figure 3. 7).



Figure 3. 7. Drum Mixer

In general volume of paste material in the SCC is greater than conventional concrete. Trial mix design is based on recommendation of several researchers as described in detail in section 2.4.3. Adjustment of SP dosage, percentage of fly ash or MIRHA and water-binder ratio will be based on result of rheological properties (Section 3.3) test (Chapter 4) and also strength target of compressive strength of cube test (Chapter 5). The detail information of mix proportion in the detail are given in Table A1, to the table A7 in Appendix-A and also discussed in section 4.2.

3. 3. Rheological Properties

Fresh concrete test of self compacting concrete is a tool to identify the ability of concrete for self compaction. For this purpose there are number of test such as slump flow, V-funnel and L-Box tests. In order to avoid the effects of fluidity loss of concrete, fresh concrete properties should be determined within 10 minutes after mixing. All the tests for fresh concrete were performed in accordance with The European Guidelines for Self compacting Concrete Specification - Production and Use, EFNARC [76]. The following sub sections explained the different rheological tests for SCC.

3.3.1. V-funnel test

The deformability through restricted areas can be evaluated by using the V-funnel Test. Figure 3. 8 shows the testing device for V-funnel test. In this test, first the channel completely filled with concrete, then the outlet at the bottom is opened, that allows concrete to flow out, then flow time is noted that is the measure of the test.

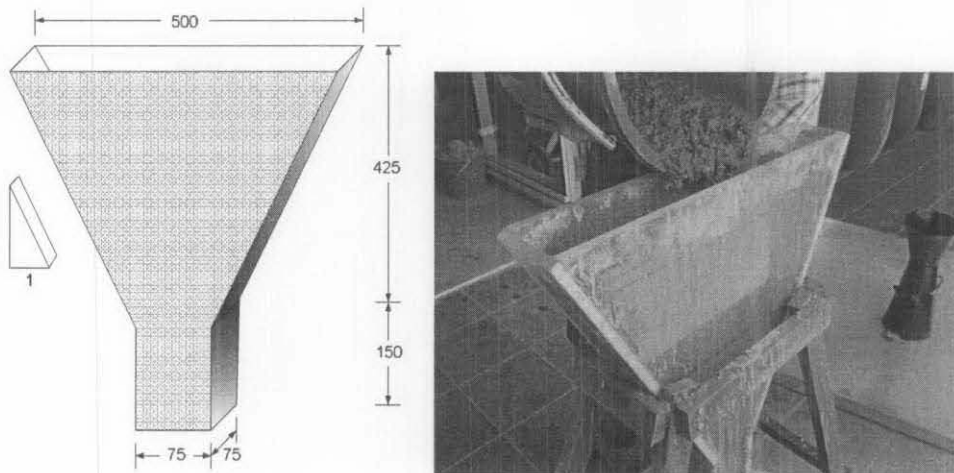


Figure 3. 8. V-funnel

3.3.2. L-box test

L-box test is used to determine the pass-through ability of self compacting concrete. The height of concrete blocked in vertical channel is noted as h_1 and the blocked height of concrete in horizontal channel is measured as h_2 . Nguyen , et al. [173] mentioned that the recommended passing ratio are 0.60 – 1. L-box dimensions and steel bars used in this study are shown in Figure 3. 9.

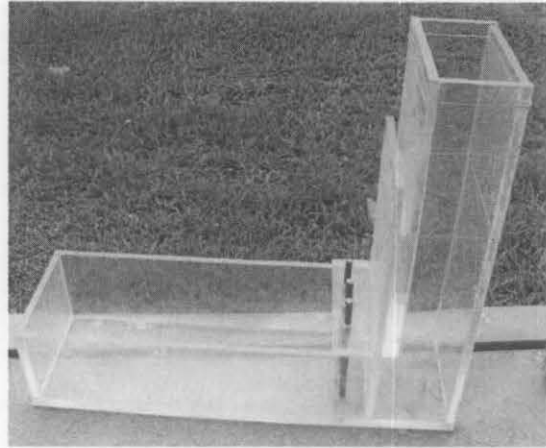
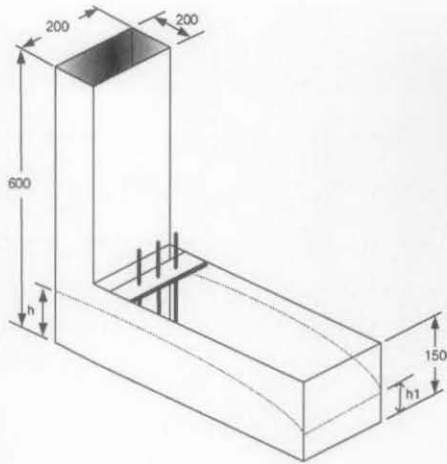


Figure 3. 9. L-Box apparatus

Value of passing through ability was given by Schutter [68] in formula:

$$P_L = \frac{H}{H_{max}} \quad (3.2)$$

Where PL = passing ratio

H = height of h1

H_{max} = 9 cm

3.3.3. T_{500} and Slump Flow Test

Slump flow tests are used to assess the horizontal flow of SCC without any obstruction. This test method is very similar to the traditional slump test used for normal concrete, instead of slumped-height; spread-diameter is measured in this test. The larger of slump flow is an indicator of high tendency of concrete to fill the formworks. However, it does not give an indication of the ability to pass through the reinforcement without blocking, but give some indication of resistance to segregation. Testing device includes a truncated cone with the internal dimensions of 200 mm diameter at the base, 100 mm diameter at the top and 300 mm height and a rigid base plate of non-absorbing material. Truncated cone is filled with SCC without tamping, followed by raising the vertical cone to allow the SCC to flow out freely. The diameter is measured in two perpendicular directions as shown in Figure 3. 10 and

Figure 3. 11. The average of two values is the slump flow. The time required for concrete to reach a slump flow diameter of 500 mm is measured and recorded as the T_{500} . This parameter is an indication of the viscosity of concrete and show how stable is the concrete. A lower time shows the greater flow ability.

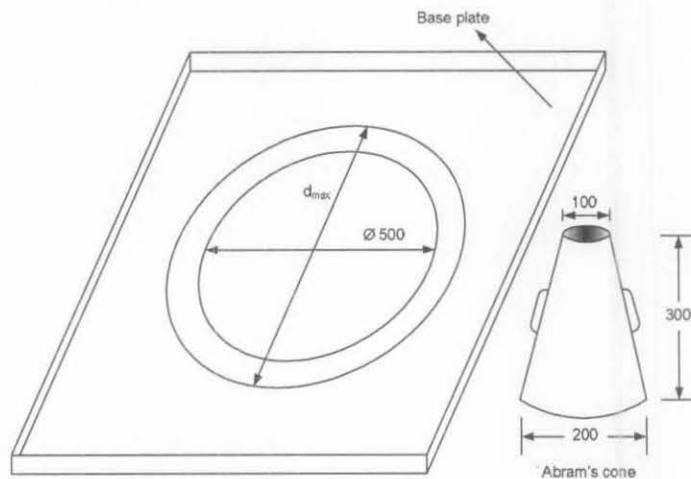


Figure 3. 10. Slump flow and T_{500} apparatus

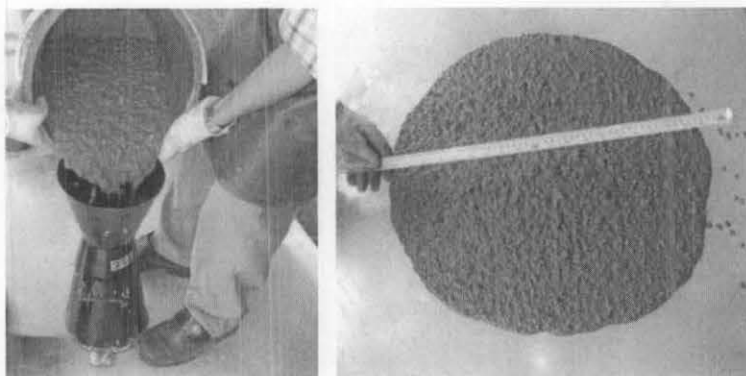


Figure 3. 11. Pouring and measurement of slump flow and T_{500}

3. 4. Mechanical Properties Test

There are a number of tests on hardened concrete those are specified in various standards that measure the physical and mechanical properties. Among all, concrete compressive strength is one of the fundamental tests that give a direct indication of its compressive resistance in structural application. Other test are related to the short-term and long term performance of concrete, such as tensile strength for cracking

resistance, porosity and permeability for durability, etc. The tests performed in this study are outlined in following sections.

3.4.1. Compressive Strength Test

In this investigation, compressive strength test was performed according BS 1881-111:1983. This standard was used for casting, curing and testing of cube specimen. Concrete cubes of 150 mm size were cast, for testing at age 1, 3, 7, 28, 90 and 360 days. Numbers of cubes to be cured were 3 times of number of test age. Cubes then were tested at every age using 3000 kN capacity compression machine as shown in Figure 3. 12.



Figure 3. 12. Compression Machine (ELE ADR 3000)

3.4.2. Flexural Strength Test

Rectangular beam of plain concrete of 100×100×500 mm size were cast and cured for testing at the age of 28 days, the flexural strength test conducted in accordance with BS 1881: Part 118: 1983. During the test the plain concrete is subjected to third point loading (mid point loading) and is known as prism bending test and can be seen in Figure 3. 13. At the point of failure maximum tensile stress is induced at the extreme bottom fiber that indicates the modulus of rupture. The modulus of rupture, R is calculated as:

$$R = \frac{PL}{(bd^2)} \quad (3.3)$$

where P = maximum total load on the beam

L = span

b = width of the beam, and

d = depth of the beam.



Figure 3. 13. Test setup profile for Flexural strength test

3.4.3. Split Cylinder test

Concrete cylinder specimens of diameter 150 mm diameter and 300 mm length were cast for testing at the age 28 days in accordance with BS 1881: Part 117: 1973 as shown in Figure 3. 14. Each concrete cylinder is placed between the platens of the testing machine lying on its horizontal axis. The load is applied until the cylinder is split into two halves.

The stress at failure state is measured at the tensile strength of concrete that is calculated as:

$$f_t = \frac{2P}{\pi LD} \quad (3.4)$$

where P = compressive load on the cylinder
 L = length of the cylinder, and
 D = diameter



Figure 3. 14. Test setup profile split cylinder test

3.4.4. Porosity Test

The porosity of concrete was carried out by coring three 50 mm diameter from concrete planks. The porosity test for this project was using vacuum saturation method. Vacuum saturation is a method of assessing the total water absorption porosity of a material. Porosity can be determined by measuring its weight gain and expressing this as a percentage of the mass of the sample. The porosity measurements were conducted on slices of cylinders cores that have been cast into (0.048 x 0.315 x 0.205) m slabs. The cored slices were put inside vacuumed desiccators for 30 minutes like shown in Figure 3. 15, and then the desiccators is filled with water for 6 hours. After 24-hours soaked in water, the samples were dried at $100 \pm 5^\circ\text{C}$.

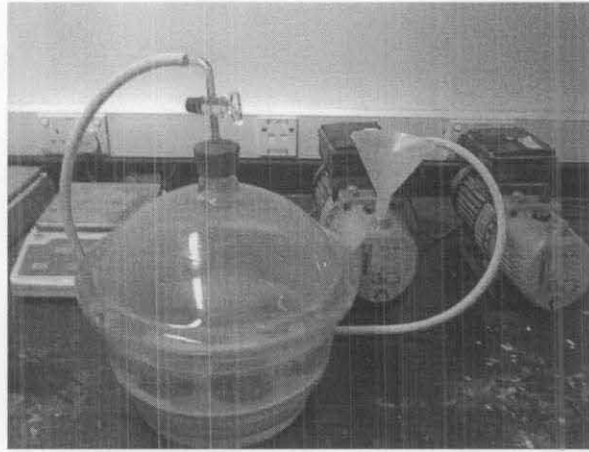


Figure 3. 15. Desiccators

Total porosity was determined by vacuum saturation method developed by RILEM CP 113 with detail procedure explained by Shafiq and Cabrera [120], and the porosity calculated as:

$$P = \frac{W_s - W_d}{W_s - W_w} \times 100 \quad (3.5)$$

Where P = total porosity in percentage

W_s = mass of saturated samples measured in the air, g

W_d = mass of oven dried samples measured in the air, g

W_w = mass of saturated samples measured in the water, g

3.4.5. Permeability

The core sample of cylinder with diameter 50 mm and height 40 mm was tested for permeability with oxygen and water permeability. The test was carried out using UTP Permeameter. Specific detail of specimen of permeability test can be seen in Table 3.

3.

Table 3. 3. Specific detail of oxygen and water permeability specimen

Specimen details	Fixed Data
Diameter, D (mm)	50
Length, L (mm)	40
Area, A (mm ²)	1.96.10 ⁻³
Pressure, p (bar)	1

Water permeability is measured by fluid penetration into sample when subjected to certain amount of pressure (1 bar). Gas permeability is the function of open porosity in the concrete and mortar sample; it decreases with the filling of pore system with water.

3.4.6. Corrosion Resistance Test

The Linear Polarization Resistance Testing was conducted on cylindrical sample tested in a beaker of 3.0% NaCl solution as shown in Figure 3. 16.

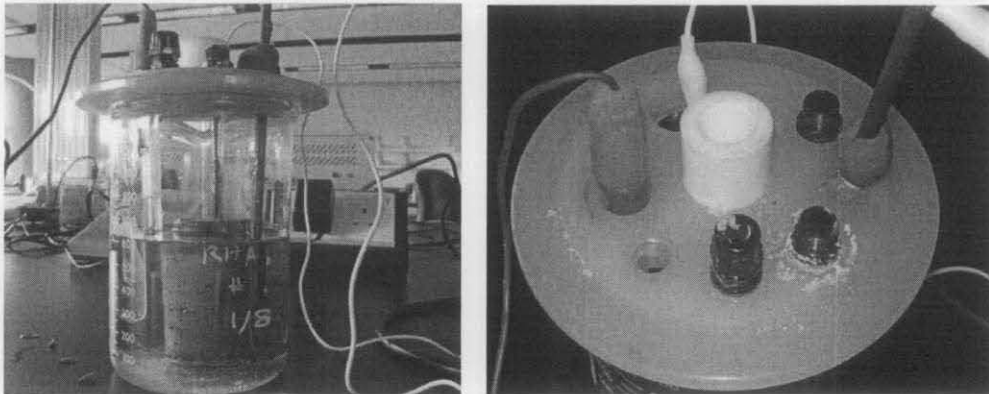


Figure 3. 16. LPR Sweep Test and Configurations of electrodes;

Configurations of electrodes as shown in Figure 3. 17 were; Working Electrode or Sample Rebar, Auxiliary Electrode and Reference Electrode.

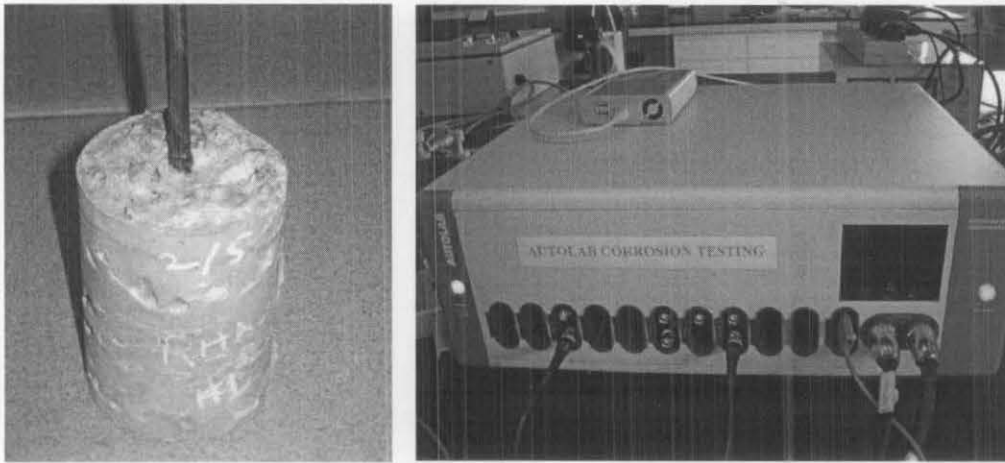


Figure 3. 17. Sample and Data logger of corrosion testing

The samples were tested at ages of 7, 28 and 90 days. The LPR method used the Autolab Test. The testing induced the corrosion to the steel reinforcement through the concrete sample by using electrochemical methods. The dimensions of sample were used to fit the Autolab Testing Machine. The 6 mm steel reinforcement bar was used in all the samples, the details are given in Figure 3. 18.

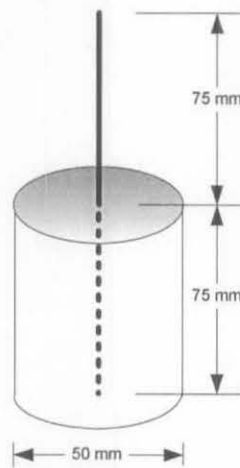


Figure 3. 18. Sample Dimensions of corrosion test

There were ten different chosen concrete mixes for this test. On average 3 samples were tested for each of the concrete mixes.

3. 5. Structural Properties Test

To validate the structural design theory as given in different standards, structural tests are necessary, particularly when any modification in material and/or procedure is introduced. The following are main purposes of structural testing:

- a. Model or full-scale testing to support in the evolution of improved analytical and design methods.
- b. Development testing for prototypes of components or ancillary equipment for performance or feasibility of construction procedure.
- c. Check testing of factory production as a control on quality of output.
- d. Investigations of structural adequacy of construction for which some reason may have become suspect.

The following sub-sections describe the details of the structural tests performed in this study.

3.5.1. Bond Characteristic

Bond characteristic was determined by pull out test. Cylindrical concrete sample have been used with an embedded steel bar that is to be pulled-out during test and complied with ASTM C900-06 "Standard Test Method for Pullout Strength of Hardened Concrete". A pull-out load as shown in Figure 3. 19 in Universal Testing Machines (UTM) was applied at the rate of 0.2 kN/s to steel bar until failure happened. Load-slip was recorded in interface every 6 second. This test was performed at the age of 28 and 90 days.

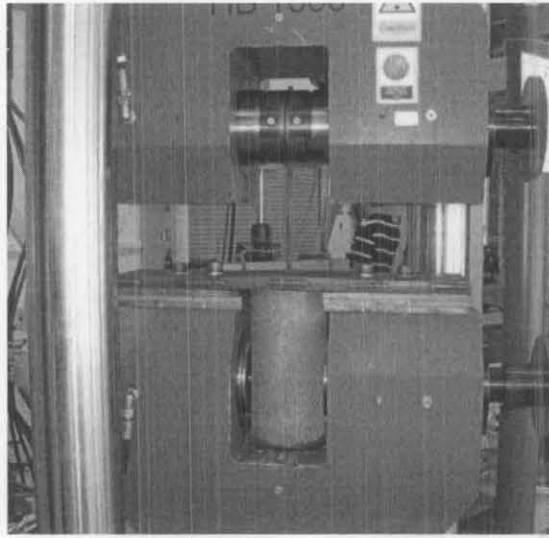


Figure 3. 19. Pull out test setup

In this study 150 diameter and 300 mm high concrete cylindrical samples with 10 or 12 mm diameter steel bars embedded in the middle were used. There were two approaches used for collation of the embedded length, L . In the first approach the contact area of all diameter steel bars with concrete was kept constant, whereas in the second approach, the embedment length was 15 times the bar diameter for all mixes and all bar sizes.

3.5.2. Testing of Reinforced Concrete Beam

3.5.2.1. Beam Detail

The dimension and size of RC beam were 1900 mm long, having a cross section of 150 × 250 mm. The main bars and shear link details are given in the Figure 3. 20. All the optimum mix SCC beam of 8 beams and control beam (normal mix) of 2 beams at age 90 days were tested in monotonic and cyclic test.

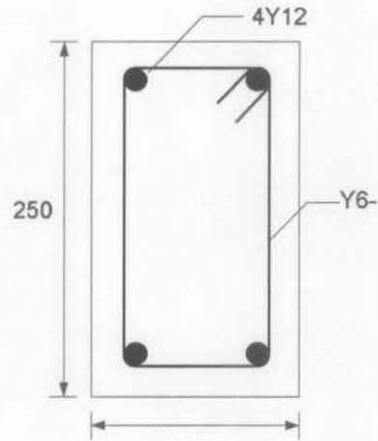


Figure 3. 20. Beam Cross Section

3.5.2.2. Monotonic and Cyclic Testing of Beam

Span of the beam was kept as 1700 mm as shown in Figure 3. 21. The beams were tested under 4-points loading using 500 kN capacity static/dynamic actuator and a loading frame. For monotonic testing the load was applied at rate of 0.2 kN/sec.

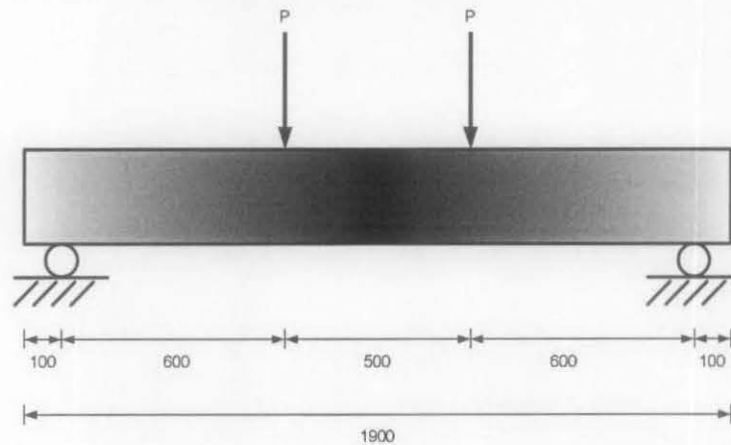


Figure 3. 21. Loading setup and dimension of beam

The failure load in static load test of a particular mix was used as a basis for setting the upper and lower level for the cyclic loading of the beam of the same mix. In cyclic testing upper level was set as 60% of the failure load and the lower level was selected as the 10% of the failure load. The beams were tested at 5 Hz either until failure or until one million cycles. The experimental setup is illustrated in Figure 3. 22 and Figure 3. 23.

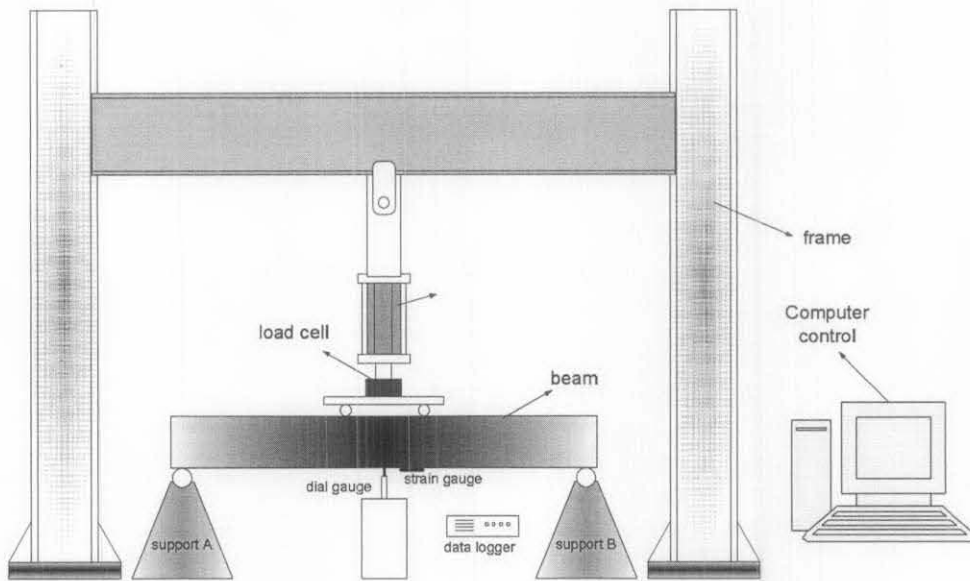


Figure 3. 22. Layout of Test Frame for Static and Cyclic Loading

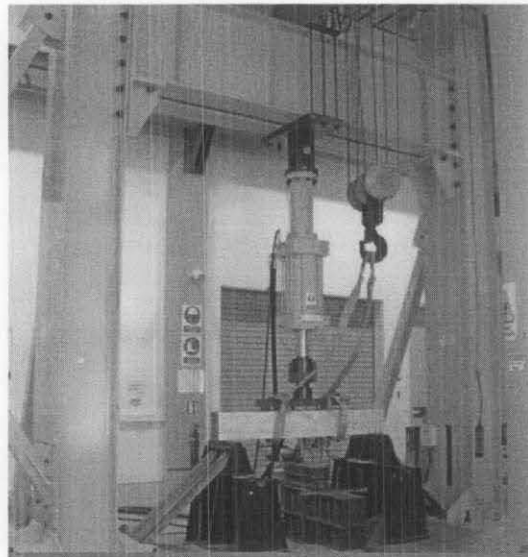


Figure 3. 23. Roell Amsler Dynamic Actuator with 500 kN capacity

The actuator was operated under load control for the fatigue loading and under displacement control for the monotonic tests, like shown in Figure 3. 24. Strains on concrete and deflections at mid span were recorded during testing in order to study

their changes under static and fatigue loading conditions. The deflection at mid span was measured using a computerized deflection measuring system.

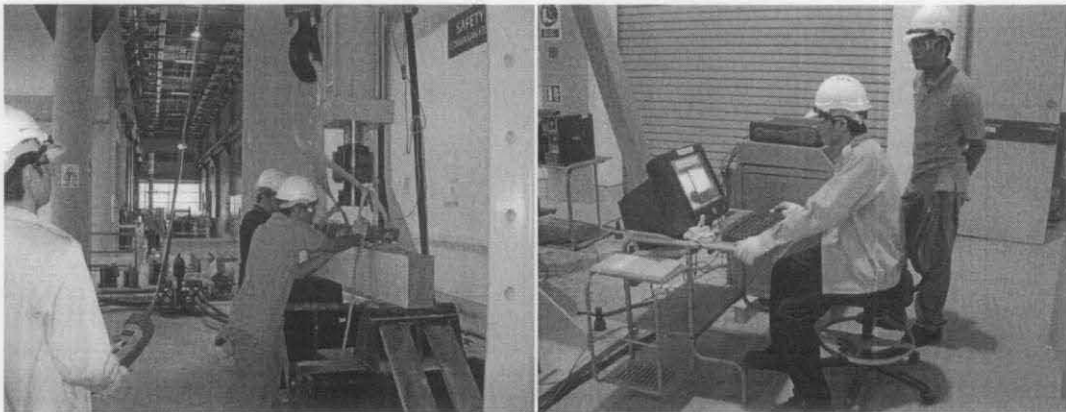


Figure 3. 24. Installment of beam and computer control of machine

Strain gauges were located on the bottom of concrete surface. LVDT was mounted to measure displacement and then can be used as comparison with displacement result by the actuator computer data as illustrated in Figure 3. 25.

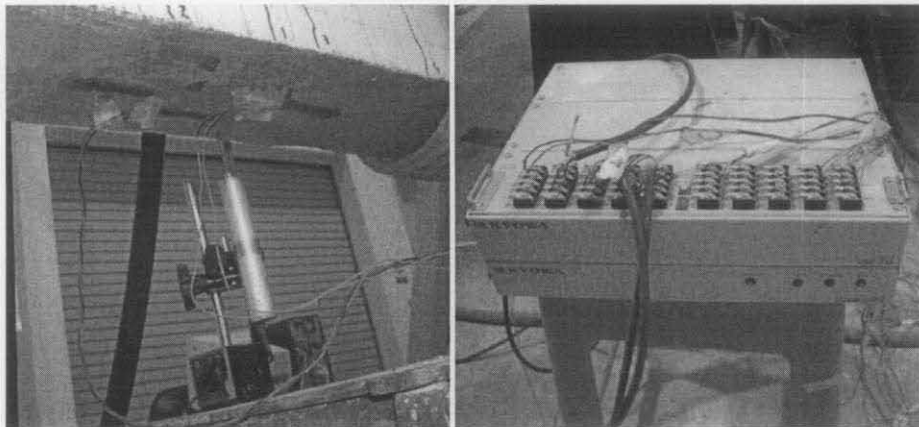


Figure 3. 25. Strain gauge location and data logger

Static beam load test was done until its fail, the crack patterns were marked in sequence of occurrence crack and value of load throughout the test. For dynamic test, the developing of crack and displacement was monitored by interfaced computer. Strain occurred in the bottom of beam was monitored using strain gages mounted at

the bottom of the beam. Typical crack pattern of static and dynamic testing of beam is shown in Figure 3. 26.

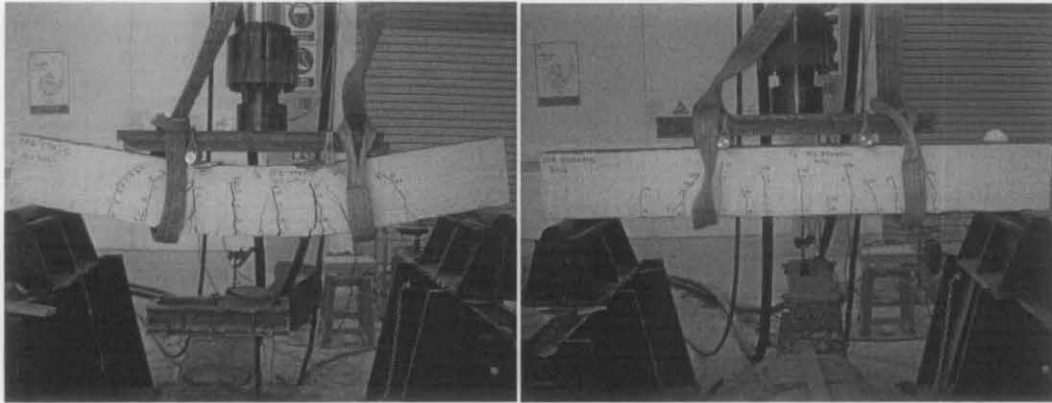


Figure 3. 26. Typical crack of static and dynamic test of beam

CHAPTER 4

RHEOLOGICAL PROPERTIES OF SCC

4. 1. Introduction

In order to obtain highly workable viscous concrete without any compaction, fresh concrete must be tested to determine the rheological properties which include its ability of self compaction, consolidation and placement in the formwork or in other word its workability in the fresh state. Rheology is defined as the study of the deformation and flow of fluid-like material in the concrete. The measurement of rheological properties can help to develop a better concrete, predict its performance and predict the mechanical properties of concrete in hardened state.

The first part of this chapter discusses various mix proportions used in this study, whereas the second part includes the technical discussion on the effects of several governing factors on the rheological properties of various mixes.

4. 2. Trial Concrete Mix

Rheological characteristics of self compacting concrete are very sensitive with respect to the mix proportions. Therefore, special attention must be paid for proportioning a mix for SCC. Grading of coarse aggregate, type and percentage of filler material and dosage of high range water reducer admixture (superplasticizer) play very important roles. For this study, fly ash and Microwave Incinerated Rice Husk Ash (MIRHA) were chosen as a filler material. There five different type of mix proportion were chosen as trial in this study, four of them were under the category of SCC where as the fifth one was the normal compacted concrete that is termed as the control mix. The mix proportional were designated as FASCC series that contained fly ash, MSCC series contained MIRHA, FMSCC series included combination of fly ash and MIRHA

and finally NPSCC series contained no pozzolans (100% OPC). The purpose of using rice husk ash is because of its abundance in Malaysia, which is burnt in highly controlled microwave environment in order to make it pozzolan in nature. In most of the available research, fly ash is commonly used as a filler material, therefore it is chosen for this study to compare the effect of MIRHA with available research on fly ash. In total 74 trial mixes from preliminary experiments in this study, only 55 were chosen to be reported in this thesis. The remaining mixes are not reported due to insignificant result in respect of variety of material proportion. The 10% fly ash content was chosen as the base filler content and to maintain the cost of concrete at competitive level 3% superplasticizers content was considered as the benchmark. This composition was based on the rheological result in this chapter (Chapter 4) also result from mechanical properties test in Chapter 5 and also result or conclusion from various research which will be described later in conclusion in Chapter 5. All these mixes are given in Table A1, to the table A7 in Appendix-A. The adjustments of mix proportion were based on the results that obtained from rheological properties and mechanical properties.

4. 3. Rheological properties

In this study the rheology of fresh concrete was tested using four different tests known as V-funnel test, L-box test, T_{500} test and slump flow test were applied on all SCC mixes. The tests were designed according to The European Guidelines for Self Compacting Concrete, EFNARC [76]. The recorded/measured values for all mixes are given in Table B1 in Appendix B. In the following sections the effects of various parameters on rheological properties are discussed.

4. 4. Effect of Water-binder Ratio on Rheological Properties

Rheological properties of self compacting concrete are highly influenced by water content. Understanding of water-binder ratio effect on rheology is the main objective that controls the acquisition of highly workable SCC.

4.4.1. Effect of Water-binder Ratio on V-funnel test

The V-funnel test is used to determine the filling ability of self compacting concrete, this ability is affected by water-binder ratio. Effect of water-binder ratio with 10% fly ash content and 3% dosage of superplasticizers on V-funnel value is shown in Figure 4. 1.

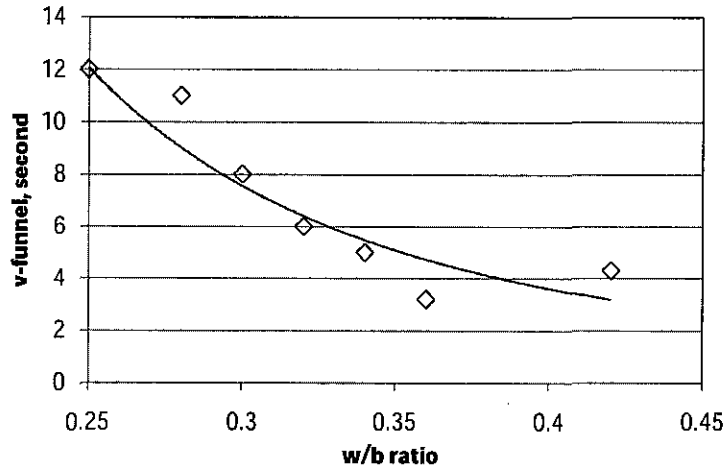


Figure 4. 1. Effects of w/b on the V-funnel test values for 10% fly ash on FASCC with 3% SP

From the analysis of Figure 4. 1, it is revealed that increasing the water-binder ratio will significantly increase the filling ability as indicated by the remolding time of concrete which indicates the flowing ability from one point to another point in the formwork. Lesser V-funnel time indicates better remolding and self compaction ability of concrete. Effects of w/b on the V-funnel test values for 10% fly ash on FASCC with 3% SP follows this relationship:

$$V_F = 0.346w_b^{-2.25} \quad (4.1)$$

$$R^2 = 0.793$$

where V_F = V-funnel time, second

w_b = water-binder ratio

It can be seen that 12 second V-funnel time was exhibited by concrete containing 0.25 w/b, whereas for the highest w/b of 0.42 gave a result of as 4.3 second and this result was about one-third of that obtained for the lowest w/b content. The determinations of self compactibility were given by several researcher and guidance

as described in section 2.4.4. However, the value of acceptance was various and rheological properties in this study need to be assessed based on site observation to determine what acceptance needs to be chosen. The guideline from “The European guidelines for self compacting concrete” EFNARC [76] describes wider coverage to the result in this study, and matches with site observation of this experiment in term of workability and flowability and now has been widely used for many researcher in the world. This guideline is utilized in this study to assess slump flow diameter, V-funnel time and T_{300} time. However, for L-box ratio, EFNARC did not describe the medium and low passing through ability so for L-box ratio the choice fell on guideline from Daczko and Constantiner [77] as describe in Table 2. 11.

Based on EFNARC guideline, FASCC for 3% SP and 10% fly ash pozzolan with $w/b < 0.3$ were categorized in class VF2, while for SCC with $w/b > 0.3$ were categorized in class VF1. All the concrete mixes for 3% SP and 10% fly ash pozzolan have satisfied the requirement, which means that lower water-binder ratio concrete can be used to produce SCC with in higher strength. While experiment work by Dinakar, et al. [22] gave the similar value of V-funnel flow time as result of SCC with 10% fly ash, 3% SP and w/b 0.29 that obtained the V-funnel time as 15 sec.

Effects of water-binder ratio on MIRHA self compacting concrete with 10% MIRHA content and 3% superplasticizers dosage is shown in Figure 4. 2.

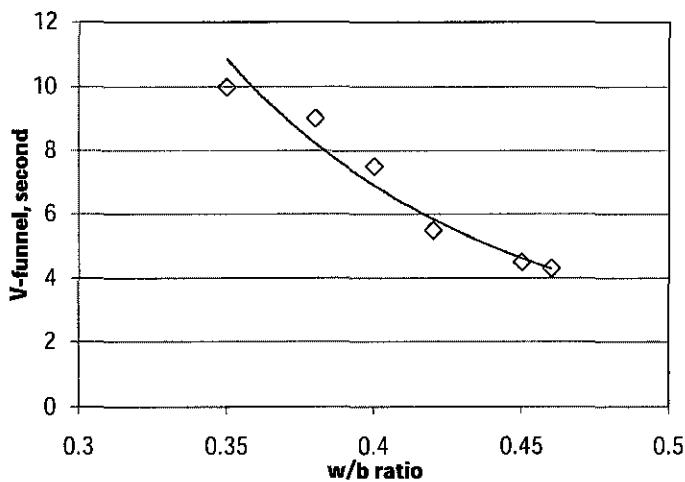


Figure 4. 2. Effects of w/b on the V-funnel test values for 10% MSCC with 3% SP

As shown in Figure 4. 2, effects of water-binder ratio together with 10% of cement replacement by MIRHA and 3% dosage of superplasticizers follow approximately a linear trend; the best statistical correlation was obtained as:

$$V_F = 0.308w_b^{-3.39} \quad (4. 2)$$

$$R^2 = 0.958$$

Cement replacement by MIRHA tends to increase the need of water compare to the fly ash, about 0.35 of water-binder ratio was needed to be applied to achieve the similar result as 0.25 in fly ash mix. This water-binder ratio of 0.25 and 3% SP result 10 second of V-funnel time. While the highest amount of water-binder ratio of 0.46 has V-funnel of 4.3 second. Based on EFNARC guidelines, MSCC for 3% SP and 10% MIRHA with w/b < 0.38 were categorized in class VF2, while for SCC with w/b > 0.38 were categorized in class VF1. All the mixes of MSCC with 10% pozzolan and 3% superplasticizers have satisfied the self compactability.

Sukumar, et al. [23] as contrast used the lower dosage of SP 0.4 – 0.7% in SCC containing fly ash, the result indicated that the water content have to be increased with minimum w/b was 0.34 to get to same rheological properties with the result in this thesis with w/b 0.25. The workability result of this study can be seen in Table 4. 1.

Table 4. 1. Rheological result of SCC

Workability test results with recommended limits								
Mix ID	w/p ratio	SP/b ratio	Slump flow (mm)	T_{50cm} slump flow (s)	V-funnel flow at T_f (s)	V-funnel at T_{min} (s)	L-Box T_{20} , T_{40} (s)	L-Box h_2/h_1
AS30	0.34	0.4	793	1.0	3	4	1.0, 1.5	1.0
BS30	0.33	0.4	675	1.5	5	6	2.0, 2.5	0.91
AS40	0.33	0.4	786	1.0	4	5	1.0, 1.5	0.99
BS40	0.33	0.4	690	2.0	5	5	2.0, 2.5	0.92
AS50	0.32	0.5	773	1.5	4	5	1.5, 2.0	0.96
BS50	0.32	0.5	685	2.0	4	5	1.5, 2.0	0.89
AS60	0.32	0.6	766	1.5	5	6	1.5, 2.0	0.95
BS60	0.31	0.6	695	2.0	4	5	1.5, 2.0	0.94
AS70	0.31	0.7	742	2.0	5	6	1.5, 2.0	0.95
BS70	0.31	0.7	680	2.0	4	6	1.5, 2.0	0.90
Recommended limits			600-800	<3	<6	< $T_f + 3$	1 ± 0.5, 2 ± 0.5	>0.8

w/p, water/powder (cement + fly ash + filler); SP/b, super plasticiser/binder (cement + fly ash).

Source: Sukumar, et al. [23]

Memon, et al. [30] found the cement replacement by RHA obtain the higher V-funnel time, using the material proportion as shown in Table 2. 2, in RHA SCC with

similar proportion which was 3.5% SP and 10% RHA and w/b 0.36 obtained 18 sec V-funnel time as shown in Figure 4. 3.

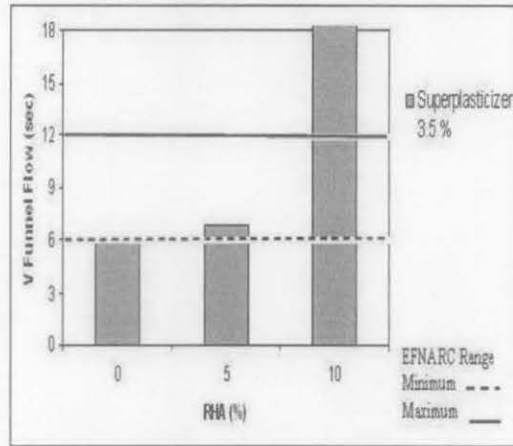


Figure 4. 3. V-funnel time with 3.5% SP, 10% RHA and 0.36 w/b

Source: Memon, et al. [30]

Figure 4. 4 and Figure 4. 5 show the effects of w/b on the mixes containing a combination of fly ash and MIRHA as the filler material. Figure 4. 4 shows the results of mixes that containing 100 kg/m^3 of fly ash and 50 kg/m^3 of MIRHA and 3% SP.

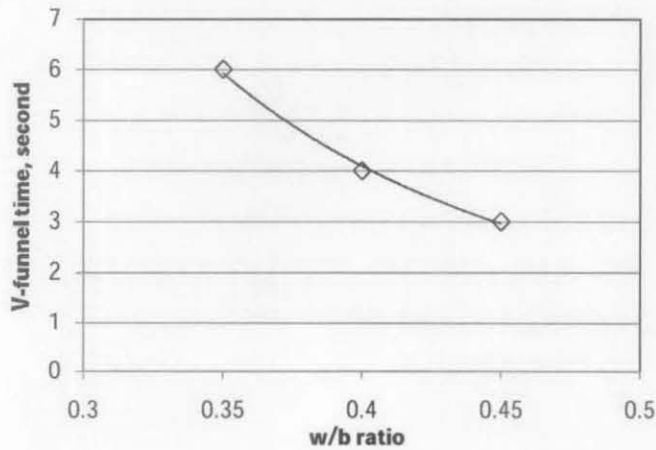


Figure 4. 4. Effects of water-binder ratio on the V-funnel test values for FMSCC with 20% FA and 10% MIRHA with 3% SP

Whereas as Figure 4. 5 shows the result of mixes that contained 50 kg/m^3 of fly ash and MIRHA 50 kg/m^3 with 3% SP.

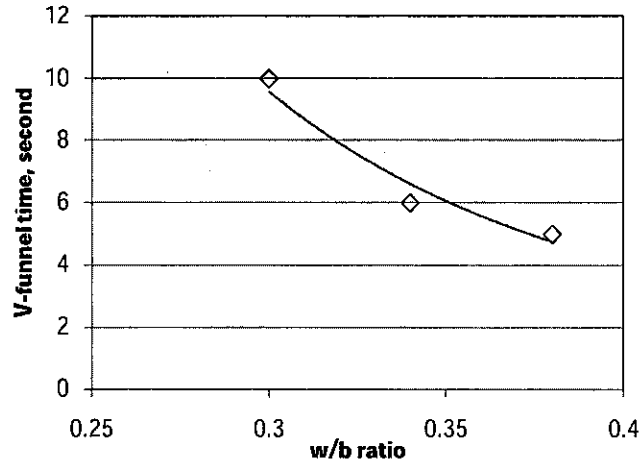


Figure 4. 5. Effects of water-binder ratio on the V-funnel test values for FMSCC with 10% FA and 10% MIRHA

The trend of the effect of w/b on mixes with combination of fly ash and MIRHA was obtained identical as shown in Figure 4. 1 and Figure 4. 2. Effect of water-binder ratio on the V-funnel test values for FMSCC with 20% FA and 10% MIRHA follow this equation:

$$V_F = 0.325w_b^{-2.76} \quad (4.3)$$

$$R^2 = 0.996$$

From Figure 4. 5, it can be seen that by presence of fly ash decreased the V-funnel time by 2 second decreasing, compare to SCC with only MIRHA pozzolan with the same water-binder ratio, same total binder and same superplasticizers content. The effect of water-binder ratio on the V-funnel test values for FMSCC with 10% FA and 10% MIRHA also had similar rheological properties compare to the 20% FA and follow this equation:

$$V_F = 0.2725w_b^{-2.95} \quad (4.4)$$

$$R^2 = 0.946$$

Based on EFNARC guidelines, all FMSCC 3% SP with 20% FA and 10% MIRHA with $w/b > 0.35$ were categorized in class VF1, while FMSCC 3% SP with 10% FA and 10% MIRHA with $w/b < 0.3$ were categorized in class VF2 and $w/b > 0.3$ were categorized in class VF1.

Figure 4. 6 shows the V-funnel results of concrete with 100% cement and having different w/b.

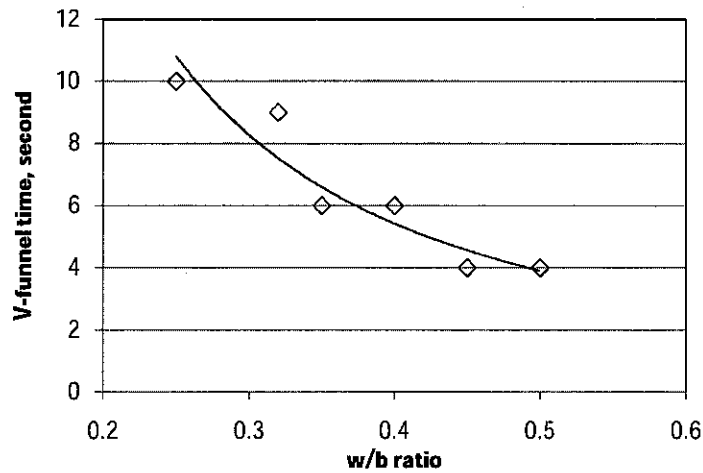


Figure 4. 6. Effect of water-binder ratio on V-funnel test of NPSCC

When a w/b of 0.25 was used the V-funnel time was obtained as 10 seconds whereas with 0.5 w/b it was reduced to 4 second. The following statistical correlation was obtained.

$$V_F = 1.4086w_b^{-1.47} \quad (4.5)$$

$$R^2 = 0.9$$

Based on EFNARC guidelines, NPSCC for 3% SP with w/b < 0.3 were categorized in class VF2, while for SCC with w/b > 0.3 were categorized in class VF1.

Figure 4. 7 presents the comparison of the effects of w/b on the V-funnel tests of the five different categories that contained 10% filler and 3% SP and the fifth categories with 100% cement.

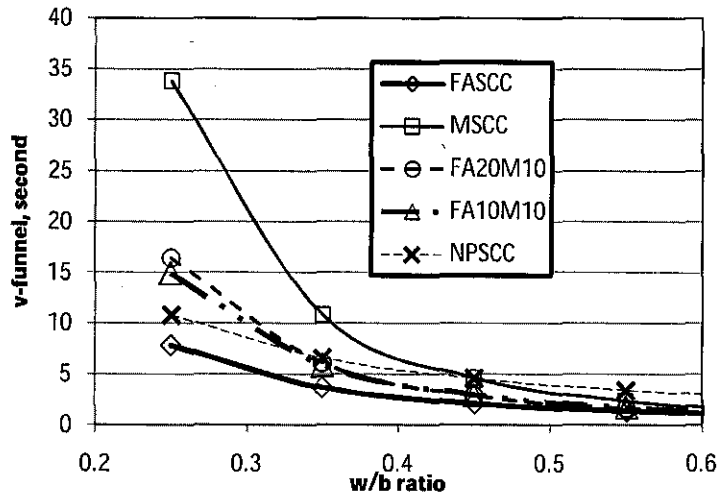


Figure 4. 7. Trend line of V-funnel time for 3% SP and 10% pozzolan and NPSCC

It can be deduced that at lower w/b such as 0.25 fly ash and 100% cement showed the lower V-funnel reading whereas at higher w/b such as 0.45 and above all mixes show V-funnel results between 4 – 4.5 seconds. This result confirmed by Felekoğlu, et al. [174], that the effect of water-binder ratio and superplasticizers dosage were significant on slump flow and V-funnel time and the result is presented in Figure 4. 8.

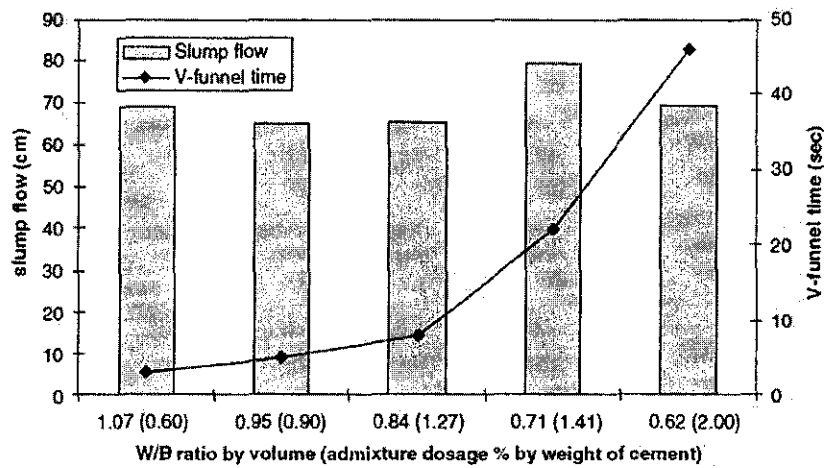


Figure 4. 8. Effect of w/b ratio and admixture dosage on slump flow and V-funnel

Source: Felekoğlu, et al. [174]

The result indicated that with the reduction of free water content simultaneously, the increase in superplasticizers dosage is not adequate to obtain similar V-funnel

times in the range of permissible slump-flow values, and the effect of water reduction on V-funnel times was more dominant than the effect of superplasticizers dosage.

4.4.2. Effect of Water-binder Ratio on L-box Test

L-box test is used to determine the passing capability of concrete from one zone to another. For example when concrete is poured from vertical chute to a beam formwork it is desired that it should spread uniformly without being hindered by steel reinforcement. To assess the passing ability of SCC, the L-box ratio acceptable range in Table 2. 11 suggested by Daczko and Constantiner [77] are detailed in Table 4. 2.

Table 4. 2. L-box ratio acceptable range

Class	L-box ratio
LB1	> 0.9
LB2	0.75 – 0.9
LB3	< 0.75

The concrete without any L-box value (the fresh concrete does not touch the front wall of L-box) is not categorized as self compacting concrete as it cannot pass through the obstacle freely.

Figure 4. 9 shows that increasing water-binder ratio linearly increases the passing ratio of fly ash self compacting concrete. Passing ratio of 0.25 water-binder ratio was obtained as low as 0.33, in other word the rheological properties or workability is low (but it can still flow easily as compared to normal concrete), so this water-binder ratio will be only suitable for beam application with very carefully water measurement in mix and also control water content in aggregate to make sure its SSD conditions.

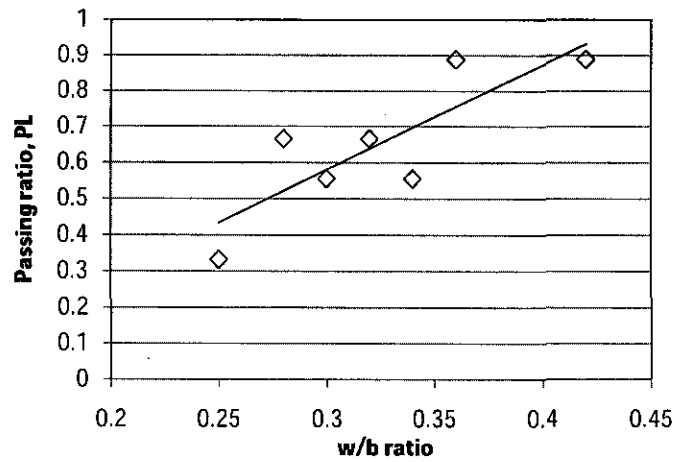


Figure 4. 9. Effects of w/b on the passing ratio, P_L for 10% fly ash with 3% SP

Based on Table 4. 2, FASCC 10% fly ash 3% SP with w/b > 0.4 were categorized in class LB1, concrete with w/b between 0.35 – 0.4 were categorized in class LB2, while concrete with w/b < 0.35 were categorized in class LB3. Water-binder ratio more than 0.4 gave the good result, but by visual investigation it was found that the fresh concrete is hard to handle due to segregation and severe bleeding. The effect of water-binder ratio on passing ratio, P_L followed the linear straight line function correlation as shown below:

$$P_L = 2.925w_b - 0.298 \quad (4. 6)$$

$$R^2 = 0.690$$

where P_L = Passing ratio

w_b = water-binder ratio

Effect of water-binder ratio on passing ratio, P_L of 10% MIRHA and 3% superplasticizers has almost same as fly ash, that are shown in Figure 4. 10.

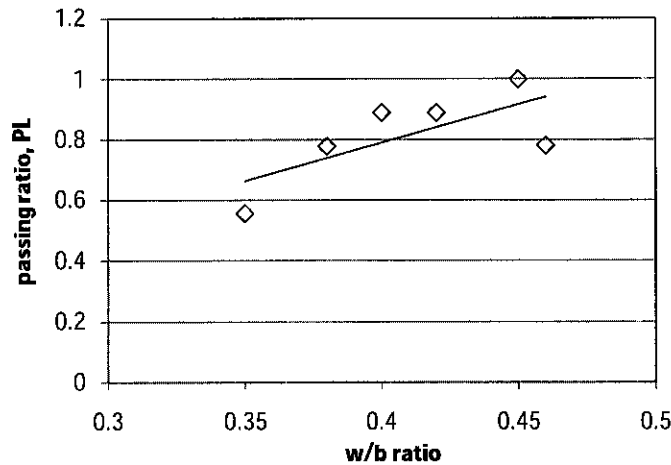


Figure 4. 10. Effects of w/b on the passing ratio for 10% MIRHA with 3% SP

Based on Table 4. 2, MSCC 10% fly ash 3% SP with $w/b > 0.43$ were categorized in class LB1, concrete with w/b between $0.38 - 0.43$ were categorized in class LB2, while concrete with $w/b < 0.38$ were categorized in class LB3. From the result shown in Figure 4. 10 following correlation was obtained:

$$P_L = 2.537w_b - 0.225 \quad (4. 7)$$

$$R^2 = 0.492$$

Memon, et al. [30] found that the results showed that the ratio of L-box increased with the increase in the quantity of superplasticizers used for flowability. The ratio decreased proportionally with the increased quantity of RHA.

Figure 4. 11 shows the effects of water-binder ratio on the passing ratio, for FMSCC 20% fly ash and 10% MIRHA with 3% SP and also FMSCC 10% fly ash and 10% MIRHA with 3% SP.

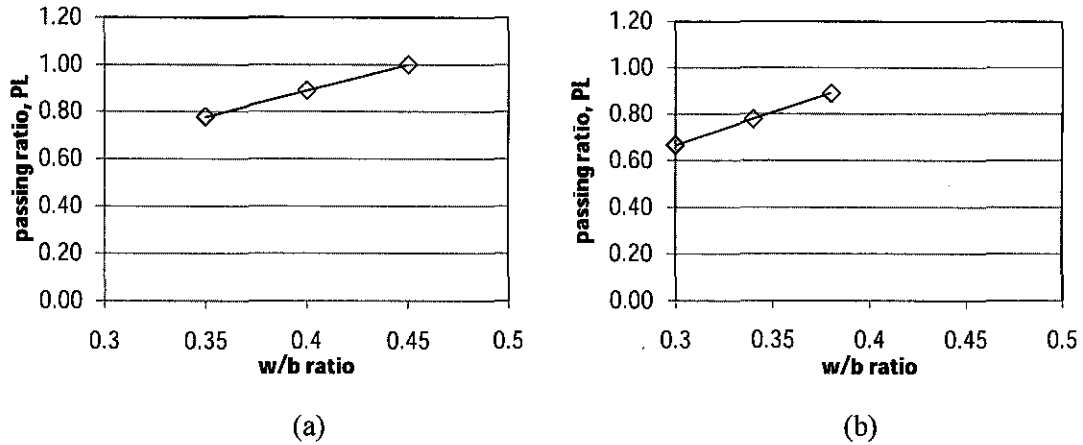


Figure 4. 11. Effects of water-binder ratio on the passing ratio, for (a) 20% fly ash and 10% MIRHA with 3% SP ; (b) 10% fly ash and 10% MIRHA with 3% SP

Based on Table 4. 2, FMSCC 20% fly ash 10% MIRHA and 3% SP with $w/b > 0.4$ were categorized in class LB1, while concrete with $w/b < 0.4$ were categorized in class LB2. FMSCC 10% fly ash 10% MIRHA and 3% SP with $w/b > 0.4$ were categorized in class LB1, concrete with w/b between 0.32 – 0.4 were categorized in class LB2, while concrete with $w/b < 0.32$ were categorized in class LB3. Combination of 20% FA & 10% MIRHA and 10% FA & 10% MIRHA with the results are plotted in Figure 4. 11 and has shown the following correlations respectively.

$$P_L = 2.222w_b \text{ and } P_L = 2.777w_b - 0.166 \quad (4. 8)$$

As compared to the correlations obtained for V-funnel test, the correlations for P_L showed low R^2 value, which means the data is scattered. Both of the mixes has almost same slope of P_L with only 0.5 difference and shift with 0.166 lower for 10% fly ash and 10% MIRHA, it was proven that fly ash increase the workability.

Figure 4. 12 shows the effect of water-binder ratio on the passing ratio of 100% cement with 3% SP concrete.

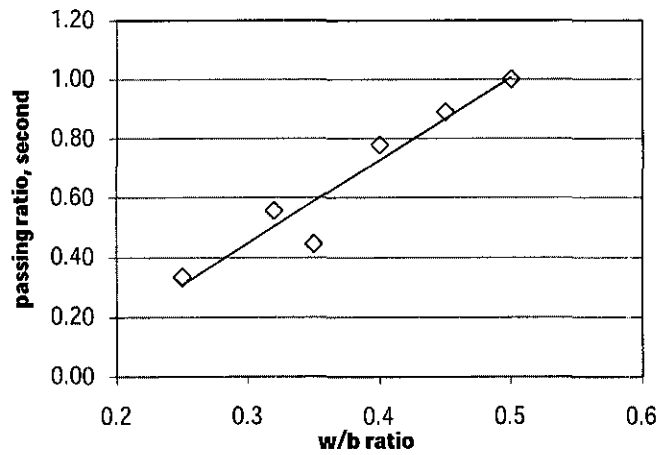


Figure 4. 12. Effects of water-binder ratio on the passing ratio, for no pozzolan with 3% SP

Based on Table 4. 2, NPSCC 3% SP with $w/b > 0.43$ were categorized in class LB1, concrete with w/b between $0.38 - 0.43$ were categorized in class LB2, while concrete with $w/b < 0.38$ were categorized in class LB3. In this case the data was well distributed and a best linear correlation was obtained as.

$$P_L = 2.785w_b - 0.387 \quad (4.9)$$

$$R^2 = 0.922$$

Figure 4. 13 contains the trend lines of all categories of concrete that are showing the relationship between w/b and the passing ratio, P_L . From the point of view of passing ratio, P_L again the FA concrete has shown the better rheology as compared to all other categories.

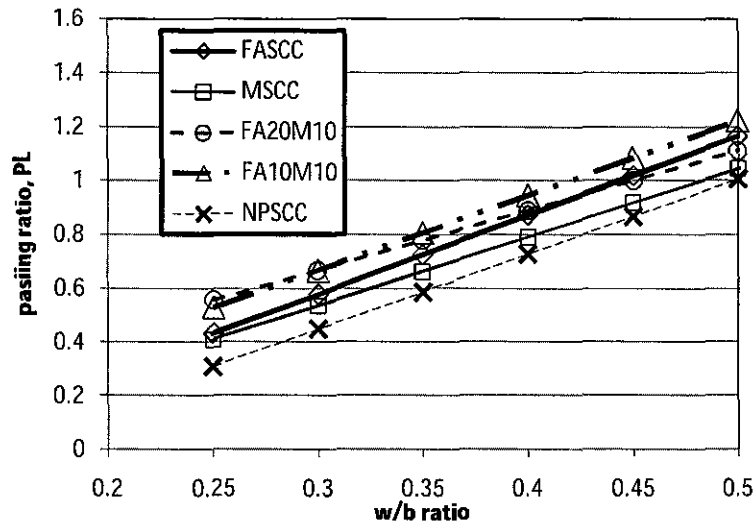


Figure 4. 13. Trend line of passing ratio for 3% SP and 10% pozzolan

Felekoğlu, et al. [174] stated that experimental measurements with L-box ratio indicate the filling and passing ability of each mixture. There is a risk of blocking of the mixture when the L-box blocking ratio is below 0.8, but there are some concerns when this mix is applied to full-scale trials. While it was reported that L-box ratio of 0.6 was found to be sufficient to obtain good filling ability. The mixtures having a water/cement ratio greater than 0.48 have a L-box ratio greater than 0.8, but water/cement ratio lower than 0.48 still can be applied.

Felekoğlu, et al. [174] also made relationship between air content and w/b, and presented graphically in Figure 4. 14. From this figure indicated that reducing free water while increasing the superplasticizers dosage resulted in an increase of viscosity. Increased air percentage attributed to the entrapped air bubbles that could not rise and escape from the surface due to high viscosity, and superplasticizers caused the air trapping during mixing as a side effect.

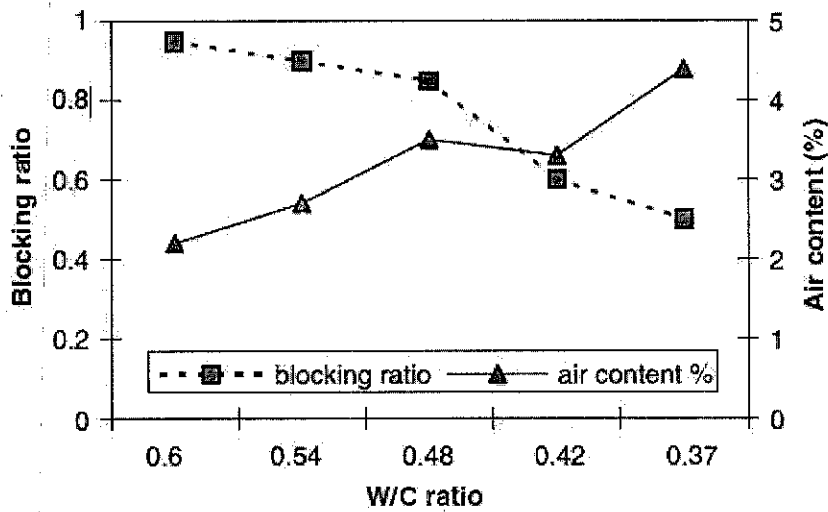


Figure 4. 14. Relationship between air content and w/b

Source: Felekoğlu, et al. [174]

4.4.3. Effect of Water-binder Ratio on T_{500} Test

T_{500} test is indication of flowability of concrete. There should be an inverse relationship between T_{500} -time and w/b. Figure 4. 15 shows the T_{500} results of 10% FA with 3% SP concrete with different w/b.

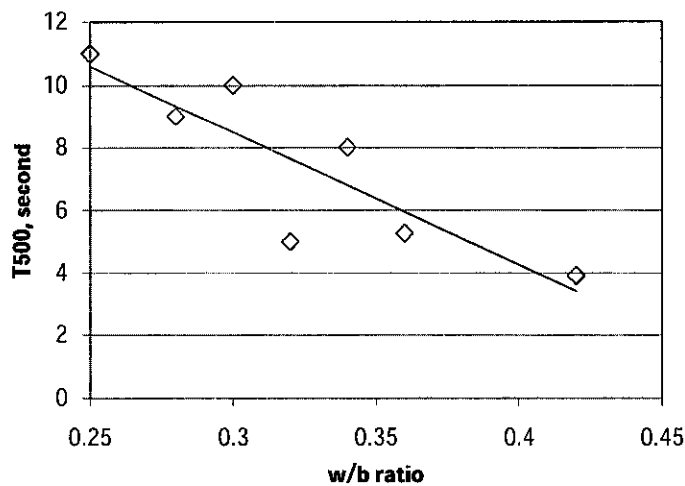


Figure 4. 15. Effects of w/b on the T_{500} for 10% fly ash with 3% SP

Based on EFNARC guideline, all FASCC for 3% SP and 10% fly ash pozzolan with any w/b were categorized in class VS2. As predicted, an inverse linear

relationship was obtained between w/b and the T_{500} time for fly ash concrete. At the lowest w/b of 0.25 the T_{500} time was 11 sec whereas at the highest w/b of 0,42 the T_{500} was 4 sec. A linear correlation formula was:

$$T_{500} = -42.18w_b + 21.13 \quad (4. 10)$$

$$R^2 = 0.74$$

where $T_{500} = T_{500}$ time, seconds
 $w_b =$ water-binder ratio

Figure 4. 16 shows the effect of w/b on the T_{500} for MSCC for 10% MIRHA and 3% SP.

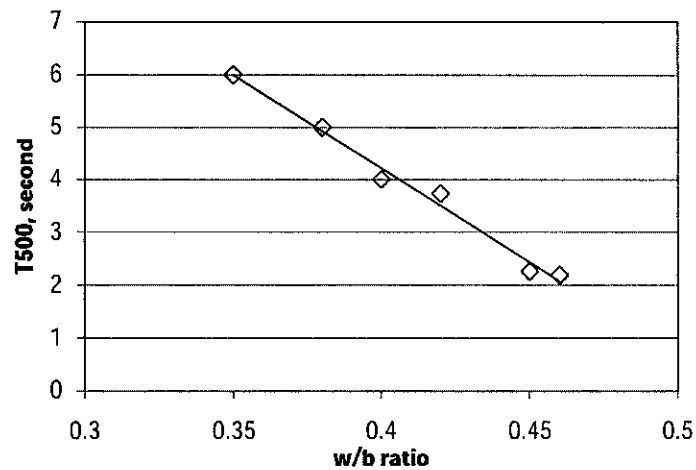


Figure 4. 16. Effects of w/b on the T_{500} for 10% MIRHA with 3% SP

Based on EFNARC guideline, all MSCC for 3% SP and 10% fly ash pozzolan with any w/b were categorized in class VS2. The lowest T_{500} time exhibited by MSCC with water-binder ratio 0.46 was 2.19 second. Effect of w/b on the T_{500} for 10% MIRHA with 3% superplasticizers follows this equation.

$$T_{500} = -35.54w_b + 18.43 \quad (4. 11)$$

$$R^2 = 0.987$$

Figure 4. 17 illustrate the T_{500} time FMSCC for 20% fly ash and 10% MIRHA with 3% SP.

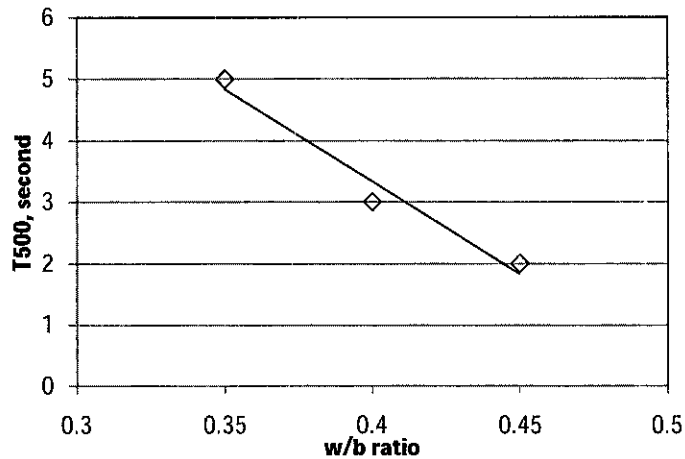


Figure 4. 17. Effects of water-binder ratio on the T_{500} , for 20% fly ash and 10% MIRHA with 3% SP

Figure 4. 17 shows that SCC for 20% fly ash and 10% MIRHA with 3% SP and water-binder ratio of 0.35 the T_{500} time was 5 second which satisfies the SCC specification based on ENFARC guideline the concrete with $w/b > 0.45$ were categorized in class VS1 and concrete with $w/b < 0.45$ were categorized in class VS2. The relationship between water-binder ratio and the T_{500} , for 20% fly ash and 10% MIRHA with 3% superplasticizers was in accordance with following equation.

$$T_{500} = -30w_b + 15.33 \quad (4.12)$$

$$R^2 = 0.964$$

Figure 4. 18 depict the effects of water-binder ratio on the T_{500} , for 10% fly ash and 10% MIRHA with 3% SP

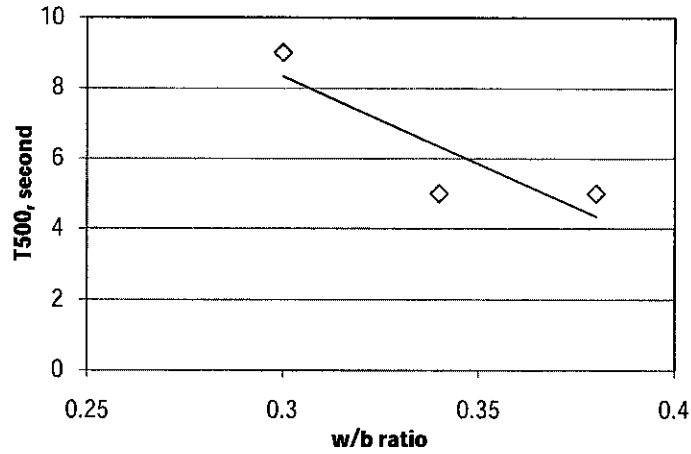


Figure 4. 18. Effects of water-binder ratio on the T_{500} , for 10% fly ash and 10% MIRHA with 3% SP

Figure 4. 18 shows that for SCC with 10% fly ash and 10% MIRHA, 3% SP and 0.3 water-binder ratio the T_{500} time was 9 second which satisfies the SCC specification. The shortest time was obtained for SCC with 0.38 water-binder ratio and was 5 second, which also confirmed the SCC requirement from EFNARC and were categorized in class VS2. Effects of water-binder ratio on the T_{500} , for 10% fly ash and 10% MIRHA with 3% superplasticizers follow this relationship.

$$T_{500} = -50w_b + 23.33 \quad (4.13)$$

$$R^2 = 0.75$$

Figure 4. 19 represent the effects of water-binder ratio on T_{500} , for no pozzolan SCC with 3% SP

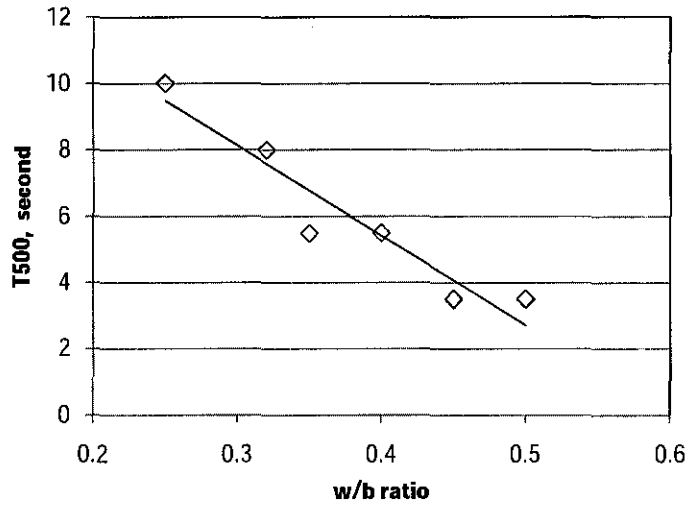


Figure 4. 19. Effects of water-binder ratio on T_{500} , for no pozzolan SCC with 3% SP

The 100% OPC SCC with 0.25 water-binder ratio showed 10 second of T_{500} time. On the other hand the shortest T_{500} time was 3.5 second for SCC with 0.5 w/b. Based on ENFARC guideline all concrete were categorized in class VS2. Effects of water-binder ratio on T_{500} , for no pozzolan SCC with 3% superplasticizers showed the following correlation.

$$T_{500} = -27.01w_b + 16.22 \quad (4.14)$$

$$R^2 = 0.908$$

Comparison of T_{500} trends of all SCC categories are plotted in Figure 4. 20.

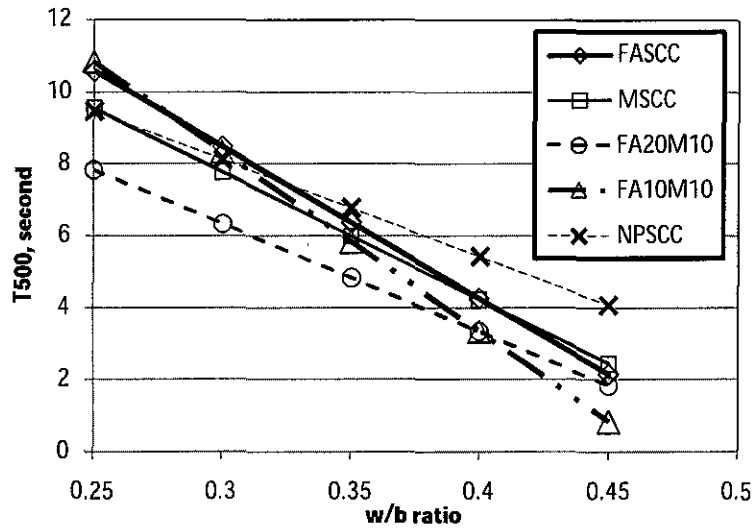


Figure 4. 20. Trend line of T_{500} for 3% SP and 10% pozzolan

It can be seen from Figure 4. 20 shows that fly ash self compacting concrete has shortest time for reaching 500 mm of diameter in high water-binder ratio but longest time in low water-binder ratio. In other words, the relationship FASCC had highest slope compared to the other SCC. While the no pozzolan SCC had the lowest speed of flow compare to other SCC.

4.4.4. Effects of Water-binder Ratio on Slump Flow Test

Flow ability is the simplest way to determine the compactibility of self compacting concrete. This test also gives an indication of consistency and viscosity of concrete. Figure 4. 21 illustrates the effects of w/b on the slump flow values for 10% fly ash with 3% SP

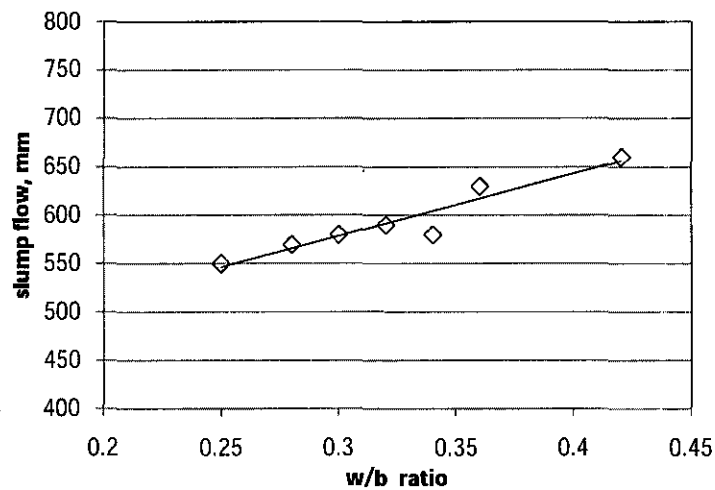


Figure 4. 21. Effects of w/b on the slump flow values for 10% fly ash with 3% SP

A diameter of 550 mm of slump flow for 10% FA and 3% SP concrete with 0.25 w/b was obtained. The slump flow of all seven mixes was varied between 550 mm and 660 mm. The 660 mm diameter was obtained for concrete with w/b of 0.42.

Based on EFNARC guideline, FASCC for 3% SP and 10% fly ash pozzolan with w/b < 0.375 were categorized in class SF1, while for SCC with w/b > 0.375 were categorized in class SF2. A good correlation slump flow and the w/b obtained as:

$$S_F = 643w_b + 385.7 \quad (4. 15)$$

$$R^2 = 0.905$$

where S_F = Slump flow diameter, mm

w_b = water-binder ratio

Figure 4. 22 shows the effects of w/b on the slump flow values for 10% MIRHA with 3% SP

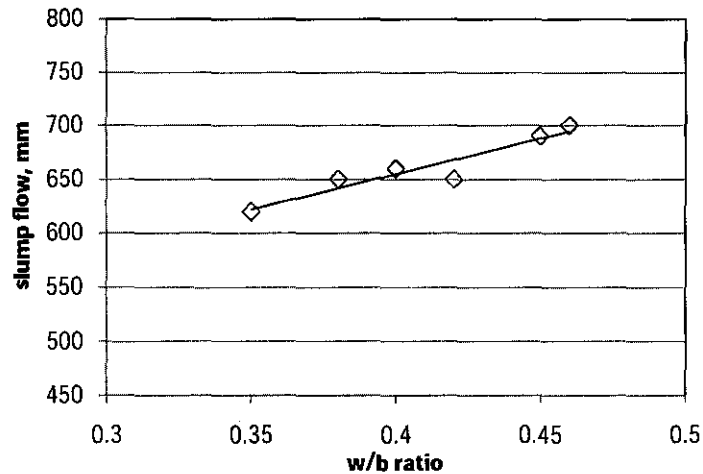


Figure 4. 22. Effects of w/b on the slump flow values for 10% MIRHA with 3% SP

From Figure 4. 22 it is illustrated that MSCC with water-binder ratio 0.35 reached 620 mm of slump flow diameter while the MSCC with water-binder ratio 0.45 reached 690 mm. Based on EFNARC guideline, MSCC for 3% SP and 10% fly ash pozzolan with w/b < 0.375 were categorized in class SF1, while for SCC with w/b > 0.375 were categorized in class SF2. Effects of water-binder ratio on the slump flow values for 10% MIRHA with 3% superplasticizers can be described using this relationship.

$$S_F = 659w_b + 391.4 \quad (4. 16)$$

$$R^2 = 0.892$$

Figure 4. 23 depicts the effects of w/b on the slump flow values for 20% fly ash and 10% MIRHA with 3% SP

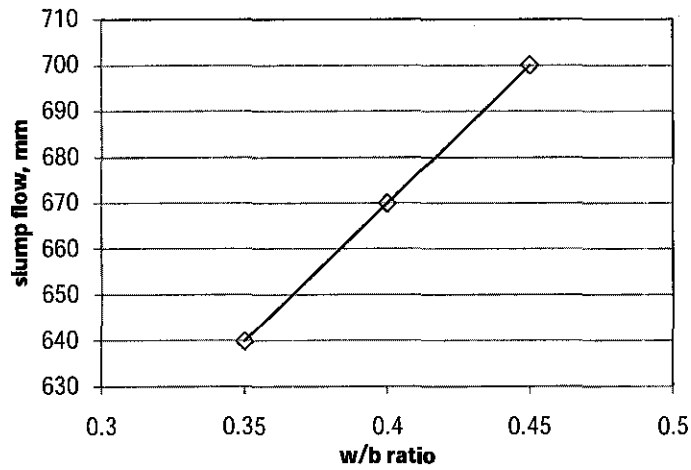


Figure 4. 23. Effects of w/b on the slump flow values for 20% fly ash and 10% MIRHA with 3% SP

Figure 4. 23 shows that SCC 20% fly ash and 10% MIRHA and water-binder ratio 0.35 had 640 mm diameter of slump flow, while the water-binder ratio 0.45 reached 700 mm diameter of slump flow. Based on EFNARC guideline, FMSCC for 3% SP and 20% fly ash 10% MIRHA with $w/b < 0.375$ were categorized in class SF1, while for SCC with $w/b > 0.375$ were categorized in class SF2. Effects of w/b on the slump flow values for 20% fly ash and 10% MIRHA with 3% superplasticizers were found to follow the relationship.

$$S_F = 600w_b + 430 \quad (4. 17)$$

$$R^2 = 1.0$$

Almost similar experiment was work by Memon, et al. [30] obtain the slump flow result as shown in Figure 4. 24. The result indicated the slump flow increased with the increase in the quantity of superplasticizer, while the flow decreased with the increased quantity of RHA.

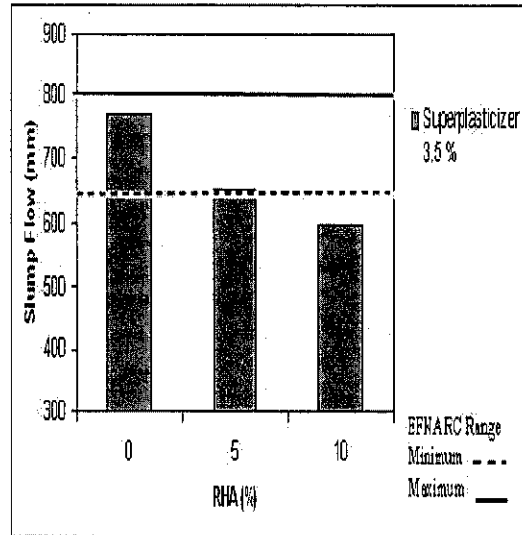


Figure 4. 24. Slump flow with 3.5% SP, 10% RHA and 0.36 w/b

Source: Memon, et al. [30]

Figure 4. 25 illustrates effects of w/b on the slump flow values for 10% fly ash and 10% MIRHA with 3% superplasticizer

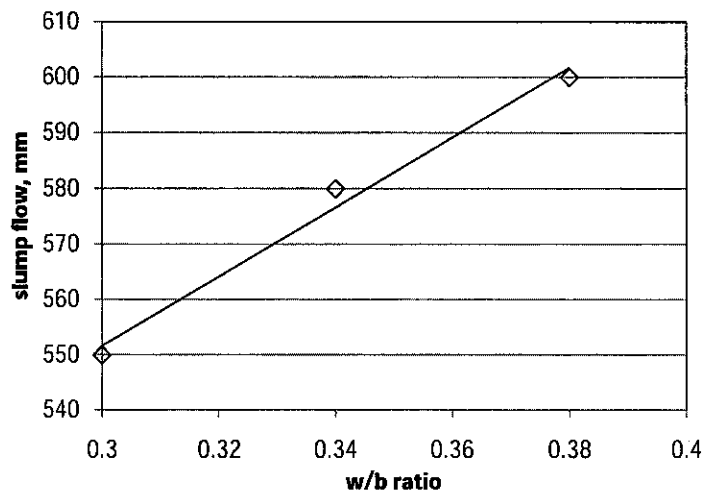


Figure 4. 25. Effects of w/b on the slump flow values for 10% fly ash and 10% MIRHA with 3% SP

Based on EFNARC guideline, all FMSCC for 3% SP and 10% fly ash 10% MIRHA with were categorized in class SF1 and were found to follow the relationship.

$$S_F = 625w_b + 364.1 \quad (4. 18)$$

$$R^2 = 0.986$$

Figure 4. 26 shows effects of w/b on the slump flow values for no pozzolan SCC with 3% superplasticizer.

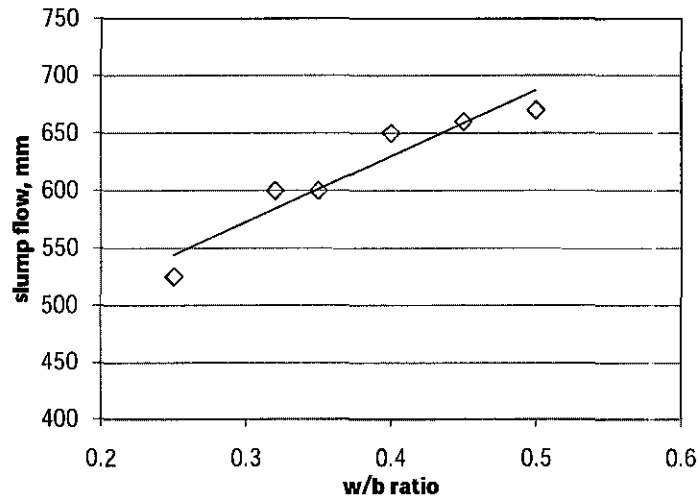


Figure 4. 26. Effects of w/b on the slump flow values for no pozzolan SCC with 3% SP

Based on EFNARC guideline, NPSCC with 3% SP and 20% fly ash 10% MIRHA with w/b < 0.4 were categorized in class SF1, while NPSCC with w/b > 0.4 were categorized in SF2 and were found to follow the relationship.

$$S_F = 572.6w_b + 400.8 \quad (4.19)$$

$$R^2 = 0.911$$

Figure 4. 27 presents the comparison of trends of all categories of mixes.

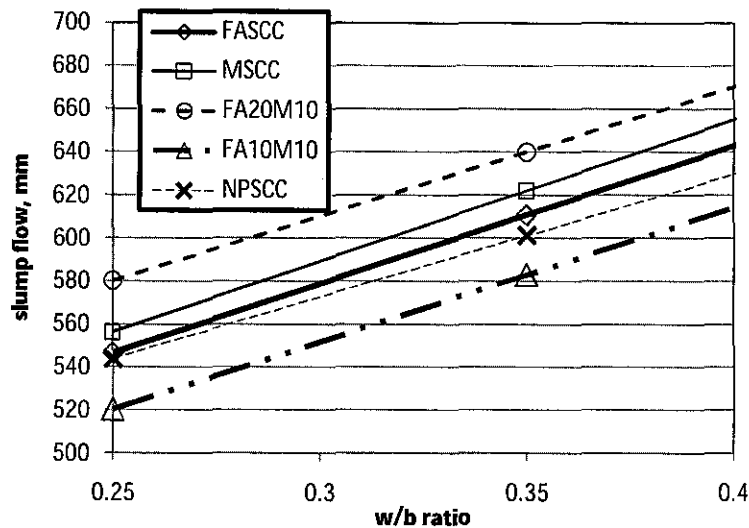


Figure 4. 27. Trend line of slump flow for 3% SP and 10% pozzolan and NPSCC

It was observed that all trend lines are almost parallel to each other. It was noticed that the concrete mix with a combination of 20% FA and 10% MIRHA showed the highest value of slump flow at all w/b. It was due to the reason that 20% fly ash content refined the consistency of concrete to a high degree.

4. 5. Effect of Superplasticizers to Rheological Properties

In this study the superplasticizers of Naphthalene Formaldehyde Sulphonate Type F High Range Water Reducer type was used, it is the most expensive among all component of SCC; therefore its optimum dosage will not only be technical value but also from the economic point of view. Increasing the superplasticizers content might be expected to give better performance in rheological properties, but too much superplasticizers will tend to cause severe segregation and bleeding. Neville [60] discussed the amount of superplasticizers for increasing the workability of the mix, they suggested that the normal dosage of superplasticizers should be between 0.3 – 0.8% by weight of binder, with the liquid superplasticizers containing only about 40% of active material. When superplasticizers is used to reduce the water content in fresh concrete, the dosage should be greater than 1.2 – 4.8%. To understand the wider range

of superplasticizer, the effect of 1.4% - 6% dosage of superplasticizers on the rheological properties were investigated in this study.

4.5.1. Effect of Superplasticizers on V-funnel Test

The effect of superplasticizers content on the V-funnel test results is shown in Figure 4. 28 and Figure 4. 29.

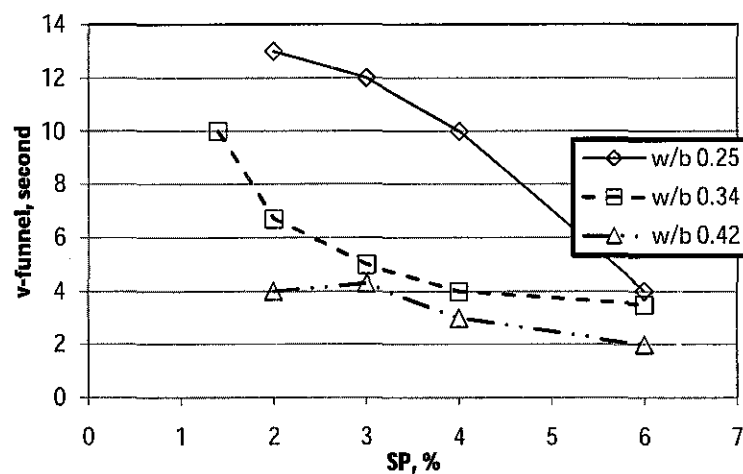


Figure 4. 28. Effects of superplasticizers content on the V-funnel test values for 10% fly ash with different w/b

Based on EFNARC guideline, FASCC with w/b 0.25 and 10% fly ash with SP > 5% were categorized in class VF1, while for SCC with SP < 5% were categorized in class VF2. FASCC with w/b 0.34 and 10% fly ash with SP > 2% were categorized in class VF1, while for SCC with SP < 2% were categorized in class VF2. And all FASCC with w/b 0.42 and 10% fly ash with any percentage of SP were categorized in class VF1.

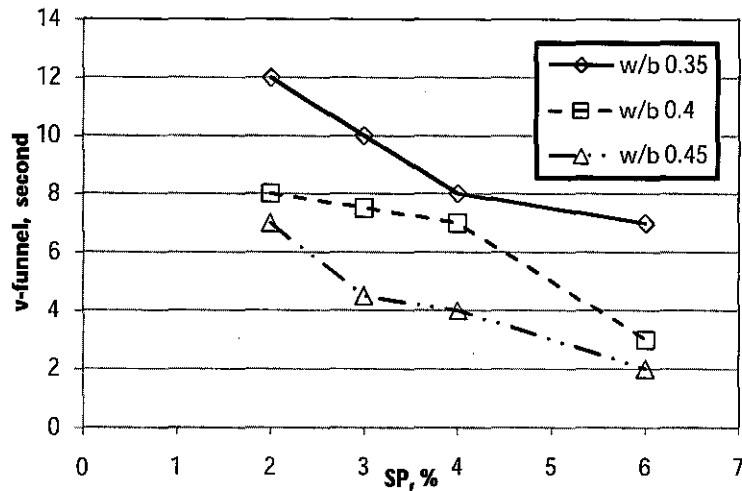


Figure 4. 29. Effects of superplasticizers content on the V-funnel test values for 10% MIRHA with different w/b

Based on EFNARC guideline, MSCC with w/b 0.35 and 10% MIRHA with SP > 4% were categorized in class VF1, while for SCC with SP < 4% were categorized in class VF2. MSCC with w/b 0.4 and 10% fly ash with SP > 2% were categorized in class VF1, while for SCC with SP < 2% were categorized in class VF2. And all MSCC with w/b 0.45 and 10% fly ash with any percentage of SP were categorized in class VF1.

The Figure 4. 28 shows the effects of using 1.4, 2, 3, 4 and 6% superplasticizers contents on the V-funnel test results of 10% FA concrete with 0.25, 0.34, and 0.42 w/b. Observations showed that V-funnel time of less than 3 second usually causes the bleeding and segregation during the placement of concrete into the mould. It was observed that for 10% FA concrete at w/b of 0.34 and 0.42 there was a variation of 1.5 sec in V-funnel readings with the increase in SP content from 3% to 6%. Whereas at a w/b of 0.25 the effect of SP dosage was very significant. At 3% V-funnel was 12 sec where at 6% SP it was 4 sec. Use fly ash as filler in self compacting concrete needs water-binder ratio in the range as 0.25 until 0.34 with 1 – 4% dosage of superplasticizer. While fly ash self compacting concrete with water-binder ratio more than 0.34 in any dosage of superplasticizers will tend to cause bleeding and segregation and resulted in a serious honeycombing after the demoulding and resulted in low of compressive strength. Use of MIRHA self compacting concrete still can be

accepted with water-binder ratio of 0.35 with 1 – 6% dosage of superplasticizers and water-binder ratio 0.4 with dosage 1 – 5%. For water-binder ratio of 0.45 can be accepted with very carefully dosage of superplasticizer.

Frommenwiler [175] stated that from a concrete technology point of view, a w/c of 0.25 is sufficient for the hydration of the cement, while in normal concrete, such w/c are not workable. Depending on fines filler content, the workability even of these mixes are not necessarily yet flow, while segregation and bleeding are other problems facing in relation to high water contents. In order to reduce the water content and for improving workability, superplasticizers are essential. Figure 4. 30 shows the correlation w/c ratio and concrete workability.

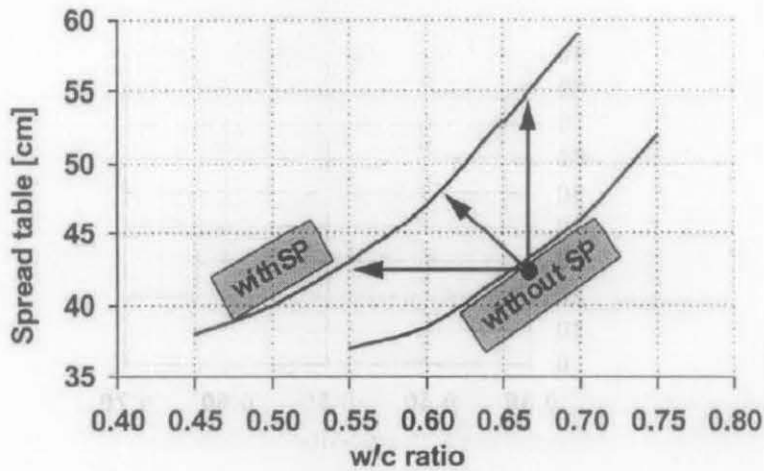


Figure 4. 30. Correlation between w/c and workability of concrete

Source: Frommenwiler [175]

4.5.2. Effect of Superplasticizers on L-box Test

The effect of superplasticizers to the L-box test is shown in Figure 4. 31 and Figure 4. 32.

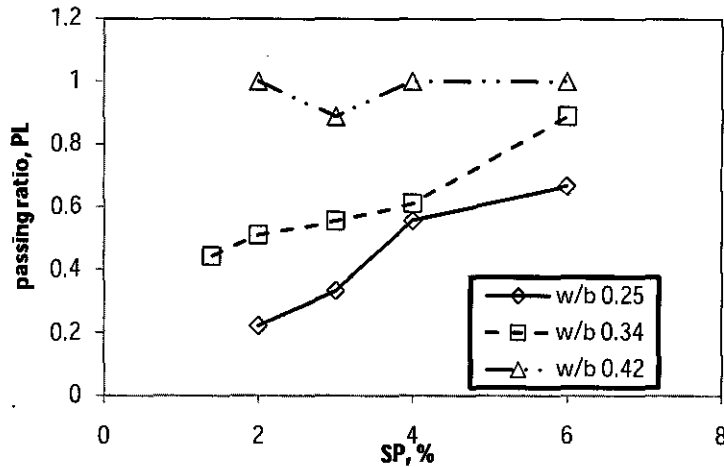


Figure 4. 31. Effects of superplasticizers content on the passing ratio for 10% fly ash with different w/b

Based on Table 4. 2, FASCC 10% fly ash w/b 0.25 with SP < 6% were categorized in class LB3, concrete with w/b 0.34 and SP < 5% were categorized in class LB2, while all concrete with w/b 0.42 were categorized in class LB1.

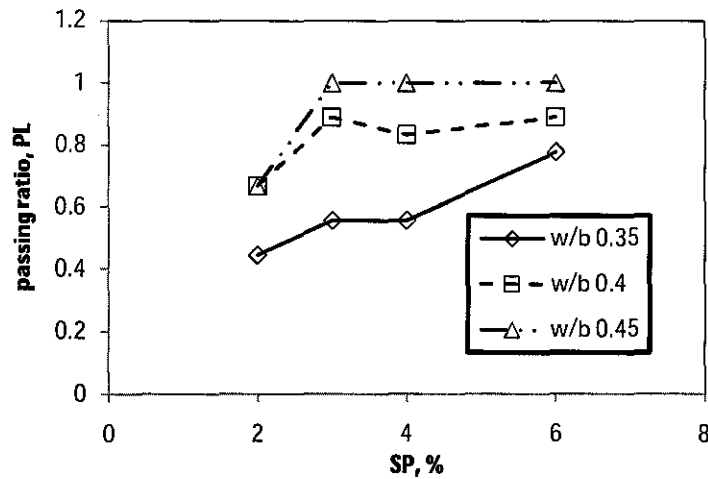


Figure 4. 32. Effects of superplasticizers content on the passing ratio for 10% MIRHA with different w/b

Based on Table 4. 1, FASCC 10% fly ash w/b 0.25 with SP < 6% were categorized in class LB3, concrete with w/b 0.34 and SP < 5% were categorized in class LB2, while all concrete with w/b 0.42 were categorized in class LB1. Figure 4. 31 also illustrates that the water-binder ratio of 0.25 with 2% of superplasticizers dosage has low passing ability. The MIRHA self compacting concrete with water-

binder ratio of 0.35 still performed well with any dosage of superplasticizer. Mixes with water-binder ratio of 0.4 – 0.45 performed well with LB1 class but the segregation and bleeding was occurred severely in SP dosage of 4 – 6%.

4.5.3. Effect of Superplasticizers on T_{500} Test

The effect of superplasticizers content on the T_{500} time is shown Figure 4. 33 for fly ash mixes and Figure 4. 34 for MIRHA mixes respectively.

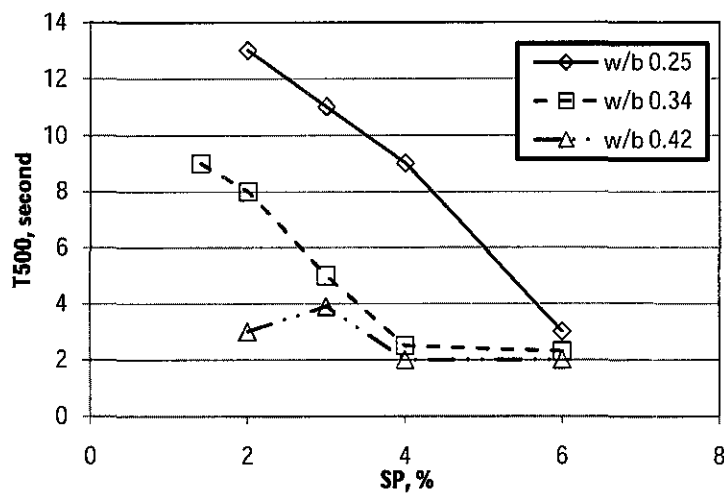


Figure 4. 33. Effects of superplasticizers content on the T_{500} for 10% fly ash with different w/b

Based on EFNARC guideline, all FASCC in any w/b and 10% fly ash pozzolan were categorized in class SF2.

The effects of superplasticizers content on the T_{500} for 10% MIRHA with different w/b in SCC are illustrated in Figure 4. 34.

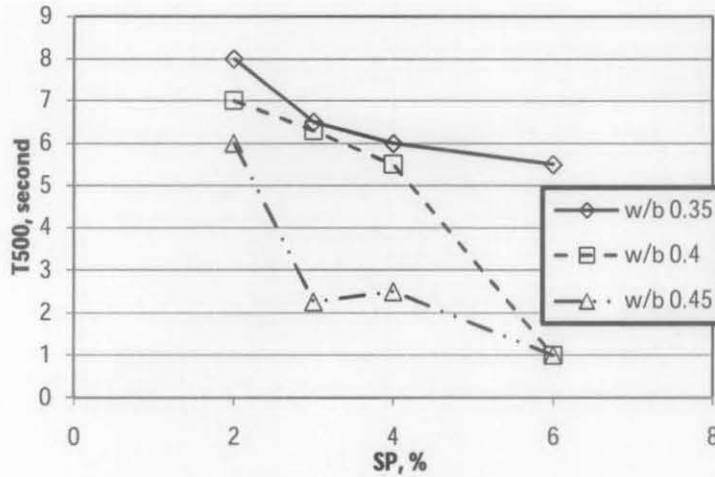


Figure 4. 34. Effects of superplasticizers content on the T_{500} for 10% MIRHA with different w/b

Based on EFNARC guideline, MSCC 10% MIRHA w/b 0.35 were categorized in class VS2, concrete with w/b 0.4 and SP between 2 – 5% were categorized in class VS2 while the concrete with w/b 0.4 that contain SP > 5 were categorized in class VS1 and concrete with w/b 0.45 and SP between 2 – 5% were categorized in class VS2 while the concrete with w/b 0.4 that contain SP > 5 were categorized in class VS1. It's clearly shown that by increasing the amount of superplasticizers will significantly increase the flowing speed. FASCC had higher speed of flowing as compared to the MSCC.

4.5.4. Effect of Superplasticizers on Slump Flow Test

The result of effect of superplasticizers on slump flow test are shown in Figure 4. 35 and Figure 4. 36.

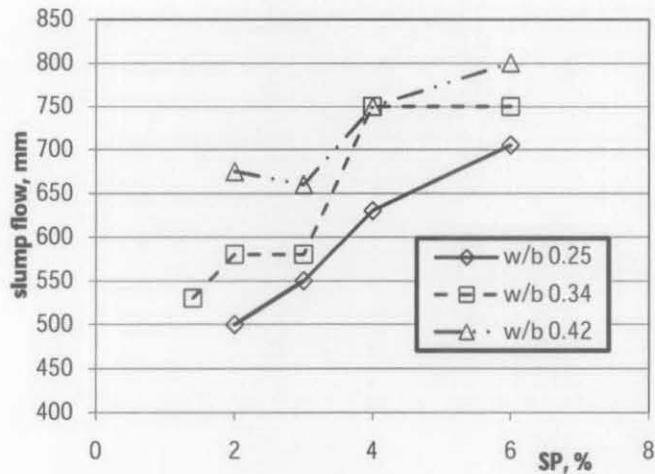


Figure 4. 35. Effects of superplasticizers content on the slump flow for 10% fly ash with different w/b

Based on EFNARC guideline the FASCC 10% fly ash and w/b 0.25 with 2% SP was unaccepted SCC also the concrete with w/b 0.34 and SP 1.4% was out of acceptable range that the minimum slump flow diameter should be 550 mm. The concrete with w/b 0.25 and SP 3 – 4% were categorized in class SF1 and the concrete with SP > 4% were categorized in class SF2. FASCC 10% fly ash and w/b 0.34 with SP 2 – 3% were categorized in class SF1, and concrete with SP > 3% were categorized in class SF2. FASCC 10% fly ash and w/b 0.42 with SP 2 – 4% were categorized in class SF2, while concrete with SP > 4% were categorized in class SF3.

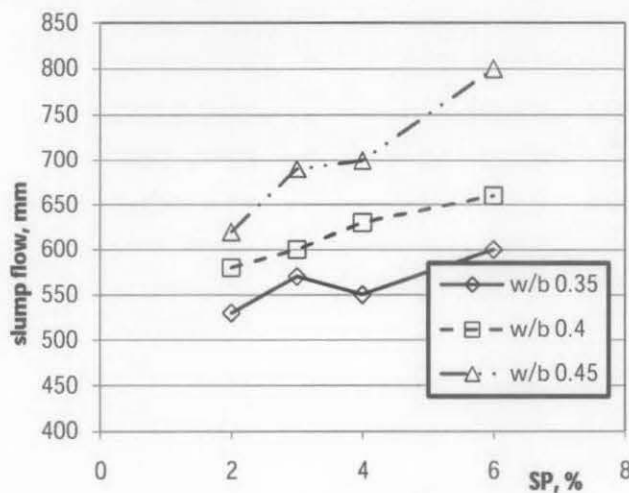


Figure 4. 36. Effects of superplasticizers content on the slump flow for 10% MIRHA with different w/b

Based on EFNARC guideline the MSCC 10% MIRHA ash and w/b 0.35 with 2% SP was out of acceptable range. The concrete with w/b 0.35 and SP > 2% were categorized in class SF1. MSCC 10% MIRHA and w/b 0.4 with SP 2 – 5% were categorized in class SF1, and concrete with SP > 5% were categorized in class SF2. MSCC 10% MIRHA and w/b 0.45 with SP 2% were categorized in class SF2, while concrete with SP 2 – 5% were categorized in class SF2 and concrete with SP > 5% were categorized in class SF3..

Ravindrarajah, et al. [95] investigated the influence the superplasticizers to the slump flow in SCC. Figure 4. 37 shows effect of superplasticizers dosage in self compacting concretes to the slump flow. Superplasticizers start to influence to the concrete on dosage 0.2%. The slump flow was increased with the increase of the superplasticizers dosage.

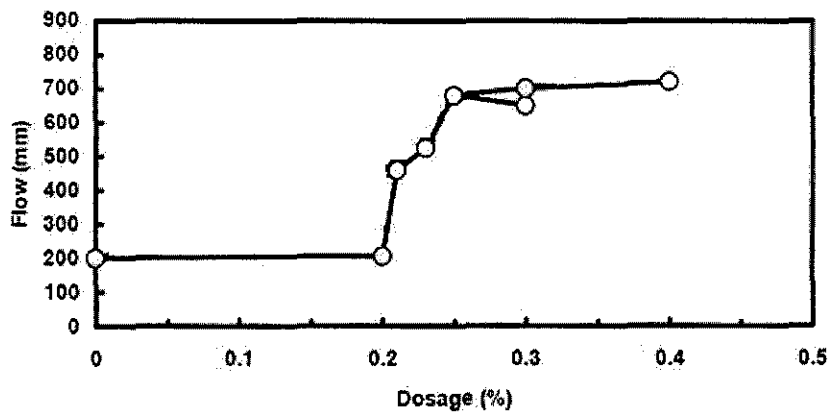


Figure 4. 37. Effect of superplasticizers on slump flow

Source: Ravindrarajah, et al. [95]

4. 6. Effect of Pozzolan Amount on Rheological Parameter

Pozzolan as a cement replacement in self compacting concrete will affect significantly the rheological properties because of its different rate of water absorption compared to the OPC. Figure 4. 38 to Figure 4. 39 show this effect of different content of pozzolan in self compacting concrete.

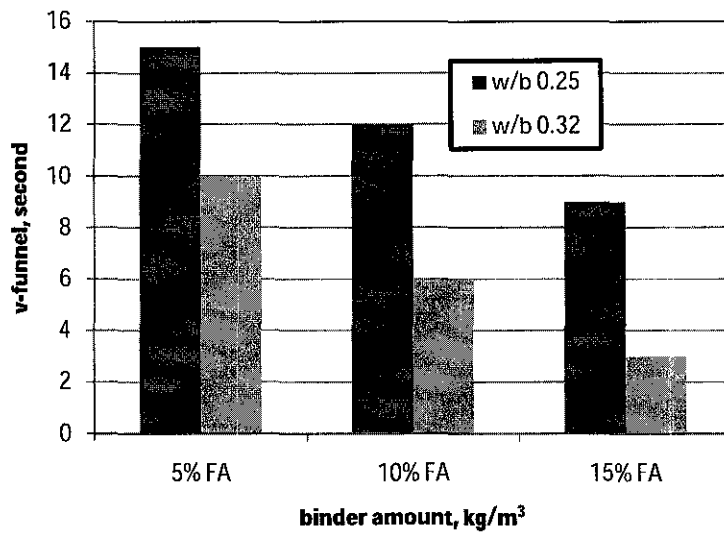


Figure 4. 38. Effects of different cement/fly ash content on the V-funnel test values of 3% SP mixes with different w/b

Based on EFNARC guideline, FASCC w/b 0.25 and 5, 10 and 15% fly ash with SP 3% were categorized in class VF2, for SCC with w/b 0.32; 5% FA and SP 3% were categorized in class VF2, while SCC 3% SP with w/b 0.32; 10 and 15% fly ash were categorized in class VF1.

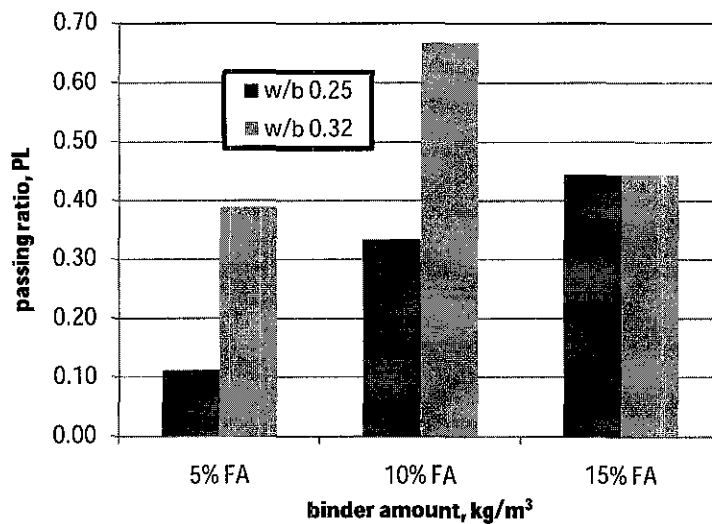


Figure 4. 39. Effects of different cement/fly ash content on the passing ratio, P_L of 3% SP mixes with different w/b

Based on Table 4. 1, FASCC w/b 0.25 and 5, 10 and 15% fly ash with SP 3% and also FASCC w/b 0.32 and 5, 10 and 15% fly ash with 3% SP were categorized in

class LB3. Figure 4. 39 shows that 10% fly ash content, achieved the parameter of good SCC, this confirmed by Ravindrarajah, et al. [26] as shown in Table 4. 3.

Table 4. 3. Mix proportion and rheological properties

Mix	Cement (kg/m ³)	Fly ash (kg/m ³)	Fly ash addition (%)	Slump Flow (mm)	T ₀ (sec.)	T _{5min} (sec.)	Super Plastciser (kg/m ³)
1	350	147	10	650	15	44	2.68
2	350	147	10	665	13	29	2.68
3	350	147	10	605	12	18	2.68
4	350	147	10	750	7	10	2.68
5	350	161	20	695	13	17	2.75
6	350	168	25	740	8	12	2.79

Source: Ravindrarajah, et al. [26]

Figure 4. 40 shows the effects of different cement/fly ash content on the T₅₀₀ test values of 3% SP mixes with different w/b

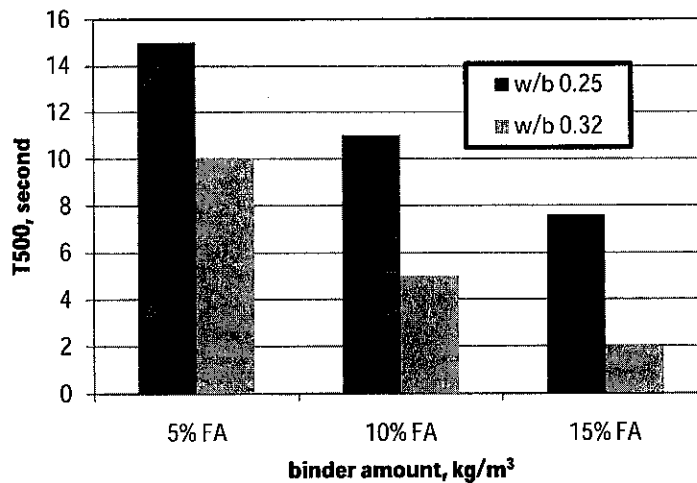


Figure 4. 40. Effects of different cement/fly ash content on the T₅₀₀ test values of 3% SP mixes with different w/b

Based on EFNARC guideline, FASCC w/b 0.25 and 5, 10 and 15% fly ash with SP 3% and also FASCC w/b 0.32 and 5, 10 and 15% fly ash with 3% SP were categorized in class VS2.

Figure 4. 41 shows the effects of different cement/fly ash content on the slump flow test values of 3% SP mixes with different w/b.

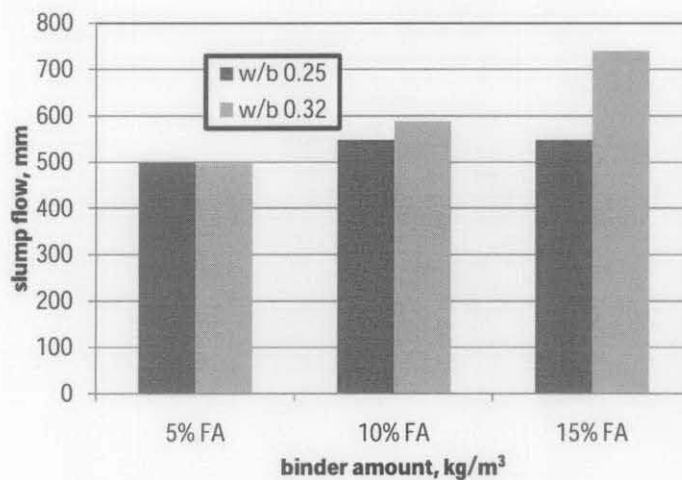


Figure 4. 41. Effects of different cement/fly ash content on the slump flow test values of 3% SP mixes with different w/b

Based on EFNARC guideline, FASCC w/b 0.25 and 0.32 with 5% fly ash; SP 3% were out of range of the SCC acceptance. FASCC w/b 0.25; 10 and 15% fly ash with SP 3% were categorized in class SF1. FASCC w/b 0.32 and 10% fly ash with 3% SP were categorized in class VS1. FASCC w/b 0.32 and 15% fly ash with 3% SP were categorized in class SF2.

Figure 4. 38 to Figure 4. 41 show that the presence of fly ash will significantly increase the self compactability. This behavior also confirmed by Chao-Lung and Meng-Feng [113] that pozzolanic materials including fly ash or MIRHA are densely packed to reduce the amount of cement paste required and pozzolanic material is used to fill void of blended aggregates and therefore increase workability

Dinakar, et al. [22] investigated the influence of fly ash on flow properties. It can also be inferred that both cement content and fly ash had a contrary relation with respect to slump flow, as shown in Figure 4. 42. Increasing the cement content will decrease the amount of fly ash and the slump flow also decrease. This phenomenon is due to the spherical particle shape of fly ash, which acts in a similar way to ball bearings in the concrete which produce higher slump flows. The result also showed

that at high slump flows of around 800 mm the fly ash self compacting concretes still had high segregation resistant.

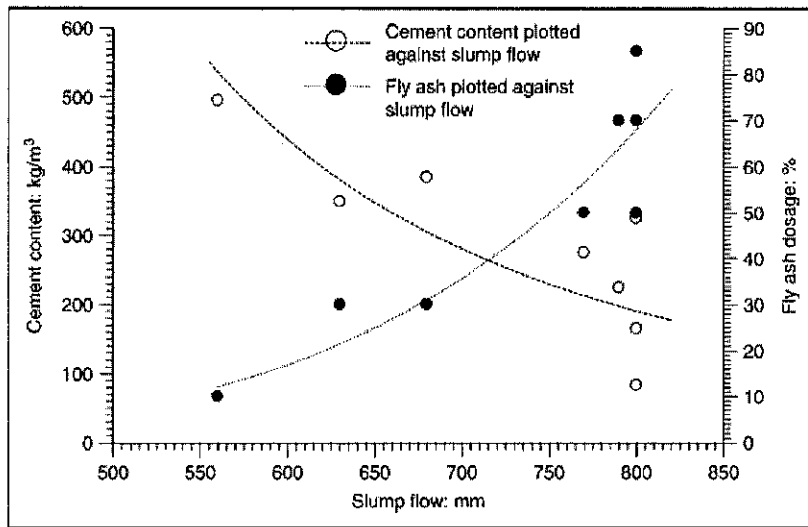


Figure 4. 42. Influence of cement content and fly ash on slump flow

Source: Dinakar, et al. [22]

4.7. Summary

The summarization of SCC acceptance of all mixes can be seen in Table 4. 4

Table 4. 4. SCC acceptance based on rheological properties

NO	Mixes	EFNARC [76]			Daczko and Constantiner [77] L-box	SCC acceptance
		Slump flow	V-funnel	T500		
1	FA5-0.25-3	x	v	v	v	x
2	FA10-0.25-3	v	v	v	v	v
3	FA15-0.25-3	v	v	v	v	v
4	FA5-0.32-3	x	v	v	v	x
5	FA10-0.32-3	v	v	v	v	v
6	FA15-0.32-3	v	v	v	v	v
7	FA10-0.25-3	v	v	v	v	v
8	FA10-0.28-3	v	v	v	v	v
9	FA10-0.3-3	v	v	v	v	v
10	FA10-0.32-3	v	v	v	v	v
11	FA10-0.34-3	v	v	v	v	v
12	FA10-0.36-3	v	v	v	v	v
13	FA10-0.42-3	v	v	v	v	v
14	FA10-0.25-2	x	v	v	v	x
15	FA10-0.25-3	v	v	v	v	v
16	FA10-0.25-4	v	v	v	v	v
17	FA10-0.25-6	v	v	v	v	v
18	FA10-0.34-2	v	v	v	v	v
19	FA10-0.34-3	v	v	v	v	v
20	FA10-0.34-4	v	v	v	v	v
21	FA10-0.34-6	v	v	v	v	v
22	FA10-0.42-2	v	v	v	v	v
23	FA10-0.42-3	v	v	v	v	v
24	FA10-0.42-4	v	v	v	v	v
25	FA10-0.42-6	v	v	v	v	v
26	M10-0.35-2	x	v	v	v	x
27	M10-0.35-3	v	v	v	v	v
28	M10-0.35-4	v	v	v	v	v
29	M10-0.35-6	v	v	v	v	v
30	M10-0.4-2	v	v	v	v	v
31	M10-0.4-3	v	v	v	v	v
32	M10-0.4-4	v	v	v	v	v
33	M10-0.4-6	v	v	v	v	v
34	M10-0.45-2	v	v	v	v	v
35	M10-0.45-3	v	v	v	v	v
36	M10-0.45-4	v	v	v	v	v
37	M10-0.45-6	v	v	v	v	v
38	M10-0.35-3	v	v	v	v	v
39	M10-0.38-3	v	v	v	v	v
40	M10-0.4-3	v	v	v	v	v
41	M10-0.42-3	v	v	v	v	v
42	M10-0.45-3	v	v	v	v	v
43	M10-0.46-3	v	v	v	v	v
44	FA20-M10-0.35-3	v	v	v	v	v
45	FA20-M10-0.4-3	v	v	v	v	v
46	FA20-M10-0.45-3	v	v	v	v	v
47	FA10-M10-0.3-3	v	v	v	v	v
48	FA10-M10-0.34-3	v	v	v	v	v
49	FA10-M10-0.38-3	v	v	v	v	v
50	NP-0.25-3	x	v	v	v	x
51	NP-0.32-3	v	v	v	v	v
52	NP-0.35-3	v	v	v	v	v
53	NP-0.4-3	v	v	v	v	v
54	NP-0.45-3	v	v	v	v	v
55	NP-0.5-3	v	v	v	v	v

Notes: v = accepted SCC; x = unaccepted SCC

Table 4. 4 indicated that 5 mixes were out of SCC acceptable range from total 55 mixes. These unaccepted SCC will be still tested in compressive strength test and durability test. From the result of the rheological characteristic as obtained in this study, following is the summary of major findings:

1. Because of the nature of fly ash it requires less water as compared to MIRHA for obtaining similar level workability. For 10% MIRHA with 3% SP content a w/b of 0.35 was required to achieve the similar rheology as that obtained for 10% FA with 3% SP and 0.25 w/b.
2. V-funnel time for all categories of mixes was varied between 4 sec to 12 sec. For the lowest w/b using 10% FA with 3% SP the time was 12 sec and for the same mix with the highest w/b of 0.42 the measured time was 4 sec.
3. The variation in slump flow was measured between 550 to 650 mm for FA mixes and between 540 to 690 for MIRHA mixes. It means there is about 35% variation in the flowability, which indicate that the water content did appreciable effect the viscosity and consistency of the mixes.
4. L-box test indicates that through congested steel reinforcement whether the concrete with block can pass through due to its own. From higher w/b to lower w/b the passing ratio was obtained as 80% - 90% higher. It means higher w/b significantly affect the passing ability of SCC.
5. The result of the L-box test indicates that the water-binder ratio has a profound effect on the concretes passing ability through congested steel.
6. A medium to high w/b variation with SP content from 3% - 6% did not significantly change the rheological properties of different concrete mixes. 3% SP content with any w/b did not cause bleeding and segregation in any of the mixes.

From experiment indicated that SCC showed less tolerant of changes than ordinary concrete. Self compacting concrete is sensitive in changes amount of water that have large effects on its rheological properties. Furthermore more effort should be taken care to minimize failure in mixing. Some recommendation are given by several researchers, Grace and CoConn [176] stated to produce SCC producer must have quality control program in place with adequate rheological properties measurement, batching accuracy and moisture control in aggregate. Always check and

adjust for moisture in aggregates. Furthermore impose tighter control limits on SCC than on ordinary concrete. Various acceptable for successful SCC must be chosen based on site observation, not every acceptance is suitable to our mix due to the differences of many factors such as type of aggregate, superplasticizer, climate, etc. How much variation can be tolerated depends on the materials used and needs to be determined through testing. SCC performance targets, and mix design, are based on the structural requirements of the element to be placed, as well as the flowability required for placement.

CHAPTER 5

MECHANICAL PROPERTIES OF SCC

5.1. Introduction

This chapter discusses the results of the mechanical properties of SCC containing fly ash and MIRHA as the filler materials. For investigating the mechanical properties of compressive strength, modulus of rupture and the tensile strength were determined. The compressive strength of concrete is one of the fundamental design parameters. In this study the compressive strength was measured from the concrete age of one day until one year. While modulus of rupture and tensile strength are needed for crack width control.

As discussed in Chapter 4 the basic variables affecting of rheological concrete properties were of water-binder ratio and the superplasticizers content. The effects of these variables into the mechanical properties are discussed detail in following sections.

5.2. Compressive Strength of SCC

Compressive strength of different self compacting concrete mixes was determined at 1, 3, 7, 28, 180 and 360 days which complies with BS 1881-111:1983. The detailed results are given in Appendix-B

5.2.1. Effects of Water-binder Ratio

Amount of water in terms of binder content plays important role for compressive strength development at different ages. Particularly for SCC, the amount of water is very important for achieving the rheological properties target as detail discussed in

Chapter 4. Where high amount of water is necessary for workability in the fresh state of concrete, it has much adverse effects on the compressive strength. The following sub-sections discuss the effects of w/b on various types of SCC.

5.2.1.1. Effects of Water-binder Ratio on Compressive Strength of FASCC

Effects of water-binder ratio on compressive strength of 10% fly ash based self compacting concrete with 3% superplasticizers and w/b in the range of 0.25 to 0.42 are discussed in this section. The results of these effects are presented in Figure 5. 1.

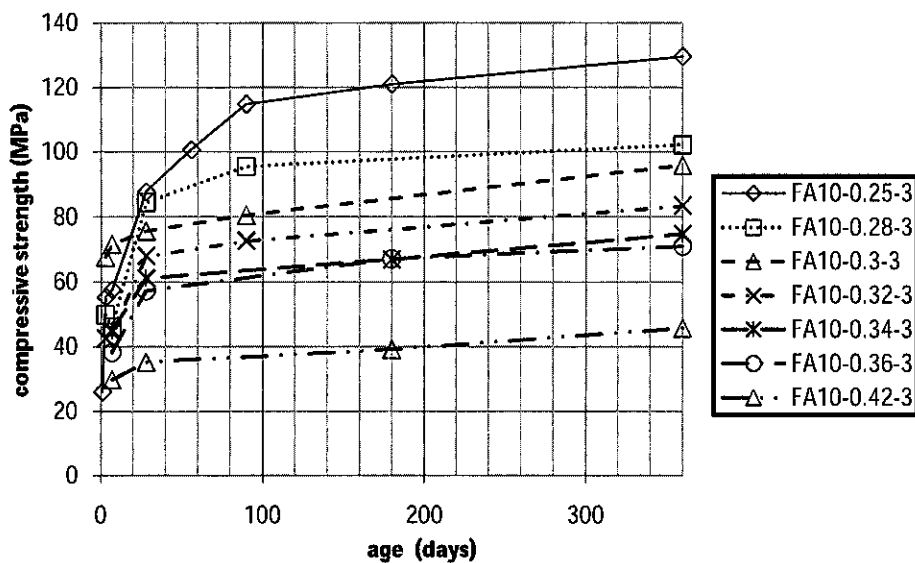


Figure 5. 1. Strength developments of FASCC with 10% fly ash and 3% SP in variation of w/b

As observed in Figure 5. 1 the highest value of compressive strength of 129.5 MPa was obtained at the age of one year with a lowest w/b of 0.25. While as the same mix with higher w/b of 0.42 yielded a value of 45.7 MPa at one year. This is a significant variation in compressive strength, which is almost 3 times. This significant change is solely caused by variation of water content whereas all other ingredients were kept constant. Similarly at the age of 28 days 35.2 MPa was obtained with a w/b of 0.42 and 87.67 MPa was achieved with a w/b of 0.25. The variation is in the same order of magnitude to the difference that was obtained at one year.

It can be seen from Figure 5. 1 that for high compressive strengths, the strength was developed in 3 stages, 7 to 28 days, 28 to 90 days and 90 days to one year. From 7 day till 28 days the gain in compressive strength was 24 to 39%. For example at the age of 7 day with w/b 0.25, the strength was 57.44 MPa, and reached 87.67 MPa at the age of 28 days. From 28 days until 90 days the increment in strength was 16 to 33 MPa. For concrete with w/b 0.28 a strength of 84.5 MPa was measured at 28 days, and was increases to 95.5 MPa at the age of 90 days. From the age of 90 days until one year the strength was increased from 4 to 9%. With w/b of 0.25 strength of 114.77 MPa was determined at the age of 90 days that attained 129.5 MPa when cured for one year. SCC with w/b of 0.28 a value of 95.5 MPa was determined at 90 days that was increase 4% until one year of age that was measured as 102.24 MPa.

Concrete with high w/b compressive strength was developed into two stages such as 7 – 28 days and from 28 days until one year. For FASCC with w/b 0.42 after 7 days 29.78 MPa was measured, whereas at 28 days it reached to 35.2 MPa, which is about 37% increment. Onwards from 28 days until one year age an increment of 5.51 MPa in strength was observed that is calculated as 18% increment. It can be generalized that from mixing until 28 days until one year of age it was developed from moderate to slower rate.

The investigation of optimum water-binder ratio was examined by Poon, et al. [9]. The results have shown that with a fly ash content of 25% and 45%, concrete with a 28-day compressive strength of 80 MPa could be obtained at the w/b of 0.24, while w/b lower than 0.24 gave lower result of compressive strength. A plot of water-binder ratio against concrete strength is given in Figure 5. 2.

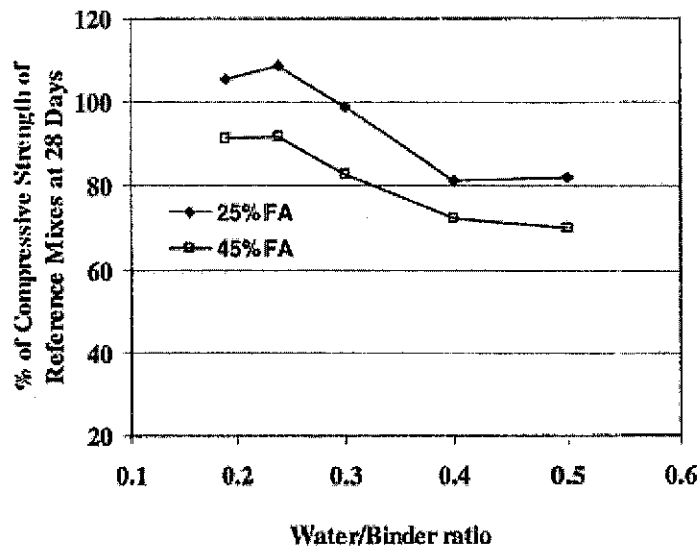


Figure 5. 2. Strength performance of fly ash concrete with different w/b ratios

Source: Poon, et al. [9]

Since with lower w/b concrete strength after 28 days was developed from moderate to higher rate until 90 days that means that fly ash has worked as filler as well as pozzolanic material. On the hand compressive strength with high w/b after 28 days was developed at very slow rate, that means in such concrete fly ash has acted as filler material only.

In order to correlate w/b with the compressive strength measured at 28 days, results are plotted in Figure 5. 3.

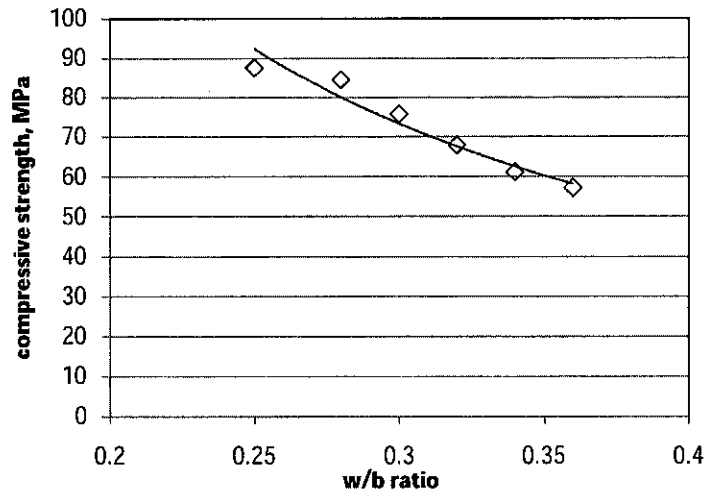


Figure 5. 3. FASCC compressive strength contain 3% SP at variation of water-binder ratio at 28 days

The best correlation between 28 days compressive strength and the w/b for 10% FA concrete with 3% SP as:

$$f'_c = 15.974w_b^{-1.26} \quad (5.1)$$

$$R^2 = 0.949$$

Where f'_c = compressive strength on 28 days

w_b = water-binder ratio

While Sukumar, et al. [23] used the lower dosage of SP ranging 0.4 to 0.7% in SCC containing fly ash, as result the need of water content have to be increased with minimum w/b was 0.34 due to the demand of acceptable rheological properties. These combination of low SP and relative high water content produce the lower compressive strength as compared to the result in this thesis with minimum w/b 0.25 which obtained 87.67 MPa whereas Sukumar, et al. [23] only achieved 81.25 MPa. The mix proportion and result can be seen in Table 5. 1 and Table 5. 2 respectively.

Table 5. 1. Mix proportion for various grade of SCC

Mix ID	Cement (kg/m ³)	Fly ash (kg/m ³)	Quarry dust (kg/m ³)	FA (kg/m ³)	CA (kg/m ³)	w/p ratio	SP % of binder	VMA % of binder
AS30	250	275	--	842	772	0.34	0.4	0.1
BS30	133	275	117	842	772	0.34	0.4	0.1
AS40	333	215	--	835	766	0.33	0.4	0.1
BS40	246	215	87	835	766	0.33	0.4	0.1
AS50	417	153	--	828	759	0.32	0.5	0.1
BS50	357	153	60	828	759	0.32	0.5	0.1
AS60	500	101	--	820	753	0.32	0.6	0.1
BS60	463	101	37	820	753	0.31	0.6	0.1
AS70	583	50	--	813	745	0.31	0.7	0.1
BS70	566	50	17	813	746	0.31	0.7	0.1

Source: Sukumar, et al. [23]

Table 5. 2. Compressive strength of SCC

Table 5
Compressive strength of SCC and the expected strength of conventional concrete as per IS: SP: 23-1982

Mix ID	1 day	3 days	7 days	14 days	28 days
<i>Compressive strength (N/mm²) obtained for different SCC mixes</i>					
AS30	8.14	18.12	27.60	34.91	39.62
BS30	6.05	13.89	21.27	27.32	32.50
AS40	10.32	23.24	35.26	44.18	50.24
BS40	8.12	18.21	28.41	34.63	42.30
AS50	12.76	28.28	43.54	54.52	61.82
BS50	10.22	23.10	34.69	43.65	52.00
AS60	14.61	32.18	49.81	62.45	70.93
BS60	12.36	27.31	41.83	52.03	61.90
AS70	16.21	35.68	55.92	70.68	81.25
BS70	14.30	31.42	48.80	60.90	71.50

Source: Sukumar, et al. [23]

5.2.1.2. Effect of Water-binder Ratio on Compressive Strength of MSCC

Effect of water-binder ratio on compressive strength of MIRHA self compacting concrete with 3% superplasticizers is drawn in Figure 5. 4. As discussed in Chapter 4 MIRHA required higher amount of water compared to fly ash concrete in order to achieve the same workability. Therefore the lowest w/b was kept 0.35 and highest w/b as 0.46 for this group of concrete mixes.

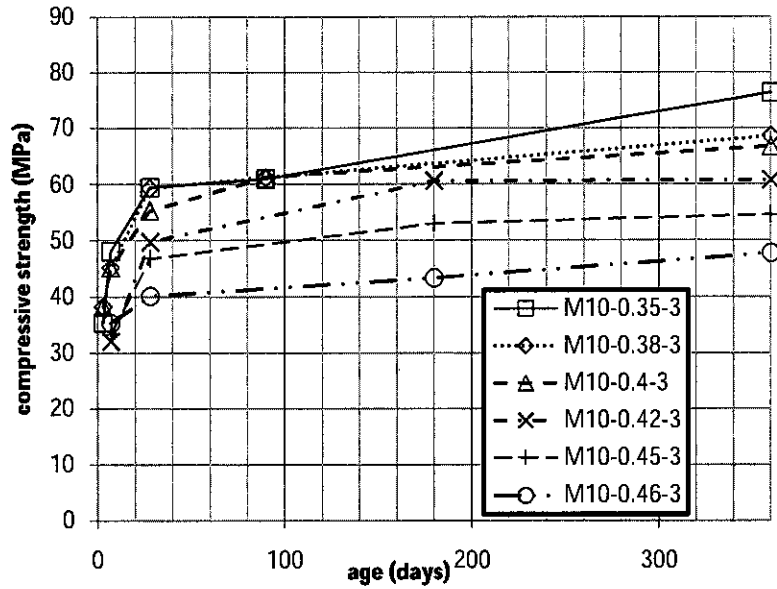


Figure 5. 4. Strength developments of MSCC with 10% MIRHA and 3% SP in variation of w/b

Because of the high water requirement in MSCC, it needs minimum w/b of 0.35 as compared FASCC with only w/b 0.25. The highest compressive strength at the age of one year in MSCC with w/b of 0.35 was 76.4 MPa. In comparison for 10% fly ash concrete with 3% SP with minimum w/b 0.25 the compressive strength was 129.5 MPa which is almost 69% greater than result of MSCC in one year strength.

For MIRHA concrete the compressive strength was generally developed into two stages, 7 days until 28 days and 28 days to one year. At the age of 28 days the highest increment of 70% in compressive strength with respect to 7 days strength was observed for MSCC with w/b of 0.35, i.e. 7 days strength was measured as 48.06 MPa and at the age 28 days it was found as 59.47 MPa. After 28 days the strength development rate was reduced to quite slow. At the age of one year the compressive strength was determined as 76.4 MPa which was 18% higher than the 28 days strength. 28% higher than the 28 days strength.

At higher w/b such as with 0.46 the 7 days strength was achieved as 35.29 MPa that was increased to 40.1 MPa at the age of 28 days, which is about 15% increment. At the age of one year the compressive strength was reached to 47.72 MPa, which was 20% increment.

With the lowest w/b of 0.35 the 28 days compressive strength was obtained as 59.47 MPa, in comparison to this the 28 days strength of 10% FA and 3% SP concrete with w/b of 0.34 was obtained as 61.18 MPa.

In general on an average there was a total 15% increment in strength at the age of one year with respect to 28 days strength. Therefore MIRHA did not contribute to for strength development after 28 days. It can be argued that MIRHA has acted as filler material in SCC. In order to correlate w/b with the compressive strength measured at 28 days, results are plotted in Figure 5. 5.

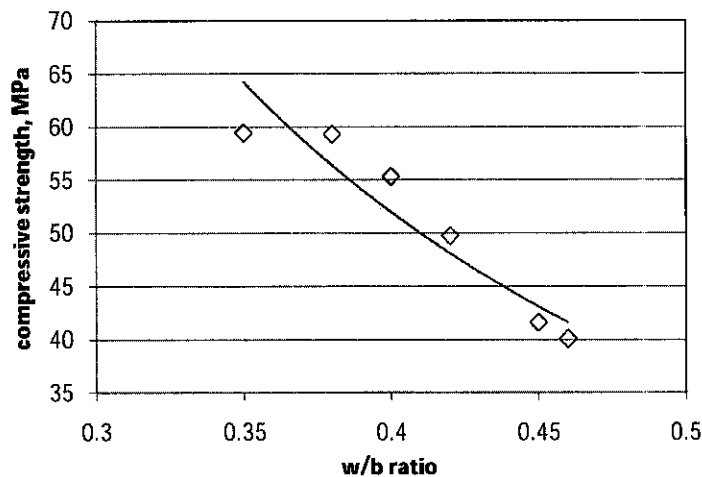


Figure 5. 5. MIRHA SCC compressive strength at 3% SP 10% MIRHA and at different water-binder ratio

Effect water-binder ratio on MIRHA self compacting concrete with 3% dosage of superplasticizers was shown to follow the relationship:

$$f'_c = 12.143w_b^{-1.586} \quad (5.2)$$

$$R^2 = 0.893$$

These results also confirmed by Nuruddin, et al. [20] with similar minimum w/b 0.35 and utilized MIRHA as filler in concrete, with optimum MIRHA filler 10 – 15% which achieved 65.01 MPa. As shown in Table 5. 3.

Table 5. 3. Compressive Strength Development of Concrete Samples

Mix	w/c	MIRHA	Compressive Strength (MPa)			
Code		(%)	3 days	7 days	28 days	56 days
A0	0.35	0	40.56	49.41	67.41	71.13
A1		5	28.24	32.63	51.91	56.82
A2		10	31.46	40.09	58.11	62.06
A3		15	31.15	41.43	58.11	65.01
B0	0.40	0	28.20	34.31	39.92	51.40
B1		5	30.51	38.15	55.33	62.32
B2		10	38.37	41.98	58.72	66.05
B3		15	35.08	42.18	60.39	67.71
C0	0.45	0	17.39	22.29	40.02	47.70
C1		5	28.91	35.09	51.33	60.92
C2		10	25.04	33.63	51.40	57.32
C3		15	24.83	32.67	54.01	59.16

Source: by Nuruddin, et al. [20]

Ahmadi, et al. [31] examined SCC containing rice husk ash, which the results showed higher compressive strength in SCC than normal concrete, with around 31% to 41% of normal concrete compressive strength. But until 60 days mixes containing rice husk ash indicated lower compressive strength rather than samples with no replacement, this decreasing can be countered by increasing the rate of pozzolanic reactions of rice husk ash in the matrix. And increasing the amount of rice husk ash replacement showed a significant effect on strength of normal concrete than SCC mixes. The optimum percentage of replacement was the mixes which containing 20% rice husk ash as shown in Figure 5. 6, which also indicated that by increasing the amount of replacement, water to binder ratio rises up.

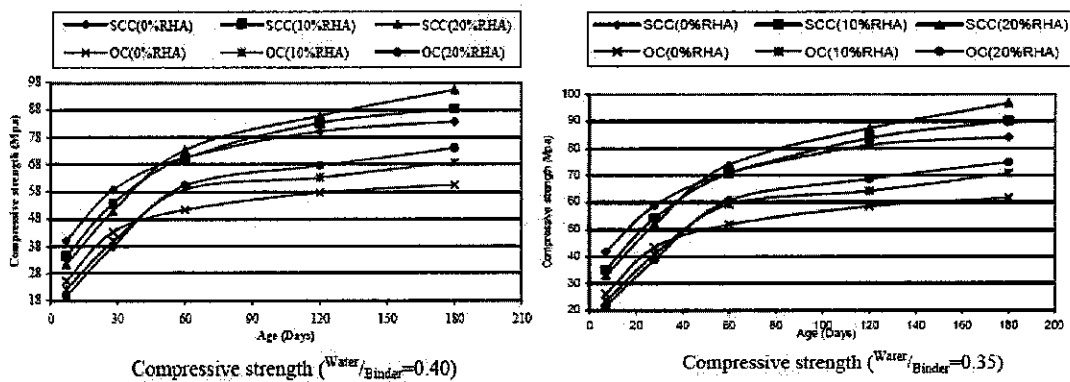


Figure 5. 6. Strength development of SCC containing RHA

Source: Ahmadi, et al. [31]

5.2.1.3. Effect of Water-binder ratio to Compressive Strength of FMSCC

In this group, three concrete mixes were prepared with a combination of 20% fly ash and 10% MIRHA using a w/b of 0.35, 0.4 and 0.45 respectively. Another three mixes were made with combination of 10% fly ash and 10% MIRHA using 0.3, 0.34 and 0.38 w/b. Among all six mixes, FA10-M10-0.3-3 concrete that contained 0.3 w/b was observed as the best mix which had the highest strength as show in Figure 5. 7. For this concrete mix 7 days strength was determined as 50.01 MPa was increased by at the rate of 30% until 28 days it was obtained as 65.17 MPa.

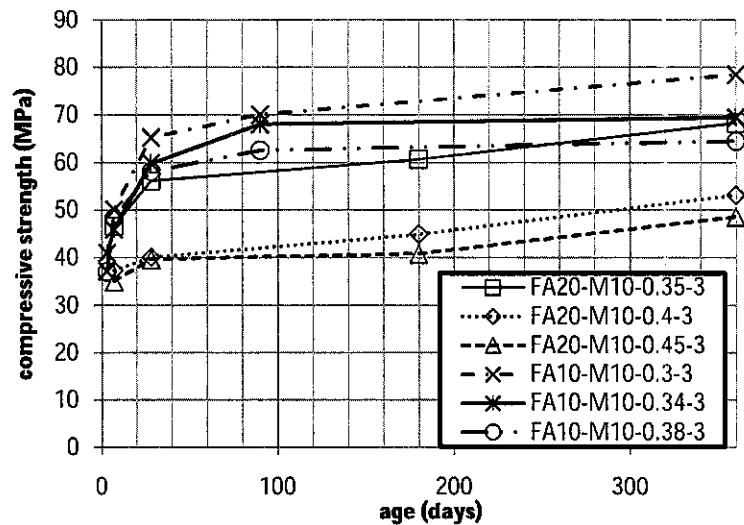


Figure 5. 7. Compressive strength of FMSCC with 3% SP at different water-binder ratio

However, concrete with 10% FA, 3% SP and w/b 0.3 had a 28 days strength of 75.72 MPa, which is about 16% higher than the 28 days strength of corresponding FMSCC. At the age of one year compressive strength of FA10-M10-0.3-3 concrete was 69.37 MPa, which was about 20% higher than the corresponding 28 days strength. The lowest compressive strength was observed for MSCC mixes that contained 0.4 and 0.45 w/b. With 0.45 w/b the 7 days strength was 34.94 MPa, at 28 days and one year it was 39.66 and 48.54 MPa respectively. The 10% MIRHA with 3% SP and 0.45 w/b concrete was better than FA20-M10-0.45-0.3 concrete. For such concrete 7 days strength was found as 33.23 MPa, 28 days 46.8 MPa and one year

value was developed to 54.61 MPa. It can be concluded that 10% FA gave the better result with compare to the 20% FA when it mix with MIRHA.

5.2.1.4. Effect of Water-binder Ratio to compressive Strength of NPSCC

No pozzolan self compacting concrete is SCC that only incorporate superplasticizers as admixtures without any cement replacement or pozzolan. Mix proportion with amount OPC of 500 kg/m^3 and 3% superplasticizers dosage and variation of water-binder ratio. Figure 5. 8 show the compressive strength of NP SCC with OPC 500 kg/m^3 .

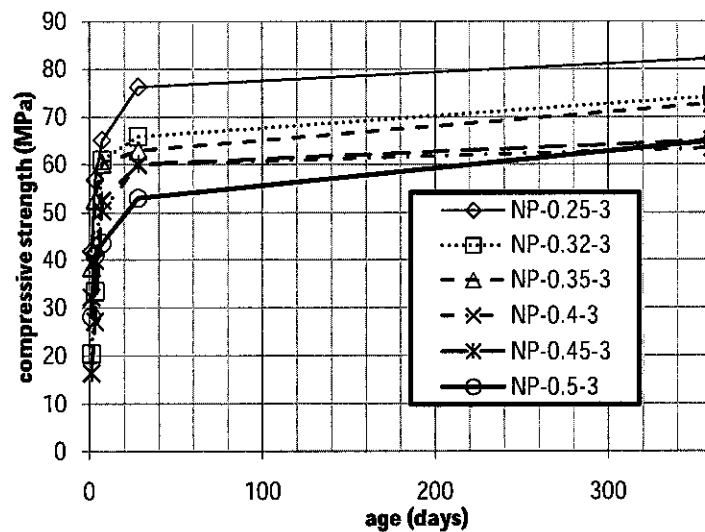


Figure 5. 8. Compressive strength of NP SCC with OPC 500 kg/m^3

Figure 5. 8 shows the compressive strength development of 100% OPC concrete with 3% SP with the variation of w/b from 0.25 to 0.5. At the age of 28 days 53.08 MPa strength was determined for concrete with w/b of 0.5, whereas for concrete with a w/b of 0.25 the compressive strength was 76.4 MPa, and this was 50% higher than the concrete strength with w/b of 0.5. For all the concrete mixes the strength continued to slowly develop until one year of age, increasing by 5 to 8%.

Figure 5. 9 shows the 28-day NP SCC compressive strength with 3% SP and at different water-binder ratio

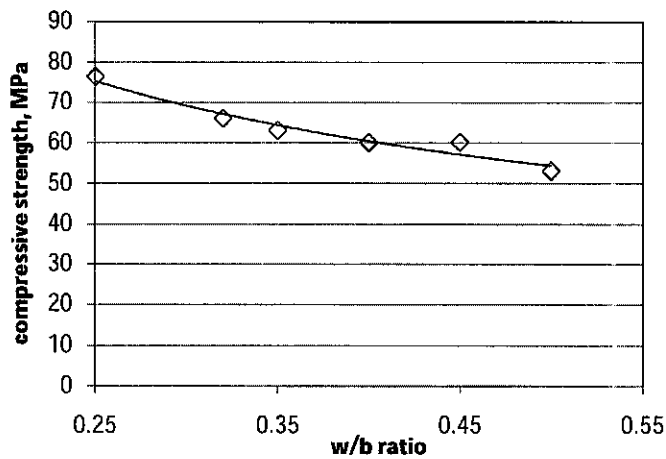


Figure 5. 9. NP SCC compressive strength with 3% SP and at different water-binder ratio

Figure 5. 9 contains 28-day compressive of concrete that was plotted against w/b, following was the best correlation obtained analysis.

$$f'_c = 39.25w_b^{-0.47} \quad (5.3)$$

$$R^2 = 0.944$$

The low water-binder ratio has proved its efficiency to achieve high strength concrete, and it is clearly indicated in all figures above. But lower water-binder ratio will also affect to lower rheological properties and some time could not achieve standard rheological properties. In this case NP-0.25-3 was fail in rheological test and will not be used in structural beam test.

5.2.2. Effect of Superplasticizers on Compressive Strength of SCC

5.2.2.1. Effect of Superplasticizers to Compressive Strength of FASCC

Self compacting concrete with 10 % fly ash and variation of 2 – 6% dosage of superplasticizers with water-binder ratio of 0.25, 0.34 and 0.42 were investigated to determine effect of superplasticizers on the compressive strength. Figure 5. 10 shows the compressive strength of different concrete at different ages.

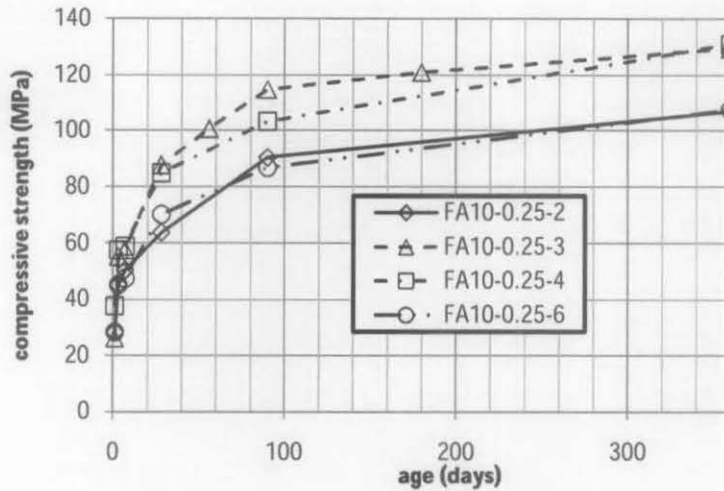


Figure 5. 10. Effect of superplasticizers on FASCC with water-binder ratio 0.25 and 10% fly ash

It can be seen from Figure 5. 10 that concrete with w/b of 0.25 with 3% and 4% superplasticizers content developed higher strength than the concrete mixes made of 2% and 6% SP content. As the age of 28 days concrete with 3% and 4% SP content yield 87.67 and 84.9 that was about 18% higher than the 28 days strength of 6% SP content. With the mix containing 3% superplasticizers showed superior strength between 28 days and one year. While the mix containing 2% SP and w/b 0.25 was fail in rheological properties test as describe in Chapter 4 and showed the low strength.

Dinakar, et al. [22] in their research also found the similar result, with the material proportion as shown in Table 2. 1. The mix proportion with 3% SP obtained the optimum compressive strength that can be seen in Table 5. 4. The result clearly shown that the 3% SP and 10% fly ash obtain 102.5 MPa compressive strength followed by the concrete with 2.5%SP and 30% SP which yielded the similar compressive strength as 103.25 MPa.

Table 5. 4. Mechanical properties of various mixtures

No.	Name	Fly ash: %	Compressive strength: MPa					Split ten. str.: MPa (90 days)
			3 days	7 days	28 days	90 days	180 days	
1	NC20	0	-	-	29.0	35.6	38.85	3.26
2	SCC558	85	-	-	14.64	22.07	27.74	1.70
3	NC30	0	21.8	31.0	43.0	44.5	45.0	4.27
4	SCC557	70	12.2	19.3	34.9	45.52	57.25	5.66
5	SCC757	70	8.0	20.98	34.83	44.96	55.81	4.52
6	NC60	0	50.5	59.0	74.0	76.0	76.0	5.70
7	SCC555	50	22.0	35.21	57.9	66.72	79.50	6.80
8	SCC655	50	22.65	32.33	50.07	60.63	72.05	6.22
9	NC90	0	72.8	76.0	78.00	80.0	84.0	6.27
10	SCC553	30	40.52	54.93	77.08	91.95	103.25	7.35
11	SCC530	30	36.0	41.0	71.62	75.26	89.53	7.92
12	NC100	0	71.0	78.0	87.0	86.0	88.0	6.28
13	SCC551	10	54.6	67.05	86.41	90.75	102.5	7.92

Source: Dinakar, et al. [22]

An investigation of optimum superplasticizers dosage was made by Rixom and Mailvaganam [99]. They showed that the maximum compressive strength of SCC made of 400 kg/m³ OPC was achieved with 4.4% of superplasticizers content, shown in Figure 5. 11.

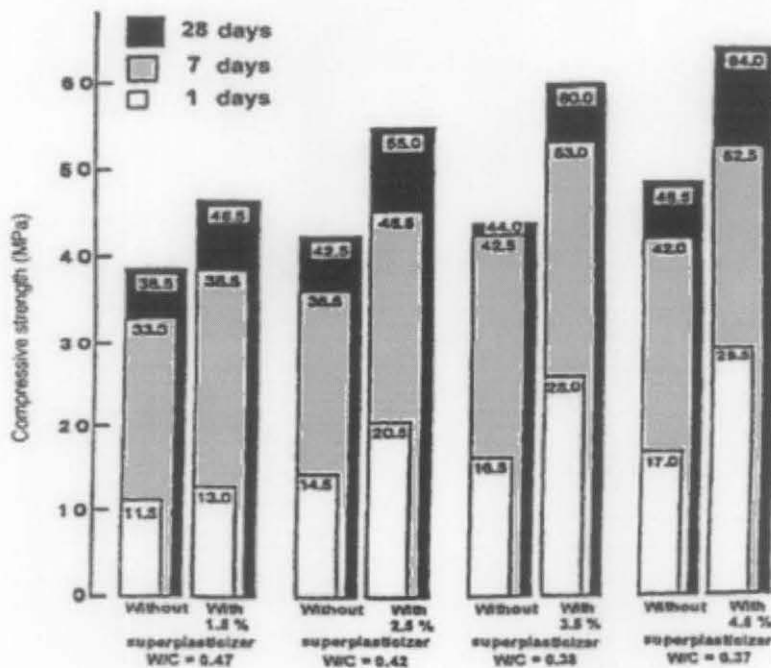


Figure 5. 11. Strength development of NC and high-strength SCC

Source: Rixom and Mailvaganam [99]

Compressive strength of 10% FASCC with 0.34 w/b containing different dosage of superplasticizers is shown in Figure 5. 12.

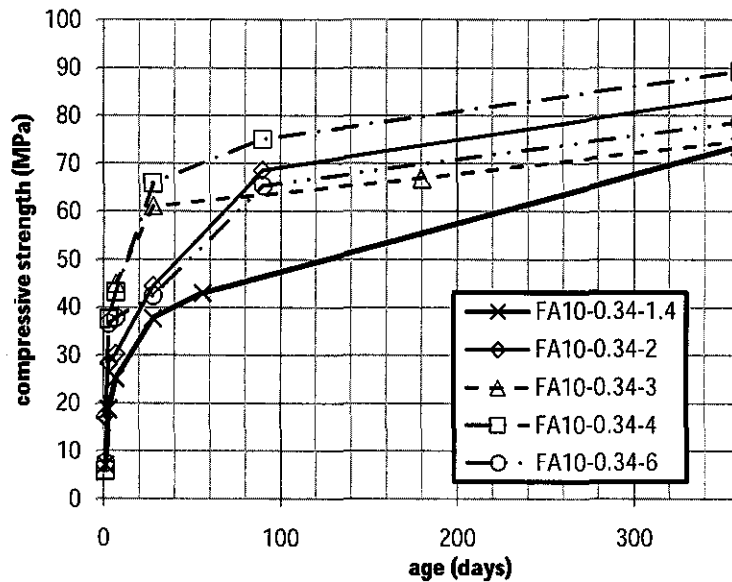


Figure 5. 12. Effect of superplasticizers on FASCC with water-binder ratio 0.34 and 10% fly ash

From Figure 5. 12. shows that the concrete with 4% superplasticizers developed higher strength than all other mixes. The concrete containing 2% dosage of superplasticizers developed compressive strength similar to that of the mixes with 6% dosage. While concrete with water-binder ratio 0.34 has lower compressive strength compared with concrete with water-binder ratio 0.25 and concrete with 2% superplasticizers had highest compressive strength after one year of curing. With the high dosage of superplasticizers the compressive decreased, which was also mentioned by Tarun and Shiw [177], who found that when superplasticizers dosage was increased beyond normal dosage, concrete performance started to deteriorate.

Figure 5. 13 illustrates the compressive strength development of 10% FASCC with a w/b of 0.42.

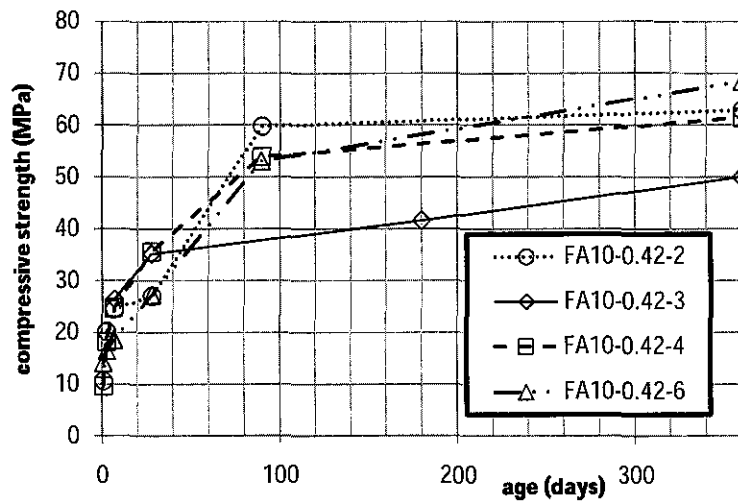


Figure 5. 13. Compressive strength of FASCC with water-binder ratio 0.42 variation of superplasticizer

At the age of 28 days concrete with 2, 3 and 4% SP content showed similar strength which was between 35 and 36 MPa, whereas at 90 days concrete with 2% SP content showed the highest strength of 59.81 MPa. Concrete with 4% SP content achieved 53.83 MPa of compressive strength. For this concrete group there was a very small increment in the compressive strength all the way until one year of age, which was between 4 to 6%. The dosage of SP did not effectively affect to the strength in high water-binder ratio.

Figure 5. 14 summarizes the effects of SP content on 28 days strength of concrete containing 0.25, 0.34 and 0.42 w/b. The figure illustrates the optimum SP content.

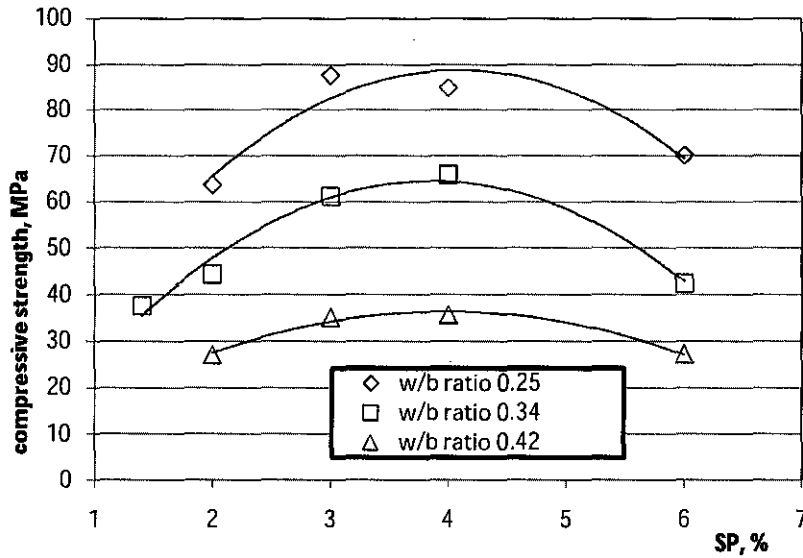


Figure 5. 14. Correlation of FASCC compressive strength and superplasticizers content

Increasing the water-binder ratio will reduce the effect of superplasticizers like shown in the Figure 5. 14. Effect superplasticizers on fly ash self compacting concrete with water-binder ratio 0.25 follow the relationship:

$$f'_c = -4.656S_p^2 + 38.72S_p + 5.245 \quad (5.4)$$

$$R^2 = 0.994$$

Where f'_c = compressive strength on 28 days

S_p = dosage of superplasticizers in%

And for water-binder ratio 0.34 will follow this relationship:

$$f'_c = -4.774S_p^2 + 36.94S_p - 6.916 \quad (5.5)$$

$$R^2 = 0.968$$

And for water-binder ratio 0.42 will follow this relationship:

$$f'_c = -2.263S_p^2 + 18.02S_p + 0.502 \quad (5.6)$$

$$R^2 = 0.975$$

This result was confirmed by the result of Rixom and Mailvaganam [99] who used no pozzolan SCC but Pierre, et al. [96] who also used no pozzolan SCC found the

different conclusion that the optimum percentage of superplasticizers was 1% like show in the Figure 5. 15.

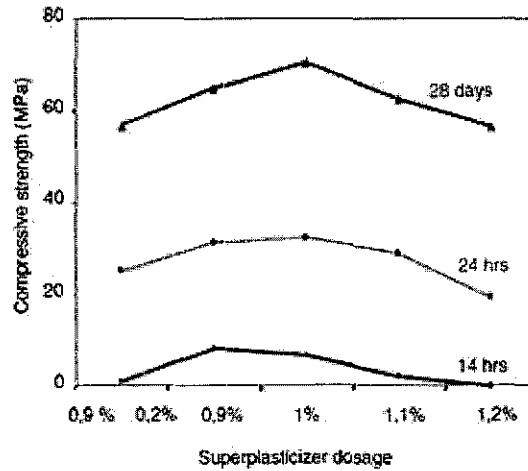


Figure 5. 15. Effect of superplasticizers content to the compressive strength

Source: Pierre, et al. [96]

The differences between two optimum content is explained by investigation by Gene [63], that some of the factors that affect to the workability also effect the compressive strength such as: quantity of cementitious materials, characteristics of these materials, consistency, grading of fine aggregate, shape of sand grains, grading and shape of coarse aggregate, proportion of fine to coarse aggregate, percentage of air entrained, type and quantity of pozzolan or other supplementary cementitious material, quantity of water, mixture and ambient temperatures, amount and characteristic of admixtures used and time in transit.

5.2.2.2. Effect of Superplasticizers on Compressive Strength of MSCC

One of the objectives of this research was to produce SCC with minimum 50 MPa as a high strength concrete using locally available materials i.e. rice husk and also to study the effect of partial replacement of cement by varied percentages of MIRHA with different dosage of superplasticizer. The results of compressive strength from these mix design are indicated in Figure 5. 16 to Figure 5. 18.

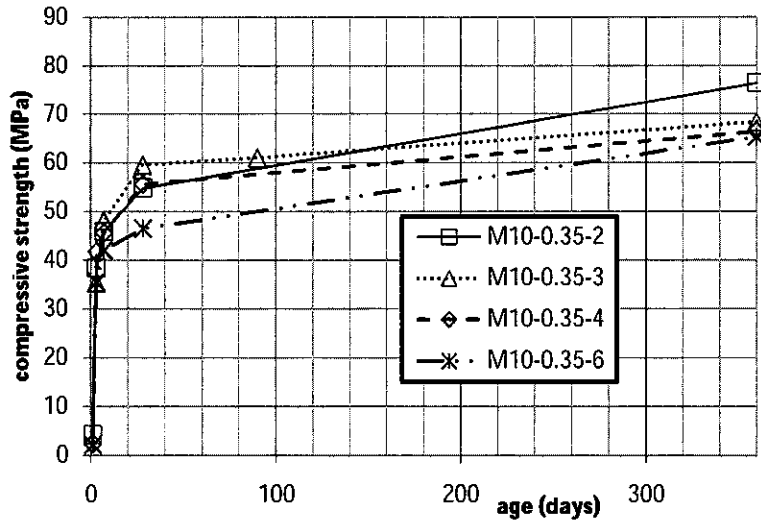


Figure 5. 16. Compressive strength of MSCC w/b 0.35 in variation of superplasticizer

In 28 days MSCC with 3% SP reached the highest compressive strength with 59.47 MPa, but in one year MSCC with 2% SP reached the highest compressive strength but based on rheological test this proportion was not categorized as SCC as result in Chapter 4. The lowest development strength was MSCC with 6% SP. The self compacting concrete with water-binder ratio 0.25 gave no result in rheological property and it was not suitable for self compact ability and not included in this discussion.

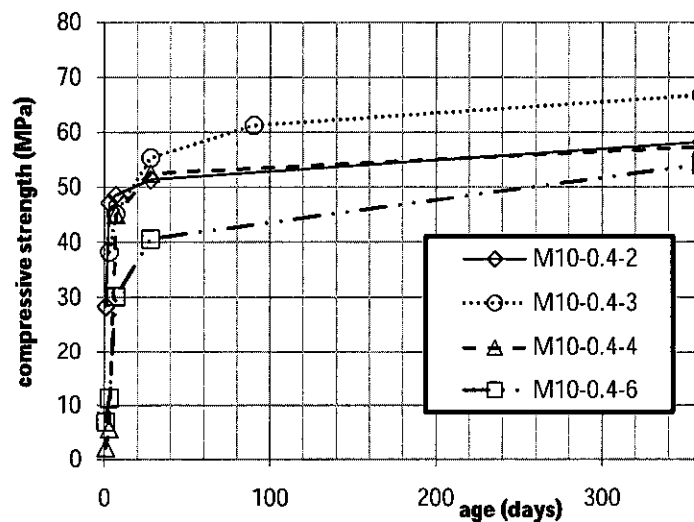


Figure 5. 17. Compressive strength of MSCC with water-binder ratio 0.4 in variation of superplasticizer

While the mix proportion with water-binder ratio of 0.4 shows highest in 4% dosage of superplasticizers and indicate lower strength in 6% dosage of superplasticizer.

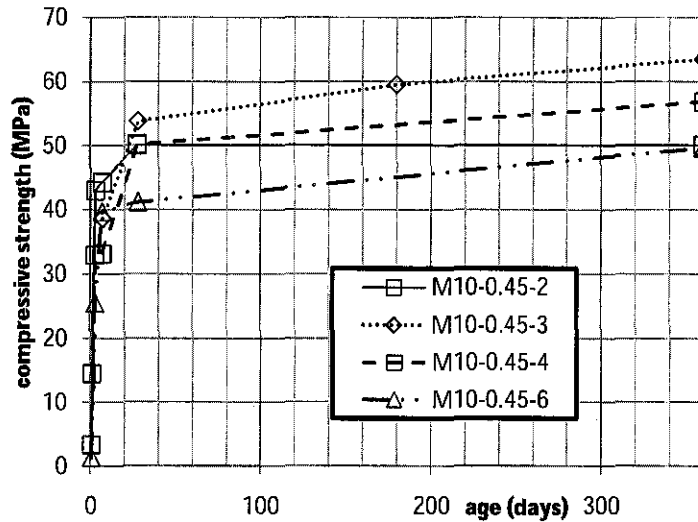


Figure 5. 18. Compressive strength of MSCC with water-binder ratio 0.45 variation of superplasticizer

Based on the results obtained from Figure 5. 18, the results indicate that mix proportion of MIRHA based self compacting concrete with water-binder ratio 0.45 with 3% gave highest strength and again the mix proportion of MIRHA self compacting concrete with 2% and 6% gave lowest strength compare with all mix proportion in MIRHA self compacting concrete.

The effect of superplasticizers to the compressive strengths 28 days of hydration is shown in Figure 5. 19.

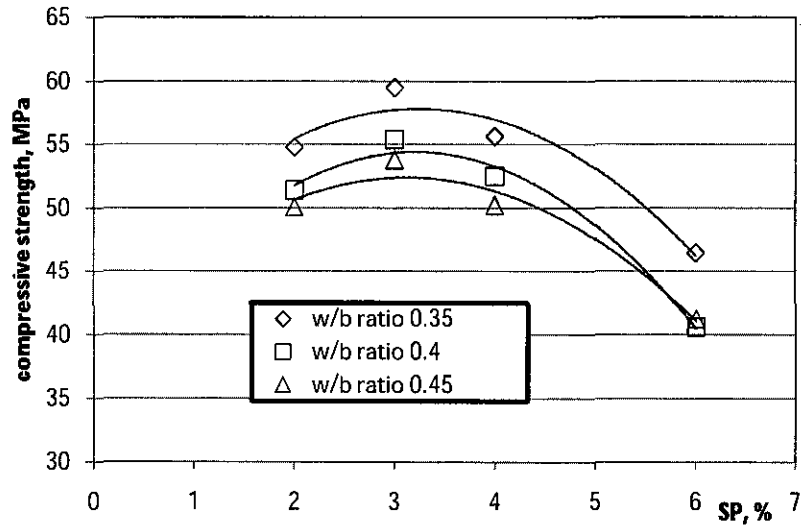


Figure 5. 19. Correlation of MSCC compressive strength and superplasticizers content

Effect superplasticizers on MIRHA self compacting concrete with water-binder ratio 0.35 follow the relationship:

$$f'_c = -1.525S_p^2 + 9.911S_p + 41.69 \quad (5.7)$$

$$R^2 = 0.939$$

And for water-binder ratio 0.4 will follow this relationship:

$$f'_c = -1.790S_p^2 + 11.5S_p + 35.89 \quad (5.8)$$

$$R^2 = 0.985$$

And for water-binder ratio 0.42 will follow this relationship:

$$f'_c = -1.374S_p^2 + 8.596S_p + 38.92 \quad (5.9)$$

$$R^2 = 0.958$$

The results indicated that the optimum dosage of superplasticizers was found between 2 – 4% and suggestion amount of water to produce self compacting concrete is: for fly ash self compacting concrete the minimum water-binder ratio is 0.25 and maximum is 0.35.; for MIRHA self compacting concrete minimum the water-binder ratio is 0.35 and maximum is 0.4. Self compacting concrete with cement replacement by fly ash or MIRHA with water-binder ratio more than 0.42, will tend to segregate and severe bleeding. From graph above also revealed that fly ash will be influenced significantly by increasing water-binder ratio rather than MIRHA self compacting

concrete. this result also confirmed by Nuruddin, et al. [20] with minimum w/b was 0.35 when the concrete use the rice husk ash replacement.

5.2.3. Effect of Different fly ash Content

The effect of fly ash content on the compressive strength of SCC is investigated in this section of 5%, 10% and 15% fly ash content. The results are plotted in Figure 5. 20 for two groups, the first group are based on w/b of 0.25 and the second group composed of 0.32 w/b.

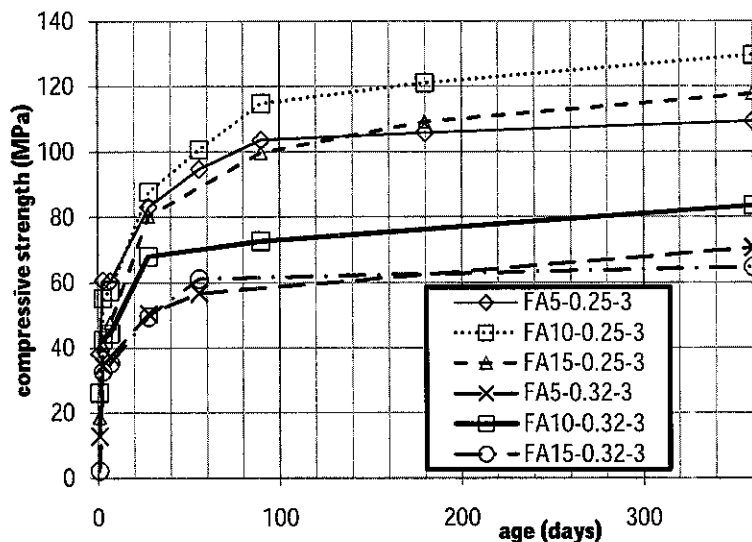


Figure 5. 20. Effects of different fly ash content on compressive strength

At the age of 28 days 10% FA with 0.25 w/b showed the highest compressive strength of 87.67 MPa which was found further increased to 129.5 MPa at the age of one year. At the age of 28 days 5% and 15% FA content and 83.09 and 80.29 MPa strength respectively. Similarly concrete with w/b of 0.32, 10% FA content showed the highest strength at all ages. At 28 days it was found as 67.9 MPa that was reached to 83.41 MPa at one year. While concrete 5% FA; 2% SP with w/b 0.25 and concrete 5% FA; 3%SP with w/b 0.35 achieved 80.29 MPa and 50.37 MPa respectively were not categorized as SCC as result in rheological test in Chapter 4.

As reported by some researcher such as Azli [178] found the optimum content of silica fume as 10%, Pantawee and Sinsiri [179] used the diatomite from natural

pozzolan and the optimum pozzolan content was found between 5 – 10% and the result is shown Figure 5. 21.

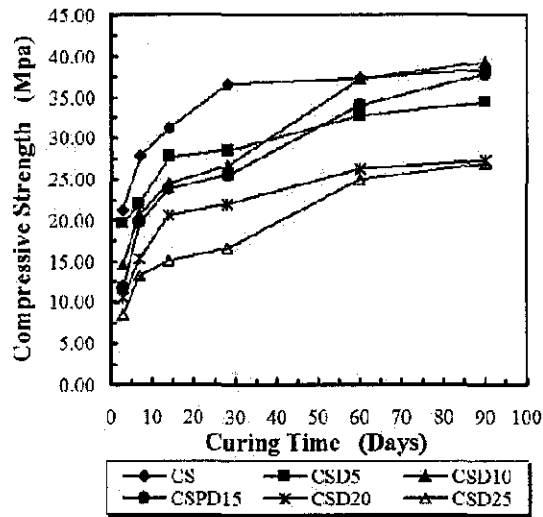


Figure 5. 21. Strength development of concrete with diatomite aspozzolan

Source: Pantawee and Sinsiri [179]

The 10% fly ash as optimum percentage also confirmed by Wanga, et al. [180] by their research of effect the fly ash content on amount of filling water. The amount of the filling water is related to the packing density of system as stated by Chengzhi, et al. [181]. The replacement of fly ash as pozzolanic material affects the packing density of system, as result may alter the amount of the filling water and finally achieved the better compressive strength and durability properties. The optimum filling water as an effect of content of fly ash can be seen in Figure 5. 22.

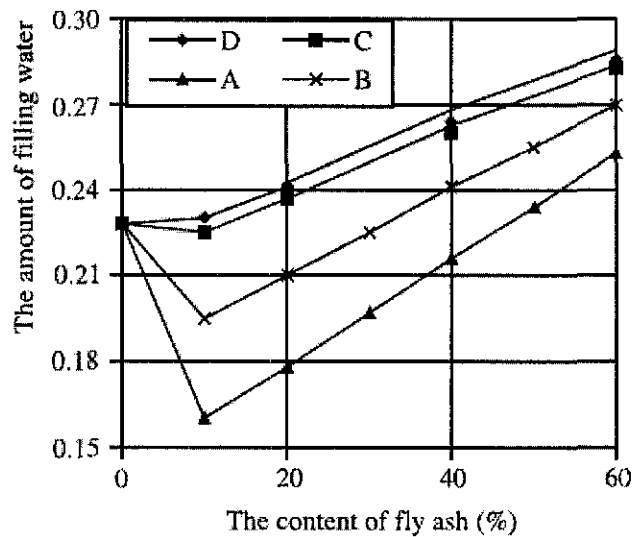


Figure 5. 22. The influence of the content of fly ash on the amount of filling water

Source: Wanga, et al. [180]

The similar result also found by Nochaiya, et al. [182] with investigation in compressive strength of the SCC containing fly ash and/or silica fume. Fly ash is generally known to decrease the mechanical properties of concrete at an early age and the early age bonding of fly ash particles to the cement matrix (by radiating bundles of fibrous C-S-H) is very weak. However, the mixes with SF were found to have higher compressive strength than fly ash mixes when compared to the same fly ash content. In term of effect of fly ash to the concrete it shown that the optimum percentage fly ash was 10% that similar with the result of this thesis that can be seen in Figure 5. 23.

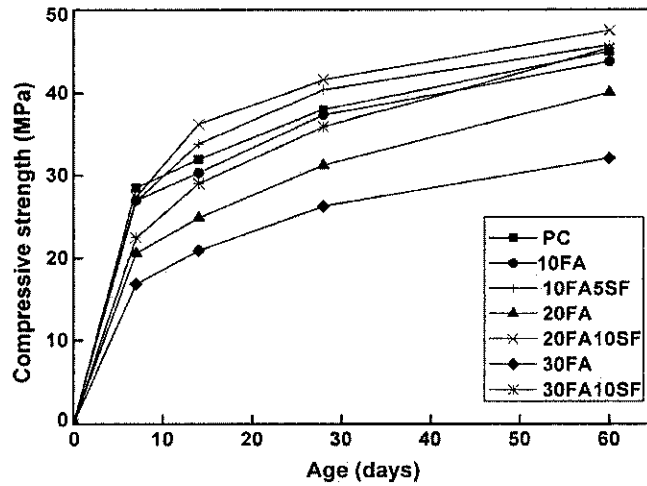


Figure 5.23. Compressive strength of Portland cement–fly ash–silica fume concrete

Source: Nochaiya, et al. [182]

The interesting finding from the result of work by Nochaiya, et al. [182] that it was found that in concrete containing fly ash, the water requirement decreased as the fly ash content increased as shown in Figure 5.24. However, the water absorption is low when the unburned carbon in fly ash is below around 1%. The concrete containing fly ash and silica fume, the water requirements were higher than for those mixes without silica fume as compared to the mixes with the same fly ash content. This phenomenon is due to the extremely fine particle size of silica fume with resulting in a greater.

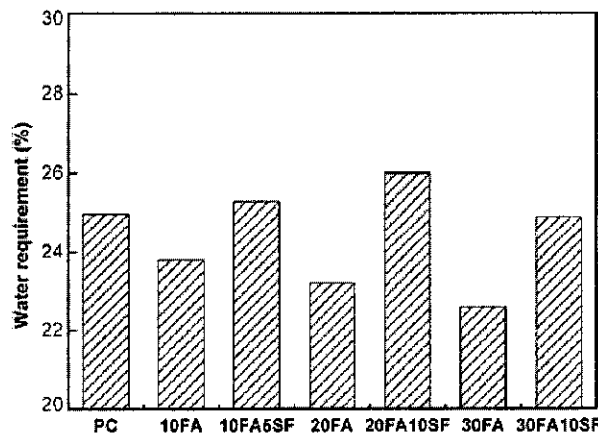


Figure 5.24. Water requirement of concrete containing fly ash and/or silica fume

Source: Nochaiya, et al. [182]

While Saraswathy, et al. [18] investigated effect of different type activated fly ash. The result showed that 10% fly ash as the optimum percentage which produced the highest compressive strength as shown in Figure 5. 25.

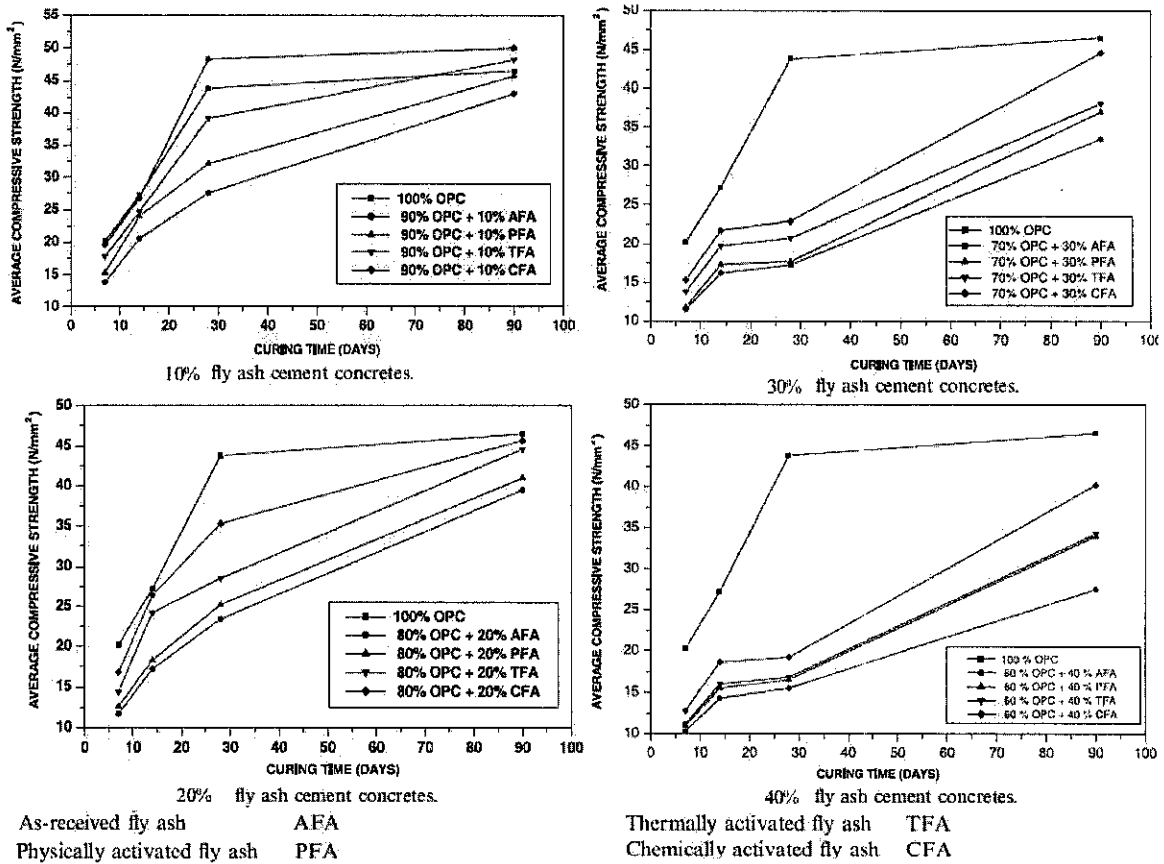


Figure 5. 25. Compressive strength vs. curing time for OPC and fly ash cement concretes

Source: Saraswathy, et al. [18]

The optimum content of MIRHA was investigated by Kamal, et al. [21] in different burning temperature of MIRHA. The lower hydration process was the reason of lower strength of 20%, 15% and 5% MIRHA concrete at early days. Pozzolanic reaction in 10% MIRHA concrete showed more rapid development in producing C-S-H gel as the curing days continued that indicated by the increment percentage of compressive strength. The result showed that 10% is the optimum level of replacement, as shown in Figure 5. 26.

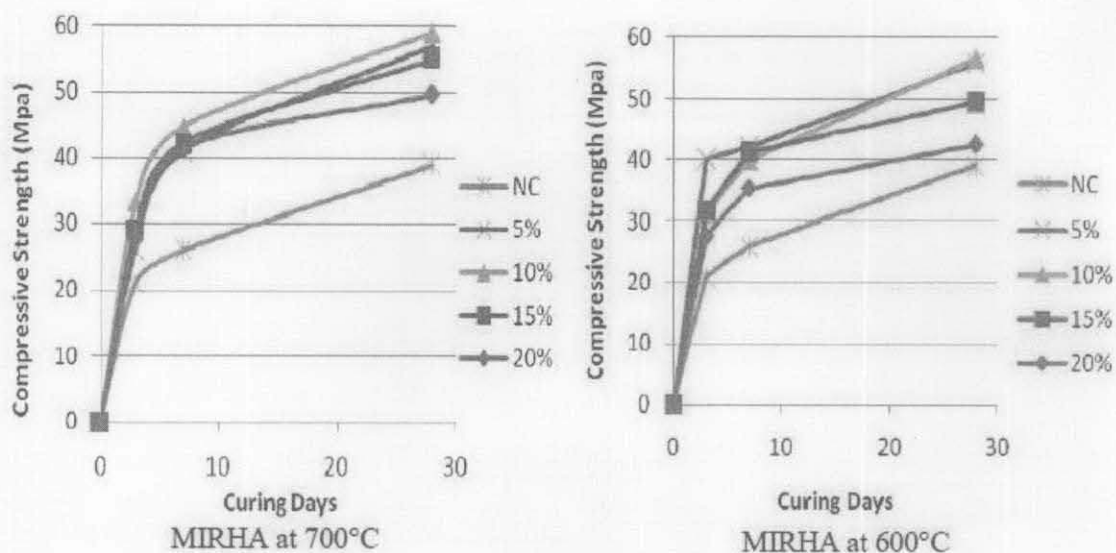


Figure 5. 26. Strength development 700°C and 600°C burning temperature of MIRHA

Source: Kamal, et al. [21]

The similar investigated also done by Muhammad and Waliuddin [19] with different particle size of RHA. The result indicated that 10% RHA were optimum content in all different particle size of RHA as shown in Figure 5. 27.

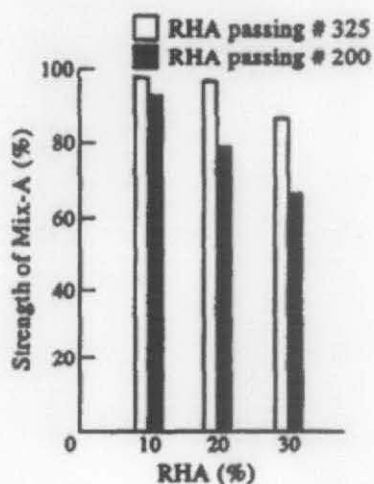


Figure 5. 27. Effect of fineness on strength gain at 28 days

Source: Muhammad and Waliuddin [19]

While Namagga and Atadero [13] used Class C fly ash had another optimum percentage of fly ash.in self compacting concrete. They found that self compacting

concrete with 25 – 35 fly ash that contain high lime as optimum range of class C fly ash..

The optimum mix proportion based on compressive strength can be compared using Figure 5. 28.

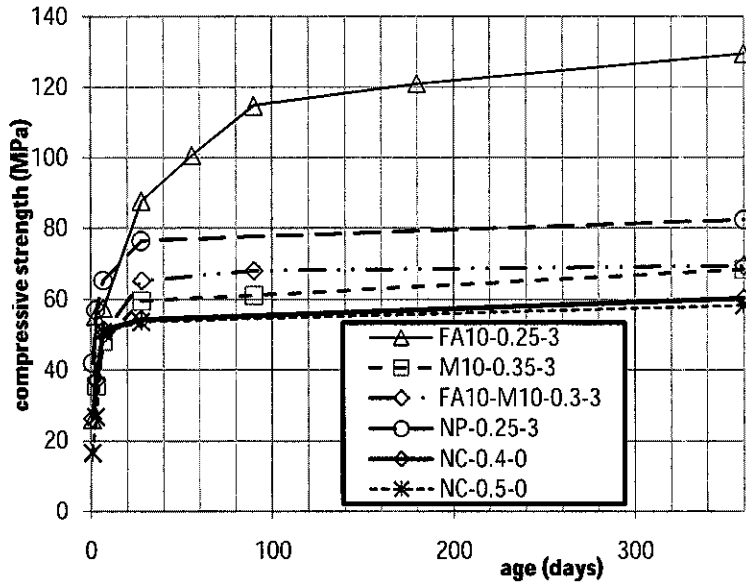


Figure 5. 28. Optimum SCC mix design based on compressive strength

Figure 5. 28 shows that FASCC had highest compressive strength, while the MSCC had lowest strength but the strength was still higher than control mix.

5. 3. Flexural Strength Test

Modulus of rupture represents the flexural strength of concrete. This value is calculated as the apparent tensile stress induced in the extreme tension fiber of a plain concrete beam specimen under the load based third-point loading that produces rupture when tested in accordance with the BS 1881: Part 118: 1983.

In this study the flexural strength, f_{fl} or Modulus of Rupture of each representative mix was measured at the age of 90 days. Modulus of rupture of 10% FA with w/b of 0.25, 0.3 and 0.32, 10% FA + 10% MIRHA concrete with w/b of 0.3, 0.34 and 0.38 and 10% MIRHA mixes with w/b of 0.35, 0.38 and 0.4 are plotted in Figure 5. 29. For all 10 mixes the average value was obtained between 4.5 and 6.5 MPa. In general

10% fly ash mixes and 10% FA+10% MIRHA mixes showed the better performance as compared to the 10% MIRHA mixes.

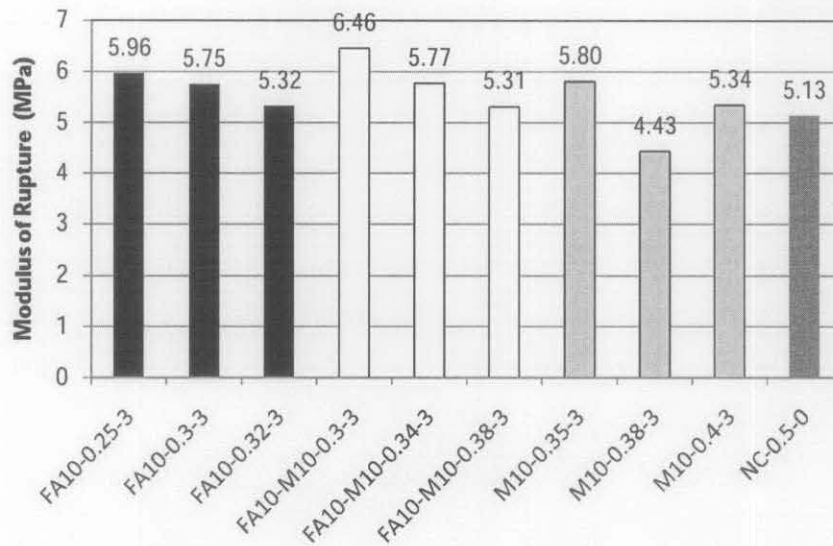


Figure 5. 29. Modulus of Rupture of SCC

5. 4. Split Tensile Test

Split tensile strength of cylinders of each mix was measured at the curing age of 90 days. The results of split tensile strength mixes are shown on Figure 5. 30. Generally, the graph shows an increment in the split tensile strength of the concrete as the percentage of fly ash increases.

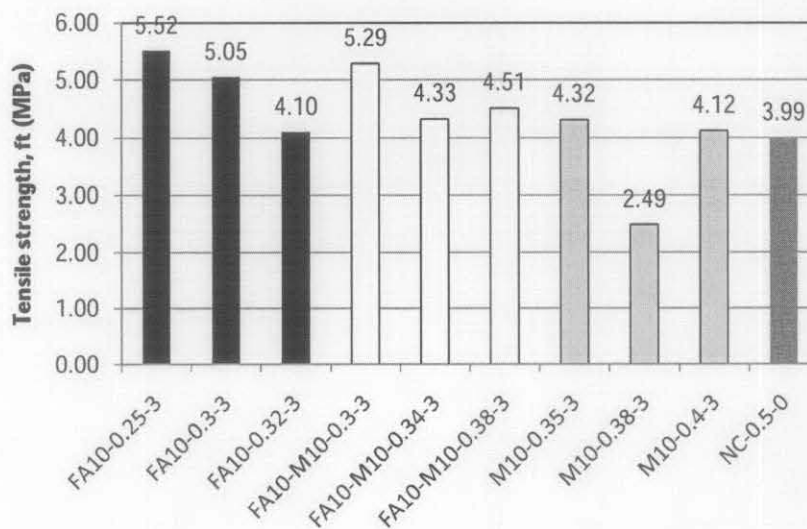


Figure 5. 30. Split tensile of SCC

From Figure 5. 30 shows that FASCC with water-binder ratio 0.25 achieved the highest split tensile with 5.52 MPa tensile strength. While the lowest split tensile was achieved by MSCC with water-binder ratio 0.38 and lower than control specimen.

Castel, et al. [104] investigated the tensile strengths in SCC, which the result indicated that the split tensile strengths measured on vibrated concrete are always superior to the ones obtained on SCC, as are the compressive strengths in Table 5. 5. For a constant compressive strength, SCC and vibrated concrete have a similar split tensile strength measured by using splitting test.

Table 5. 5. Tensile strength obtained by using the splitting test

	SCC25	VC25	SCC40	VC40
$f_{t,splitting}$ (MPa)	2.6	2.9	3.4	4.0
$f_{t,splitting}/f_{c28}$	0.087	0.083	0.077	0.082
$f_{t,splitting}/f_{c28}^{2/3}$	0.269	0.271	0.273	0.299
Ratio SCC/VC	0.90		0.85	

Source: Castel, et al. [104]

Druta [105] found that SCC mixtures exhibited greater values in both splitting tensile and compressive strength after being tested, compared to normal concrete. The splitting tensile strength increased around 30%, while the compressive strength was around 60% greater. The SCC tensile strengths after 7 days were almost as high as those obtained after 28 days for normal concrete, this phenomenon was due to the use of mineral and chemical admixtures, which usually improve the bonding between aggregate and cement paste, and finally increasing the strength of concrete.

While Sukumar, et al. [23] used the lower dosage of SP ranging in SCC containing fly ash with the mix proportion in

Table 5. 1, the result showed the similar result with result of this thesis as obtain in Table 5. 6.

Table 5. 6. Splitting tensile strength of SCC

Curing period (days)	Tensile strength in N/mm ² for different grades of SCC mixes									
	AS30	AS40	AS50	AS60	AS70	BS30	BS40	BS50	BS60	BS70
1	1.40	1.65	2.01	1.56	2.14	1.21	1.49	1.26	1.94	1.98
3	2.40	2.99	3.42	3.30	3.65	2.60	2.47	2.98	3.38	3.61
7	3.12	3.96	4.58	4.85	5.48	2.76	3.35	3.76	4.35	4.84
14	3.66	4.60	5.64	5.64	6.67	3.25	3.98	4.75	5.24	5.73
28	4.06	5.01	5.95	6.72	7.54	3.72	4.53	5.06	5.79	6.45

Source: Sukumar, et al. [23]

5. 5. Summary

This section highlights the summary of the principal finding as:

1. Water-binder ratio significantly affects the compressive strength of all types of SCC.
 - a. For 10% fly ash concrete containing 3% SP, at 0.42 w/b the 28 days compressive strength was obtained as 35.2 MPa whereas when a w/b of 0.25 was used the 28 days compressive strength was obtained as 87.67 MPa. It is concluded that maintaining all mix proportion variation in w/b from 0.42 to 0.25 increased the 28 days strength to about 1.5 times. So, the amount of water content can economize the cost of self compacting concrete.
 - b. For 10% MIRHA concrete with 3% SP content 28 days compressive strength of concrete with a w/b of 0.35 was obtained 59.47 MPa, whereas concrete with a w/b of 0.46 yielded 28 days compressive strength of 40.1 MPa. In MIRHA with the variation of high to low w/b the strength increment was obtained as 50%.
 - c. For similar w/b both 10% FA and 10% MIRHA concrete showed similar compressive strength with very close margin. In general MIRHA is suitable for producing 28 days compressive strength as high 50-60 MPa cause compliance of SCC rheological requirement it needs as low as 0.35 w/b, if the SP content is fixed at its optimum level of 3% dosage. Whereas fly ash is suitable for producing higher 28 days

strength such as 80 MPa because it requires low water content as 0.25 w/b for complying the rheological characteristic of SCC.

- d. At lower w/b such as 0.25 to 0.32 there was an increases of 30 – 40% was observed for 10% FA concrete from 28 days to 90 days, which means with lower w/b fly ash highly acted as pozzolanic as well filler material in SCC. For 10% MIRHA concrete such increment was found between 15% to 20% indicates that mostly MIRHA acted as a filler material. However these were little pozzolanic activity took place in the mixes.
 - e. The concrete with 10% OPC attained 5 to 14% lower compressive strength as composed to corresponding 10% fly ash and/or 10% MIRHA based concrete.
 - f. 10% fly ash combined with 10% MIRHA performed better than the 20% FA+10% MIRHA mixes. In comparison to 10% FA mixes and 10% MIRHA mixes FMSCC mixes showed 11% - 17% lower compressive strength.
2. 10% replacement of cement either by fly ash or by MIRHA is found optimum that showed best result. Figure 5. 28 illustrates the optimum mixes for fly ash, MIRHA and 100% OPC. Furthermore, all types of SCC achieved the high strength concrete with the compressive strength were more than 50 MPa.
 3. From the flexural strength test, in general 10% fly ash mixes and 10% FA+10% MIRHA mixes showed the better performance as compared to the 10% MIRHA mixes, and the indication that all type of SCC showed the better modulus rupture than normal concrete.
 4. The split tensile test result indicated that all type of SCC performed with better strength. FASCC with w/b 0.25 achieved the highest split tensile with 5.52 MPa tensile strength which 39% higher than normal concrete. While MSCC achieved higher tensile strength as compared with normal concrete with almost 8.2%.

The optimum percentage of fly ash and MIRHA were found as 10% weight of paste content and 3% SP was also contribute the highest performance in term of rheological properties and compressive strength result and this value also was confirmed by several researchers Wang, et al. [180]; Nochaiya, et al. [182]; Saraswathy, et al. [18]; Dinakar, et al. [22]; Ravindrarajah, et al. [26] in 10% fly ash

content; Muhammad and Waliuddin [19]; Kamal, et al. [21]; Nuruddin, et al. [20] in 10% MIRHA replacement; Dinakar, et al. [22] in 3% dosage of SP. Furthermore, this proportion will be used in structural behavior test with 3% SP and 10% pozzolan. While the w/b will be applied accordance with its optimum water content that result the highest compressive strength.

CHAPTER 6

DURABILITY OF SCC

6. 1. Introduction

Durability of concrete is defined as the level of its resistance against deterioration mechanism when it is subjected to aggressive environment such as marine conditions during service life. One of the fundamental objectives of the development of SCC is to apply in big size beams that contains congested steel reinforcement such as those used as bridge girders. Because of the potential application of SCC in structures that posed concern of long term durability, an investigation of durability properties such porosity, permeability and corrosion resistance is necessary.

6. 2. Total Porosity Test of SCC

Porosity of concrete is an important factor that controls its short and long term performance. In early ages of concrete, its porosity determines the compressive strength. Porosity of concrete affects the rate of movement of aggressive substances such chloride ions or supply of oxygen inside the concrete. The diffusion and/or permeation of aggressive ions results in poor durability, particularly corrosion of embedded steel reinforcement in concrete. There are many variables such as w/b, SP content may affect the porosity of SCC. In the following sub-section the influence of such variables is discussed.

6.2.1. Effect of Water-binder Ratio on Total Porosity

From the results of compressive strength as discussed in Chapter 5, those mixes showed the high compressive strength from each group were opted for further

investigation and durability characteristics. For FASCC mix with 3% SP, two mixes with w/b of 0.25 and 0.32 were selected for porosity.

Figure 6. 1 shows the total porosity of 5% FA, 10% FA and 15% FA mixes with 3% SP content and the w/b of 0.25 and 0.32. The porosity was measured at the age of 28 days.

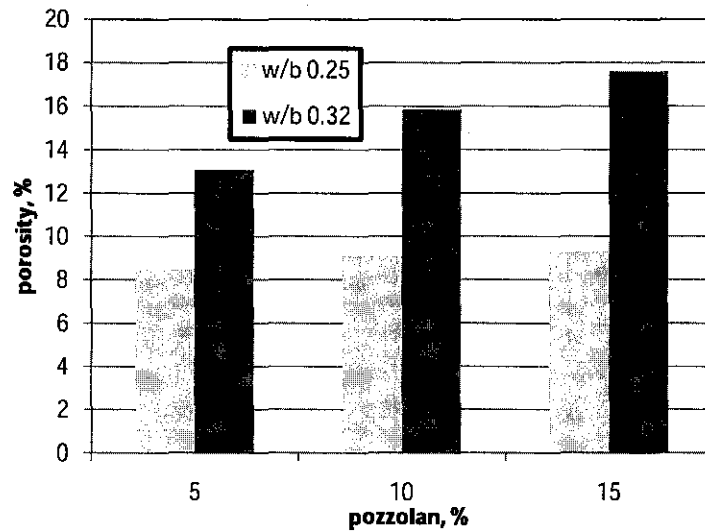


Figure 6. 1. Total porosity of concrete made of 5%, 10% and 15% FA content with a w/b of 0.25 and 0.32 at the age of 28 days

Total porosity of three mixes with w/b of 0.32 was measured 39% to 48% higher than that of the mixes made of w/b of 0.25. It is the significant change in the porosity of concrete that may cause appreciable reduction in durability when w/b is increased to 0.32. When comparing the affects of 5%, 10% and 15% FA content, concrete with 5% FA content showed the lowest porosity whereas SCC with 15% FA content posed the highest porosity. But it can be noticed that all of 5% FA in this porosity test were fail in rheological test as described in Chapter 4. When a w/b of 0.25 was used the porosity of 5% FA mix was measured as 8.2% for 10% FA mixes it was measured as 8.9% and the highest porosity value of 9.2% was determined for 15% FA concrete. It means that there was a variation of 5% to 7% in porosity value was measured between two successive mixes. The porosity of 5% FASCC with a w/b of 0.32 was obtained as 13.2% whereas as for 10% FASCC it was increased to the value of 15.9% and for 15% it was found 17.8%.

As mentioned above the difference in the value in the value of total porosity is larger for 5%, 10% and 15% FA content in concrete that is made of a w/b of 0.32. As discussed in Chapter 5 when the w/b was increased the pozzolanic reaction was delayed. So, it is due to this reason with w/b of 0.32 there was a big in porosity value between 5% FASCC and 10% FASCC and between 10% and 15% FASCC. While Poon, et al. [9] stated that if fly ash ash content increased, the average pore diameters decreased, but the measured porosity increased. The decreasing of w/b ratio resulted in lower porosity for the normal concrete and fly ash concrete, and this statement also was confirmed by Cabrera and Hasan [119] stated that in terms of durability related parameters, the lowest porosity and oxygen permeability were given by the fly ash concrete.

Figure 6. 2 shows the total porosity of MSCC. Three mixes with a lower w/b of 0.35, middle w/b of 0.4 and the highest w/b of 0.45 were chosen for porosity test.

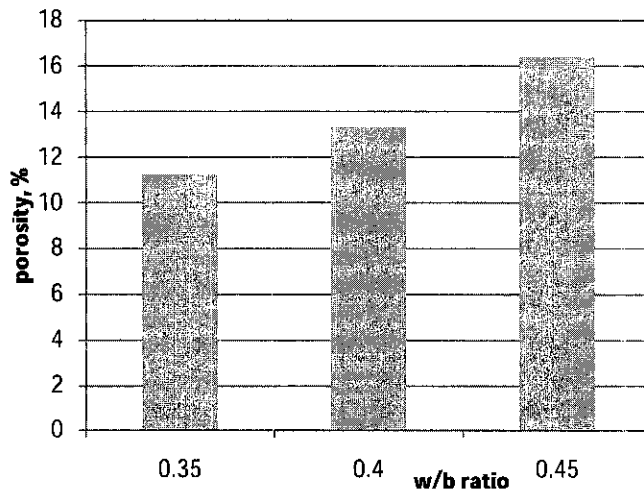


Figure 6. 2. Effect of water-binder ratio on porosity of 10% MSCC

When the w/b was kept at low as 0.35 the porosity was obtained as 11.3% where as for concrete with a w/b of 0.4, it was 13.3%, which is about 16% higher than that of concrete with w/b of 0.35. When the amount of water was further increased to a w/b of 0.45, its porosity was determined as 16.1%, which is 20% higher than the 0.4 w/b concrete and 36% higher than the lowest water content. From the above discussion high w/b, higher cement replacement results high porosity, hence, its durability may be lowered

6.2.2. Effects of Superplasticizers on Porosity

The effects of superplasticizers on concrete are described in detail by Neville [60]. Superplasticizers contains long molecules to wrap around cement particles and give them negative charge, this charge causes them repel each other, resulting the deflocculation and dispersion of cement particles. Due to this chemical reaction the very high workability of concrete could be achieved, porosity of concrete can be reduced and may produce very high strength concrete. Whereas Azli [178] stated that the superplasticized fresh concrete can be placed with little or no compaction and not be subjected to excessive bleeding or segregation

The advantage of using superplasticizers as mentioned by Park and Tia [183] that permeability and drying shrinkage of superplasticized concrete were significantly less than those of conventional concrete.

Porosity of 10% FASCC with a w/b of 0.25,0.34 and 0.42 with different dosage of SP and measured at the age of 28 days is presented in Figure 6. 3.

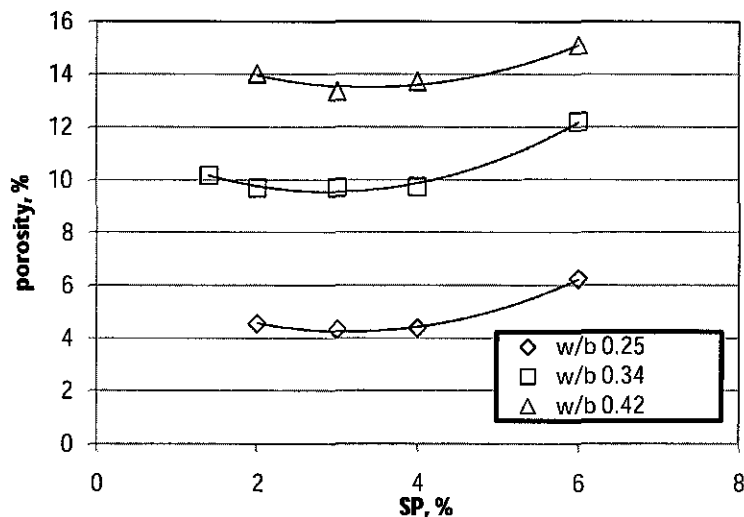


Figure 6. 3. Effect of SP dosage on porosity in 10% FASCC with different water-binder ratio

As shown in Figure 6. 3 it can be deduced that the optimum dosage of superplasticizers is 3 – 4% based on lower porosity, while 2%SP with w/b 0.25 were not specified as SCC as describe in Chapter 4. Ane, et al. [184] stated that superplasticizers are able to reduce the porosity of the hardened concrete by allowing

the fresh material to become workable with low water-binder ratio. Effects of SP on porosity of FASCC with water-binder ratio of 0.42 and 10% fly ash are mathematically described as:

$$P_C = 0.238S_p^2 - 1.613S_p + 16.22 \quad (6.1)$$

$$R^2 = 0.967$$

Where S_p = Superplasticizers content in%

P_C = porosity of concrete in%

Effects of SP on porosity of FASCC with water-binder ratio 0.34 and 10% fly ash follows this equation:

$$P_C = 0.276S_p^2 - 1.610S_p + 11.88 \quad (6.2)$$

$$R^2 = 0.988$$

Effect of SP on porosity of FASCC with water-binder ratio 0.25 and 10% fly ash follows this equation:

$$P_C = 0.242S_p^2 - 1.528S_p + 6.662 \quad (6.3)$$

$$R^2 = 0.996$$

The influence of superplasticizers investigated by Etsuo, et al. [185] that superplasticizers will disperse cement particles, and consequently the pore structures of hardened samples reflect the coagulated structure of the particles in fresh cement paste.

From Figure 6. 3 it can also be concluded that superplasticizers dosage more than 4% tend to make high porosity, it means SP dosage more than 4% is not feasible. While Figure 6. 4 shows the effect of SP dosage on porosity in MIRHA SCC with different water-binder ratio

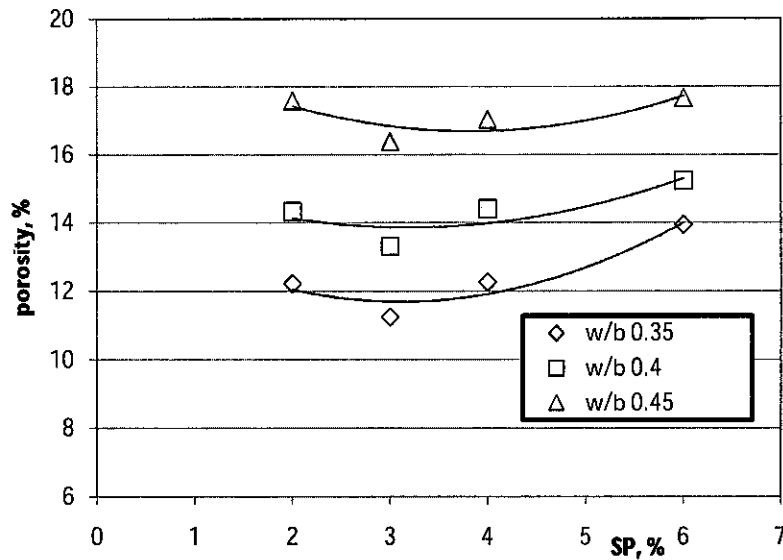


Figure 6. 4. Effect of SP dosage on porosity in MIRHA SCC with different water-binder ratio

Similarly, the effects of superplasticizers on MIRHA self compacting concrete showed almost the same behavior as discussed for fly ash self compacting concrete. And also the concrete with 2% SP and w/b 0.35 was not categorized as SCC like mentioned in Chapter 4. Effects of SP on porosity of MSCC with water-binder ratio of 0.45 and 10% MIRHA follow this equation:

$$P_c = 0.221S_p^2 - 1.696S_p + 19.93 \quad (6.4)$$

$$R^2 = 0.669$$

Effects of SP on porosity of MSCC with water-binder ratio 0.4 and 10% MIRHA follows this equation:

$$P_c = 0.277S_p^2 - 1.727S_p + 14.38 \quad (6.5)$$

$$R^2 = 0.905$$

Effect of SP on porosity of MSCC with water-binder ratio 0.35 and 10% MIRHA follows this equation:

$$P_c = 0.182S_p^2 - 1.169S_p + 15.74 \quad (6.6)$$

$$R^2 = 0.706$$

6.2.3. Correlation Between Porosity and Compressive Strength

The high strength concrete can be achieved easily with low porosity; in other word the high strength concrete must also show high performance concrete behavior in term of workability, strength and durability. The correlation between compressive strength and porosity should be close to each other; in fact that high performance concrete has a particularly dense structure of hydrated cement paste which contains discontinuous capillary pore system. Thus the high performance concrete possesses a high resistance to external attack.

In Figure 6. 5, the total porosity of different FASCC mixes is plotted against the corresponding compressive strength.

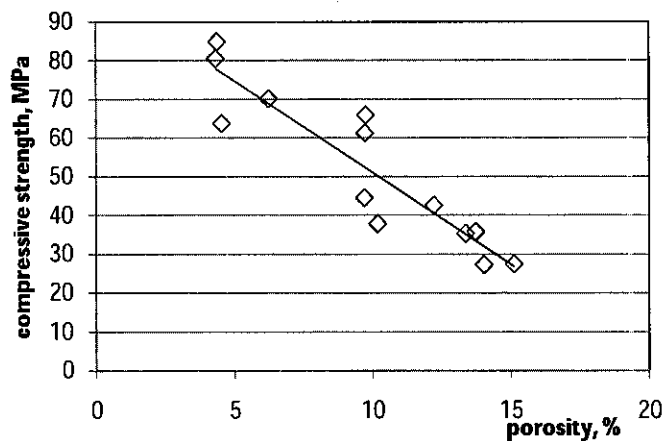


Figure 6. 5. Correlation between porosity and comp. strength in FASCC

Both porosity and compressive strength was measured at 28 days. An inverse relationship between porosity and compressive strength was observed, which is defined as:

$$f'_c = -4.732P_c + 98.32 \quad (6.7)$$

$$R^2 = 0.842$$

Where f'_c = compressive strength on 28 days

P_c = porosity of concrete in%

Figure 6. 6 shows the relationship between total porosity and compressive strength of MSCC.

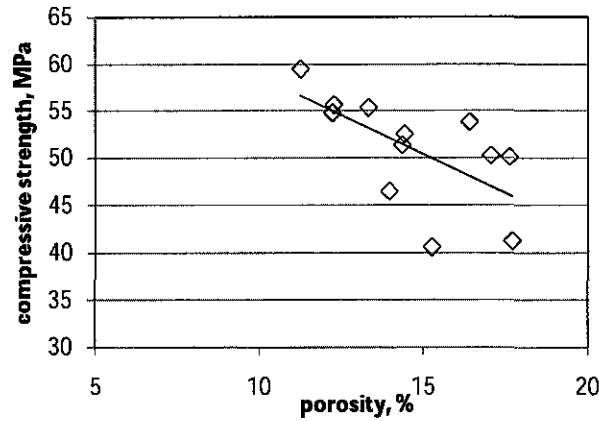


Figure 6. 6. Correlation between porosity and compressive strength in MSCC

The following correction through statistical analysis was obtained as:

$$f'_c = -1.662P_c + 75.29 \quad (6. 8)$$

$$R^2 = 0.402$$

In both figure (Figure 6. 5 and Figure 6. 6) can be concluded that the porosity of concrete is always depend on its compressive strength.

6. 3. Permeability of Concrete

Permeability of concrete is defined as the tendency of flow of fluid such as liquid or gasses through its microstructure. The flowing fluid may contain aggressive ions for example chloride ions, which may continuously diffuse within the concrete pore system. Upon reaching a threshold value, the diffused ions may cause the deterioration of structure; corrosion of embedded steel is one of such cases. The water and/or gas (oxygen) permeability is usually used as durability indicator.

6.3.1. Water Permeability

Water permeability of concrete is controlled by many factors, including porosity, pressure head, and testing time. The depth of water penetration is used to calculate the water permeability using the Valanta's equation. Higher ability of the concrete resist water intrusion result as in the lower water permeability.

The Valanta's equation was defined by Shafiq and Cabrera [120]:

$$K_w = \frac{d^2 v (\mu)}{2Th (\rho g)} \quad (6.9)$$

- Where K_w = water permeability, m^2
 d = depth of water penetration, m
 v = total porosity, fraction
 T = time of penetration, s
 h = the applied pressure, m
 μ = viscosity of water, N s/m²
 ρ = density of water, kg/m³
 g = acceleration due to gravity, m/s²

In this study, water permeability of three fly ash mixes having 5%, 10% and 15% fly ash content with a w/b of 0.25 was determined. Since fly ash concrete with 0.25 w/b has shown very high 28 days strength of 80 MPa and lower than 8.5% porosity, therefore investigation of permeability of such concrete mix may indicate the long term durability. Water permeability of FASCC in different pozzolan content are presented in Figure 6. 7.

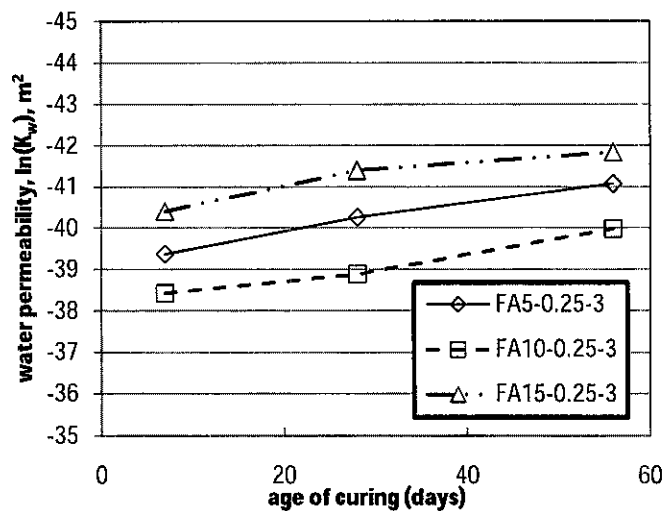


Figure 6. 7. Water permeability of FASCC

For concreting into marine environment a value of water permeability lower than 10^{-18} or $e^{-41.45}$ is considered reasonable for ensuring more than 50 years of service life

without major maintenance and repair as stated by Shafiq [186]. Value of 28 days and 90 days permeability of all three mixes indicate high potential durability. While Dinakar, et al. [111] investigated the permeability of SCC containing fly ash with different dosage of SP. The permeability represented the durability characteristic of concrete. The absorption characteristics represent the volume of pores and their capillarity. The results indicated that the low strength concretes were showing higher absorption than high strength concretes. The initial absorption values of all self compacting fly ash concretes were higher than NC and the absorption increased with an increase in replacement fly ash content as shown in Figure 6. 8.

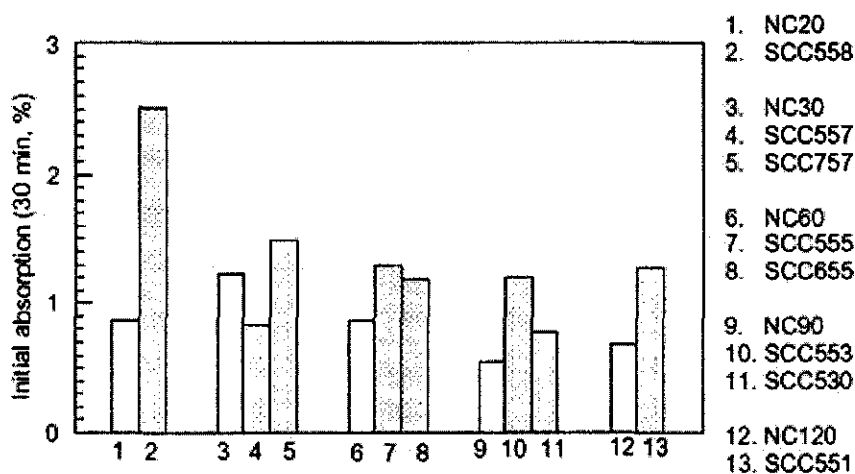


Figure 6. 8. Initial absorption values of the concretes investigated

Source: Dinakar, et al. [111]

Dinakar, et al. [111] also found that the percentage permeable voids are also higher for self compacting fly ash concretes than vibrated concretes. For all the SCC with high volume replacements of fly ash, the corresponding permeable voids were also found to be higher. This is well represented in Figure 6. 9. This fact due to the high replacements of fly ash, high water contents and high superplasticizers dosages utilized in self compacting concretes, which finally produce increased porosity.

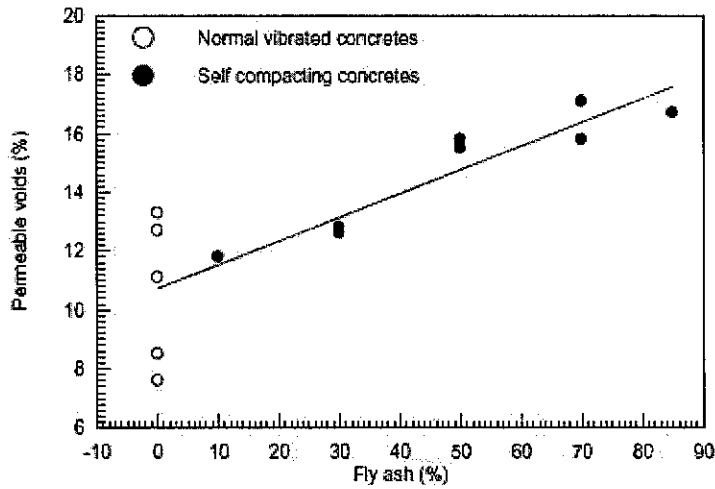


Figure 6. 9. Variation of permeable voids with fly ash replacement

Source: Dinakar, et al. [111]

6.3.2. Gas Permeability

Oxygen permeability was used in this study to investigate the gas permeability.

Oxygen permeability is calculated using:

$$K_0 = \frac{2\mu p_2 VL}{A(p_{in}^2 - p_{out}^2)} 10^{-5} \quad (6.10)$$

- Where
- K_0 = oxygen permeability, m^2
 - Q = volume flow rate, m^3/s
 - L = sample thickness, m
 - p_{in} = pressure at inlet, bar
 - p_{out} = pressure at outlet, bar
 - A = cross-sectional area of sample, m^2

Similar to water permeability, oxygen permeability is also used as an indicator of potential durability. The corrosion product on the surface of embedded steel reinforcement is formed by the continuous supply of oxygen. Rate flow of oxygen defines as the coefficient of intrinsic permeability K . If in-service concrete shows the coefficient of intrinsic permeability K , lower than 10^{-16} or $e^{-36.84} m^2$, this would indicate good potential durability, Shafiq [186].

At the age of 28 days and 56 days, 15% FASCC concrete showed the coefficient of intrinsic permeability K , as 2×10^{-16} or $e^{-36.15} m^2$ and 1.5×10^{-16} or $e^{-36.44} m^2$

respectively, which comply the requirement of high potential durability, FA5 and FA10 are also showed reasonable value of the coefficient of oxygen permeability.

Figure 6. 10 shows the oxygen permeability of fly ash SCC in different ages and different fly ash content.

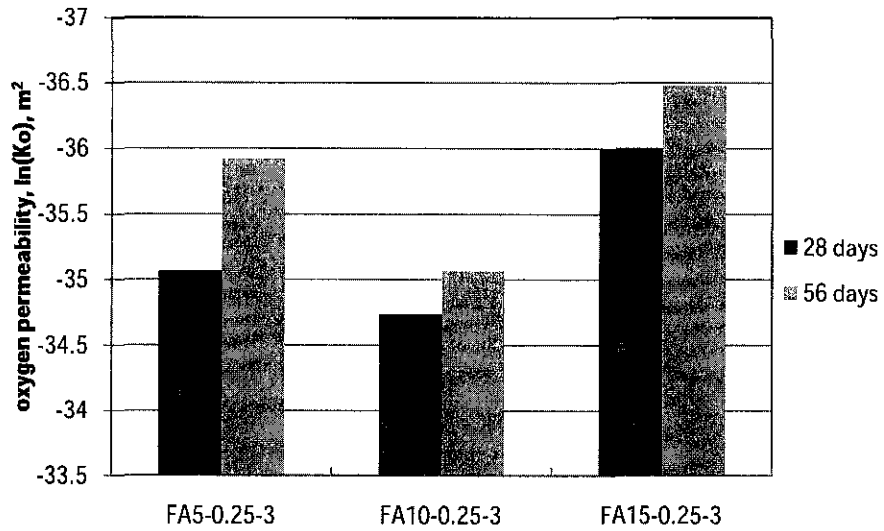


Figure 6. 10. Oxygen permeability of fly ash SCC in different ages

For MIRHA-SCC, 5% MSCC showed the lowest value of oxygen permeability as 1×10^{-16} or $e^{-36.84}$ m² that was measured at the age of 28 days. The 15% MIRHA concrete showed the permeability value of 1×10^{-15} or $e^{-34.54}$ m², which is slightly higher than the requirements of the tight concrete as shown in Figure 6. 11.

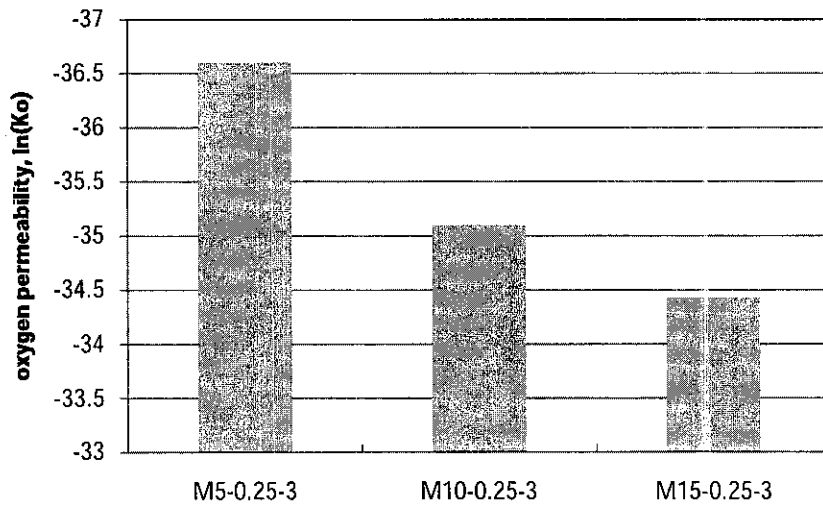


Figure 6. 11. Oxygen permeability of MSCC

Assié, et al. [109] investigated the durability properties of SCC with concern in porosity and permeability. The results of water and mercury porosity are displayed in Figure 6. 12 for SCC and vibrated concrete (VC) mixes. Water porosity is slightly higher for the SCC mixes than the corresponding VC in any class of strength. While the results of mercury porosity lead to a similar conclusion which resulted SCC presents slightly higher mercury porosity than VC. However, the mercury porosity is lower than water porosity for both type of concrete.

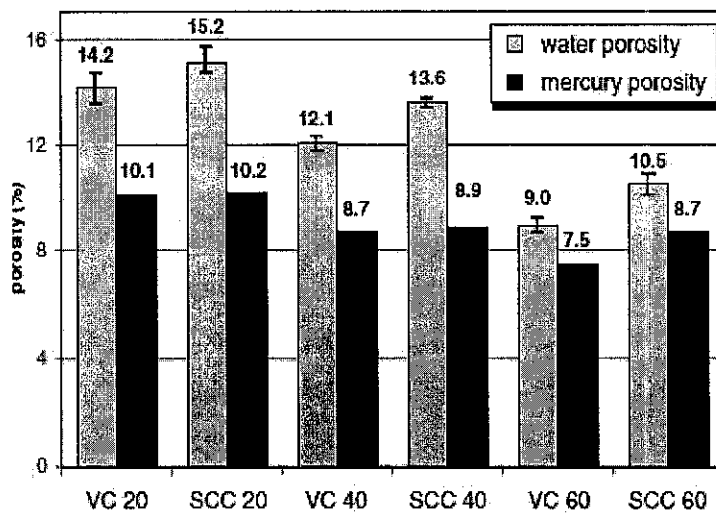


Figure 6. 12. Water and mercury porosity of concrete

Source: Assié, et al. [109]

In oxygen permeability Assié, et al. [109] found that the oxygen permeability of SCC is lower than that of VC as shown in Figure 6. 13. This trend showed that high-performance concretes are more sensitive the microcracking generated by drying on HPC compare to concrete with a higher w/b.

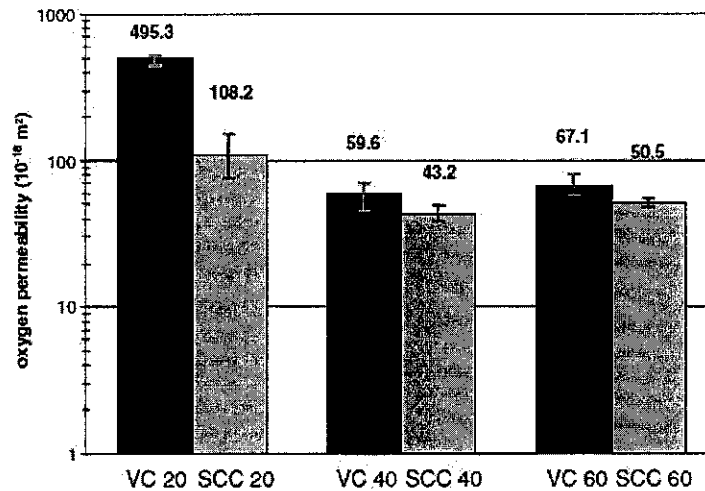


Figure 6. 13. Oxygen permeability of SCC

Source: Assié, et al. [109]

Assié, et al. [109] found that capillary absorption of SCC is higher than that of VC with a similar order of magnitude and conclude that SCC has higher durability class.

6. 4. Corrosion Characteristics

The embedded steel reinforcement in concrete is initially protected by passive layer that is formed by surrounding concrete. Basically, as a result of cement hydration, free lime cause the high alkalinity of the passive layer. During service conditions, air and moisture can penetrate into concrete through its pore system. If the surrounding air is marine environment, it carries large concentration of chloride ions. These chloride ions depassivate the alkaline layer by forming calcium chloride, and the supply of oxygen causes the formation of ferric oxide, which turns into rust product

In this study, the corrosion potential was determined using Linear Polarization Resistance Testing using the cylindrical samples which were tested in a beaker containing 3.0% NaCl solution. Table 6. 1 shows the LPR results of various concrete mixes, which are drawn in Figure 6. 14.

Table 6. 1. Analyzed LPR of SCC

Mix	LPR ($\Omega \cdot \text{cm}\hat{\text{A}}^2$)	LPR ($\Omega \cdot \text{cm}\hat{\text{A}}^2$)	I corr ($\text{mA}/\text{cm}\hat{\text{A}}^2$)	I corr ($\text{mA}/\text{cm}\hat{\text{A}}^2$)	Corrosion Rate (mm/year)	Corrosion Rate (mm/year)
	28 days	56 days	28 days	56 days	28 days	56 days
FA10-0.34-3	10014.3	6604.85	0.002632	0.003994675	0.0305	0.046298475
FA10-0.36-3	14489.5	10974.33333	0.001819	0.002389583	0.02108	0.02769545
FA10-0.42-3	7247.83	8789.592	0.003602	0.003193	0.04175	0.037
M10-0.42-3	5128.42	6699.438	0.005415	0.004207	0.06276	0.09751
M10-0.45-3	4476.25	8258.125	0.005836	0.003301575	0.06764	0.038265275
M10-0.46-3	7697.35	5140.75	0.003389	0.005110975	0.03928	0.059236225
FA10-M10-0.35-3	6686.38	10722.5	0.004841	0.0025306	0.05611	0.029329733
FA10-M10-0.4-3	11529.6	8100.75	0.002343	0.00440305	0.02715	0.051031417
FA10-M10-0.45-3	6109.6	9411.625	0.004447	0.003467	0.05154	0.08036
NC-0.4-0	4537.4	5622.516667	0.005774	0.004840633	0.06692	0.0561029

From the result in Table 6. 1, than the following charts are drawn

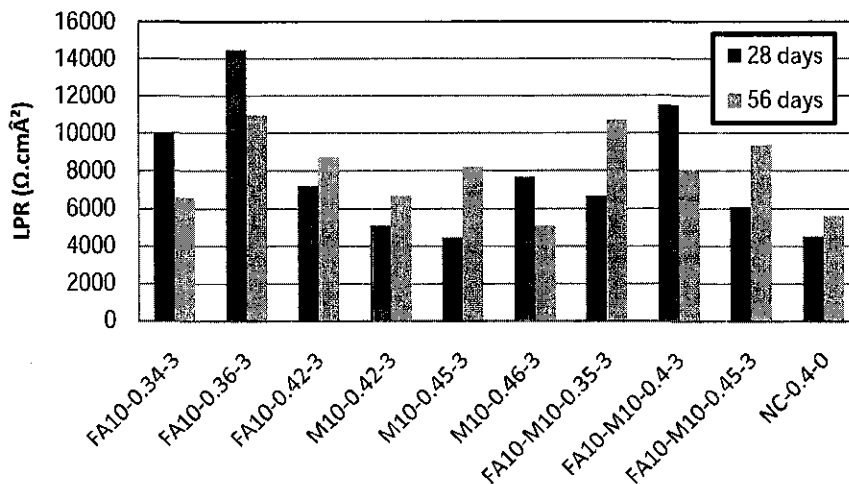


Figure 6. 14. LPR Testing Results for Sample Age 7 Days and 28 Days

From the results presented in Figure 6. 14 it can be noted that the Normal Concrete had the lowest Linear Polarization Resistivity which is 4537.4 $\text{ohm} \cdot \text{cm}\hat{\text{A}}^2$ for 7 days and 5622.517 $\text{ohm} \cdot \text{cm}\hat{\text{A}}^2$ for 28 days. This was followed by MIRHA SCC as middle corrosion resistant of concrete. The highest corrosion resistant of self compacting concrete was achieved by fly ash SCC and also combination of fly ash and MIRHA SCC had similar result. These results are in line with the investigation of Ketil [187]; Miranda, et al. [125] it was found that the micro-silica additions in concrete reduce the network of interconnected porosity and by this means the

penetration of chlorides from the external surface into the concrete could be decreased.

Song and Saraswathy [188] proposed four corrosion risks in the concrete as shown in Figure 6. 2. Normal concrete was the worst quality of corrosion resistant compare with all type of SCC with very high risk of corrosion with LPR $4537 \Omega \cdot \text{cm} \hat{\text{A}}^2$ in 28 days, while FASCC were categorized as low risk of corrosion with LPR $14489 \Omega \cdot \text{cm} \hat{\text{A}}^2$.

Table 6. 2. Corrosion risk from resistivity

Resistivity (Ohm.cm.)	Corrosion risk
Greater than 20,000	Negligible
10,000 to 20,000	Low
5,000 to 10,000	High
Less than 5,000	Very high

Source: Song and Saraswathy [188]

Figure 6. 15 illustrates the result of corrosion current; I_{corr} ($\text{mA}/\text{cm} \hat{\text{A}}^2$) reading for different mixes in 7 days and 28 days.

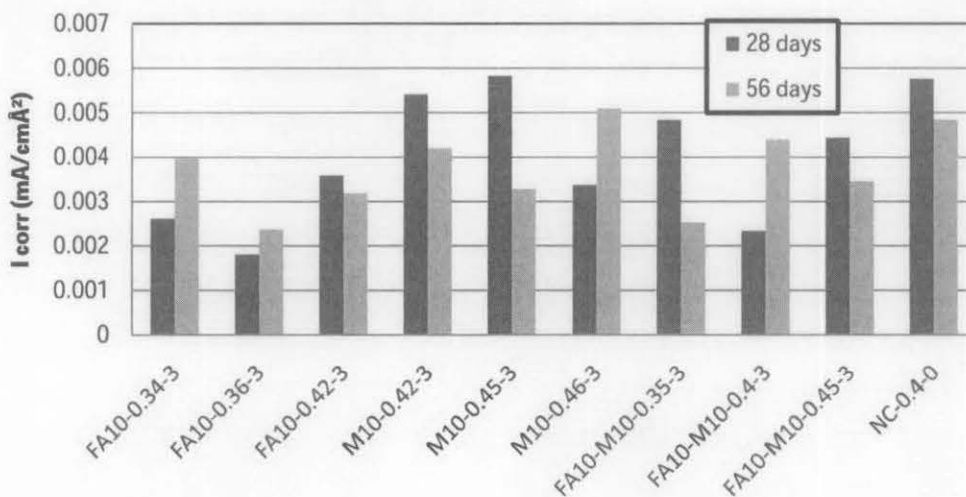


Figure 6. 15. I_{corr} ($\text{mA}/\text{cm} \hat{\text{A}}^2$) reading for different mixes in 7 days and 28 days.

Figure 6. 15 illustrates fly ash self compacting concrete showed the lowest current of corrosion. The factor causing higher corrosion rate and lower resistivity in the normal concrete mix is due to the fact that most of the water forms the capillary pores inside it. More capillary pores result in easier chloride penetration and the ease of the electron to transfer from the chloride to the reinforcement steel.

To determine criteria of potential corrosion Clear [189] recommended the following interpretations:

Table 6. 3. Corrosion criteria

Corrosion expected	i_{corr}
No corrosion expected	$< 0.2 \mu\text{A cm}^{-2}$
Corrosion possible in 10 to 15 years	$0.2 \text{ to } 1.0 \mu\text{A cm}^{-2}$
Corrosion expected in 2 to 10 years	$1.0 \text{ to } 10 \mu\text{A cm}^{-2}$
Corrosion expected in 2 years or less	$> 10 \mu\text{A cm}^{-2}$

Source: Clear [189]

Based on Table 6. 3 all the results were expected in 2 to 10 years corrosion, as the result were between $1.0 \text{ to } 10 \mu\text{A cm}^{-2}$ or $0.001 \text{ to } 0.01 \text{ mA cm}^{-2}$. The comparison of these result are given by Saraswathy, et al. [18] who investigated the corrosion resistant of steel embedded in concrete containing fly ash, the result showed that among the activation systems studied, fly ash improved the compressive strength to a certain extent, only 10% and 20% replacements. Since the fly ash concrete surface layer is etched by a strong alkali to facilitate more cement particles to join together and also the addition of CaO which is further promoting the growth of CSH gel and Ca(OH)_2 which is more advantageous to enhance the strength development and increase the corrosion-resistance of steel embedded in concrete. The fly ash blended cement concrete showed higher resistivity values than normal concrete which indicates the fly ash concretes are more closely packed and perhaps the connected pores are fewer and smaller. The reason of highly packed of this concrete is due to pozzolan reacts with the free lime liberated during setting to form CSH gel. The result is displayed in Figure 6. 4 and showed the similar corrosion rate per year with the result as shown in Figure 6. 16.

Table 6. 4. Corrosion rate of normal concrete and fly ash concrete

System	Replacement level (%)	Area rusted (%)	Corrosion rate (mmpy)
OPC	Control	50	0.0739
PFA	10	25	0.0362
	20	30	0.0534
	30	35	0.0681
	40	40	0.1567

Source: Saraswathy, et al. [18]

Figure 6. 16 presents show the results of the corrosion rate, fly ash self compacting concrete showed the lowest rate of corrosion per year. Furthermore, fly ash concrete has a higher compressive strength; higher resistivity and lower corrosion rate compared to all the other mix and in particular mix with fly ash. This is due to the effectiveness of the fly ash to react with the cement to produce more quality binder; and the other factor of successfully achievement of high resistant to corrosion is that fly ash has much finer particles than MIRHA.

Figure 6. 16 illustrates the corrosion Rate (mm/year) reading for different mixes in 7 days and 28 days.

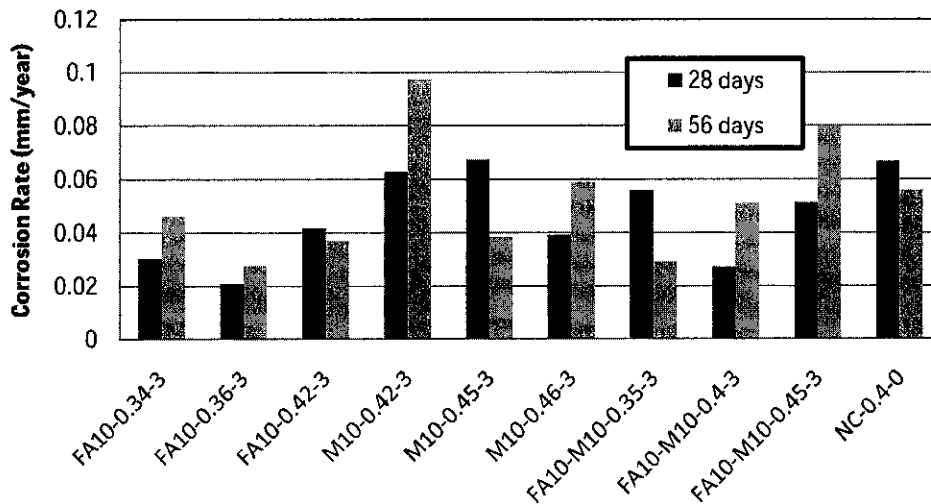


Figure 6. 16. Corrosion Rate (mm/year) reading for different mixes in 7 days and 28 days.

From the result also show some inconsistency of the data, when the w/b was 0.34 obtained the corrosion rate as 0.035 mm/year while the w/b was 0.36 the corrosion

rate should be higher but in this case it decreased as 0.02108. This inconsistency was due to the dimension effect of the mould that tends to produce more porous concrete when the small w/b concrete pours into the small dimension of mould.

6.5. Summary

Determination of durability properties in the laboratory is a long term process, even using accelerated method. Since for specification of high performance concrete, requirement of potential durability is an important factor. Therefore few of the mixes that showed high compressive strength and other mechanical properties were chosen for durability investigation. Following are some notable findings:

1. At similar w/b fly ash based concrete showed lower porosity and oxygen permeability as compared to the corresponding MIRHA mixes. It may be due to the reason that MIRHA need more water for chemical reaction and probably it may cause pore system to be long capillary pore system.
2. At lowest w/b of 0.25; 5%, 10% and 15% fly ash content showed the value of total porosity, oxygen and water permeability within a difference of 5% to 8%.
3. All concrete mixes (fly ash based and/or MIRHA based) showed intrinsic value of oxygen and water permeability in the range of 10^{-16} to 10^{-19} m^2 . This value of the coefficient of oxygen and water permeability is within the specification for acceptable durability requirement.
4. Corrosion potential, rate and current as determined for various mixes contained low on high water-binder ratio showed that the concrete with w/b of 0.25 offered high resistance against corrosion, whereas concrete with high w/b such as 0.4 and above showed moderate to poor resistance. The highest corrosion resistant of self compacting concrete was achieved by fly ash SCC and also combination of fly ash and MIRHA SCC had similar result. All SCC performed better corrosion resistance compared to normal concrete.

The results clearly indicated that durability properties of all types of SCC performed in line with mechanical properties especially compressive strength, which indicate that optimum mix design are suitable and reliable to be used.

CHAPTER 7

STRUCTURAL BEHAVIOR OF SCC

7. 1. Introduction

In last two chapters, properties of concrete that investigated in this research program were discussed in details. The results showed that with optimum w/b content, superplasticizers dosage (such as 3%), 10% pozzolan and very high 28 days compressive strength up to 80 MPa can be achieved. Such concrete showed qualifications for very high potential durability. Therefore, in this chapter structural properties of concrete beams those were tested under static and dynamic load and the bond characteristics are discussed.

7. 2. Bond Characteristic

Proper compaction flowing without segregation or bleeding is the main objective of self compacting concrete; therefore it is expected to develop a normal bond with reinforcement.

Bonding characteristic of embedded steel bar was investigated by the pull-out test. Three different diameters of steel bars were used those were partly embedded at the center of concrete cylinder. The three different diameter bars were embedded by two methods, in first method the bars were embedded in concrete by 15 times of diameter of bar, in the second method embedded length was calculated based on equal contact area of all diameter bar in concrete, detail are given in Table 7. 1 and Table 7. 2.

Table 7. 1. Calculation for embedded reinforcement for constant area.

diameter of embedded steel bar(mm)	perimeter of steel bar (mm)	length of embedded steel bar(mm)	contact area(mm ²)
10	31.42	240	7541
12	37.70	200	7541
16	50.27	150	7541

Table 7. 2. Calculation for embedded reinforcement for 15 times of bar diameter.

diameter of embedded steel bar (mm)	15 x diameter of embedded steel bar (mm)	Contact area(mm ²)
10	150	4713
12	180	6786
16	240	12065

For pull out test, the concrete samples were tested at the age of 28 days. Table 7. 3 shows the pull-out force and the ultimate bond strength of 10,12 and 16 mm diameter bars embedded in different concrete based on same contact area.

Table 7. 3. Pull-out results and bond strength of constant area:

Mix	dia (mm)	embedded length L (mm)	ult. Pull out P (kN)	bond strength f_b (Mpa)
FA5-0.32-3	10	240	49.37	6.55
FA5-0.32-3	12	200	80.6	10.69
FA5-0.32-3	16	150	85.28	11.31
FA10-0.32-3	10	240	49.92	6.62
FA10-0.32-3	12	200	69.45	9.21
FA10-0.32-3	16	150	73.26	9.72
FA15-0.32-3	10	240	49.51	6.57
FA15-0.32-3	12	200	67.31	8.93
FA15-0.32-3	16	150	93.57	12.41
NP-0.25-3	10	240	50.38	6.68
NP-0.25-3	12	200	81.7	10.84
NP-0.25-3	16	150	99.46	13.19
NP-0.32-3	10	240	50	6.63
NP-0.32-3	12	200	77.54	10.28
NP-0.32-3	16	150	74.21	9.84

Table 7. 4. Pull-out results and bond strength of 15× of embedded length

Mix	dia (mm)	embedded length L (mm)	ult. Pull out P (kN)	bond strength f_b (Mpa)
FA5-0.32-3	10	150	49.14	10.43
FA5-0.32-3	12	180	78.24	11.53
FA5-0.32-3	16	240	81.53	6.76
FA10-0.32-3	10	150	49.29	10.46
FA10-0.32-3	12	180	78.79	11.61
FA10-0.32-3	16	240	96.43	7.99
FA15-0.32-3	10	150	49.53	10.51
FA15-0.32-3	12	180	74.40	10.96
FA15-0.32-3	16	240	117.68	9.75
M10-0.35-2	10	150	43.66	9.26
M10-0.35-2	12	180	66.74	9.84
M10-0.35-2	16	240	85.47	7.08
M10-0.35-4	10	150	41.91	8.89
M10-0.35-4	12	180	58.41	8.61
M10-0.35-4	16	240	101.78	8.44
M10-0.35-6	10	150	27.30	5.79
M10-0.35-6	12	180	66.01	9.73
M10-0.35-6	16	240	133.07	11.03
M10-0.4-2	10	150	45.02	9.55
M10-0.4-2	12	180	57.33	8.45
M10-0.4-2	16	240	103.53	8.58
M10-0.4-4	10	150	39.81	8.45
M10-0.4-4	12	180	64.55	9.51
M10-0.4-4	16	240	81.46	6.75
M10-0.4-6	10	150	9.75	2.07
M10-0.4-6	12	180	34.25	5.05
M10-0.4-6	16	240	106.58	8.83
M10-0.45-2	10	150	42.14	8.94
M10-0.45-2	12	180	67.77	9.99
M10-0.45-2	16	240	62.60	5.19
M10-0.45-4	10	150	28.60	6.07
M10-0.45-4	12	180	56.42	8.31
M10-0.45-4	16	240	102.00	8.46
M10-0.45-6	10	150	25.68	5.45
M10-0.45-6	12	180	66.01	9.73
M10-0.45-6	16	240	90.86	7.53
NP-0.25-3	10	150	47.19	10.01
NP-0.25-3	12	180	80.28	11.83
NP-0.25-3	16	240	121.97	10.11
NP-0.32-3	10	150	50.49	10.71
NP-0.32-3	12	180	76.85	11.33
NP-0.32-3	16	240	119.78	9.93
NC-0.4-0	10	150	42.58	9.03
NC-0.4-0	12	180	65.23	9.61
NC-0.4-0	16	240	111.11	9.21

Result of ultimate bond strength that contained in Table 7. 3 and Table 7. 4 are clustered in various groups, for drawing various discussions to describe the effects of different parameters on the ultimate bond strength. Figure 7. 1 shows the ultimate strength of FASCC with 5%, 10% and 15% fly ash content for which w/b was 0.32 and SP was 3%.

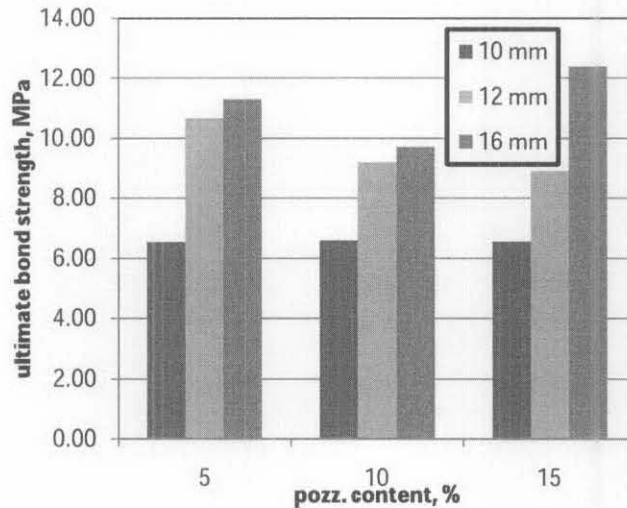


Figure 7. 1. Effects of different fly ash content on bond strength with constant embedment area

The embedment length of 10 mm, 12 mm and 16 mm diameter bars was chosen based on constant contact area. The 16 mm diameter showed the highest bond strength in all concrete mixes. The 16 mm diameter bar showed 46% to 88% higher bond strength as compared to 10 mm diameter bar. The 10 mm diameter showed the same bond strength for all three mixes. For 12 mm diameter bar 5% FASCC showed 10.69 MPa of bond strength in comparison of 9.21 and 8.39 MPa that was obtained for 10% FA and 15% FA mixes respectively. For 16 mm bar 15% FA showed the higher strength.

Figure 7. 2 shows the bond strength results of 5%, 10% and 15% FASCC mixes which had an embedment length of 15 times the bar diameter.

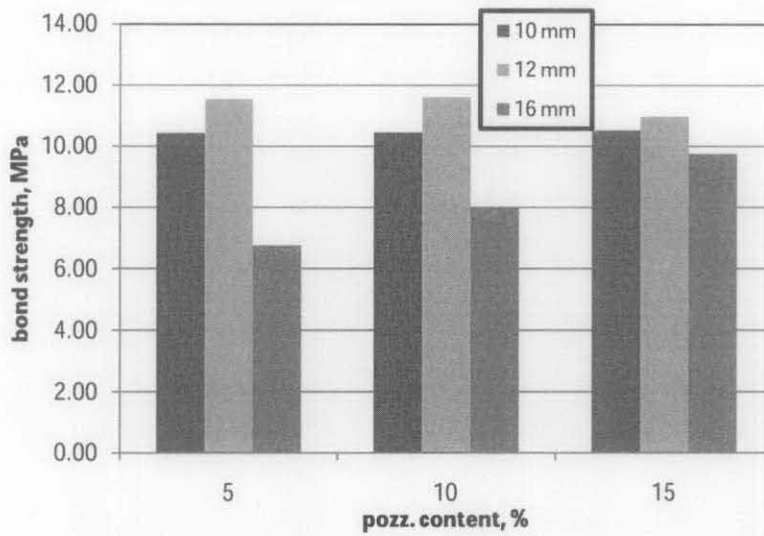


Figure 7. 2. Effects of 5, 10 & 15% FA content bond strength 15 times diameter of embedment length

In this case the maximum bond strength was found as 11.61 MPa and the lowest value was 6.76 MPa. The 12 mm diameter bar has shown the highest bond strength in each of the group, whereas the 16 mm diameter bar showed the lowest bond.

Figure 7. 3 and Figure 7. 4 show that increasing of superplasticizers content reduce the anchorage bond stress. And from these figure also show that bond strength values increased when larger steel bar diameter is used.

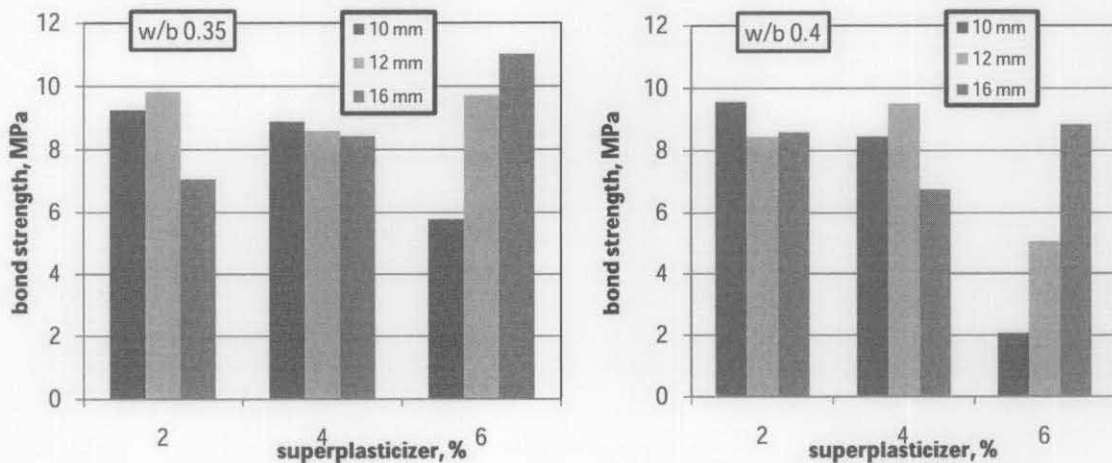


Figure 7. 3. Effect of superplasticizers on bond strength with w/b 0.35 and 0.4

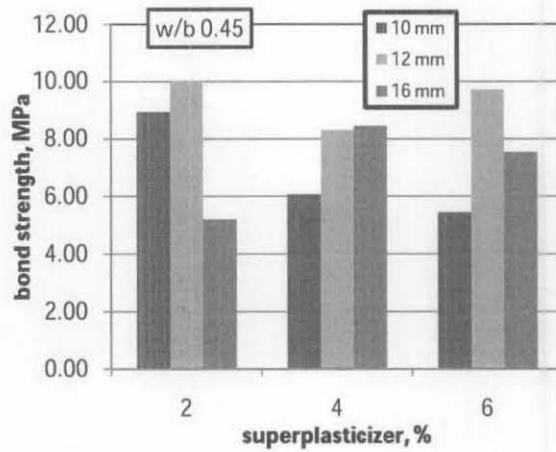


Figure 7. 4. Effect of superplasticizers on bond strength with w/b 0.45

The effect of superplasticizers on bond strength in line with the compressive strength in w/b of 0.4 that showed that 4% SP dosage was the higher bond strength with 40% higher than the bond strength of FASCC with 6% SP dosage.

Figure 7. 5 depicts clearly that increasing the water-binder ratio will reduce bond strength, and again that superplasticizers content increased so the bond strength decreased.

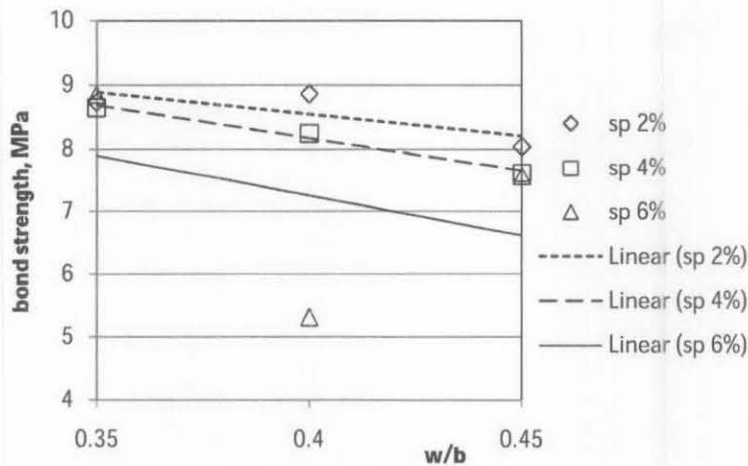


Figure 7. 5. Effect of water-binder ratio on bond strength in different sp content

The investigation of bond strength of reinforcing bars embedded in full-scale heavily reinforced concrete sections made with industrial self compacting concrete and compared with that of normal concrete was studied by Hassan, et al. [131]. The

bond stress was tested for bars located at three different heights that are 150 mm, 510 mm, and 870 mm from the bottom of the pullout specimens and at different tested ages 1, 3, 7, 14, and 28 days. The results also indicated that the bond stress was slightly higher in the SCC pullout specimen compared to the normal concrete pullout specimen as shown in Figure 7. 5.

Table 7. 5. Bond stress for SCC and NC pullout specimens

	SCC	NC
	Top bar	Top bar
1 day		
Measured bond stress (u) (MPa)	10.08	10.19
3 days		
Measured bond stress (u) (MPa)	16.99	16.56
7 days		
Measured bond stress (u) (MPa)	18.26	17.83
14 days		
Measured bond stress (u) (MPa)	18.37	17.62
28 days		
Measured bond stress (u) (MPa)	19.75	18.90

Source: Hassan, et al. [131]

The other investigation was done by Valcuende and Parra [129] who studied bonding properties of SCC. The result indicated that the ultimate bond strength of SCC is slightly higher in normal concrete as shown in Table 7. 6. Most of specimen was fail in pull out modes. This failure was caused the steel reached stresses close to yield stress, when the compressive strength of the concrete is increased, the higher stresses transmitted by the bars that generate an increase in the radial component of the bond stress and increase bond effects. Usually the tensile strength which largely determines bond failure, increases relatively less than the compressive strength; and that may result in a failure by splitting instead of by pull-out. There may be various reasons for this phenomenon, such as consolidation of the steel–concrete interface and the slightly lower tensile strength in SCC.

Table 7. 6. Mechanical properties and pull-out test results

Concrete	Age (days)	f_c (MPa)	f_t (MPa)	Mean bond stress			Ultimate bond stress			Mode of failure
				τ_b (MPa)	$\tau_b/\sqrt{f_c}$	COV (%)	τ_u (MPa)	$\tau_u/\sqrt{f_c}$	COV (%)	
S-65-32	28	30.21	2.40	11.66	2.12	1.42	18.00	3.27	3.37	Pull-out
	90	37.31	2.82	13.46	2.20	5.28	19.57	3.53	5.57	Pull-out
S-55-32	28	35.77	2.73	13.56	2.27	1.56	21.66	3.62	3.74	Pull-out
	90	44.18	3.20	16.55	2.49	3.69	25.43	3.83	5.23	Pull-out
S-55-42	28	50.18	3.52	17.55	2.48	1.99	27.97	3.95	2.62	Pull-out
	90	59.50	4.14	19.09	2.47	4.41	29.45	3.82	2.36	Pull-out
S-45-42	28	61.15	4.09	20.08	2.64	1.74	39.98	3.83	0.59	Pull-out
	90	69.02	4.80	22.68	2.70	4.65	32.38	3.90	2.65	Splitting
N-65-32	28	27.75	2.65	8.42	1.62	7.24	15.39	3.05	6.22	Pull-out
	90	35.52	3.20	10.71	1.80	9.91	20.25	3.40	5.70	Pull-out
N-55-32	28	33.76	3.08	10.74	1.82	3.64	19.18	3.39	3.95	Pull-out
	90	43.21	3.72	12.28	1.87	7.69	21.53	3.28	3.10	Pull-out
N-55-42	28	42.40	3.67	12.67	1.94	7.76	23.63	3.67	1.67	Pull-out
	90	51.73	4.29	15.88	2.21	3.86	25.65	3.80	2.25	Pull-out
N-45-42	28	56.50	4.22	16.19	2.33	4.04	29.69	3.81	0.35	Pull-out
	90	63.09	4.98	19.66	2.48	2.83	31.35	3.95	1.45	Splitting

f_c : Compressive strength; f_t : tensile strength; τ_b : mean bond strength; τ_u : ultimate bond strength; COV: coefficient of variation.

Source: Valcuende and Parra [129]

7. 3. Behavior of SCC Structure under Static Loading

Bending capacity of reinforced concrete beams subjected to static loading was investigated using computer models and experimental testing for selected mixes. The computer model determine the reliability of the experiment setup based on the expected ultimate loading from the specimen so it can fit into the range of load in actuator machine and also to determine the tendency of failure type of the beams so it can feasible to be tested. The crack patterns of the computer model establish this tendency.

7.3.1. Computer Modeling

The described model has been applied to study the feasibility of loading setup under static load on the beam test. Modeling of beam experiment was carried out by nonlinear analysis program using ATENA (Advanced Tool for Engineering Nonlinear Analysis). ATENA is a nonlinear analysis software developed by Červenka Consulting. This program is used for analysis of concrete and reinforced concrete structures, which can simulates real behavior of concrete and reinforced concrete structures including concrete cracking, crushing and reinforcement yielding.

This program was used to find the stress pattern of the specimen and also the displacements and the particular strains. The program utilizes an iterative procedure to

produce the forces and displacements when members consist of materials that exhibits non-linear behavior. The stiffness of each member is calculated by section-analysis and the stiffness method is applied at each iterative step as a non-linear method. The load is applied in increments with 80 step of increment loading and the program created the result at each load step using standard Newton-Rhapson and standard arc length iteration, Červenka and Červenka [190]. This model using SBETA (StahlBETonAnalyse) constitutive model which describe by Červenka, et al. [191]. The material model SBETA includes the following effects of concrete behavior: non-linear behavior in compression including hardening and softening, fracture of concrete in tension based on the nonlinear fracture mechanics, biaxial strength failure criterion, reduction of compressive strength after cracking, tension stiffening effect, reduction of the shear stiffness after cracking (variable shear retention), two crack models: fixed crack direction and rotated crack direction. The increment load of 1.5 kN was applied to the model, with compressive strength concrete of $f_c' = 51$ MPa and split tensile stress of concrete for cracking analysis was $f_t = 3.6$ MPa. Modulus young was define as much as $E_c = 3.9 \cdot 10^4$ MPa. The result showed that the initial crack was occurred when loading achieved as 22.5 kN, and finally the failure mode arise as the increment load reach with maximum load 120 kN. Input of ATENA program and initial crack and final crack of beam model can be seen in Appendix-C

Figure 7. 6 illustrates the computer model used to run the program, and how the beam was meshed by several solid elements.

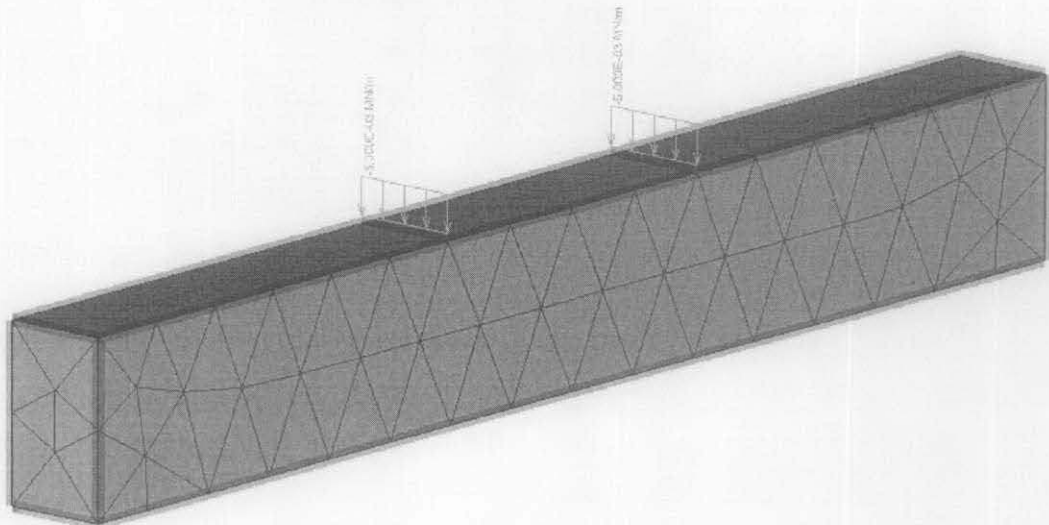


Figure 7. 6. Finite Element mesh model of a beam

The stress of σ_x in after yielding condition is shown below. Where hot color represent tensile stress and cold color represent compression stress.

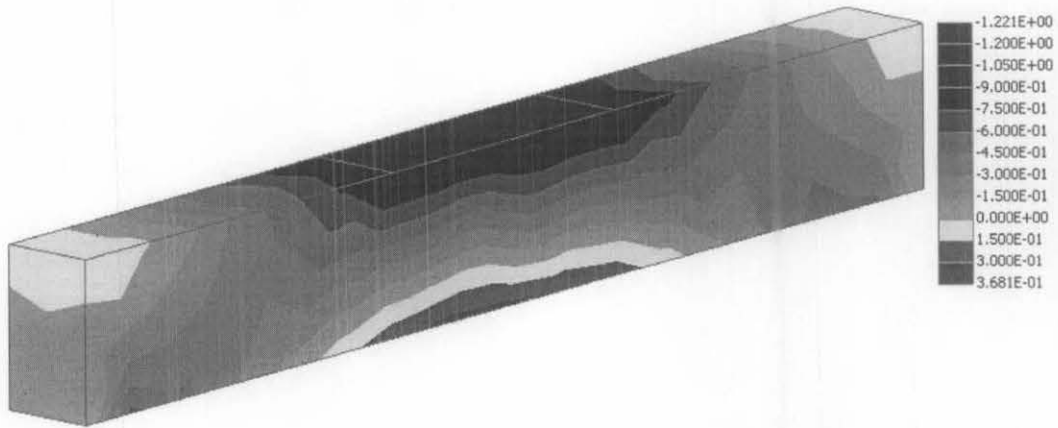


Figure 7. 7. Stress contour of σ_x in a beam in first increment load

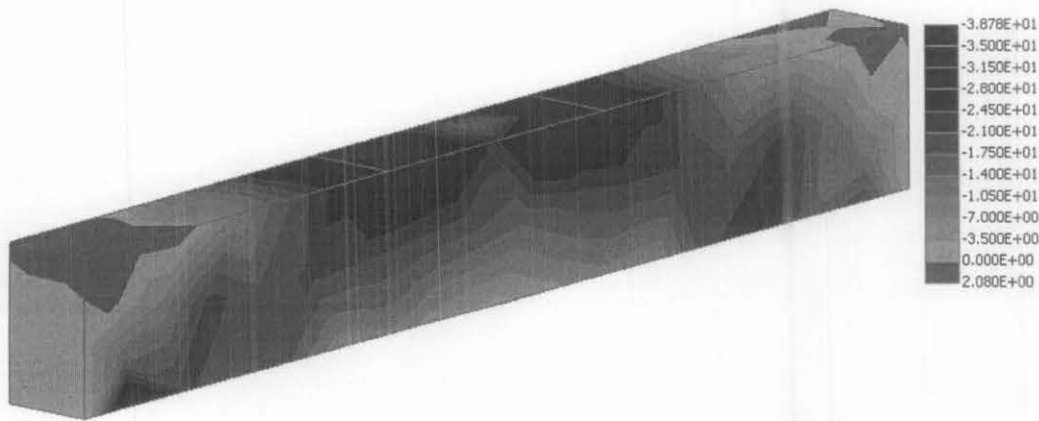


Figure 7. 8. Stress contour of σ_x in a beam in final increment load

Figure 7. 7 shows the stress contour, σ_x on beam subjected to a line loading in line with that used in the experiment. In the first increment load, distribution of stress is still in the linear condition. The middle top fiber of beam is in compression stress, while the bottom fiber of beam is in tensile stress. Figure 7. 8 shows the stage of final increment load that illustrate the failure of beam. Contour area of tensile stress of beam decrease in this stage due to cracking and crushing in tensile area. Therefore compression stress will be dominant and finally crush the concrete.

Principal stress is the maximum of the stresses in the solid element and it is maximum stress on which there is no shear stress.

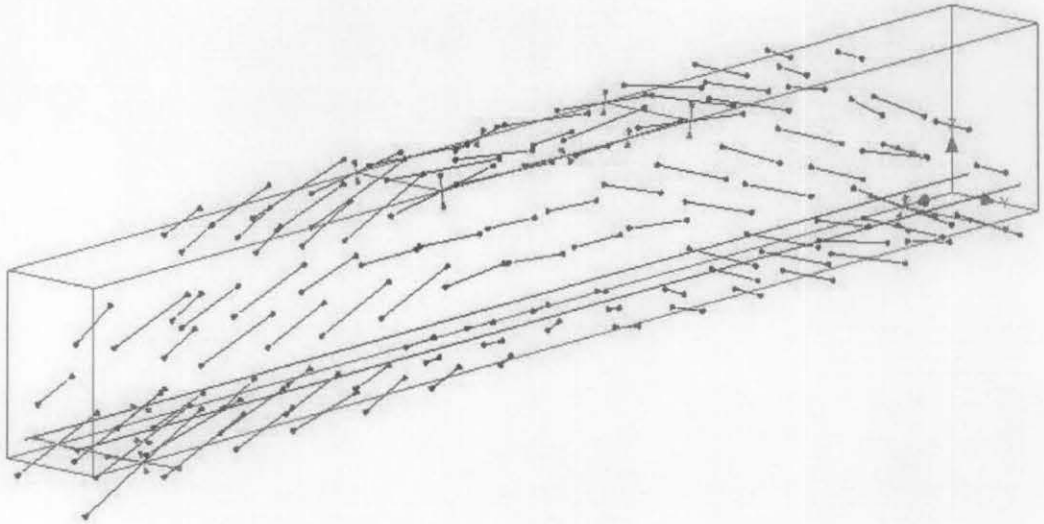


Figure 7. 9. Tensor of Principal stress of beam

Figure 7. 9 illustrates the principal stress which form a curve from support to middle of top fiber. The figure also shows that the maximum impact of stress will concentrate in this area.

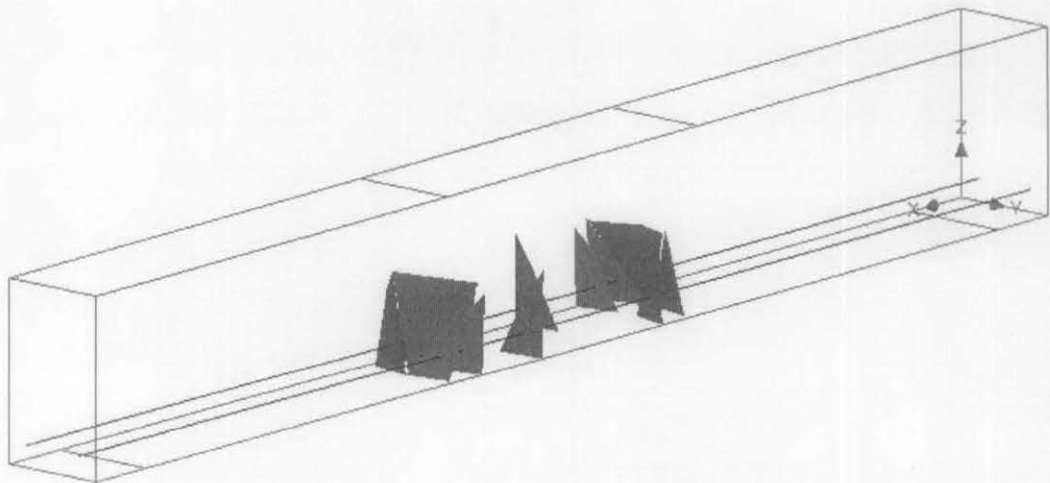


Figure 7. 10. First crack in of beam

Figure 7. 10 shows that first crack occur in the middle bottom of the beam and growing to the top of beam, and the failure type is bending failure so the experiment setup can be used.

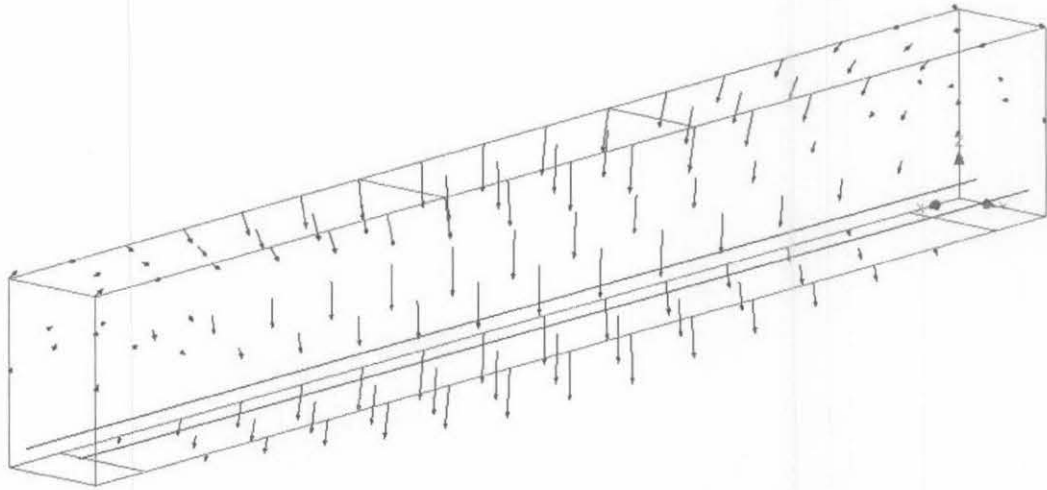


Figure 7. 11. Typical displacement vector of beam

Figure 7. 11 shows that the displacement in the middle of the beam is larger than in the end of the same beam.

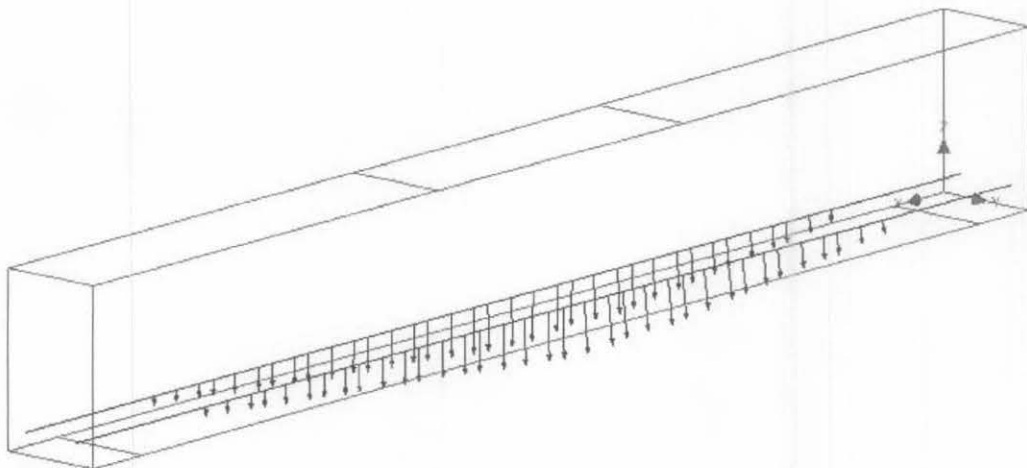


Figure 7. 12. Typical displacement vector of steel reinforcement

Figure 7. 12 depicts the clearly situation that only middle of steel reinforcement will deflect while the end section of steel will still remain in its position.

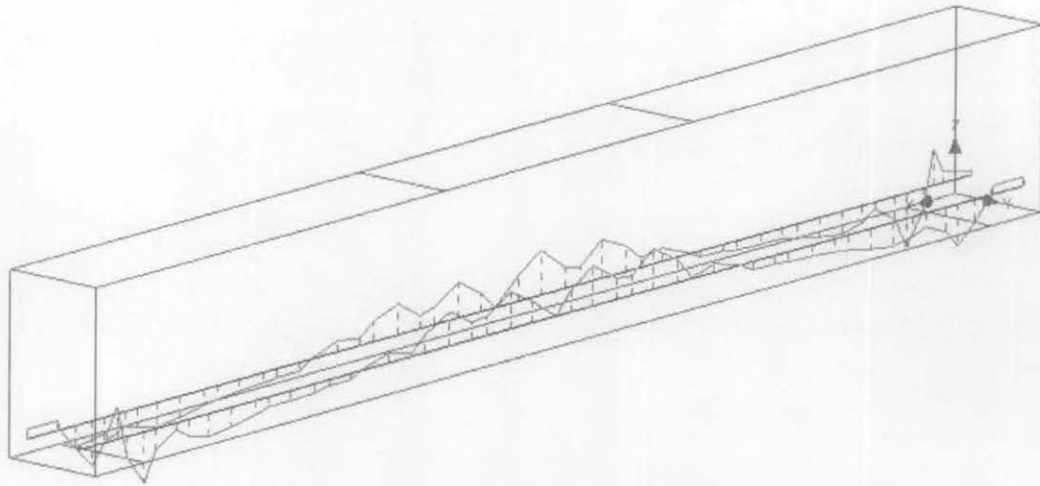


Figure 7. 13. Typical stress on steel reinforcement in longitudinal axes

Figure 7. 13 shows that the maximum stress on the steel reinforcement is in the middle and decrease gradually at the end. It can be seen from Figure 7. 6 to Figure 7. 13 that the experiment setup can be used in the experiment included the dimension of beam, the span of beam and loading.

7.3.2. Beam Testing under Static Load

Five beams were tested under static load in order to compare the influence of the mix design. Four-point bend tests for self compacting concrete beams containing fly ash and MIRHA and also normal concrete were performed to determine the static behavior. The load was applied at the rate of 0.2 kN/second. All tests were performed at the Universiti Teknologi PETRONAS (UTP) using closed-loop servo-controlled testing machines equipped with load cells of 500 kN capacity.

Static load beam used the optimum mix design from the result of compressive strength that mentioned earlier in Chapter 5. The displacement-load diagram of five beam of static load can be seen below.

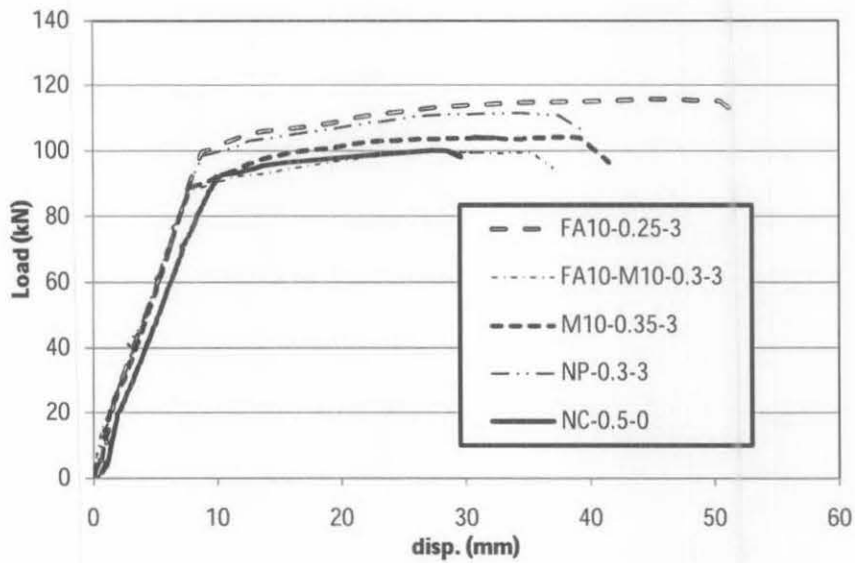


Figure 7. 14. Load-displacement diagram of SCC beam static load test

Figure 7. 14 shows the performance and behavior of five different mixes of beam specimen those were chosen as the optimum from each group under static load test. From the all result of beam static load test than can be synthesized as performance parameter as illustrated in Table 7. 7. This table also shows the type of failure and initial cracks which are not included in Figure 7. 14.

Table 7. 7. Result of final test of static beam load

specimen	f'_c	P_u	d_u	P_y	d_y	P_c	d_c	P_{fc}	P_{dc}	Failure type
FA10-0.25-3	71.86	115.63	45.66	99.53	8.83	110.15	52.19	30	80	fs
FA10-M10-0.3-3	65.89	100.33	27.84	85.72	7.57	94.61	37.06	25	80	fs
M10-0.35-3	59.47	104.21	28.50	85.44	7.53	96.43	41.58	25	50	s
NP-0.3-3	65.11	111.58	32.78	99.03	9.11	106.53	39.33	30	70	fs
NC-0.5-0	54.28	100.15	28.14	92.9	10.74	94.45	34.15	30	70	s

Where:

- f'_c = compressive strength at age 28 days, MPa
- P'_u = ultimate static load, kN
- d'_u = displacement in ultimate static load, mm
- P_y = initial yield load, kN
- d_y = displacement in initial yield load, mm
- P_c = crush load, kN
- d_c = displacement in crush load, mm
- P_{fc} = initial flexural crack load, kN
- P_{dc} = initial diagonal crack load, kN

- s = shear failure
- fs = flexural failure, slipping off

The results extracted from Table 7. 7 to compare the performance in each mix of the beam can be assembled in the several charts in Figure 7. 15 and Figure 7. 16.

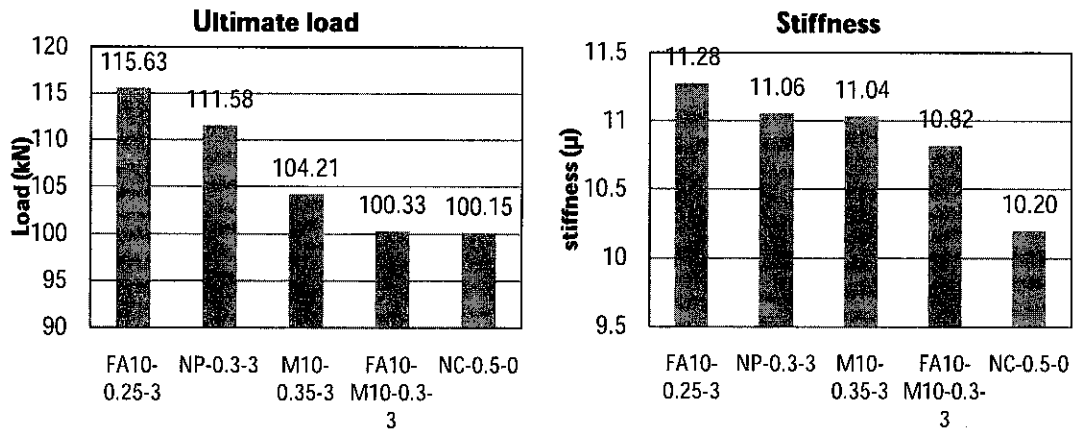


Figure 7. 15. Ultimate load and stiffness of SCC beam static load test

Figure 7. 15 shows that the beam with fly ash self compacting concrete performed better than the other beams and its ultimate load was 115.63 kN. This is in line with the compressive strength behavior as discussed earlier in Chapter 5. The worst performance of beam was normal concrete beam which only achieved 100.15 kN of ultimate load. While no pozzolan self compacting concrete also performed well with ultimate load of 111.58 kN and follow by MIRHA self compacting concrete, but combination of fly ash and MIRHA unexpectedly and performed almost same as normal concrete.

Fly ash self compacting concrete beam also shows a high stiffness compared to the other tested beam with 11.28 kN/mm, while the normal concrete showed the worst stiffness with a value of 10.2 kN/mm. MIRHA SCC and no pozzolan SCC performed almost similar stiffness of 11.06 kN/mm and 11.04 kN/mm for MIRHA and no pozzolan SCC respectively.

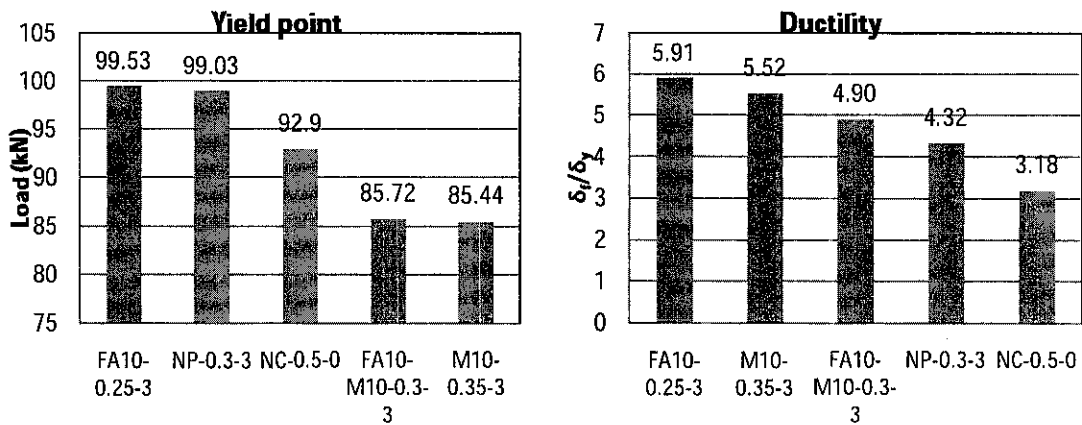


Figure 7. 16. Yield point load and ductility of SCC beam static load test

Yield point load is very essential to determine the performance of the structure and become the limit of the beam subjected to the loading in its linear stage. Fly ash SCC beam and no pozzolan SCC performed almost similar with 99.53 kN and 99.03 kN for fly ash and no pozzolan SCC, respectively. While in this yield point parameter the normal concrete performed better than MSCC and FMSCC for static test with 92.9 kN yield point load. Combination of fly ash and MIRHA SCC and MIRHA SCC did not perform well and only achieved 85.72 kN and 85.44 kN, respectively.

Fly ash performed surprisingly with high ductility; generally the high strength concrete has low ductility. This beam performed well with 5.91 of ductility follow by MIRHA SCC with 5.52. The worst ductility again achieved by normal concrete beam with 3.18. The ductility is very important for energy absorption as mentioned by Weena, et al. [168]; Spadeal and Bencardino [192]. The ductility of concrete in the real structure is influenced by strength of concrete and confined section of concrete structure. Therefore using confining reinforcement in earthquake resisting structures is very common for many structural designers, in order to increase the ductility of the structural members.

To simplify the performance, for all five beam that representative of optimum mix design in self compacting concrete, the benchmark of performance can be drawn in Figure 7. 17.

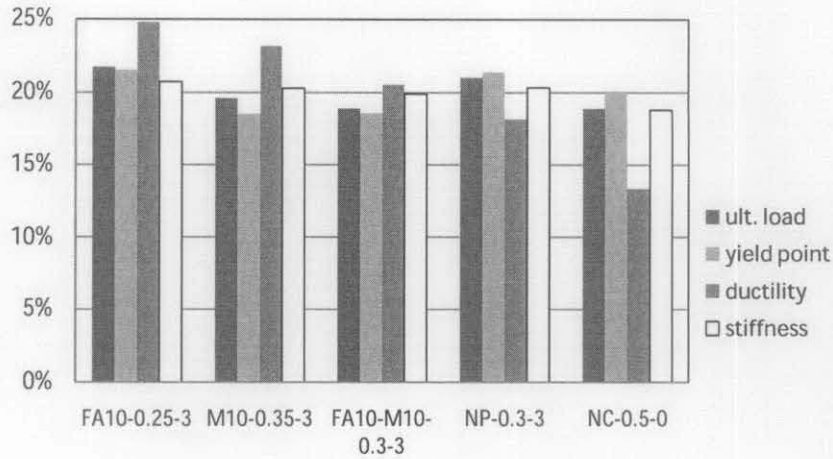


Figure 7. 17. Performance benchmark of static loading test

From Figure 7. 17 clearly shows that self compacting concrete containing fly ash is the best mix and show the best performance in all aspect. It means that FASCC is not only the stronger mix that has shown highest elastic yield, high compressive strength, 80 MPa at 28 days it has also shown high ductility and the area under the load deflection curve (modulus of toughness). This also was indicated in modulus of rupture and tensile strength result. Furthermore this result also in line with the mechanical properties as discussed in earlier chapter. Total performance of FASCC was 88.78%, MSCC was 81.54%, FMSCC was 77.84%, NPSCC was 80.83% and the lowest performance was normal concrete with 71.00%. For all that parameter than can be concluded that all SCC types performed better than normal concrete as a control specimen. It shown also that FASCC has the best performance beam which was 8.8% higher than the normal concrete beam.

These results are also in accordance with previous similar studies by Hassan, et al. [121] who investigated the structural behavior with beam static load test with comparing the SCC beam and normal concrete (NC) beam. SCC beams also showed lower ultimate shear strength compared to NC beams with maximum ultimate shear strength increase of 17% was observed in NC beams as detailed in Table 7. 8. The post-diagonal cracking shear resistance and ductility in beams of SCC were also low compared to NC beams, this phenomenon due to less aggregate interlock as a consequence of a lower quantity of coarse aggregate in SCC.

Table 7. 8. Load-deflection results of SCC and NC beams

Beam designation	Total load (kN)			$P_u/P_d(\%)$	Deflection in each beam (mm)	
	At first flexural crack (P_f)	At first diagonal crack (P_d)	At failure (P_u)		At first diagonal crack load (δ_d)	At failure load (δ_f)
SCC-0	90	141	298	211.3	0.97	2.77
NC-0	90	135	330	244.4	0.77	3.2
SCC-1	105	153	319	208.5	1.1	3.3
NC-1	103	149	380	255.0	1.12	4.11
SCC-2	97	-	212	-	-	2.01
NC-2	75	-	280	-	-	23.28

Source: Hassan, et al. [121]

7.3.3. Crack Pattern of Static Test

Crack pattern visualize the growing of crack and its development. During the experiment, every new crack of concrete than was marked as the sequence of crack and development of crack will be marked with the associated loading. All crack patterns are displayed in Figure 7. 18. to Figure 7. 22.

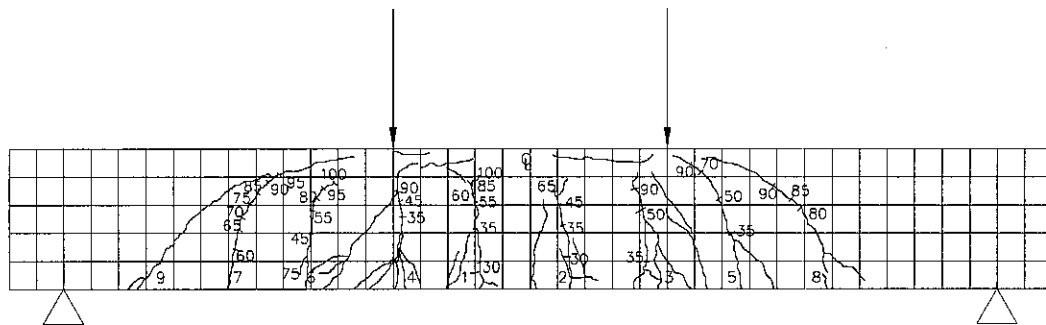


Figure 7. 18. Crack pattern of FASCC beam specimen (flexural failure)

During the static tests, the fly ash self compacting concrete beam, flexural cracks developed first in the pure bending region with initial flexural load of 30 kN in crack number 1, this crack occurred almost at the same time with crack number 2. These middle cracks due to flexural displacement propagated to the middle top of beam. The diagonal tensile cracks developed as the loading increased when load reached 80 kN. These diagonal tensile cracks propagated from the bottom to the loading points at an angle of 45° degrees. The increase in diagonal crack grows independently of the flexural crack growth. The flexural crack relatively did not grow after the diagonal crack occurred. Figure 7. 14 shows in the static tests, the load-deflection curve shows

a non-linear behavior and the strains in the stirrups are closely related to the diagonal cracking in the tested beam. When load increased to more than 100 kN the formation of new significant cracks in the beam has not been recorded also the associated loading which cause the crack due to the difficulty of recording. However, the sketch of pattern cracks then can be drawn by tracing the photograph using the CAD program. Details of all the static experimental results are reported in Table 7. 7.

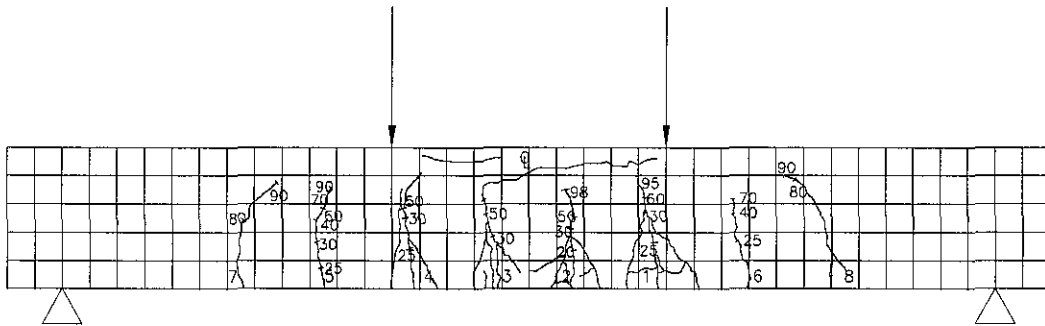


Figure 7. 19. Crack pattern of FMSCC beam specimen (flexural failure)

The crack of fly ash and MIRHA SCC propagated in lower loading with 25 kN of initial flexural crack. The diagonal cracks were developed with associated load of 80 kN at around angle of 65°.

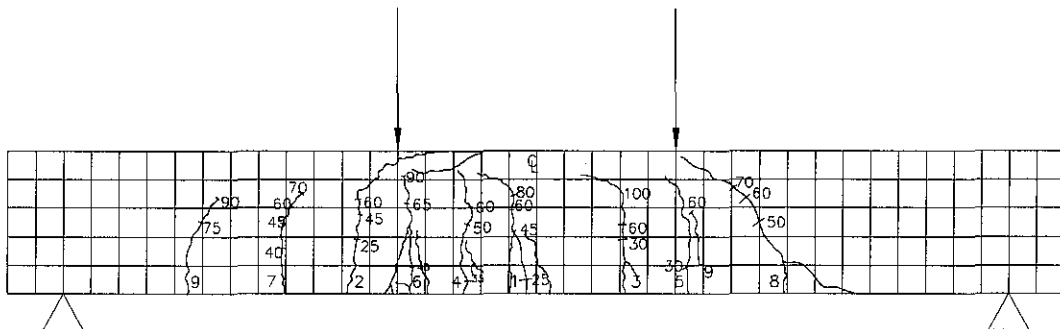


Figure 7. 20. Crack pattern of MSCC beam specimen (shear failure)

The crack of MIRHA SCC propagated in lower loading with 25 kN of initial flexural crack. The diagonal cracks were developed with associated load of 50 kN at an angle of 45°. From the diagonal crack grow in a very early stage of incremental load, it was noticed that MIRHA SCC has a low resistant stage to the shear load.

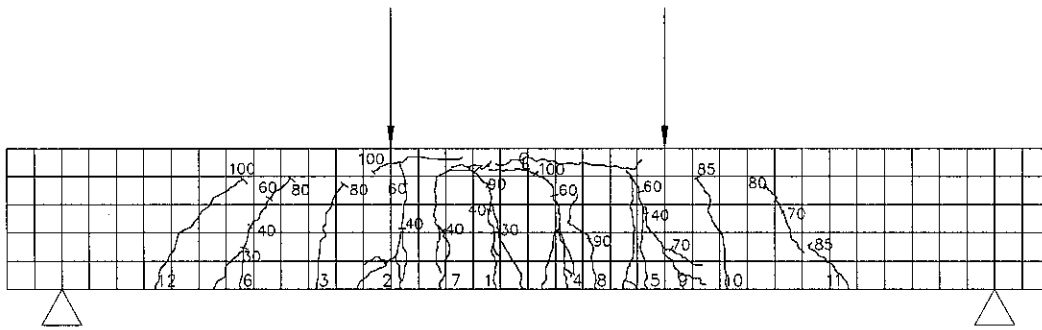


Figure 7. 21. Crack pattern of NPPSCC beam specimen (bending failure)

Figure 7. 21 shows that for the no pozzolan self compacting concrete beam, flexural cracks developed first in the bottom middle of beam with initial flexural load of 30 kN and then propagated to the middle top of the beam. The diagonal tensile cracks developed as the loading increased when the load reached 70 kN and these diagonal tensile cracks propagated from the bottom to the loading points at 45°.

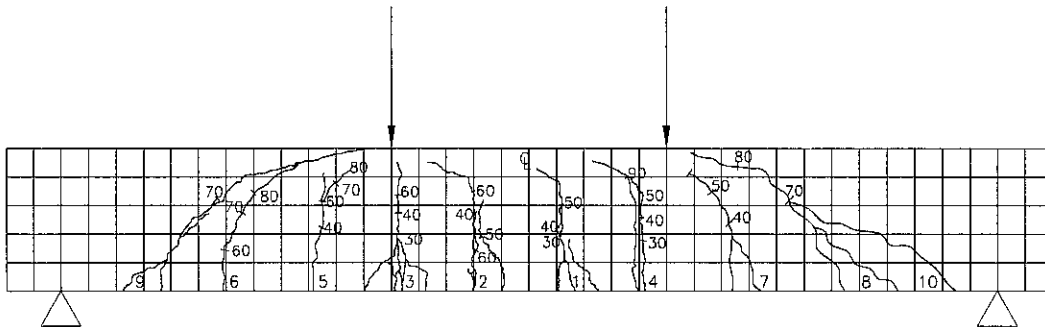


Figure 7. 22. Crack pattern of Normal Concrete beam specimen (shear failure)

Figure 7. 22 shows that, for the normal concrete beam, flexural cracks developed first in the bottom middle of the beam with initial flexural load of 30 kN and then propagated to the middle top of beam. The diagonal tensile cracks developed as the loading increased when the load reached 70 kN These diagonal tensile cracks propagated from the bottom to the loading points at 45°.

Kae-Hwan and Jae-Jung [193] mentioned that during the static tests, flexural cracks developed first in the pure bending region, but diagonal tensile cracks are developed as the loading increased. For the beams without stirrups, these diagonal tensile cracks propagated from the middle of the web to the supports and to the loading points at 45°. In this case, the shear cracking load and the ultimate shear

strength increases linearly with the increase of the amount of polymer. For the beams with stirrups, the diagonal tensile cracks initiated from the midpoints of each stirrup and propagated at 45°. In most cases, three or four diagonal tensile cracks occur symmetrically on the opposite sides of the beams. In the static tests, the load-deflection curve shows a non-linear behavior and the strains in the stirrups are closely related to the diagonal cracking in the tested beam.

While Castel, et al. [104] investigated the cracking behavior of SCC and vibrated concrete with the result as shown in Figure 7. 23

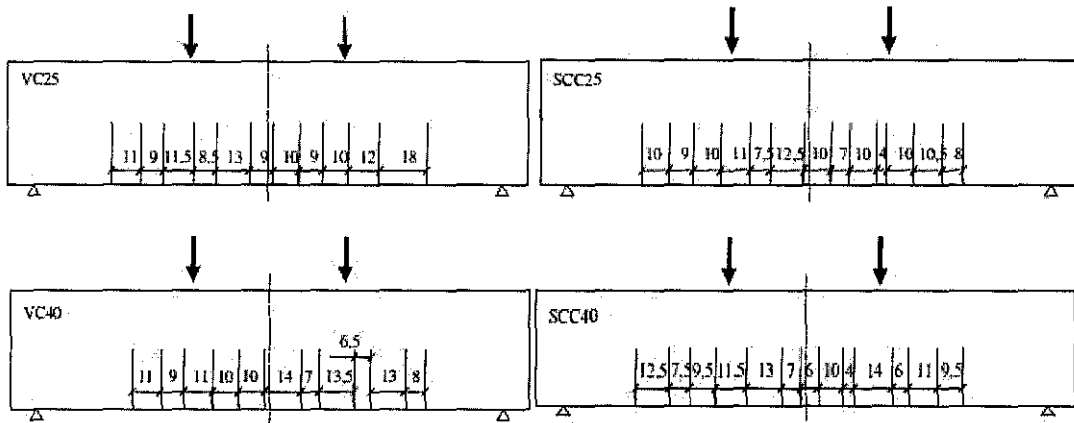


Figure 7. 23. Cracking map of 70-80% of the ultimate length-all length in cm

Source: Castel, et al. [104]

Figure 7. 23 shows that in high loading values, the average crack spacing of the SCC is slightly lower due to a higher number of cracks and the cracks distribution is slightly less regular than the one observed on VC beams. The failure modes for all the beams were compressive concrete crushing after the tension steel yielding as shown in the Figure 7. 23.

Hassan, et al. [128] investigated the strength, cracking and deflection performance of self compacting concrete beams subjected to shear failure. The result showed that there is an overall similarity between the beams in terms of crack width, crack heights, crack angles or overall failure mode as shown in Figure 7. 24. However, SCC beams exhibited slightly less number of cracks than NC beams. The other hand number of diagonal shear cracks was lower in SCC beams compared to NC beams.

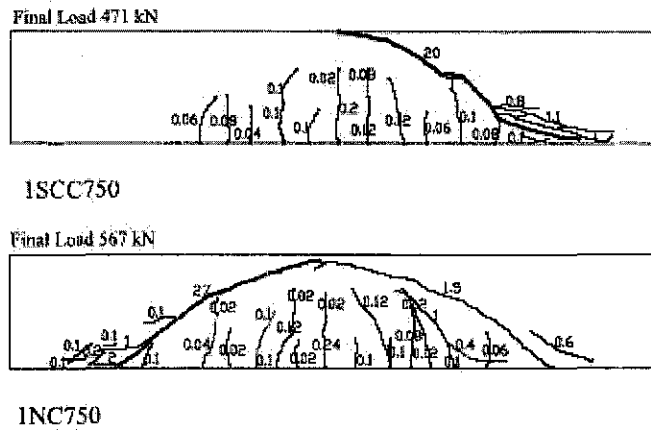


Figure 7. 24. Crack pattern in SCC and normal concrete

7. 4. Behavior of SCC Structure under Dynamic Loading

Concrete is one material that often used in structures that subjected to cyclic loads. The flexural behavior of a reinforced concrete beam under cyclic loading is analyzed through several parameters, which represent its behavior and performance due to cyclic and dynamic loading.

7.4.1. Result of Dynamic Test

Five beams of SCC which were chosen as the optimum among each group were tested under dynamic loading test. The result of all type of self compacting concrete in this study can be seen in Table 7. 9. and Table 7. 10.

Table 7. 9. Result of fatigue testing

specimen	f'_c	P'_u	P_{min}	P_{max}	R^*	testing frequency	N_u	N_u
FA10-0.25-3	71.86	115.63	9.953	59.718	0.52	5	650,000	-
FA10-M10-0.3-3	65.89	100.33	8.572	51.432	0.51	5	1,000,000	>1,000,000
M10-0.35-3	59.47	104.21	8.544	51.264	0.49	5	1,000,000	>1,000,000
NP-0.3-3	65.11	111.58	9.903	59.418	0.53	5	580,000	-
NC-0.5-0	54.28	100.15	9.29	55.74	0.56	5	1,000,000	>1,000,000

Table 7. 10. Result of fatigue testing (continued)

specimen	V_{co}	P_{fc}	P_{dc}	P_{max}/P_y	k_{max}	k_{min}	P_y	Failure/crack type
FA10-0.25-3	40	30	80	0.6	19.27	15.43	99.53	fh
FA10-M10-0.3-3	40	25	80	0.6	17.69	13.03	85.72	fs
M10-0.35-3	25	25	50	0.6	16.79	14.37	85.44	fs
NP-0.3-3	35	30	70	0.6	18.92	14.88	99.03	fh
NC-0.5-0	35	30	70	0.6	17.38	12.62	92.9	fs

Where:

- f'_c = compressive strength at age 28 days (MPa)
- P'_u = ultimate static load (kN)
- P_{min} = minimum of fatigue load (kN)
- P_{max} = maximum of fatigue load (kN)
- R^* = ratio of ultimate cyclic load and ultimate static load
- N_u = number of cyclic to failure
- N'_u = number of stirrups or tensile bars breaking
- V_{co} = $P_{dc}/2$ (kN)
- P_{fc} = initial flexural crack load (kN)
- P_{dc} = initial diagonal crack load (kN)
- k_{max} = maximum stiffness (kN/mm)
- k_{min} = minimum stiffness (kN/mm)
- P_y = initial yield load (kN)
- fh = flexural failure, plastic hinge
- fs = flexural failure, slipping off

The first flexural cracking load in the middle of beam was visually observed. The formation of first diagonal crack was also observed visually during the loading and was also verified during the experiment. Table 7. 10 presents the loads at first flexure and also shear crack, and failure loads of all SCC and normal concrete beams. From the result indicated that there was significant difference was observed between SCC and NC beams with respect to the all parameter. First flexural crack load for SCC beams varied from 25 kN to 40 kN, while the first diagonal dominant shear cracks were varied from 50 kN to 80 kN. In general, SCC beams exhibited high stiffness than normal concrete. The comparison result of dynamic beam test was done by Hassan, et al. [139], the result in Table 7. 11 also shows that SCC beam performed better than the NC beams.

Table 7. 11. Cracking loads and crack characteristic of experimental SCC/NC beams

Beam designation	Total applied load (P; kN)			Ratio (%)		Number of crack at failure
	At first flexural crack (P_{f1})	At first diagonal crack (P_{f2})	At failure (P_u)	$100 P_{f1}/P_u$	$100 P_{f2}/P_u$	
1SCC150	32	49	146	22	34	6
1NC150	32	50	154	21	32	5
2SCC150	33	53	161	21	33	6
2NC150	33	50	168	20	30	6
1SCC250	58	74	228	25	32	6
1NC250	60	82	243	25	34	5
2SCC250	60	83	252	24	33	7
2NC250	54	85	269	20	32	6
1SCC363	90	141	298	30	47	8
1NC363	90	135	330	27	41	6
2SCC363	96	146	325	30	45	7
2NC363	94	132	349	27	38	5
1SCC500	109	200	348	31	57	10
1NC500	120	190	403	30	47	8
2SCC500	120	240	438	27	55	9
2NC500	135	265	456	30	45	8
1SCC750	180	320	471	38	68	11
1NC750	188	325	567	33	57	12
2SCC750	222	390	601	37	65	12
2NC750	205	350	650	32	54	9

Source: Hassan, et al. [139].

7.4.2. S-N Curves of Dynamic Test

In cycle fatigue situations, materials performance can be characterized by an S-N curve, also known as a Wöhler curves. The fatigue experiment clearly showed that fatigue occurs by crack growth from surface defects until the specimen can no longer support the applied load. This phenomenon also can be explained by Figure 7. 8, that tensile stress in the beam decreases due to cracking in tensile area and hence the compression stress will be dominant and finally the concrete was crushed.

The S-N curve is a graph of the magnitude of a level of stress (S) against the logarithmic scale of cycles to failure (N). S-N curves are derived from tests on samples of the material to be characterized where a regular sinusoidal load is applied by a testing machine which also counts the number of cycles to failure. The result of S-N curves of all SCC type can be seen in Figure 7. 25 to Figure 7. 27.

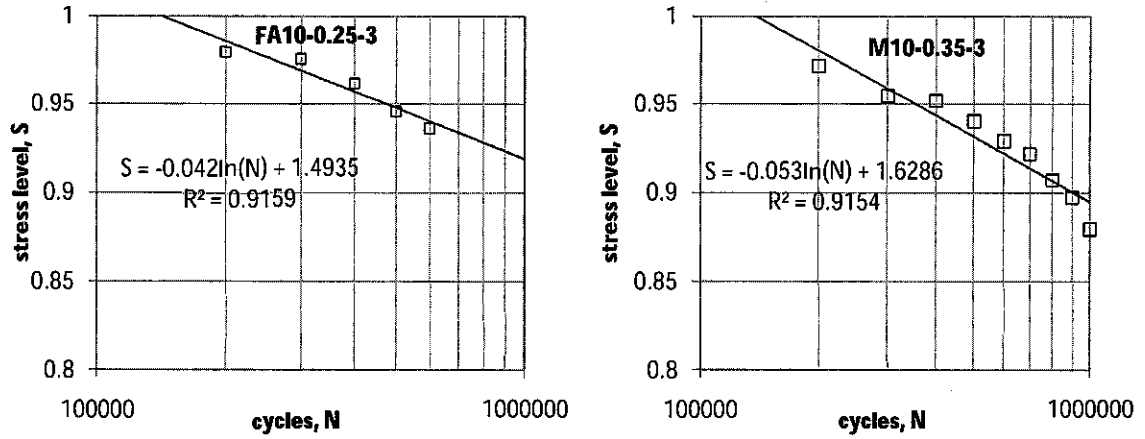


Figure 7. 25. S-N curves of FASCC and MSCC

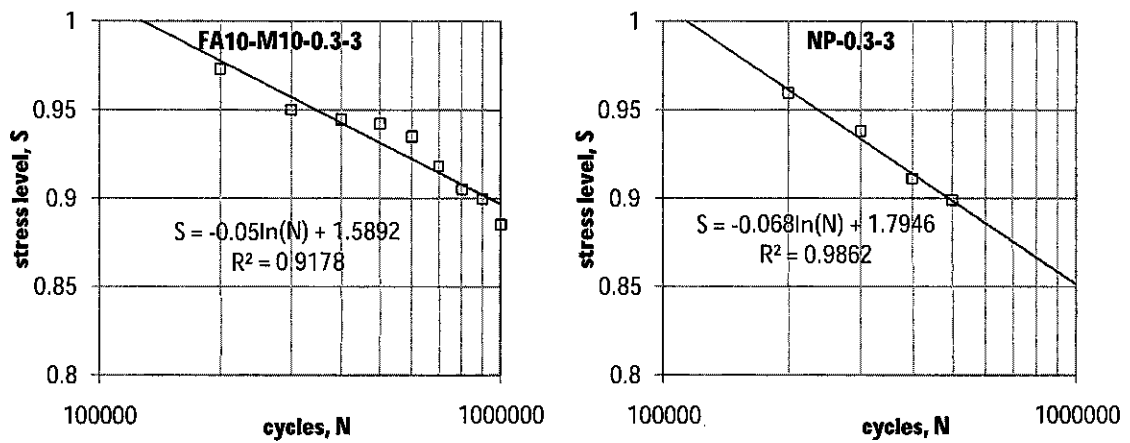


Figure 7. 26. S-N curves of FMSCC and NPSCC

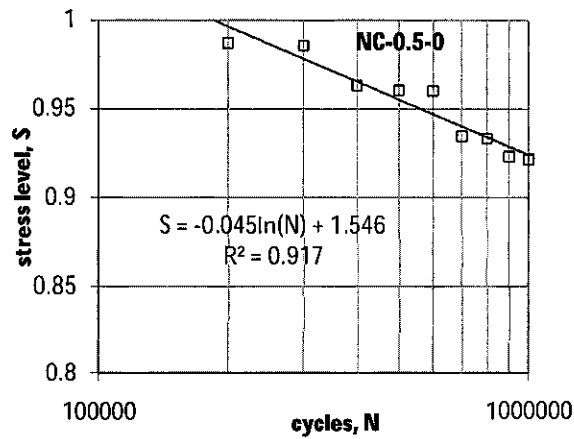


Figure 7. 27. S-N curves of normal concrete

Figure 7. 25 shows that FASCC had lowest rate of decay slope of 0.042 with almost 50% lower from no pozzolan 100% OPC with 0.068 rate of decay slope. On

the other hand from Figure 7. 25 also shows that fatigue life of fly ash self compacting concrete was short compared with other types of SCC with the brittle failure as illustrated in Figure 7. 28. The reason for this short fatigue life is a combination of higher ultimate fatigue load and higher compressive strength. This phenomenon was confirmed by Nilson [194] that high-strength concrete may be relatively free of internal microcracking in early history of static load, even up to about 75% of ultimate load. However, high-strength concrete is more brittle than low-strength concrete and it is lacking much of the ductility that accompanies progressive crack growth.

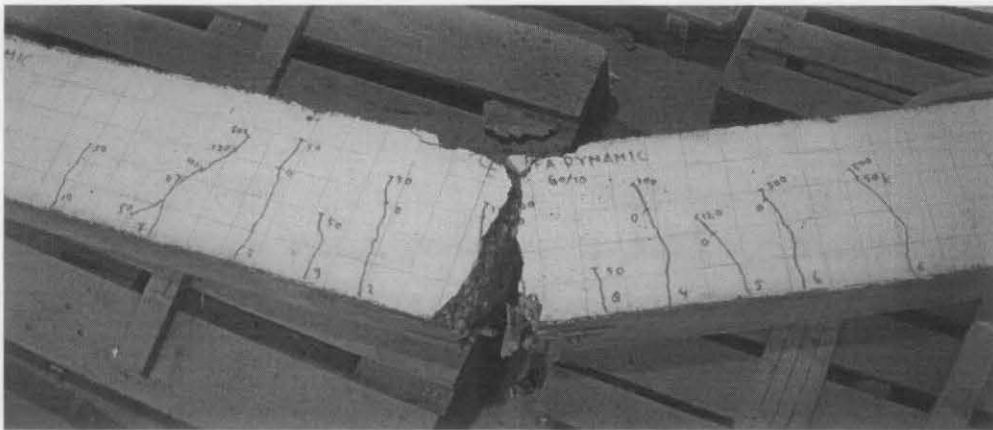


Figure 7. 28. Brittle failure of FASCC in dynamic test

This brittleness of high strength concrete also confirmed by Xiaobin, et al. [195] and the steel bars as the reinforced concrete can only restrain the development of the cracks, but cannot totally eliminate the concrete cracking. Zhou, et al. [196] found that high strength concrete tend to be more brittle with increasing strength. On other hand, the research done by Glenn [197] found that the use of high-strength concrete for seismic design still has the ability to remain ductile and avoid brittle modes of failure. From his study, it is concluded that the high strength concrete can be applied for ductile moment-resisting frames, results in a ductile hysteretic behavior with excellent energy dissipation similar to that of the normal strength concrete behavior. It was observed that the confinement reinforcement within the joint of the high-strength specimen was far from yielding at the maximum applied load. It is also concluded that the amount of confinement reinforcement could be modified for higher strength concretes because it provides an excessive amount of confinement reinforcement.

7.4.3. Flexural Stiffness of a Specimen in a Dynamic Test

Flexural stiffness; as mentioned by Kuang, et al. [198]; is one of the parameters that can be used to evaluate the decay of structural resistances to the cyclic loads. This flexural stiffness can be calculated by secant stiffness method. The result of flexural stiffness of all SCC in dynamic test can be seen in Figure 7. 29.

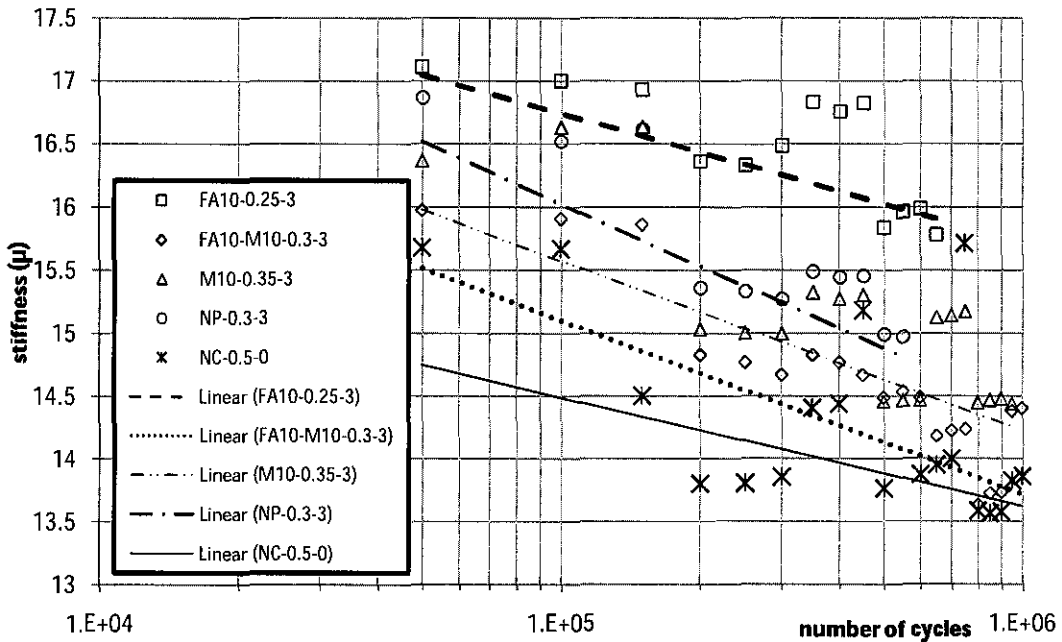


Figure 7. 29. Number of cycle vs Flexural stiffness

Figure 7. 29 shows that the FASCC beams performed better than the other types of SCC, with high stiffness and low decay of its flexural stiffness. The stiffness of fly ash self compacting concrete beam follows this equation.

$$k = -1.896.10^{-6}n + 17.14094 \quad (7.1)$$

$$R^2 = 0.618$$

The stiffness of the combination of fly ash and MIRHA self compacting concrete beam follows this equation.

$$k = -1.899.10^{-6}n + 15.60945 \quad (7.2)$$

$$R^2 = 0.713$$

The stiffness of MIRHA self compacting concrete beam follows this equation.

$$k = -1.922 \cdot 10^{-6}n + 16.07623 \quad (7.3)$$

$$R^2 = 0.566$$

The stiffness of no pozzolan self compacting concrete beam follows this equation.

$$k = -3.408 \cdot 10^{-6}n + 16.68483 \quad (7.4)$$

$$R^2 = 0.711$$

The stiffness of normal concrete beam follows this equation.

$$k = -1.189 \cdot 10^{-6}n + 14.80497 \quad (7.5)$$

$$R^2 = 0.187$$

FASCC beam has highest flexural stiffness of 17.11 as compared with the flexural stiffness from normal concrete as a control sample with 15.68 that around 9.1% lower than FASCC beam.

7.4.4. Displacement and Load of Specimen in Dynamic Test.

The displacement-load graph is used to describe cumulative displacements in cyclic loading test, therefore explain the fatigue of the specimen as shown in Figure 7.30 to Figure 7.32.

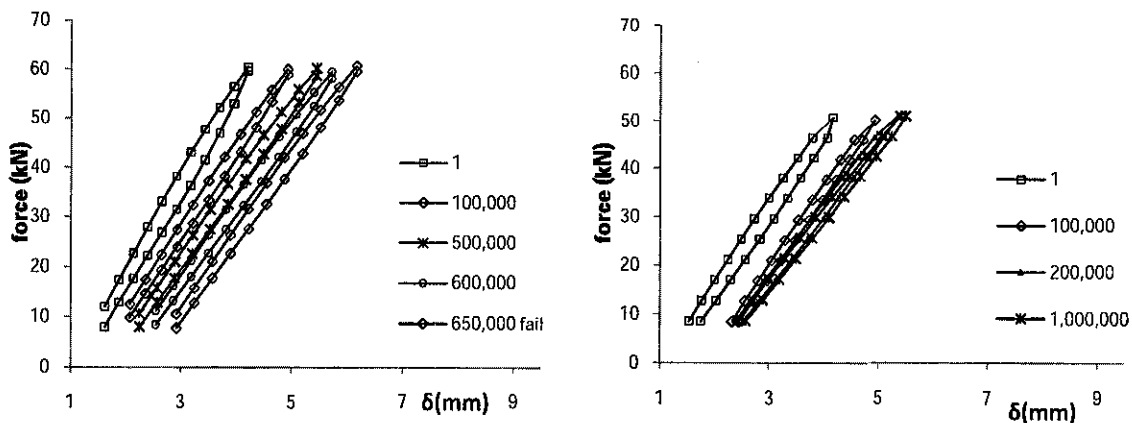


Figure 7.30. Displacement-load diagram for FASCC and MSCC

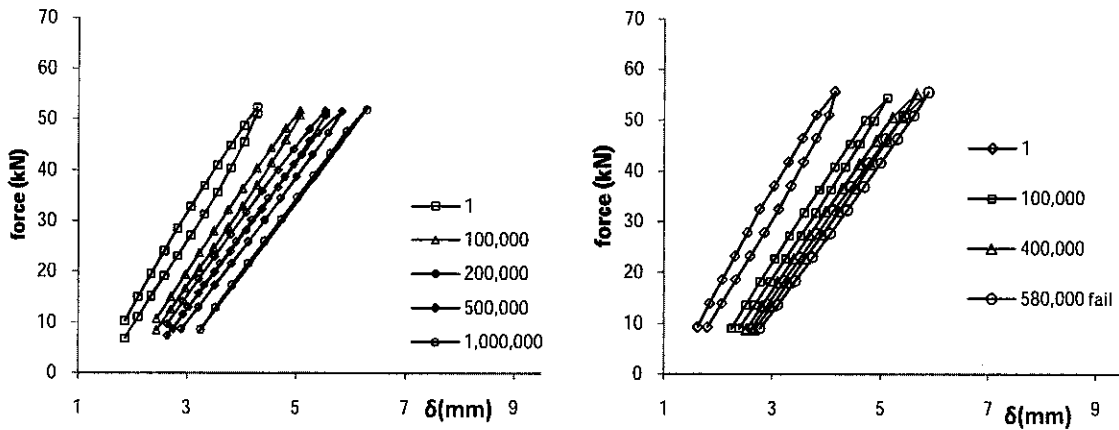


Figure 7.31. Displacement-load diagram for FMSCC and diagram for NPSCC

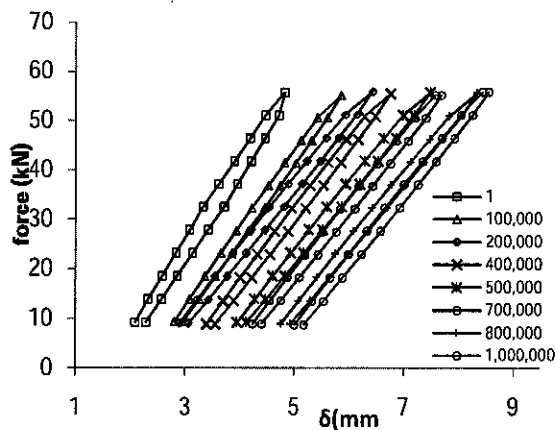


Figure 7.32. Displacement-load diagram for normal concrete

Figure 7.30 to Figure 7.32 depict the cumulative displacement of FASCC, MSCC, FMSCC, NPSCC and NC beam specimen. It can be seen that beam with self compacting concrete had the smallest displacement compare to normal concrete specimen. The displacement shift of MIRHA self compacting concrete was small compare to other specimen which indicated that the crack growth were developed rapidly. While in the beam with normal concrete, the shift displacement were big and indicated that crack growth were developed slowly.

7.4.5. Crack Pattern of Dynamic Test

In the fatigue experiments, a minimum cyclic loading was fixed at 10% - 60% of yield load, with the frequency set at 5 Hz. The displacements at the mid span, strain in the bottom of beam and crack growth were measured at first cycles and every new crack

was marked with associated cycles. The results of the fatigue experiments are shown in Table 7. 9. It can be noticed that the displacement increased and grown with the increase of loading cycles.

Figure 7. 33 shows that the crack occurred instantly as the start of the test. The crack growth during the fatigue tests began with micro cracking in the middle of the beam, which progressed to form larger surface cracks and grew into diagonal cracks, as shown in Figure 7. 33.

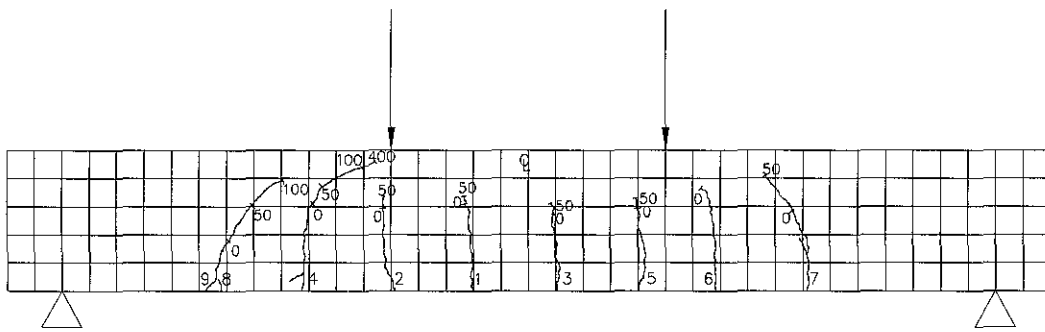


Figure 7. 33. FASCC crack pattern of dynamic test (number of cyclic in thousands)

At this stage, the diagonal cracks grew at 45° and the maximum crack width was 0.2 – 0.8 mm approximately. The mid span deflection also increased as the number of cyclic loading increased. The maximum crack width increased rapidly before 50,000 cycles. After 50,000 cycles, middle cracks were stop, and the diagonal crack width increased slowly. It can be concluded that there is a threshold cycle value for which crack width increases during a given fatigue life. Finally fracture was occurred in 650,000 numbers of cycles.

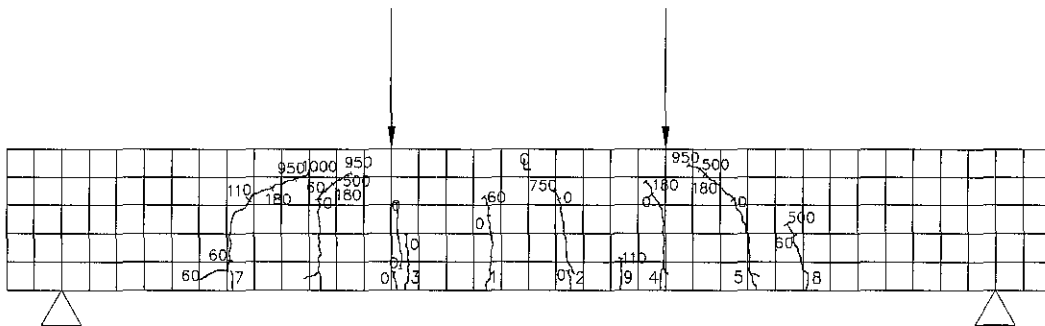


Figure 7. 34. MSCC crack pattern of dynamic test

The crack pattern of MIRHA SCC specimen had almost similar phenomenon in growing middle crack, but the middle cracks still growing until 750,000 cycles. The diagonal crack grew until the end of one million cycles.

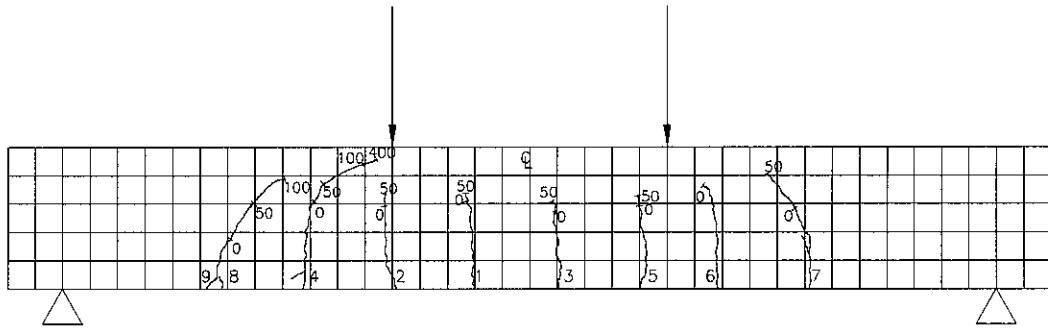


Figure 7. 35. FMSCC crack pattern of dynamic test

The crack pattern of FA and MIRHA SCC also had similar sequences of crack growing and still resist its ductility until one million cycles.

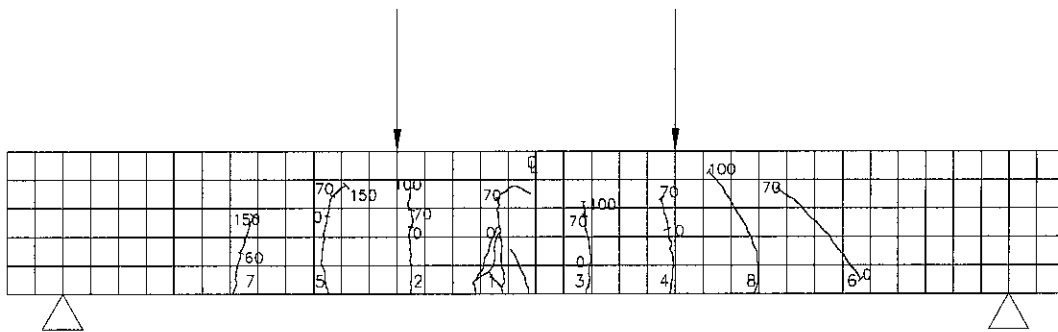


Figure 7. 36. NPSCC crack pattern of dynamic test

The bending crack formed more complex with interconnection micro crack in sequence one of crack. Some of middle crack still grew until 100,000 numbers of cycles.

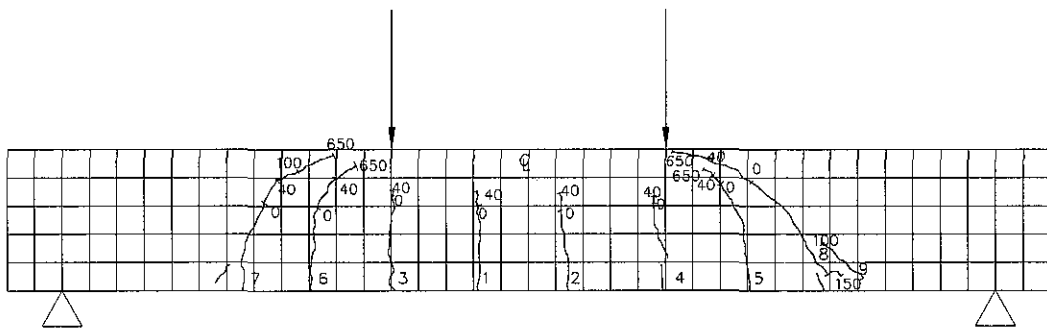


Figure 7. 37. Normal concrete crack pattern of dynamic test

The crack pattern of normal concrete had typical crack in dynamic test, and also it had very similar pattern crack with FMSCC.

7.5. Summary

Based on results as discussed in Chapter 7; it was found that SCC showed best level of mechanical and durability properties and also achieved high compressive strength concrete. Furthermore, its performance was judged to determine its effectiveness and feasibility in structural application. Some notable findings are stated as follows:

1. Bond strength
 - a. 16 mm diameter embedded bar showed the highest bond strength in all concrete mixes. 16 mm diameter bar showed 46% to 88% higher bond strength as compared to 10 mm diameter bar. 10 mm diameter showed the same bond strength for all three mixes. For 12 mm diameter bar 5% FASCC showed 10.69 MPa of bond strength in comparison of 9.21 and 8.39 MPa that was obtained for 10% FA and 15% FA mixes respectively. For 16 mm bar 15% FA showed the higher strength.
 - b. The increase in superplasticizers content reduce the anchorage bond stress, the bond strength values increased when larger steel bar diameter is used. The effect of superplasticizers on bond strength was obtained in line with the compressive strength as the concrete with w/b of 0.4 with 4% SP dosage showed the maximum bond strength that was 40% higher than the bond strength of FASCC with 6% SP dosage. The increasing the water-binder ratio reduced the bond strength.

FASCC with w/b of 0.4 yielded 70% lower bond strength as compared to that obtained in FASCC with w/b of 0.35.

2. Static load test of RC beams

- a. Beams with FASCC performed better than the beams made of other mixes; ultimate load of FASCC-3%SP-0.25 w/b was obtained as 115.63 kN, lowest ultimate load was obtained for normal compacted concrete that was found 100.15 kN. Fly ash self compacting concrete beams also showed the high stiffness as compared to the other beams it was obtained as 11.28 kN/mm, MIRHA SCC and 100% OPC SCC showed similar level of stiffness as 11.06 kN/mm and 11.04 kN/mm respectively
- b. Fly ash SCC beams and 100% OPC SCC showed the elastic yield load (load at first crack) as 99.53 kN and 99.03 kN respectively. Combination of fly ash and MIRHA SCC and MIRHA-SCC achieved a value of 85.72 kN and 85.44 kN respectively. FA-SCC beams showed a ductility factor of 5.91 which was higher than that measured for MIRHA-SCC as 5.52. Normal compacted concrete beams showed a lowest ductility factor as 3.18.
- c. Typical cracks during the static load tests were found as the flexural cracks that developed first in the pure bending region at the applied load range of 25 to 30 kN. These cracks in the middle-third region were caused due to flexural displacement propagated to the middle top of the beam. The diagonal tensile cracks developed when the loading increased to 50 - 80 kN. These diagonal tensile cracks propagated from the bottom to the loading points at an angle of 45° to about 65°. The development in diagonal cracks growth was found independent of the flexural cracks growth. The development of flexural cracks growth was almost stopped when the development of the diagonal cracks growth initiated. In the static tests, the load-deflection curve showed a non-linear behavior and the strains in the stirrups are closely related to the diagonal cracking in the tested beam.

3. Cyclic Load test (Fatigue behavior)

- a. FASCC conceived the lowest rate of S-N curve slope decay that was found as 0.042, which is almost 35% lower than that of 100% OPC as it was measured as 0.068. Fatigue life of FASCC was found shorter as compared to other type of SCC. The reason for this short fatigue life may be the higher ultimate fatigue load and higher compressive strength. FASCC beam has highest flexural stiffness of 17.11 as compared the lowest flexural stiffness from normal concrete as a control sample with 15.68 that around 9.1% lower than FASCC beam.
- b. The typical crack in dynamic test occurred instantly at the start of test. The crack growth during the fatigue tests began with micro cracking in the middle-third zone of the beam, which progressed to form larger surface cracks and grew into diagonal cracks. At this stage, the diagonal cracks grew at 45° and the maximum crack width was found about 0.2 – 0.8 mm. The deflection at the mid span also increased as the number of cyclic increased. The maximum crack width increased rapidly before 50,000 cycles. After 50,000 cycles, middle cracks were stop, and the diagonal crack width increased slowly. It can be concluded that there is a threshold cycle value for which crack width increases during a given fatigue life.

CHAPTER 8

CONCLUSIONS

8. 1. Introduction

In view of the objectives of this research that were set at the start, the conclusions corroborate and confirm all the objectives. Based on the results that have been discussed in Chapter 4 to Chapter 7, several conclusions are drawn and discussed in the following sections.

8. 2. Fresh Concrete Properties

Based on the results and discussion made on the fresh concrete properties in Chapter 4, the following conclusions are drawn:

1. Because of the nature of fly ash, it requires less water as compared to MIRHA for obtaining similar level.
2. The higher w/b significantly affects the rheological properties. There was about 35% variation in the flow ability, 80% in passing through ability and 38% in filling ability which indicates that the water content did appreciable effect on the viscosity and consistency of the mixes, and
3. Medium to high w/b variation with SP content from 3% to 6% did not significantly change the rheological properties of different concrete mixes. High dosage of SP which was more than 5% would cause the fresh concrete to bleed and segregate, while fresh concrete with less than 3% SP content with any w/b did not cause bleeding and segregation in any of the mixes.

8. 3. Mechanical Properties

Major conclusions relevant to mechanical properties:

1. Water-binder ratio significantly affected the compressive strength of all types of SCC. Maintaining all mix proportion variation in w/b from 0.42 to 0.25 increased the 28 days strength to about 1.5 times. So, the amount of water content can economize the cost of self compacting concrete.
2. In MIRHA with the variation of high to low w/b, the strength increment was obtained as 50%. For similar w/b, both 10% FA and 10% MIRHA, concrete showed similar compressive strength with very close margin. In general MIRHA is suitable for producing 28-day compressive strength as high as 50 to 60 MPa, and due to fulfillment of SCC rheological requirement it needs as low as 0.35 w/b if the SP content is fixed at its optimum level of 3% dosage. On the other hand, fly ash is suitable for producing higher 28-day strength such as 80 MPa because it requires low water content such as 0.25 w/b for complying the rheological characteristic of SCC.
3. Lower w/b fly ash highly acted as pozzolanic as well as filler material in SCC. For 10% MIRHA concrete such increment was found between 15% to 20% that indicates that mostly MIRHA acted as a filler material. However, there was little pozzolanic activity that took place in the mixes.
4. The result showed that the range of 2% to 4% amount of SP content are the optimum for producing SCC with fly ash and/or rice husk ash.
5. 10% replacement of cement either by fly ash or by MIRHA is found to be optimum that showed the best result.
6. All types of SCC showed better modulus of rupture than normal concrete, while the split tensile test result indicated that all types of SCC performed better strength. FASCC with w/b 0.25 achieved the highest split tensile with 5.52 MPa tensile strength which was 39% higher than normal concrete, while MSCC achieved higher tensile strength as compared with normal concrete with almost 8.2%.
7. The results confirmed that it is possible to get high strength and high durability concrete economically using MIRHA by burning local available rice husk. The utilization of MIRHA into the concrete mix proportions has given various

effects to the concrete properties. Utilization of MIRHA was able to extract the quality and quantity of amorphous SiO₂, with an optimum amount of MIRHA significantly improving the compressive strength performance. As a final point, all types of SCC achieved high strength concrete with the compressive strength more than 50 MPa at 28 days indicating that both fly ash and MIRHA are appropriate as filler and pozzolan to enhance the compressive strength of concrete.

8. In general it was found that fly ash SCC showed better mechanical properties as compared to the MIRHA SCC and normal concrete.

8. 4. Durability

From durability investigation, the following are some notable findings:

1. At similar w/b, fly ash based concrete showed lower porosity and oxygen permeability as compared to the corresponding MIRHA mixes. It may be due to the reason that MIRHA needs more water for chemical reaction and probably it may cause pore system to be long capillary pore system.
2. All concrete mixes (fly ash based and/or MIRHA based) showed intrinsic value of oxygen and water permeability in the range of 10^{-16} to 10^{-19} m². This value of the coefficient of oxygen and water permeability is within the specification for acceptable durability requirement.
3. Corrosion potential, rate and current as determined for various mixes contained low on high water-binder ratio showed that the concrete with w/b of 0.25 offered high resistance against corrosion, whereas concrete with high w/b such as 0.4 and above showed moderate to poor resistance. The highest corrosion resistant of self compacting concrete was achieved by fly ash SCC and also combination of fly ash and MIRHA SCC had similar result. All SCC performed better corrosion resistance compared to normal concrete.
4. All data from durability properties test gave promising result as indication that fly ash and MIRHA are suitable for categorization of high performance concrete that it can perform good workability (Chapter 4) and also showed high compressive strength (Chapter 5) and good durability as compared to normal vibrated concrete (Chapter 6).

8. 5. Structural Behavior

Structural behavior test showed good result as expected, since the all type of SCC performed as high performance concrete as described in previous conclusion. SCC showed the best level of mechanical and durability properties and also achieved high compressive strength concrete. Furthermore, its performance was judged to determine its effectiveness and feasibility in structural application. Some of the findings are concluded below:

1. For bond strength, 16 mm diameter embedded bar showed the highest bond strength in all concrete mixes. For 12 mm diameter bar, 5% FASCC showed 10.69 MPa of bond strength in comparison of 9.21 and 8.39 MPa that was obtained for 10% FA and 15% FA mixes respectively. For 16 mm bar 15% FA showed the higher strength.
2. The increase in superplasticizers content reduce the anchorage bond stress, while the bond strength values increased when a larger steel bar diameter is used. The effect of superplasticizers on bond strength was obtained in line with the compressive strength as the concrete with w/b of 0.4 with 4% SP dosage showed the maximum bond strength that was 40% higher than the bond strength of FASCC with 6% SP dosage. Thus, increasing the water-binder ratio reduced the bond strength.
4. In static load test of RC beams, beams with FASCC performed better than the beams made of other mixes. Fly ash self compacting concrete beams showed high stiffness as compared to the other beams, with a value of 11.28 kN/mm. MIRHA SCC and 100% OPC SCC showed similar levels of stiffness as 11.06 kN/mm and 11.04 kN/mm respectively
5. Fly ash SCC beams and 100% OPC SCC showed an elastic yield load (load at first crack) of 99.53 kN and 99.03 kN respectively. Combination of fly ash and MIRHA SCC and MIRHA-SCC achieved a value of 85.72 kN and 85.44 kN respectively. FASCC beams showed a ductility factor of 5.91, which was higher than that measured for MIRHA-SCC as 5.52. Normal compacted concrete beams showed the lowest ductility factor of 3.18.

6. Typical cracks during the static load tests were found as flexural cracks that developed first in the pure bending region at the applied load range of 25 to 30 kN. These cracks in the middle-third region were due to flexural displacement propagated to the middle top of the beam. Diagonal tensile cracks were developed when the loading was increased from 50 to 80 kN. These diagonal tensile cracks propagated from the bottom to the loading points at an angle of 45° to about 65°. The development of diagonal cracks growth was found independent of the flexural cracks growth. The development of flexural cracks growth was almost stopped when the development of the diagonal cracks growth initiated. In the static tests, the load-deflection curve showed a non-linear behavior and the strains in the stirrups are closely related to the diagonal cracking in the tested beam.
7. In cyclic load test (Fatigue behavior), FASCC conceived the lowest rate of S-N curve slope decay that was found as 0.042, which is almost 35% lower than that of 100% OPC as it was measured as 0.068. Fatigue life of FASCC was found shorter as compared to other type of SCC. The short fatigue life was due to the combination of the higher ultimate fatigue load and higher compressive strength. FASCC beam has the highest flexural stiffness of 17.11 as compared to the lowest flexural stiffness from normal concrete (control sample) with a value of 15.68 which is about 9.1% lower than FASCC beam.
8. The crack growth during the fatigue tests began with micro cracking in the middle-third zone of the beam, which progressed to form larger surface cracks and grew into diagonal cracks. The maximum crack width increased rapidly before 50,000 cycles. After 50,000 cycles, middle cracks stopped, and the diagonal crack width increased slowly. It can be concluded that there is a threshold cycle value for which crack width increases during a given fatigue life.

8. 6. Recommendations

Although a detailed research program has been performed during this research study, however, there are still many gaps identified for further research. Some of them are described as below:

1. Extensive research is needed to test on other types of cement replacement materials, such as silica fume, ground granulated blast furnace slag, GGBS

- and quarry dust. In this study the total binder content was kept at 500 kg/m^3 , different binder content may also be required in further research.
2. In this study, durability testing was limited to minimum number of mixes with few tests performed. In future research, durability of SCC is to be undertaken in greater detail. For example, chloride migration tests, carbonation tests and microstructure using Scanning Electron Microscopy (SEM).
 3. The role of different types and grading and shape of coarse and fine aggregates including recycled aggregate would be another interesting area for future research.
 4. Statement from Gene [63] who mentioned some factors that affect the workability which are: proportion of fine to coarse aggregate, percentage of air entrained, quantity of water, ambient temperatures and time in transit would also be other important factor in future investigation as all this kind factor could affect the behavior of SCC significantly.

Reference

- [1] H. Okamura and M. Ouchi, "Self compacting concrete," *Journal of Advance Concrete Technology*, vol. Vol., 1, No. 1, 5-15, 2003.
- [2] C. S. Poon and D. W. Ho, "A feasibility study on the utilization of r-FA in SCC," *Cement and Concrete Research* 34 (2004) 2337-2339, 2004.
- [3] C. Djelal, Y. Vanhove, and A. Magnin, "Tribological behaviour of self compacting concrete," *Cement and Concrete Research*, vol. 34 (2004) 821-828, 2004.
- [4] M. Ahmaruzzaman, "A review on the utilization of fly ash," *Progress in Energy and Combustion Science* (2009) 1-37, 2009.
- [5] K. Norazlan, "The Geotechnical Properties of Pulverised Fuel Ash (PFA) as Road Embankment Construction Material," in *Faculty of Civil Engineering*. vol. Master of Engineering (Civil-Geotechnic) Johor, Malaysia: Universiti Teknologi Malaysia, 2008.
- [6] O. Omar, "Rice production and potential for hybrid rice in Malaysia," in *International Plantation Industry Conference and Expo - IPiCEX 2008* Shah Alam, 2008.
- [7] F. Adam, I. A. Rahman, and M. I. Saleh, "Production and characterization of rice husk ash as a source of pure silica," in *Proceedings of the first National Seminar on Ceramic Technology*, 1989, pp. 261-273.
- [8] F. Adam, "Penyediaan Dan Kajian Penjerapan Silika Daripada Abu Sekam Padi." vol. Master of Science Penang: Universiti Sains Malaysia 1991.
- [9] C. S. Poon, L. Lam, and Y. L. Wong, "A study on high strength concrete prepared with large volumes of low calcium fly ash," *Cement and Concrete Research* 30 (2000) 447-455, 2000.
- [10] L. Lam, Y. L. Wong, and C. S. Poon, "Degree of hydration and gel/space ratio of high-volume fly ash/cement systems," *Cement and Concrete Research* 30 (2000) 747-756, 2000.
- [11] Y. M. Zhang, W. Sun, and H. D. Yan, "Hydration of high-volume fly ash cement pastes," *Cement & Concrete Composites* 22 (2000) 445-452, 2000.
- [12] P. Termkhajornkit, T. Nawa, and K. Kurumisawa, "Effect of water curing conditions on the hydration degree and compressive strengths of fly ash-cement paste," *Cement & Concrete Composites* 28 (2006) 781-789, 2006.
- [13] C. Namagga and R. A. Atadero, "Optimization of Fly Ash in Concrete: High Lime Fly Ash as Replacement for Cement and Filler Material," in *2009 World of Coal Ash (WOCA) Conference* Lexington, KY, USA, 2009.
- [14] S. Antiohos and S. Tsimas, "Investigating the role of reactive silica in the hydration mechanisms of high-calcium fly ash/cement systems," *Cement & Concrete Composites* 27 (2005) 171-181, 2005.
- [15] M. Singh and M. Garg, "Durability of cementing binders based on fly ash and other wastes," *Construction and Building Materials* 21 (2007) 2012-2016, 2007.
- [16] S. H. Lee, H. J. Kim, E. Sakai, and M. Daimon, "Effect of particle size distribution of fly ash-cement system on the fluidity of cement pastes," *Cement and Concrete Research* 33 (2003) 763-768, 2003.

- [17] M. J. McCarthy and R. K. Dhir, "Towards maximising the use of fly ash as a binder," *Fuel* 78 (1999) 121–132, 1999.
- [18] V. Saraswathy, S. Muralidharan, K. Thangavel, and S. Srinivasan, "Influence of activated fly ash on corrosion-resistance and strength of concrete," *Cement & Concrete Composites* 25 (2003) 673-680, 2003.
- [19] S. I. Muhammad and A. M. Waliuddin, "Effect of rice husk ash on high strength concrete," *Construction and Building Materials, Vol. 10, No. 1, pp. 521-526, 1996, 1996.*
- [20] M. F. Nuruddin, A. Kusbiantoro, and N. Shafiq, "Microwave Incinerated Rice Husk Ash (MIRHA) And It's Effects On Concrete Strength," *IMS International Conference, American University of Sharjah, 2008.*
- [21] N. L. M. Kamal, M. F. Nuruddin, and N. Shafiq, "The Influence Of Burning Temperatures and Percentage Inclusion of Microwave Incinerated Rice Husk Ash (MIRHA) On Normal Strength Concrete," *ICCBT 2008 - A - (47) - pp531-538, 2008.*
- [22] P. Dinakar, K. G. Babu, and M. Santhanam, "Mechanical properties of high-volume fly ash self-compacting concrete mixtures," *Structural Concrete, vol 9, No 2, pp. 109 - 116, 2008.*
- [23] B. Sukumar, K. Nagamani, and R. S. Raghavan, "Evaluation of strength at early ages of self-compacting concrete with high volume fly ash," *Construction and Building Materials* 22 (2008) 1394–1401, 2008.
- [24] M. Liu, "Self-compacting concrete with different levels of pulverized fuel ash," *Construction and Building Materials, online version, pp. 001-008, 2010.*
- [25] M. Nehdi, M. Pardhanb, and S. Koshowski, "Durability of self-consolidating concrete incorporating high-volume replacement composite cements," *Cement and Concrete Research* 34 (2004) 2103– 2112, 2004.
- [26] R. S. Ravindrarajah, D. Siladyi, and B. Adamopoulos, "Development of High-Strength Self-Compacting Concrete with Reduced Segregation Potential," in *Proceedings of the 3rd International RILEM Symposium , Reykjavik, Iceland, 17-20 August 2003, (RILEM Publications), 1 Vol., 1048 pp., ISBN: 2-912143-42-X 2003.*
- [27] N. Bouzoubaâ and M. Lachemib, "Self-compacting concrete incorporating high volumes of class F fly ash Preliminary results," *Cement and Concrete Research* 31 (2001) pp. 413-420, 2001.
- [28] M. Sonebi, "Medium strength self-compacting concrete containing fly ash: Modelling using factorial experimental plans," *Cement and Concrete Research* 34 (2004) 1199–1208, 2004.
- [29] M. Sahmaran and I. O. Yaman, "Hybrid fiber reinforced self-compacting concrete with a high-volume coarse fly ash," *Construction and Building Materials* 21 (2007) 150–156, 2007.
- [30] S. A. Memon, M. A. Shaikh, and H. Akbar, "Production of Low Cost Self Compacting Concrete Using Rice Husk Ash," in *First International Conference on Construction In Developing Countries (ICCIDC-I) "Advancing and Integrating Construction Education, Research & Practice" August 4-5, 2008, Karachi,, Pakistan, 2008.*

- [31] M. A. Ahmadi, O. Alidoust, I. Sadrinejad, M. Nayer, and "Development of Mechanical Properties of Self Compacting Concrete Contain Rice Husk Ash," *World Academy of Science, Engineering and Technology* 34, pp. 168 - 171, 2007.
- [32] M. Collepardi, "Self-Compacting Concrete: What is New," in *Proceedings of the First North America Conference on the Design and Use of Self-Consolidating Concrete*, Evanston, USA, 2003, pp. 377-380.
- [33] J. A. Peter, N. Lakshmanan, Manoharan, and P. Devadas, "Investigations on the Static Behavior of Self-Compacting Concrete Under-Reamed Piles," *Journal of Materials in Civil Engineering information* Vol. 18 No. 3, 2006.
- [34] S. Abhishek, Shethji, and C. Vipulanandan, "Flow Properties of Self Consolidating Concrete with Time," *CIGMAT-2004 Conference & Exhibition*, 2004.
- [35] O. Celik and L. D. Stephen, "FINAL REPORT EVALUATION OF SELF-CONSOLIDATING CONCRETE," *Virginia Department of Transportation and the University of Virginia*, 2003.
- [36] W. Timo, "FRESH PROPERTIES OF SELF-COMPACTING CONCRETE (SCC)," *Otto-Graf-Journal* Vol. 14, 2003.
- [37] P. P. Ambedkar, "Self Compacting Concrete Its Properties and Test," *Construction and Management, MIT College, Pune*, 2008.
- [38] X. Youjun, L. Baoju, Y. Jian, and Z. Shiqiong, "Optimum mix parameters of high-strength self-compacting concrete with ultrapulverized fly ash," *Cement and Concrete Research*, vol. 32 (2002) 477-480, 2002.
- [39] K. Stefan and B. Wolfgang, "Assessment of the fresh concrete properties of self compacting concrete," *FTB (Ready-mixed Concrete Research Association)*, pp. pp. 113 -124, 2003.
- [40] S. L. D'Aloia, L. L. Roy, and J. Cordin, "Rheological behaviour of fresh cement pastes formulated from a Self Compacting Concrete (SCC)," *Cement and Concrete Research* 36 (2006) 1203-1213, 2006.
- [41] S. E. Chidiac, O. Maadani, A. G. Razaqpur, and N. P. Mailvaganam, "Correlation of Rheological Properties to Durability and Strength of Hardened Concrete," *JOURNAL OF MATERIALS IN CIVIL ENGINEERING © ASCE*, vol. / JULY/AUGUST 2003 / 391, 2003
- [42] R. Nicolas, "A thixotropy model for fresh fluid concretes: Theory, validation and applications," *Cement and Concrete Research*, vol. 36 (2006) 1797-1806, 2006.
- [43] G. Jacek and S. Janusz, "Influence of superplasticizers on rheological behaviour of fresh cement mortars," *Cement and Concrete Research* 34 (2004) 235-248, 2004.
- [44] P. Coussot, "Rheometry of Pastes, Suspensions, and Granular Materials," *John Wiley & sons, New Jersey*, 2005.
- [45] M. H. Ozkul and U. A. Dogan, "RHEOLOGICAL PROPERTIES AND SEGREGATION RESISTANCE OF SCC PREPARED BY PORTLAND CEMENT AND FLY ASH," *Measuring, Monitoring and Modeling Concrete Properties*, 463-468., 2006.

- [46] H. Klaus and Y. Klug, "A Database for the Evaluation of Hardened Properties of SCC," *LACER*, vol. No. 7, 2002, 2002.
- [47] H. J. H. Brouwers and H. J. Radix, "Self-Compacting Concrete: Theoretical and experimental study," *Cement and Concrete Research* 35 (2005) 2116 – 2136, 2005.
- [48] E. Ozbay, A. Oztas, A. Baykasoglu, and H. Ozbebek, "Investigating mix proportions of high strength self compacting concrete by using Taguchi method," *Construction and Building Materials* 23 (2009) 694–702, 2009.
- [49] S. Nan, H. KungChung, and C. HisWen, "A simple mix design method for self-compacting concrete," *Cement and Concrete Research*, vol. 31 (2001) 1799–1807, 2001.
- [50] W. R. Grace and CoConn, "Mixture Proportioning Self-Consolidating Concrete (SCC)," *TECHNICAL BULLETIN TB - 1503*, FA/GPS/IMGrace Construction Products, vol. TB-1503E, 2005.
- [51] M. Jianxin and D. Jörg, "Ultra High Performance Self Compacting Concrete," *LACER No. 7*, 2002.
- [52] R. K. Dhir, W. Z. Zhu, and M. J. McCarthy, "Use of Portland PFA Cement in Combination with Superplasticizing Admixtures," *Cement and Concrete Research*, Vol. 28, No. 9, pp. 1209–1216, 1998.
- [53] A. Bilal, "Mix Design of Self-Compacting Concrete," *The Sixth Annual U.A.E. University Research Conference ENG - 95* 1995.
- [54] C. Ping-Kun, "An approach to optimizing mix design for properties of high-performance concrete," *Cement and Concrete Research*, vol. 34 (2004) 623–629, 2004.
- [55] P. K. Chang, Y. N. Peng, and C. L. Hwang, "A design consideration for durability of high performance concrete," *Cem. Concr. Compos*, vol. 23 (2001) 375–380., 2001.
- [56] F. M. Z. Muhammad, M. N. Islam, and B. Hassan, "An expert system for mix design of high performance concrete," *Advances in Engineering Software* vol. 36 (2005) 325-337, 2005.
- [57] A. Ricardo, Einsfeld and S. L. Marta, Velasco, "Fracture parameters for high-performance concrete," *Cement and Concrete Research* 36 (2006) 576 – 583, 2006.
- [58] M. R. Taylor, F. D. Lydon, and B. I. G. Barr, "Mix proportions for high strength concrete," *Construction and Building Materials*, Vol. 10, No. 6, pp. 445-450, 1996.
- [59] A. K. Mullick, "High Performance Concrete for Bridges and Highway Pavements," *Advanced in Bridgr Engineering*, vol. March 24 - 25, 2006.
- [60] A. M. Neville, *Properties of Concrete*. London: Pearson Education Limited, 1995.
- [61] A. Noumowé, H. Carré, A. Daoud, and H. Toutanji, "High-Strength Self-Compacting Concrete Exposed to Fire Test," *JOURNAL OF MATERIALS IN CIVIL ENGINEERING* © ASCE / NOVEMBER/DECEMBER 2006 pp. 754, 2006.

- [62] L. D. A. Schwartzentruber, R. L. Roy, and J. Cordin, "Rheological behaviour of fresh cement pastes formulated from a Self Compacting Concrete (SCC)," *Cement and Concrete Research* 36 (2006) 1203–1213, 2006.
- [63] D. D. Gene, "Factors Influencing Concrete Workability," in *Significan of test and properties of concrete and concrete-making material, volume 1*, Joseph, F, Lamond, Pielert, J, and H, Eds., 2006, p. 59.
- [64] T. Wüstholz, "FRESH PROPERTIES OF SELF-COMPACTING CONCRETE (SCC)," *Otto-Graf-Journal Vol. 14*, 2003.
- [65] L. François and T. Sedran, "Mixture-proportioning of high-performance concrete," *Cement and Concrete Research* 32 (2002) 1699–1704, 2002.
- [66] K. Stefan and G. Horst, "Controlling the workability properties of self compacting concrete used as ready-mixed concrete " *FTB (Ready-mixed Concrete Research Association)*, pp. pp. 103 - 112, 2000.
- [67] L. Zhuguo, O. Takaaki, and T. Yasuo, "Flow Performance of High-Fluidity Concrete," *JOURNAL OF MATERIALS IN CIVIL ENGINEERING © ASCE / NOVEMBER/DECEMBER 2004*, 2004.
- [68] G. D. E. Schutter, "GUIDELINES FOR TESTING FRESH SELF-COMPACTING CONCRETE," *European Research Project: MEASUREMENT OF PROPERTIES OF FRESH SELF-COMPACTING CONCRETE*, 2005.
- [69] W. C. Yun, J. K. Yong, C. S. Hwa, and Y. M. Han, "An experimental research on the fluidity and mechanical properties of high-strength lightweight self-compacting concrete," *Cement and Concrete Research*, vol. 36 (2006) 1595–1602, 2006.
- [70] O. Masahiro, Kochi, N. Sada-aki, O. Thomas, S.-E. Hallberg, and L. Myint, "APPLICATIONS OF SELF-COMPACTING CONCRETE IN JAPAN, EUROPE AND THE UNITED STATES " *ISHPC international seminar of high performance concrete*, 2003.
- [71] P. L. Domone, "Self-compacting concrete: An analysis of 11 years of case studies," *Cement & Concrete Composites* 28 (2006) 197–208, 2006.
- [72] M. Lachemi, K. M. A. Hossain, V. Lambrosa, P. C. Nkinamubanzi, and N. Bouzoubaa, "Self-consolidating concrete incorporating new viscosity modifying admixtures," *Cement and Concrete Research* 34 (2004) 917–926, 2004.
- [73] S. G. Bapat, S. B. Kulkarni, and K. S. Bandekar, "A Silent Concrete in Scenic Valley," *An International Journal of Nuclear Power - Vol. 18 No. 1 (2004) pp. 43-51*, 2004.
- [74] M. S. Ravikumar, C. Selvamony, S. U. Kannan, and S. B. Gnanappa, "Behaviour of Self Compacted Self Curing Kiln Ash Concrete with Various Admixtures " *ARPJN Journal of Engineering and Applied Sciences, VOL. 4, NO. 8, OCTOBER*, 2009.
- [75] I. S. Mohammad, I. Ichiro, and M. Takashi, "A study on the applicability of vibration in fresh high fluidity concrete," *Cement and Concrete Research*, vol. 35 (2005) 1834- 1845, 2005.

- [76] EFNARC, "The European guidelines for self compacting concrete," *The European Federation of Specialist Construction Chemicals and Concrete Systems. - specification, production and use*, 2005.
- [77] J. A. Daczko and D. Constantiner, "Rheodynamic Concrete," *Proceedings of the 43rd Congresso Brasileiro do Concreto*, 2001.
- [78] D. J. Akers, "Building Material," in *Building Design and Construction Handbook (6th Edition)*, F. Merritt and J. T. Ricketts, Eds.: Knovel © 2001 McGraw-Hill 2001, pp. 4.9 - 4.10.
- [79] S. Gofii, A. Guerrero, M. P. Luxán, and A. Macías, "Activation of the fly ash pozzolanic reaction by hydrothermal conditions," *Cement and Concrete Research* 33 (2003) 1399–1405, 2003.
- [80] P. Anne-Mieke and D. S. Geert, "Cement hydration in the presence of high filler contents," *Cement and Concrete Research* 35 (2005) 2290 – 2299, 2005.
- [81] N. B. Singh, V. D. Singh, R. Sarita, and C. Shivani, "Effect of lignosulfonate, calcium chloride and their mixture on the hydration of RHA-blended portland cement," *Cement and Concrete Research* 32 (2002) 387–392, 2002.
- [82] N. Shafiq, M. F. Nuruddin, and I. Kamaruddin, "Comparison of engineering and durability properties of fly ash blended cement concrete made in UK and Malaysia," *Advances in Applied Ceramics*, vol.106 314-318, 2007.
- [83] C. S. Poon, S. C. Kou, L. Lam, and Z. S. Lin, "Activation of fly ash/cement systems using calcium sulfate anhydrite (CaSO₄)," *Cement and Concrete Research* 31 (2001) 873–881, 2001.
- [84] T. Jatuphon, J. Chai, and K. Kraiwood, "Effect of Water-Binder Ratio and Replacement of Rice Husk-Bark Ash on Pozzolanic Reaction of Mortar," *International Conference on Pozzolan, Concrete and Geopolymer Khon Kaen, Thailand, May 24-25, 2006*, 2006.
- [85] A. Fernández-Jiménez and A. Palomo, "Composition and microstructure of alkali activated fly ash binder: Effect of the activator," *Cement and Concrete Research* vol. 35 (2005) 1984 - 1992, 2005.
- [86] G. P. Vagelis, "Effect of fly ash on Portland cement systems Part I. Low-calcium fly ash," *Cement and Concrete Research*, vol. 29 (1999) 1727–1736, 1999.
- [87] V. G. Papadakis, M. N. Fardis, and C. G. Vayenas, "Hydration and carbonation of pozzolanic cements," *ACI Mater*, vol. J 89 (1992) 119., 1992.
- [88] P. Bertil, "A Comparison Between Mechanical Properties of Self-Compacting Concrete and The Corresponding Properties of Normal Concrete," *Cement and Concrete Research*, vol. 31 (2001) 193-198, 2001.
- [89] M. Sari, E. Prat, and J. F. Labastire, "High strength self-compacting concrete Original solutions associating organic and inorganic admixtures," *Cement and Concrete Research* 29 (1999) 813-818, 1999.
- [90] G. Rodrigues de Sensale, "Strength development of concrete with rice-husk ash," *Cement and Concrete Composites*, vol. 28 (2006) 158 - 160, 2005.
- [91] T. Pipat, "Role of Fly Ash on The Fluidity of Paste," ws3-er.eng.hokudai.ac.jp/egpsee/alumni/abstracts/Pipat, 2002.

- [92] B. H. Bharatkumar, R. Narayanan, B. K. Raghuprasad, and D. S. Ramachandramurthy, "Mix proportioning of high performance concrete," *Cement & Concrete Composites* 23 (2001) 71-80, 2001.
- [93] A. Leemann and F. Winnefeld, "The effect of viscosity modifying agents on mortar and concrete," *Cement & Concrete Composites* 29 (2007) 341-349, 2007.
- [94] J. Bjömström and S. Chandra, "Effect of superplasticizers on the rheological properties of cements," *Materials and Structures / Matériaux et Constructions*, Vol. 36, December 2003, pp 685-692, 2003.
- [95] R. S. Ravindrarajah, F. Farrokhzadi, and A. Lahoud, "Properties of Flowing Concrete and Self-Compacting Concrete With High-Performance Superplasticier," *Proceedings of the 3rd International RILEM Symposium , Reykjavik, Iceland, 17-20 August 2003, Edited by O. Wallevik and I. Nielsson , (RILEM Publications), 1 Vol., 1048 pp., ISBN: 2-912143-42-X, 2003.*
- [96] C. Pierre, J. Shipping, and K. ByungGi, "Cement/superplasticizer interaction The case of polysulfonates," *Bulletin des Laboratoires des Points et Chaussées*, vol. 233-July-August 2001 - ref 4.73 - pp. 89-99, 2001.
- [97] A. Borsoi, M. Collepardi, S. Collepardi, E. N. Croce, and M. Passuelo, "Influence of Viscosity Modifying Admixture on the Composition of SCC," *Eighth CANMET/ACI International Conference on Superplasticizers and Other Chemical Admixtures in Concrete*, 2006.
- [98] P. Jean, Yves, K. H. Khayat, and E. Wirquin, "Coupled effect of time and temperature on variations of yield value of highly flowable mortar," *Cement and Concrete Research* 36 (2006) 832 – 841, 2006.
- [99] M. R. Rixom and N. P. Mailvaganam, "Chemical Admixtures for Concrete," *E. & F. N. Spoon Ltd., Edition: 3, p. 94, 1999.*
- [100] H. W. Reinhardt and M. Stegmaier, "Influence of heat curing on the pore structure and compressive strength of self-compacting concrete (SCC)," *Cement and Concrete Research* 36 (2006) 879-885, 2006.
- [101] V. Corinaldesi and G. Moriconi, "Durable fiber reinforced self-compacting concrete," *Cement and Concrete Research* 34, pp. 249-254, 2004.
- [102] M. J. McCarthy, P. A. J. Tittle, K. H. Kii, and R. K. Dhir, "Mix proportioning and engineering properties of conditioned PFA concrete," *Cement and Concrete Research* 31 (2001) 321 -326, 2001.
- [103] O. Celik and N. J. Carino, "Concrete Strength Testing," in *Significance of Tests and Properties of Concrete and Concrete -Making Materials* Bridgeport: American Society for Testing and Materials, 2006, p. pp. 125.
- [104] A. Castel, T. Vidal, and R. François, "Bond and cracking properties of self-consolidating concrete," *Construction and Building Materials, online version (2010) 001-010, 2010.*
- [105] C. Druta, "Tensile Strength and Bonding Characteristics of Self-Compacting Concrete," in *Faculty of the Louisiana State University and Agricultural and Mechanical College. vol. Master of Science in Engineering Science* Bucharest: Polytechnic University of Bucharest, 2003.

- [106] R. V. Balendran, A. Nadeem, T. Maqsood, and H. Y. Leung, "Flexural and Split Cylinder Strengths of HSC at Elevated Temperatures " *Fire Technology*, Volume 39, Number 1 / January, 2003.
- [107] M. J. Shannag, "High strength concrete containing natural pozzolan and silica fume," *Cement & Concrete Composites* 22 (2000) 399-406, 2000.
- [108] S. Bhanjaa and B. Sengupta, "Influence of silica fume on the tensile strength of concrete," *Cement and Concrete Research* 35 (2005) 743-747, 2005.
- [109] S. Assié, G. Escadeillas, and V. Waller, "Estimates of self-compacting concrete 'potential' durability," *Construction and Building Materials* 21 (2007) 1909-1917, 2007.
- [110] R. J. Detwiler and P. C. Taylor, "Specifier's Guide to Durable Concrete," vol. EB221, Portland Cement Association, Skokie, Illinois, USA, 2005, 68 pages, 2005.
- [111] P. Dinakar, K. Babu, and M. Santhanam, "Durability properties of high volume fly ash self compacting concretes," *Cement & Concrete Composites* 30, 2008.
- [112] S. Chandra, *Properties of concrete with admixture, Structure and Performance of Cements* vol. Second Edition. London: St Edmundsbury Press, Bury St Edmonds, Suffolk, 2002.
- [113] H. Chao-Lung and H. Meng-Feng, "Durability design and performance of self-consolidating lightweight concrete," *Construction and Building Materials* 19 (2005) 619-626, 2005.
- [114] P. W. Brown, D. Shi, J. P. Skalny, and W. R. Grace, *Concrete Microstructure Porosity and Permeability, POROSITY/PERMEABILITY RELATIONSHIPS*. Washington, DC: Strategic Highway Research Program, National Academy of Sciences, 2101 Constitution Avenue N.W., 1993.
- [115] P. K. Chang, Y. N. Peng, and C. L. Hwang, "A design consideration for durability of high-performance concrete," *Cement & Concrete Composites* 23 (2001) 375-380, 2001.
- [116] A. K. Al-Tamimi and M. Sonebi, "Assessment of Self-Compacting Concrete Immersed in Acidic Solutions," *JOURNAL OF MATERIALS IN CIVIL ENGINEERING, ASCE*, vol. Vol. 15, No. 4, August 1, 2003.
- [117] N. Hearn, D. Hooton, R., and M. Nokken, R., "Pore Structure, Permeability, and Penetration Resistance Characteristic of Concrete," in *Significan of test and properties of concrete and concrete-making material, volume 1*, F. L. Joseph and J. H. Pielert, Eds., 2006, p. 238.
- [118] W. Zhu and P. J. M. Bartos, "Permeation properties of self-compacting concrete," *Cement and Concrete Research* 33 (2003) 921-926, 2003.
- [119] J. G. Cabrera and A. S. A. Hasan, "Performance Properties of Concrete Repair Materials," *Construction and Building Materials, Vol. 11 Nos 5-6*, pp. 283-290, 1997.
- [120] N. Shafiq and J. G. Cabrera, "Effects of initial curing condition on the fluid transport properties in OPC and fly ash blended cement concrete," *Cement and Concrete Composites* 26 (2004) 381-387, 2004.

- [121] A. A. A. Hassan, K. Hossain, and M. Lachemi, "Structural assessment of corroded self-consolidating concrete beams," *Engineering Structures* 32 (2010) 874-885, 2010.
- [122] G. Batis and T. Routoulas, "Steel rebars corrosion investigation with strain gages," *Cement & Concrete Composites* 21 (1999) 1633171, 1999.
- [123] A. A. Gürten, K. Kayakırılmaz, and M. Erbil, "The effect of thiosemicarbazide on corrosion resistance of steel reinforcement in concrete," *Construction and Building Materials* 21 (2007) 669-676, 2007.
- [124] N. Birbilis and L. J. Holloway, "Use of the time constant to detect corrosion speed in reinforced concrete structures," *Cement & Concrete Composites* 29 (2007) 330-336, 2007.
- [125] J. M. Miranda, A. Ferná'ndezJime'nez, J. A. Gonza'lez, and A. Palomo, "Corrosion resistance in activated fly ash mortars," *Cement and Concrete Research* 35 (2005) 1210- 1217, 2005.
- [126] C. Prinya, R. Sumrerng, and S. Vute, "Effect of carbon dioxide on chloride penetration and chloride ion diffusion coefficient of blended Portland cement mortar," *Construction and Building Materials xxx* (2007) xxx-xxx, 2007.
- [127] M. Boroni, "Concrete Self Compacting Concrete for High Performance Structures," *Fédération Internationale du Béton Proceedings of the 2nd International Congress June 5-8, 2006 - Naples, Italy ID 13-42 Session 13*, 2006.
- [128] A. A. A. Hassan, K, M, A. Hossain, and M. Lachemi, "Strength, cracking and deflection performance of large-scale self-consolidating concrete beams subjected to shear failure," *Engineering Structures* (2010), doi:10.1016, online version, pp. 001 - 010, 2010.
- [129] M. Valcuende and C. Parra, "Bond behaviour of reinforcement in self-compacting concretes," *Construction and Building Materials* 23 (2009) 162-170, 2009.
- [130] M. R. Esfahani, M. Lachemi, and M. R. Kianoush, "Top-bar effect of steel bars in self-consolidating concrete (SCC)," *Cement & Concrete Composites* 30 (2008) 52-60, 2008.
- [131] A. A. A. Hassan, K, M, A. Hossain, and M. Lachemi, "Bond strength of deformed bars in large reinforced concrete members cast with industrial self-consolidating concrete mixture," *Construction and Building Materials* 24 (2010) 520-530, 2010.
- [132] A. Effendy, "The Properties and Flexural Behaviour of Self Compacting Concrete Using Palm Oil Fuel Ash and Admixture," in *Faculty of Civil Engineering*. vol. Master of Civil Engineering Johor: Unervisiti Teknologi Malaysia, 2008.
- [133] V. B. Lambros, "Self-consolidating concrete : rheology, fresh properties and structural behaviour." vol. Master of Applied Science Toronto, Ontario, Canada: Ryerson University, 2003.
- [134] L. H. Han and G. H. Yao, "Experimental behaviour of thin-walled hollow structural steel (HSS) columns filled with self-consolidating concrete (SCC)," *Thin-Walled Structures* 42 (2004) 1357-1377, 2004.

- [135] L. H. Han and G. H. Yao, "Behaviour of concrete-filled hollow structural steel (HSS) columns with pre-load on the steel tubes," *Journal of Constructional Steel Research* 59 (2003) 1455–1475, 2003.
- [136] J. A. Peter, N. Lakshmanan, and P. D. Manoharan, "Investigations on the Static Behavior of Self-Compacting Concrete Under-Reamed Piles," *Journal of Materials in Civil Engineering*, Vol. 18, No. 3, June 1, 2006.
- [137] F. M. d. A. Filho, M. K. E. Debs, and A. L. c. H. C. E. Debs, "Bond-slip behavior of self-compacting concrete and vibrated concrete using pull-out and beam tests," *Materials and Structures* (2008) 41:1073–1089, 2008.
- [138] H. E. Chabib, M. Nehdi, and M. H. E. Naggar, "Behavior of SCC confined in short GFRP tubes," *Cement & Concrete Composites* 27 (2005) 55–64, 2005.
- [139] A. A. A. Hassan, K. M. A. Hossain, and M. Lachemi, "Behavior of full-scale self-consolidating concrete beams in shear," *Cement & Concrete Composites* 30 (2008) 588–596, 2008.
- [140] F. Dehn, K. Holschemacher, and D. Weiße, "Self-Compacting Concrete (SCC) Time Development of the Material Properties and the Bond Behaviour," *LACER* No. 5, 2000.
- [141] D. Frank, H. Klaus, and W. e. Dirk, "Self-Compacting Concrete (SCC) Time Development of the Material Properties and the Bond Behaviour," *LACER* No. 5, 2000.
- [142] S. K. Ghosh and M. Saatcioglu, *Ductility and seismic behavior, High Performance Concrete and Applications* LONDON Edward Arnold, A member of the Hodder Headline Group, 1994.
- [143] N. Ulrika, "Concrete Structures Subjected to Blast and Fragment Impacts: Numerical Simulations of Reinforced and Fibre-reinforced Concrete," in *Department of Civil and Environmental Engineering Division of Structural Engineering, Concrete Structures* Göteborg, Sweden CHALMERS UNIVERSITY OF TECHNOLOGY, 2008.
- [144] A. S. Ezeldin and P. N. Balaguru, *Fatigue and bond properties, High Performance Concrete and Applications* London: Edward Arnold, A member of the Hodder Headline Group, 1994.
- [145] K. Maekawa and K. Farouk, El-Kashif, "Cyclic Cumulative Damaging of Reinforced Concrete in Post-Peak Regions," *Journal of Advance Concrete Technology* Vol. 2, No. 2, 257-271, 2004.
- [146] S. Zihai and Z. Masaki, "Numerical studies on load-carrying capacities of notched concrete beams subjected to various concentrated loads," *Construction and Building Materials* 18 (2004) 173–180, 2004.
- [147] T. Houssam, Z. Liangying, D. Yong, Z. Yue, and P. Balaguru, "Cyclic Behavior of RC Beams Strengthened with Carbon Fiber Sheets Bonded by Inorganic Matrix,," *ASCE journal*, vol. 0899-1561, 2006.
- [148] S. Khaled and J. K. Raymond, "Fatigue behavior of fiber-reinforced recycled aggregate base course," *Journal of Materials in Civil Engineering*, Vol. 11, No. 2, May, 1999.
- [149] D. Minh-Tan, C. Omar, and A. RPierre-Claude, "FATIGUE BEHAVIOR OF HIGH-PERFORMANCE CONCRETE," *Journal of Materials in Civil Engineering*, Vol. 5, No. 1, February, 1993, 1993.

- [150] G. P. Christos, F. P. Michael, and A. H. Kent, "Fatigue behavior of RC beams strengthened with GFRP sheets," *Journal of Composites for Construction*, Vol. 5, No.4, November, 2001. , 2001.
- [151] M. Ben-Amoz., "Bounds on fatigue damage: relation to microstructure dependent crack growth, I. Constant amplitude cyclic damage," *International Journal of Fracture* 124: 153–177, 2003.
- [152] R. Breitenbücher and H. Ibuk, "Experimentally based investigations on the degradation-process of concrete under cyclic load," *Materials and Structures* (2006) 39:717–724, 2006.
- [153] M. Schläfli and E. Brühwiler, "Fatigue of existing reinforced concrete bridge deck slabs," *EngineeringvStructure* Vol. 20, No. 11 . pp. 991-948, 1998.
- [154] Z. Jun, S. Henrik, and C. L. Victor, "Fatigue life prediction of fiber reinforced concrete under flexural load," *International Journal of Fatigue* 21 (1999) 1033–1049, 1999.
- [155] B. Paulo, Cachim, A. Joaquim, Figueiras, and A. A. Paulo, Pereira, "Numerical modelling of fibre-reinforced concrete fatigue in bending," *International Journal of Fatigue* 24 (2002) 381–387, 2002.
- [156] A. J. Nieto, J. M. Chicharro, and P. Pintado, "An approximated methodology for fatigue tests and fatigue monitoring of concrete specimens," *International Journal of Fatigue*, vol. 28 (2006) 835–842, 2006.
- [157] V. Li, C. and M. Takashi, "Fatigue Crack Growth Analysis of Fiber Reinforced Concrete with Effect of Interfacial Bond Degradation," *Cement and Concrete Composites* 20, 339-351, 1998.
- [158] Á. Miguel, Pindado, A. Antonio, and J. Alejandro, "Fatigue behavior of polymer-modified porous concretes," *Cement and Concrete Research* 29, 1077–1083, 1999.
- [159] S. P. Singh and S. K. Kaushik, "Fatigue strength of steel fibre reinforced concrete in flexure," *Cement & Concrete Composites* 25 (2003) 779-786, 2003.
- [160] L. Peiyin, L. Qingbin, and S. Yupu, "Damage constitutive of concrete under uniaxial alternate tension–compression fatigue loading based on double bounding surfaces," *International Journal of Solids and Structures* 41. 3151–3166, 2004.
- [161] G. J. Krige and J. Mahachi, "Dynamic Behaviour of Composite Floors," *Journal of Construction Steel Research* 34 (1995) 249-269, 1995.
- [162] S. Jongsung and O. Hongseob, "Structural behavior of strengthened bridge deck specimens under fatigue loading," *Engineering Structures* 26 (2004) 2219–223, 2004.
- [163] M. K. Lee and B. I. G. Barr, "An overview of the fatigue behaviour of plain and fibre reinforced concrete," *Cement & Concrete Composites* 26 (2004) 299–305, 2004.
- [164] C. Christoph and M. Masoud, "Fatigue behaviour of CFRP L-shaped plates for shear strengthening of RC T-beams," *Journal of Composites: Part B* 35 (2004) 279–290, 2004.

- [165] M. Takashi and C. L. Victor, "Fatigue life analysis of fiber reinforced concrete with a fracture mechanics based model," *Cement & Concrete Composites* 21 (1999) 249±261, 1999.
- [166] C. Andrea, S. Andrea, and V. Sabrina, "A fracture mechanics model for a composite beam with multiple reinforcements under cyclic bending," *International Journal of Solids and Structures* 41 (2004) 5499–5515, 2004.
- [167] D. A. Hordijk and H. W. Reinhardt, "Numerical and experimental investigation into the fatigue behavior of plain concrete.," *Proc., SEM VII Int. Congr. on Experimental Mech., Las Vegas NV., 1992.*
- [168] P. L. Weena, J. G. Sanjayan, and S. Setunge, "Constitutive Model for Confined High Strength Concrete Subjected to Cyclic Loading," *JOURNAL OF MATERIALS IN CIVIL ENGINEERING © ASCE / JULY/AUGUST 2004 / 297*, 2004.
- [169] M. Bin, K. V. Subramaniam, and S. P. Shah, "Failure Mechanism of Concrete under Fatigue Compressive Load," *JOURNAL OF MATERIALS IN CIVIL ENGINEERING © ASCE / NOVEMBER/DECEMBER 2004 pp.566*, 2004.
- [170] A. E. Naaman and H. H. ammoud, "Fatigue Characteristics of High Performance Fiber-reinforced Concrete," *Cemenr and Concrete Composites* 20 (1998) 353-363, 1998.
- [171] O. Mallet, "Fatigue of reinforced concrete," *HMSO, London.*, 1991.
- [172] R. A. Barnes and G. C. Mays, "Fatigue performance of concrete beams strengthened with CFRP plates," *Journal Composite for Construction, ASCE*, vol. 3(2), 63-72., 1999.
- [173] N. Nguyen , Roussel , and P. Coussot, "Correlation between L-box test and rheological parameters of a homogeneous yield stress fluid," *Cement and Concrete Research*, vol. 36 (2006) 1789–1796, 2006.
- [174] B. Felekoğlu, S. Türkel, and B. Baradan, "Effect of water/cement ratio on the fresh and hardened properties of self-compacting concrete," *Building and Environment* 42 (2007), pp. 1795-1802, 2007.
- [175] A. Frommenwiler, "NEW GENERATION OF SUPERPLASTICIZERS FOR HIGH PERFORMANCE CONCRETE (HPC)," *MBT Holding, Switzerland*, pp. 50 - 62, 1997.
- [176] W. R. Grace and CoConn, "Self-Consolidating Concrete (SCC) Production Tips," *TECHNICAL BULLETIN TB - 1505*, pp. 2-4, 2005.
- [177] R. N. Tarun and S. S. Shiw, "Effect Of Dosage Of Superplasticizers On Concrete Microstructure And Strength," *Center for By- Products Utilization (CBU) at the University of Wisconsin-Milwaukee*, 1997.
- [178] S. A. B. Azli, "Effect Of Silica Fume To The Strength And Permeability Of High Performance Ground Granulated Blastfurnace Slag Concrete," in *Faculty of Civil Engineering*. vol. Master of Engineering (Civil – Structure) Johor: Universiti Teknologi Malaysia, 2006, p. 76.
- [179] S. Pantawee and T. Sinsiri, "THE USE OF NATURAL POZZOLANS IN LIGHTWEIGHT CONCRETE," *Cement and Concrete Research*. 34. p.2175-2179, 2008.
- [180] A. Wang, C. Zhang, and W. Sun, "Fly ash effects: I. The morphological effect of fly ash," *Cement and Concrete Research* 33 (2003) 2023-2029, 2003.

- [181] Z. Chengzhi, W. Aiqin, T. Mingshu, and L. Xiaoyu, "THE FILLING ROLE OF POZZOLANIC MATERIAL," *Building Material Industry Bureau of Beijing, Beijing, 100000, Cement and Concrete Research, Vol. 26, No. 6, pp. 943-947, 1996.*
- [182] T. Nochaiya, W. Wongkeo, and A. Chaipanich, "Utilization of fly ash with silica fume and properties of Portland cement-fly ash-silica fume concrete," *Science direct Fuel 89 (2010) 768-774, 2010.*
- [183] S. B. Park and M. Tia, "THE EFFECTS OF SUPERPLASTICIZERS ON THE ENGINEERING PROPERTIES OF PLAIN CONCRETE," *Transportation Research Board, Issue Number: 1062, p. 38-46, 1986.*
- [184] M. K. Ane, J. F. Robert, and B. Lennart, "Relating the molecular structure of comb-type superplasticizers to the compression rheology of MgO suspensions" *Cement and Concrete Research Volume 36, Issue 7 July 2006, Pages 1231-1239 2006.*
- [185] S. Etsuo, K. Takayuki, S. Tomomi, A. Kiyoshi, and D. Masaki, "Influence of superplasticizers on the hydration of cement and the pore structure of hardened cement," *Cement and Concrete Research 36 (2006) 2049-2053, 2006.*
- [186] N. Shafiq, "Transport characteristics of fluid and ions in concrete: Performance criteria for concrete durability," in *Faculty of Engineering, Civil Engineering Leeds: University of Leeds, United of Kingdom, 1999.*
- [187] V. Ketil, "Electrochemical studies of steel in cement mortar containing chloride and micro-silica," *Corrosion Science 49 (2007) 1702-1717, 2007.*
- [188] H. W. Song and V. Saraswathy, "Corrosion Monitoring of Reinforced Concrete Structures - A Review," *International Journal Electrochemical Science, 2 (2007) 1- 28, 2007.*
- [189] K. C. Clear, "Time-to-Corrosion of Reinforcing Steel in Concrete Slabs," *PHWA-RD-76-70, Washingyon, DC, 1976.*
- [190] V. Červenka and J. Červenka, *User's Manual for ATENA 3D* Prague: Červenka Consulting, 2007
- [191] V. Červenka, L. Jendele, and J. Červenka, *ATENA Program Documentation, Part 1, Theory* Prague: Červenka Concsultiing, 2007.
- [192] G. Spadeal and F. Bencardino, "BEHAVIOR OF FIBER-REINFORCED CONCRETE BEAMS UNDER CYCLIC LOADING," *Journal of Structural Engineenng, Vol. 123, No.5, May, 1997 Paper No. 13318, 1997.*
- [193] K. Kae-Hwan and K. Jae-Jung, "Fatigue strength in polymer-reinforcedc oncrete beams under cyclic loading," *Nuclear Engineeringa nd Design 156 (1995) 63-73, 1995.*
- [194] A. H. Nilson, *Design of Concrete Structures*, 13th edition ed.: McGraw-Hill Science/Engineering/Math 2003.
- [195] L. Xiaobin, T. H. Cheng, and Tzu, "Behavior of high strength concrete with and without steel fiber reinforcement in triaxial compression," *Cement and Concrete Research 36 (2006) 1679-1685, 2006.*
- [196] F. P. Zhou, R. V. Balendran, and A. P. Jeary, "Size Effect on Flexural, Splitting Tensile, and Torsional Strengths Of High-Strength Concrete," *Cement and Concrete Research, Vol. 28, No. 12, pp. 1725-1736, 1998.*

- [197] M. M. Glenn, "EFFECT OF HIGH-STRENGTH CONCRETE ON THE SEISMIC RESPONSE OF CONCRETE FRAMES," in *Department of Civil Engineering and Applied Mechanics* Montréal, Canada: McGill University, 1997.
- [198] F. Kuang, Y. Shih-Tzung, W. Chwen-Shyuan, and H. Keh-Luen, "CYCLIC BEHAVIOR OF MODERATELY DEEP HSC BEAMS," *Journal of Structural Engineering*, Vol. 119, No. 9, September, 1993 Paper No. 2624., 1993.

Appendix A

A. 1. Effects of Variation of FA Content with 3% SP and w/b of 0.25 and 0.32

NO	Mixes	OPC	FA	MIRHA	CA (20-8)	CA (8-4)	sand	w/b	w/c	water	S/P (%)	SP weight	total	pozzolan (%)
1	FA5-0.25-3	475	25	0	310	615	850	0.25	0.26	125	3	15	2400	5
2	FA10-0.25-3	450	50	0	310	615	850	0.25	0.28	125	3	15	2400	10
3	FA15-0.25-3	425	75	0	310	615	850	0.25	0.29	125	3	15	2400	15
4	FA5-0.32-3	475	25	0	310	615	850	0.32	0.34	160	3	15	2435	5
5	FA10-0.32-3	450	50	0	310	615	850	0.32	0.36	160	3	15	2435	10
6	FA15-0.32-3	425	75	0	310	615	850	0.32	0.38	160	3	15	2435	15

(unit in kg/m³)

A. 2. Effects of Variation of Water Content with 3% SP

NO	Mixes	OPC	FA	MIRHA	CA (20-8)	CA (8-4)	sand	w/b	w/c	water	S/P (%)	SP weight	total	pozzolan (%)
1	FA10-0.25-3	450	50	0	310	615	850	0.25	0.28	125	3	15	2400	10
2	FA10-0.28-3	450	50	0	310	605	845	0.28	0.31	140	3	15	2400	10
3	FA10-0.3-3	450	50	0	312	605	833	0.3	0.33	150	3	15	2400	10
4	FA10-0.32-3	450	50	0	310	615	850	0.32	0.36	160	3	15	2435	10
5	FA10-0.34-3	450	50	0	300	600	830	0.34	0.38	170	3	15	2400	10
6	FA10-0.36-3	450	50	0	297	598	825	0.36	0.40	180	3	15	2400	10
7	FA10-0.42-3	450	50	0	280	590	820	0.42	0.47	210	3	15	2400	10

A. 3. Effects of Variation of SP Content with 10% FA Content in Different w/b

NO	Mixes	OPC	FA	MIRHA	CA (20-8)	CA (8-4)	sand	w/b	w/c	water	S/P (%)	SP weight	total	pozzolan (%)
1	FA10-0.25-2	450	50	0	310	615	850	0.25	0.28	125	2	10	2400	10
2	FA10-0.25-3	450	50	0	310	615	850	0.25	0.28	125	3	15	2400	10
3	FA10-0.25-4	450	50	0	310	615	850	0.25	0.28	125	4	20	2400	10
4	FA10-0.25-6	450	50	0	310	615	850	0.25	0.28	125	6	30	2400	10
5	FA10-0.34-2	450	50	0	300	600	830	0.34	0.38	170	2	10	2410	10
6	FA10-0.34-3	450	50	0	300	600	830	0.34	0.38	170	3	15	2400	10
7	FA10-0.34-4	450	50	0	300	600	830	0.34	0.38	170	4	20	2400	10
8	FA10-0.34-6	450	50	0	300	600	830	0.34	0.38	170	6	30	2400	10
9	FA10-0.42-2	450	50	0	280	590	820	0.42	0.47	210	2	10	2400	10
10	FA10-0.42-3	450	50	0	280	590	820	0.42	0.47	210	3	15	2400	10
11	FA10-0.42-4	450	50	0	280	590	820	0.42	0.47	210	4	20	2400	10
12	FA10-0.42-6	450	50	0	280	590	820	0.42	0.47	210	6	30	2400	10

A. 4. Effects of Variation of SP Content with 10% MIRHA in Different w/b

NO	Mixes	OPC	FA	MIRHA	CA (20-8)	CA (8-4)	sand	w/b	w/c	water	S/P (%)	SP weight	total	pozzolan (%)
1	M10-0.35-2	450	0	50	310	600	815	0.35	0.39	175	2	10	2400	10
2	M10-0.35-3	450	0	50	310	600	815	0.35	0.39	175	3	15	2400	10
3	M10-0.35-4	450	0	50	310	600	815	0.35	0.39	175	4	20	2400	10
4	M10-0.35-6	450	0	50	310	600	815	0.35	0.39	175	6	30	2400	10
5	M10-0.4-2	450	0	50	300	595	810	0.4	0.44	200	2	10	2405	10
6	M10-0.4-3	450	0	50	302	592	806	0.4	0.44	200	3	15	2400	10
7	M10-0.4-4	450	0	50	300	595	810	0.4	0.44	200	4	20	2405	10
8	M10-0.4-6	450	0	50	300	595	810	0.4	0.44	200	6	30	2405	10
9	M10-0.45-2	450	0	50	290	585	805	0.45	0.5	225	2	10	2405	10
10	M10-0.45-3	450	0	50	290	585	800	0.45	0.50	225	3	15	2400	10
11	M10-0.45-4	450	0	50	290	585	805	0.45	0.5	225	4	20	2405	10
12	M10-0.45-6	450	0	50	290	585	805	0.45	0.5	225	6	30	2405	10

A. 5. Effects of Variation of Water Content with 3% SP in MSCC

NO	Mixes	OPC	FA	MIRHA	CA (20-8)	CA (8-4)	sand	w/b	w/c	water	S/P (%)	SP weight	total	pozzolan (%)
1	M10-0.35-3	450	0	50	310	600	815	0.35	0.39	175	3	15	2400	10
2	M10-0.38-3	450	0	50	305	595	810	0.38	0.42	190	3	15	2400	10
3	M10-0.4-3	450	0	50	302	592	806	0.4	0.44	200	3	15	2400	10
4	M10-0.42-3	450	0	50	300	590	804	0.42	0.47	210	3	15	2404	10
5	M10-0.45-3	450	0	50	290	585	800	0.45	0.50	225	3	15	2400	10
6	M10-0.46-3	450	0	50	287	583	800	0.46	0.51	230	3	15	2400	10

A. 6. Effects of Variation of Water Content with 3% SP in FMSCC

NO	Mixes	OPC	FA	MIRHA	CA (20-8)	CA (8-4)	sand	w/b	w/c	water	S/P (%)	SP weight	total	pozzolan (%)
1	FA20-M10-0.35-3	350	100	50	310	600	815	0.35	0.5	175	3	15	2400	10
2	FA20-M10-0.4-3	350	100	50	300	595	810	0.4	0.57	200	3	15	2405	10
3	FA20-M10-0.45-3	350	100	50	290	585	805	0.45	0.64	225	3	15	2405	10
4	FA10-M10-0.3-3	400	50	50	310	600	820	0.3	0.375	150	3	15	2400	20
5	FA10-M10-0.34-3	400	50	50	305	600	825	0.34	0.425	170	3	15	2400	20
6	FA10-M10-0.38-3	400	50	50	300	590	820	0.38	0.475	190	3	15	2400	20

A. 6. Effects of Variation of Water Content with 3% SP in NPSCC

NO	Mixes	OPC	FA	MIRHA	CA (20-8)	CA (8-4)	sand	w/b	w/c	water	S/P (%)	SP weight	total	pozzolan (%)
1	NP-0.25-3	500	0	0	310	615	850	0.25	0.25	125	3	15	2400	0
2	NP-0.32-3	500	0	0	310	615	850	0.32	0.32	160	3	15	2435	0
3	NP-0.35-3	500	0	0	310	600	815	0.35	0.35	175	3	15	2400	0
4	NP-0.4-3	500	0	0	295	590	815	0.4	0.4	200	3	15	2400	0
5	NP-0.45-3	500	0	0	280	585	810	0.45	0.45	225	3	15	2400	0
6	NP-0.5-3	500	0	0	265	575	810	0.5	0.5	250	3	15	2400	0

A. 7. Normal Concrete

NO	Mixes	OPC	FA	MIRHA	CA (20-8)	CA (8-4)	sand	w/b	w/c	water	S/P (%)	SP weight	total	pozzolan (%)
1	NC-0.4-0	500	0	0	290	590	820	0.4	0.4	200	0	0	2400	0
2	NC-0.5-0	500	0	0	265	575	810	0.5	0.5	250	0	0	2400	0

Appendix B. Compressive Strength

NO	Mixes	age (days)	compression (MPa)		
			Sample 1	Sample 2	Sample 3
1	FA10-0.25-2	1	28.16	25.07	27.07
	FA10-0.25-2	3	41.15	40.47	45.09
	FA10-0.25-2	7	47.22	46.13	50.27
	FA10-0.25-2	28	51.73	50.93	63.7
	FA10-0.25-2	90	62.42	90.32	73.62
	FA10-0.25-2	360	79.99	106.8	98.03
2	FA10-0.25-3	1	26.08	24.01	22.88
	FA10-0.25-3	3	53.62	55.17	50.14
	FA10-0.25-3	7	55.84	57.44	57
	FA10-0.25-3	28	70.92	85.37	87.67
	FA10-0.25-3	56	97.47	100.57	84.59
	FA10-0.25-3	90	114.77	94.56	75.9
	FA10-0.25-3	180	80.32	103.27	120.97
	FA10-0.25-3	360	111.84	129.5	92.57
3	FA10-0.25-4	1	6.721	35.59	37.73
	FA10-0.25-4	3	44.58	57.57	57
	FA10-0.25-4	7	55.84	57.44	58.76
	FA10-0.25-4	28	63.17	84.9	63.74
	FA10-0.25-4	90	103.2	69.36	96.61
	FA10-0.25-4	360	130.9	113	128.8
4	FA10-0.25-6	1	24.45	28.29	26.78
	FA10-0.25-6	3	43.31	43.76	45.15
	FA10-0.25-6	7	46.13	47.41	43.29
	FA10-0.25-6	28	70.08	63.53	67.64
	FA10-0.25-6	90	86.76	79.63	83.9
	FA10-0.25-6	360	62.64	107.4	70.02
5	FA10-0.34-1.4	1	7.13	7.12	6.98
	FA10-0.34-1.4	3	18.73	17.86	18.4
	FA10-0.34-1.4	7	22.78	25.21	23.95
	FA10-0.34-1.4	28	37.53	37.7	33.82
	FA10-0.34-1.4	56	36.94	42.95	42.74
	FA10-0.34-1.4	360	73.57	69.68	71.97
6	FA10-0.34-2	1	16.97	17.22	16.95
	FA10-0.34-2	3	24.8	27.79	28.23
	FA10-0.34-2	7	29.3	30.17	20.52
	FA10-0.34-2	28	36.63	41.44	44.41
	FA10-0.34-2	90	61.68	68.52	67.85
	FA10-0.34-2	360	84.08	65.23	70.77

NO	Mixes	age (days)	compression (MPa)		
			Sample 1	Sample 2	Sample 3
7	FA10-0.34-3	7	44.93	39.84	34.48
	FA10-0.34-3	28	50.6	61.18	59.77
	FA10-0.34-3	180	66.86	54.27	61.53
	FA10-0.34-3	360	74.71	60.71	71.05
8	FA10-0.34-4	1	0.47	5.797	0.863
	FA10-0.34-4	3	37.49	29.86	35.32
	FA10-0.34-4	7	38.79	38.03	43.15
	FA10-0.34-4	28	60.91	57.32	65.84
	FA10-0.34-4	90	64.75	62.9	75.02
	FA10-0.34-4	360	89.27	70.82	70.39
9	FA10-0.34-6	1	7.44	5.493	6.226
	FA10-0.34-6	3	22.84	36.5	34.93
	FA10-0.34-6	7	19.7	37.75	35
	FA10-0.34-6	28	40.65	42.45	24.95
	FA10-0.34-6	90	59.97	65.44	62.56
	FA10-0.34-6	360	78.74	66.29	63.25
10	FA10-0.42-2	1	9.901	10.6	10.68
	FA10-0.42-2	3	14.83	17.95	20.2
	FA10-0.42-2	7	21.57	23.04	24.58
	FA10-0.42-2	28	27.13	26.54	24.56
	FA10-0.42-2	90	49.2	59.81	50.35
	FA10-0.42-2	360	48.96	62.92	52.97
11	FA10-0.42-3	7	26.4	24.3	23.79
	FA10-0.42-3	28	35.2	34.23	33.5
	FA10-0.42-3	180	41.54	36.63	35.18
	FA10-0.42-3	360	49.85	40.66	39.05
12	FA10-0.42-4	1	8.91	9.54	9.61
	FA10-0.42-4	3	13.35	16.16	18.18
	FA10-0.42-4	7	19.41	20.74	24.82
	FA10-0.42-4	28	28.98	24.42	35.65
	FA10-0.42-4	90	44.28	53.83	45.32
	FA10-0.42-4	360	61.49	56.63	47.67
13	FA10-0.42-6	1	10.77	14.15	10.57
	FA10-0.42-6	3	15.87	15.21	16.45
	FA10-0.42-6	7	18.25	18.6	11.96
	FA10-0.42-6	28	27.3	23.79	24.03
	FA10-0.42-6	90	45.94	52.55	53.08
	FA10-0.42-6	360	51.57	68.47	61.62
14	FA5-0.25-3	1	33.58	25.66	38.2
	FA5-0.25-3	3	55.57	60.61	50.59
	FA5-0.25-3	7	60.34	55.93	52.5

NO	Mixes	age (days)	compression (MPa)		
			Sample 1	Sample 2	Sample 3
	FA5-0.25-3	28	75.02	79.34	83.09
	FA5-0.25-3	56	94.65	86.61	91.67
	FA5-0.25-3	90	88.26	94.55	103.5
	FA5-0.25-3	180	98.4	103.6	105.8
	FA5-0.25-3	360	109.3	68.73	106.5
15	FA10-0.25-3	1	26.08	24.01	22.88
	FA10-0.25-3	3	53.62	55.17	50.14
	FA10-0.25-3	7	55.84	57.44	57
	FA10-0.25-3	28	70.92	85.37	87.67
	FA10-0.25-3	56	97.47	100.57	84.59
	FA10-0.25-3	90	114.77	94.56	75.9
	FA10-0.25-3	180	80.32	103.27	120.97
	FA10-0.25-3	360	111.84	129.5	92.57
16	FA15-0.25-3	1	14.44	8.627	18.55
	FA15-0.25-3	3	29.69	19.82	40.65
	FA15-0.25-3	7	26.06	47.73	29.19
	FA15-0.25-3	28	75.6	70.44	80.29
	FA15-0.25-3	90	99.74	97.18	69.57
	FA15-0.25-3	180	109.1	99.03	105.4
	FA15-0.25-3	360	109.2	117.7	93.58
17	FA5-0.32-3	1	12.07	11.62	12.76
	FA5-0.32-3	3	34.36	30.99	28.31
	FA5-0.32-3	7	35.99	35.6	37.27
	FA5-0.32-3	28	49.69	50.37	44.26
	FA5-0.32-3	56	52.33	56.63	45.96
	FA5-0.32-3	360	65.65	70.55	69.83
18	FA10-0.32-3	3	42.42	0	0
	FA10-0.32-3	7	44.37	0	0
	FA10-0.32-3	28	67.9	0	0
	FA10-0.32-3	90	72.6	0	0
	FA10-0.32-3	360	83.41	0	0
19	FA15-0.32-3	1	2.236	0.5	0.549
	FA15-0.32-3	3	32.67	31.69	28.32
	FA15-0.32-3	7	35.21	33.4	33.73
	FA15-0.32-3	28	49.55	43.92	46.47
	FA15-0.32-3	56	51.9	50.45	61.18
	FA15-0.32-3	360	64.63	64.63	64.63
20	FA10-0.25-3	1	26.08	24.01	22.88
	FA10-0.25-3	3	53.62	55.17	50.14
	FA10-0.25-3	7	55.84	57.44	57
	FA10-0.25-3	28	70.92	85.37	87.67

NO	Mixes	age (days)	compression (MPa)		
			Sample 1	Sample 2	Sample 3
	FA10-0.25-3	56	97.47	100.57	84.59
	FA10-0.25-3	90	114.77	94.56	75.9
	FA10-0.25-3	180	80.32	103.27	120.97
	FA10-0.25-3	360	111.84	129.5	92.57
21	FA10-0.28-3	3	49.83	0	0
	FA10-0.28-3	7	46.06	0	0
	FA10-0.28-3	28	84.5	0	0
	FA10-0.28-3	90	95.5	0	0
	FA10-0.28-3	360	102.24	0	0
22	FA10-0.3-3	3	67.73	0	0
	FA10-0.3-3	7	71.6	0	0
	FA10-0.3-3	28	75.71	0	0
	FA10-0.3-3	90	80.6	0	0
	FA10-0.3-3	360	95.81	0	0
23	FA10-0.32-3	3	42.42	0.00	0.00
	FA10-0.32-3	7	44.37	0	0
	FA10-0.32-3	28	67.9	0	0
	FA10-0.32-3	90	72.6	0	0
	FA10-0.32-3	360	83.41	0	0
24	FA10-0.34-3	7	44.93	39.84	34.48
	FA10-0.34-3	28	50.6	61.18	59.77
	FA10-0.34-3	180	66.86	54.27	61.53
	FA10-0.34-3	360	74.71	60.71	71.05
25	FA10-0.36-3	7	31.6	28.44	38.12
	FA10-0.36-3	28	57.19	56.14	54.75
	FA10-0.36-3	180	67.06	63.75	59.77
	FA10-0.36-3	360	71.03	64.44	61.49
26	FA10-0.42-3	7	28.16	29.78	27.81
	FA10-0.42-3	28	35.2	34.23	33.5
	FA10-0.42-3	180	39.07	39.02	35.51
	FA10-0.42-3	360	45.71	40.58	39.42
27	M10-0.35-2	1	3.4	4.1	4.2
	M10-0.35-2	3	33	38.34	36.82
	M10-0.35-2	7	45.77	37.74	39.13
	M10-0.35-2	28	54.75	51.86	53.14
	M10-0.35-2	360	68.28	66.3	60.64
28	M10-0.35-3	3	35.41	0	0
	M10-0.35-3	7	48.06	0	0
	M10-0.35-3	28	59.47	0	0
	M10-0.35-3	90	60.96	0	0
	M10-0.35-3	360	76.4	0	0


NO	Mixes	age (days)	compression (MPa)		
			Sample 1	Sample 2	Sample 3
29	M10-0.35-4	1	2.4	2.1	2.3
	M10-0.35-4	3	41.71	35.83	36.46
	M10-0.35-4	7	45.57	33.4	33.73
	M10-0.35-4	28	55.6	47.32	49.12
	M10-0.35-4	360	66.4	63.4	54.52
30	M10-0.35-6	1	2.09	1.81	2.09
	M10-0.35-6	3	35.45	35.11	33.54
	M10-0.35-6	7	41.92	29.39	33.39
	M10-0.35-6	28	39.94	46.46	37.15
	M10-0.35-6	360	53.08	65.19	0
31	M10-0.4-2	1	28.29	0	0
	M10-0.4-2	3	47.07	0	0
	M10-0.4-2	7	48.51	0	0
	M10-0.4-2	28	40.38	51.36	46.63
	M10-0.4-2	360	55.34	58.16	57.15
32	M10-0.4-3	3	38.23	0	0
	M10-0.4-3	7	45.16	0	0
	M10-0.4-3	28	55.33	0	0
	M10-0.4-3	90	61.25	0	0
	M10-0.4-3	360	66.76	0	0
33	M10-0.4-4	1	2.1	0	0
	M10-0.4-4	3	5.6	0	0
	M10-0.4-4	7	45	38	0
	M10-0.4-4	28	45.68	52.5	43.48
	M10-0.4-4	360	56.3	55.4	57.34
34	M10-0.4-6	1	7	0	0
	M10-0.4-6	3	11.33	0	0
	M10-0.4-6	7	30.1	0	0
	M10-0.4-6	28	33.63	34.43	40.6
	M10-0.4-6	360	54.15	0	0
35	M10-0.45-2	1	3.4	0	0
	M10-0.45-2	3	43.04	0	0
	M10-0.45-2	7	44.32	0	0
	M10-0.45-2	28	49.99	47.32	50.08
	M10-0.45-2	360	50.1	42.14	0
36	M10-0.45-3	7	38.64	34.66	29.65
	M10-0.45-3	28	41.1	41.64	40.2
	M10-0.45-3	180	59.51	48.84	51.69
	M10-0.45-3	360	63.5	48.57	56.84
37	M10-0.45-4	1	14.48	0	0
	M10-0.45-4	3	32.93	0	0

NO	Mixes	age (days)	compression (MPa)		
			Sample 1	Sample 2	Sample 3
	M10-0.45-4	7	33.16	0	0
	M10-0.45-4	28	43.95	48.5	50.24
	M10-0.45-4	360	41.8	56.85	0
38	M10-0.45-6	1	1.3	0	0
	M10-0.45-6	3	25.53	0	0
	M10-0.45-6	7	39.69	0	0
	M10-0.45-6	28	40.28	41.21	40.75
	M10-0.45-6	360	46	40.38	49.7
39	M10-0.35-3	3	35.41	0	0
	M10-0.35-3	7	48.06	0	0
	M10-0.35-3	28	59.47	0	0
	M10-0.35-3	90	60.96	0	0
	M10-0.35-3	360	76.4	0	0
40	M10-0.38-3	3	38.23	0	0
	M10-0.38-3	7	45.16	0	0
	M10-0.38-3	28	59.33	0	0
	M10-0.38-3	90	61.25	0	0
	M10-0.38-3	360	68.6	0	0
41	M10-0.4-3	3	38.23	0	0
	M10-0.4-3	7	45.16	0	0
	M10-0.4-3	28	55.33	0	0
	M10-0.4-3	90	61.25	0	0
	M10-0.4-3	360	66.76	0	0
42	M10-0.42-3	7	31.36	30.28	32.09
	M10-0.42-3	28	41.7	49.74	48.08
	M10-0.42-3	180	48.69	60.64	60.08
	M10-0.42-3	360	48.24	59.8	60.72
43	M10-0.45-3	7	33.23	30.85	24.02
	M10-0.45-3	28	36.98	41.13	46.8
	M10-0.45-3	180	52.96	42.98	42.39
	M10-0.45-3	360	54.61	41.28	47.75
44	M10-0.46-3	7	26.49	35.29	21.82
	M10-0.46-3	28	29.11	40.1	25.98
	M10-0.46-3	180	34.35	43.31	29.62
	M10-0.46-3	360	37.19	47.72	40.76
45	FA20-M10-0.35-3	7	44.8	34.65	46.61
	FA20-M10-0.35-3	28	50.34	40.76	56.16
	FA20-M10-0.35-3	180	59.9	46.87	60.65
	FA20-M10-0.35-3	360	68.29	50.62	60.65
46	FA20-M10-0.4-3	7	32.5	37.33	32.35
	FA20-M10-0.4-3	28	39.63	40.14	39.94

NO	Mixes	age (days)	compression (MPa)		
			Sample 1	Sample 2	Sample 3
	FA20-M10-0.4-3	180	40.42	44.96	43.53
	FA20-M10-0.4-3	360	44.87	47.21	53.11
47	FA20-M10-0.45-3	7	28.91	34.94	30.14
	FA20-M10-0.45-3	28	37.55	38.82	39.66
	FA20-M10-0.45-3	180	39.8	40.76	40.45
	FA20-M10-0.45-3	360	45.37	41.17	48.54
48	FA10-M10-0.3-3	3	37.14	0	0
	FA10-M10-0.3-3	7	50.01	0	0
	FA10-M10-0.3-3	28	65.17	0	0
	FA10-M10-0.3-3	90	68.01	0	0
	FA10-M10-0.3-3	360	69.37	0	0
49	FA10-M10-0.34-3	3	40.95	0	0
	FA10-M10-0.34-3	7	45.82	0	0
	FA10-M10-0.34-3	28	59.83	0	0
	FA10-M10-0.34-3	90	62.61	0	0
	FA10-M10-0.34-3	360	64.49	0	0
50	FA10-M10-0.38-3	3	37	0	0
	FA10-M10-0.38-3	7	48.23	0	0
	FA10-M10-0.38-3	28	58.12	0	0
	FA10-M10-0.38-3	90	69.94	0	0
	FA10-M10-0.38-3	360	78.33	0	0
51	NP-0.25-3	1	31.78	33.68	41.89
	NP-0.25-3	3	56.85	48.27	45.14
	NP-0.25-3	7	65.18	49.48	62.04
	NP-0.25-3	28	69.66	61.79	76.40
	NP-0.25-3	360	80.59	82.27	80.73
52	NP-0.32-3	1	20.53	17.55	12.05
	NP-0.32-3	3	33.42	25.19	26.87
	NP-0.32-3	7	61.05	45.96	49.14
	NP-0.32-3	28	66.78	73.97	53.94
	NP-0.32-3	360	67.25	74.33	54.47
53	NP-0.35-3	1	29.7	30.62	38.43
	NP-0.35-3	3	52.64	43.88	44.25
	NP-0.35-3	7	63.28	46.24	57.98
	NP-0.35-3	28	68.97	60.58	72.08
	NP-0.35-3	360	72.41	63.6	72.8
54	NP-0.4-3	1	23.04	26.97	32.2
	NP-0.4-3	3	38.66	36.93	39.84
	NP-0.4-3	7	42.05	50.43	41.78
	NP-0.4-3	28	46.33	60.02	54.57
	NP-0.4-3	360	60.69	63.49	58.66

NO	Mixes	age (days)	compression (MPa)		
			Sample 1	Sample 2	Sample 3
55	NP-0.45-3	1	16.42	14.39	10.72
	NP-0.45-3	3	27.07	20.4	23.38
	NP-0.45-3	7	52.5	39.53	42.75
	NP-0.45-3	28	60.1	58.5	45.31
	NP-0.45-3	360	62.43	64.09	65.11
	56	NP-0.5-3	1	22.95	28.2
NP-0.5-3		3	41.01	36.64	37.71
NP-0.5-3		7	41.03	43.56	43.38
NP-0.5-3		28	44.96	48.72	53.08
NP-0.5-3		360	51.23	56.4	64.95
57		NC-0.4-0	1	22.53	24.56
	NC-0.4-0	3	32.15	36.98	34.76
	NC-0.4-0	7	36.55	51.36	50.5
	NC-0.4-0	28	49.5	54.28	45.16
	NC-0.4-0	360	0	60.2	0
	58	NC-0.5-0	1	16.6	0
NC-0.5-0		3	26.72	0	0
NC-0.5-0		7	50.7	0	0
NC-0.5-0		28	53.5	0	0
NC-0.5-0		360	58.18	56.7	55.7

Appendix C-1. ATENA Input

	Description:	beam 3d	Unit system:	Metric	side 1
	Note:	3d			
ANALYSIS INFORMATION					
Property		Value			
Description		beam 3d			
Note		3d			
Unit system		Metric			
Solver type		standard			
Run		geometrically nonlinear			
MATERIALS					
Property		MATERIAL 1			
Title		3D Nonlinear Cementitious 2			
Type		CC3DNonLinCementitious2			
Elastic modulus E [MPa]		3.927E+04			
Poisson's ratio μ [-]		0.200			
Specific material weight ρ [MN/m ³]		2.300E-02			
Coefficient of thermal expansion α [1/K]		1.200E-05			
Tensile strength F_t [MPa]		3.678E+00			
Compressive strength F_c [MPa]		-5.100E+01			
Specific fracture energy G_f [MN/m]		9.196E-05			
Critical compressive displacement W_d [m]		-5.000E-04			
Exc.,def. the shape of fail.surface ϵ [-]		0.520			
Multiplier for the direction of the pl.flow β [-]		0.000			
Fixed crack model coefficient [-]		1.000			
Plastic strain at compressive strength ϵ_{cp} [-]		-1.299E-03			
Onset of non-linear behavior in compression F_{c0} [MPa]		-7.724E+00			
Property		MATERIAL 2			
Title		Reinforcement			
Type		CCReinforcement			
Elastic modulus E [MPa]		2.100E+05			
Specific material weight ρ [MN/m ³]		7.850E-02			
Coefficient of thermal expansion α [1/K]		1.200E-05			
Reinf. type		Linear			
CONSTRUCTION CASES					
Number	Title				
1	Construction case 1				
MACRO-ELEMENTS					
MACROELEMENT 1					
MACROELEMENT 1 - JOINTS					
Number	X [m]	Y [m]	Z [m]		
1	0.0000	0.0000	0.0000	0.0000	
2	0.1000	0.0000	0.0000	0.0000	
3	1.8000	0.0000	0.0000	0.0000	

[Atena - 3D (demo version) | version 1.2.14.0 | (c)Cervenka Consulting 2007 | www.cervenka.cz]

C	Description:	beam 3d	Unit system:	Metric	side 2
	Note:	3d			


MACROELEMENT 1 - JOINTS				
Number	X [m]	Y [m]	Z [m]	
4	1.9000	0.0000	0.0000	0.0000
5	1.9000	0.0000	0.0000	0.2500
6	1.2000	0.0000	0.0000	0.2500
7	0.7000	0.0000	0.0000	0.2500
8	0.0000	0.0000	0.0000	0.2500
9	0.0000	0.1500	0.0000	0.0000
10	0.1000	0.1500	0.0000	0.0000
11	1.8000	0.1500	0.0000	0.0000
12	1.9000	0.1500	0.0000	0.0000
13	1.9000	0.1500	0.0000	0.2500
14	1.2000	0.1500	0.0000	0.2500
15	0.7000	0.1500	0.0000	0.2500
16	0.0000	0.1500	0.0000	0.2500


MAKROELEMENT 1 - LINES					
Number	Joint at the beg.	Joint at the end	Number	Joint at the beg.	Joint at the end
1	1	2	13	13	14
2	2	3	14	14	15
3	3	4	15	15	16
4	4	5	16	16	9
5	5	6	17	1	9
6	6	7	18	8	16
7	7	8	19	4	12
8	8	1	20	5	13
9	9	10	21	3	11
10	10	11	22	2	10
11	11	12	23	6	14
12	12	13	24	7	15

MAKROELEMENT 1 - SURFACES	
Number	List of boundary lines
1	1-8
2	9-16
3	1-3,19,11,10,9,17
4	4,19,12,20
5	5-7,18,15,14,13,20
6	8,18,16-17

MACROELEMENT 1 - PROPERTIES					
Type of macroelement standard, azimuth = 0.00°, zenith = 0.00°					
CS	Used	Material			
1	Yes	Ident Basic	Material 3D Nonlinear Cementitious 2	Ratio [%]	Direction

CONTACTS
BAR REINFORCEMENT
BAR REINFORCEMENT 1

	Description:	beam 3d	Unit system:	Metric	side 3
	Note:	3d			
BAR REINFORCEMENT 1 - POINTS					
Number	X [m]	Y [m]	Z [m]		
1	0.0000	0.0300	0.0300		
2	1.9000	0.0300	0.0300		
BAR REINFORCEMENT 1 - SEGMENTS					
Number	Start point	End point	Number	Start point	End point
1	1	2			
BAR REINFORCEMENT 1 - PROPERTIES					
CS	Used	Material	Area [m ²]	Bond with surrounding material	
1	Yes	Reinforcement	1.131E-04	Connection type	perfect connection
BAR REINFORCEMENT 2					
BAR REINFORCEMENT 2 - POINTS					
Number	X [m]	Y [m]	Z [m]		
1	0.0000	0.1200	0.0300		
2	1.9000	0.1200	0.0300		
BAR REINFORCEMENT 2 - SEGMENTS					
Number	Start point	End point	Number	Start point	End point
1	1	2			
BAR REINFORCEMENT 2 - PROPERTIES					
CS	Used	Material	Area [m ²]	Bond with surrounding material	
1	Yes	Reinforcement	1.131E-04	Connection type	perfect connection
EXTERNAL CABLES					
JOINT SPRINGS					
LINE SPRINGS					
SURFACE SPRINGS					
LOAD CASES - OVERVIEW					
LOAD CASE LIST					
Number	Title	Code	Coeff.[-]		
1	Body force - LC 1	Body force	1.000		
2	Supports - LC 2	Supports			
3	Forces - LC 3	Forces	1.000		
LC 1 - BODY FORCE - LC 1					
BODY FORCE					
Dir: (0.0000; 0.0000; -1.0000)					
Macroelements:					
Reinforcement bars:					
External cables:					
LC 2 - SUPPORTS - LC 2					

	Description:	beam 3d	Unit system:	Metric	side 4
	Note:	3d			

LINE SUPPORTS

Macro. / line	Coordinate system	Support in dir. of the axis		
		X	Y	Z
1/21	Global	fixed	fixed	fixed
1/22	Global	fixed	fixed	fixed

LC 3 - FORCES - LC 3

LINE FORCE LOADING

Macro. / line	Loading type	Value [MN/m]	Force direction	
			Coord. system	Orientation
1/23	continuous constant - along length	-5.000E-03	Global	Zg
1/24	continuous constant - along length	-5.000E-03	Global	Zg

SOLUTION PARAMETERS

SOLUTION PARAMETERS 1

Property	Value
Title	Standard Newton-Raphson
Method	Newton-Raphson (line search)
Iteration limit	40
Displacement Error	0.010000
Residual Error	0.010000
Absolute Residual Error	0.010000
Energy Error	0.000100
Optimize band-width	Sloan
Line Search	Yes
LS Type	With iterations
LS Unbalanced energy limit	0.800
LS Line search iteration limit	2
LS Minimum Eta	0.010
LS Maximum Eta	1.000
Update Stiffness	Each iteration
Stiffness Type	Tangent
Immediate Displacement Error Multiple	10000.0
After Step Displacement Error Multiple	1000.0
Immediate Residual Error Multiple	10000.0
After Step Residual Error Multiple	1000.0
Immediate Absolute Residual Error Multiple	10000.0
After Step Absolute Residual Error Multiple	1000.0
Immediate Energy Error Multiple	1000000.0
After Step Energy Error Multiple	10000.0

SOLUTION PARAMETERS 2

Property	Value
Title	Standard Arc Length
Method	Arc length (line search)
Arc Length Method	Consistently linearised
A-L Adjustment Method	Constant
A-L Load-Displacement Ratio	0.200
A-L Load-Displacement Method	Bergan constant
A-L Reference number of iterations	10
A-L Step-Length	Based on current load step
A-L Location	All nodes


[Alena - 3D (demo) version] | version 1.2.14.0 | ©Cervenka Consulting 2007 | www.cervenka.cz

C	Description:	beam 3d	Unit system:	Metric	side 5
	Note:	3d			

SOLUTION PARAMETERS 2	
Property	Value
Iteration limit	40
Displacement Error	0.010000
Residual Error	0.010000
Absolute Residual Error	0.010000
Energy Error	0.000100
Optimize band-width	Sloan
Line Search	Yes
LS Type	With iterations
LS Unbalanced energy limit	0.800
LS Line search iteration limit	2
LS Minimum Eta	0.010
LS Maximum Eta	1.000
Update Stiffness	Each iteration
Stiffness Type	Tangent
Immediate Displacement Error Multiple	10000.0
After Step Displacement Error Multiple	1000.0
Immediate Residual Error Multiple	10000.0
After Step Residual Error Multiple	1000.0
Immediate Absolute Residual Error Multiple	10000.0
After Step Absolute Residual Error Multiple	1000.0
Immediate Energy Error Multiple	1000000.0
After Step Energy Error Multiple	10000.0


ANALYSIS STEPS				
Number	Load cases	Phase	Solution Parameters	Coefficient [-]
1	1-3	(1) Construction case 1	Standard Newton-Raphson	1.000
2	1-3	(1) Construction case 1	Standard Newton-Raphson	1.000
3	1-3	(1) Construction case 1	Standard Newton-Raphson	1.000
4	1-3	(1) Construction case 1	Standard Newton-Raphson	1.000
5	1-3	(1) Construction case 1	Standard Newton-Raphson	1.000
6	1-3	(1) Construction case 1	Standard Newton-Raphson	1.000
7	1-3	(1) Construction case 1	Standard Newton-Raphson	1.000
8	1-3	(1) Construction case 1	Standard Newton-Raphson	1.000
9	1-3	(1) Construction case 1	Standard Newton-Raphson	1.000
10	1-3	(1) Construction case 1	Standard Newton-Raphson	1.000
11	1-3	(1) Construction case 1	Standard Newton-Raphson	1.000
12	1-3	(1) Construction case 1	Standard Newton-Raphson	1.000
13	1-3	(1) Construction case 1	Standard Newton-Raphson	1.000
14	1-3	(1) Construction case 1	Standard Newton-Raphson	1.000
15	1-3	(1) Construction case 1	Standard Newton-Raphson	1.000
16	1-3	(1) Construction case 1	Standard Newton-Raphson	1.000
17	1-3	(1) Construction case 1	Standard Newton-Raphson	1.000
18	1-3	(1) Construction case 1	Standard Newton-Raphson	1.000
19	1-3	(1) Construction case 1	Standard Newton-Raphson	1.000
20	1-3	(1) Construction case 1	Standard Newton-Raphson	1.000
21	1-3	(1) Construction case 1	Standard Newton-Raphson	1.000
22	1-3	(1) Construction case 1	Standard Newton-Raphson	1.000
23	1-3	(1) Construction case 1	Standard Newton-Raphson	1.000
24	1-3	(1) Construction case 1	Standard Newton-Raphson	1.000
25	1-3	(1) Construction case 1	Standard Newton-Raphson	1.000

[Atena - 3D (demo version) | version 1.2.14.0 | ©Oerwenka Consulting 2007 | www.oerwenka.cz]

	Description:	beam 3d	Unit system:	Metric	side 6
	Note:	3d			

Number	Load cases	Phase	Solution Parameters	Coefficient [-]
26	1-3	(1) Construction case 1	Standard Newton-Raphson	1.000
27	1-3	(1) Construction case 1	Standard Newton-Raphson	1.000
28	1-3	(1) Construction case 1	Standard Newton-Raphson	1.000
29	1-3	(1) Construction case 1	Standard Newton-Raphson	1.000
30	1-3	(1) Construction case 1	Standard Newton-Raphson	1.000
31	1-3	(1) Construction case 1	Standard Newton-Raphson	1.000
32	1-3	(1) Construction case 1	Standard Newton-Raphson	1.000
33	1-3	(1) Construction case 1	Standard Newton-Raphson	1.000
34	1-3	(1) Construction case 1	Standard Newton-Raphson	1.000
35	1-3	(1) Construction case 1	Standard Newton-Raphson	1.000
36	1-3	(1) Construction case 1	Standard Newton-Raphson	1.000
37	1-3	(1) Construction case 1	Standard Newton-Raphson	1.000
38	1-3	(1) Construction case 1	Standard Newton-Raphson	1.000
39	1-3	(1) Construction case 1	Standard Newton-Raphson	1.000
40	1-3	(1) Construction case 1	Standard Newton-Raphson	1.000
41	1-3	(1) Construction case 1	Standard Newton-Raphson	1.000
42	1-3	(1) Construction case 1	Standard Newton-Raphson	1.000
43	1-3	(1) Construction case 1	Standard Newton-Raphson	1.000
44	1-3	(1) Construction case 1	Standard Newton-Raphson	1.000
45	1-3	(1) Construction case 1	Standard Newton-Raphson	1.000
46	1-3	(1) Construction case 1	Standard Newton-Raphson	1.000
47	1-3	(1) Construction case 1	Standard Newton-Raphson	1.000
48	1-3	(1) Construction case 1	Standard Newton-Raphson	1.000
49	1-3	(1) Construction case 1	Standard Newton-Raphson	1.000
50	1-3	(1) Construction case 1	Standard Newton-Raphson	1.000
51	1-3	(1) Construction case 1	Standard Newton-Raphson	1.000
52	1-3	(1) Construction case 1	Standard Newton-Raphson	1.000
53	1-3	(1) Construction case 1	Standard Newton-Raphson	1.000
54	1-3	(1) Construction case 1	Standard Newton-Raphson	1.000
55	1-3	(1) Construction case 1	Standard Newton-Raphson	1.000
56	1-3	(1) Construction case 1	Standard Newton-Raphson	1.000
57	1-3	(1) Construction case 1	Standard Newton-Raphson	1.000
58	1-3	(1) Construction case 1	Standard Newton-Raphson	1.000
59	1-3	(1) Construction case 1	Standard Newton-Raphson	1.000
60	1-3	(1) Construction case 1	Standard Newton-Raphson	1.000
61	1-3	(1) Construction case 1	Standard Newton-Raphson	1.000
62	1-3	(1) Construction case 1	Standard Newton-Raphson	1.000
63	1-3	(1) Construction case 1	Standard Newton-Raphson	1.000
64	1-3	(1) Construction case 1	Standard Newton-Raphson	1.000
65	1-3	(1) Construction case 1	Standard Newton-Raphson	1.000
66	1-3	(1) Construction case 1	Standard Newton-Raphson	1.000
67	1-3	(1) Construction case 1	Standard Newton-Raphson	1.000
68	1-3	(1) Construction case 1	Standard Newton-Raphson	1.000
69	1-3	(1) Construction case 1	Standard Newton-Raphson	1.000
70	1-3	(1) Construction case 1	Standard Newton-Raphson	1.000
71	1-3	(1) Construction case 1	Standard Newton-Raphson	1.000
72	1-3	(1) Construction case 1	Standard Newton-Raphson	1.000
73	1-3	(1) Construction case 1	Standard Newton-Raphson	1.000
74	1-3	(1) Construction case 1	Standard Newton-Raphson	1.000
75	1-3	(1) Construction case 1	Standard Newton-Raphson	1.000
76	1-3	(1) Construction case 1	Standard Newton-Raphson	1.000

Alaris - 3D (beta version) | version 1.2.14.0 | ©Cervenka Consulting 2007 | www.cervenka.cz

	Description:	beam 3d	Unit system:	Metric	side 7
	Note:	3d			


Number	Load cases	Phase	Solution Parameters	Coefficient [-]
77	1-3	(1) Construction case 1	Standard Newton-Raphson	1.000
78	1-3	(1) Construction case 1	Standard Newton-Raphson	1.000
79	1-3	(1) Construction case 1	Standard Newton-Raphson	1.000
80	1-3	(1) Construction case 1	Standard Newton-Raphson	1.000

MONITORING POINTS

Number	Title	Type Location	Quantity - item
1	lendutan	Value at node Macroelement 1, point (0.9500; 0.0000; 0.0000) [m]	Displacements - Component 1
2	reaksi	Value at node Macroelement 1, point (0.1000; 0.0000; 0.0000) [m]	Reactions - Component 1

Appendix C-2. ATENA Output

Output of the following table only include crack attributes in step 15 as initial crack and step 80 as final crack.

	Description: Note:	beam 3d 3d	Unit system:	Metric				
ANALYSIS STEP 15								
POSITION: ELEMENTS								
MACROELEMENT 1 - CRACK ATTRIBUTES (TBL.1/2)								
Element Crack Attributes								
Group	Elem.	N.cracks [-]	Dim [-]	N.attr [-]	N1(1) [m]	N1(2) [m]	N1(3) [m]	Size1 [m]
1	11	1	3	4	9.981E-01	6.063E-02	-1.000E-02	6.061E-02
1	89	1	3	4	9.980E-01	5.905E-02	2.363E-02	6.060E-02
MACROELEMENT 1 - CRACK ATTRIBUTES (TBL.2/2)								
Element Crack Attributes								
Group	Elem.	Cod1 [m]		Sig N1 [MPa]		Sig T1 [MPa]		
1	11	3.447E-06		3.053E+00		3.504E-03		
1	89	8.935E-09		3.676E+00		1.101E-02		
BAR REINFORCEMENT 1 - CRACK ATTRIBUTES								
Element Crack Attributes								
No values have been found.								
BAR REINFORCEMENT 2 - CRACK ATTRIBUTES								
Element Crack Attributes								
No values have been found.								
ANALYSIS STEP 80								
POSITION: ELEMENTS								
MACROELEMENT 1 - CRACK ATTRIBUTES (TBL.1/3)								
Element Crack Attributes								
Group	Elem.	N.cracks [-]	Dim [-]	N.attr [-]	N1(1) [m]	N1(2) [m]	N1(3) [m]	Size1 [m]
1	1	1	3	4	3.076E-01	3.196E-02	9.510E-01	5.941E-02
1	2	1	3	4	-2.989E-01	2.641E-01	9.170E-01	5.737E-02
1	4	1	3	4	-7.235E-02	-6.789E-02	9.951E-01	6.220E-02
1	9	1	3	4	9.779E-01	2.835E-02	-2.072E-01	5.944E-02
1	10	2	3	4	9.716E-01	2.342E-01	-3.511E-02	5.905E-02
1	11	1	3	4	9.981E-01	6.047E-02	-1.019E-02	6.068E-02
1	12	1	3	4	8.839E-01	-4.338E-01	-1.746E-01	5.371E-02
1	13	2	3	4	9.711E-01	-2.376E-01	2.190E-02	5.901E-02
1	14	1	3	4	9.709E-01	-3.367E-02	2.370E-01	5.901E-02
1	32	1	3	4	9.643E-01	-1.366E-01	-2.268E-01	5.630E-02
1	34	1	3	4	8.874E-01	-1.478E-01	-4.366E-01	4.447E-02
1	35	1	3	4	7.199E-01	-3.690E-01	5.878E-01	4.668E-02
1	38	1	3	4	3.461E-01	9.139E-01	-2.122E-01	5.203E-02
1	42	1	3	4	-5.094E-01	7.137E-01	4.808E-01	4.598E-02
1	43	2	3	4	-2.525E-01	5.510E-01	7.954E-01	5.772E-02
1	45	1	3	4	1.872E-01	5.031E-01	8.437E-01	5.868E-02
1	46	1	3	4	4.365E-01	6.875E-01	6.032E-01	5.137E-02
1	53	1	3	4	3.454E-01	7.290E-01	5.910E-01	6.890E-02
1	55	1	3	4	-2.755E-01	9.558E-01	-1.027E-01	3.257E-02
1	56	2	3	4	-4.079E-01	9.063E-01	-1.101E-01	2.768E-02
1	57	1	3	4	3.391E-01	9.327E-01	-1.230E-01	3.116E-02
1	59	1	3	4	-3.957E-01	6.560E-01	6.427E-01	7.007E-02
1	60	1	3	4	-3.461E-01	5.090E-01	7.881E-01	6.898E-02
1	65	1	3	4	-2.460E-01	8.928E-02	9.652E-01	6.030E-02

(Atena - 3D (denovo) version 1.2.14.0) (c)Cemventis Consulting 2007 | www.cemventis.cz

	Description:	beam 3d	Unit system:	Metric
	Note:	3d		

MACROELEMENT 1 - CRACK ATTRIBUTES (TBL.1/3)								
Element Crack Attributes								
Group	Elem.	N.cracks [-]	Dim [-]	N.attr [-]	N1(1) [m]	N1(2) [m]	N1(3) [m]	Size1 [m]
1	66	1	3	4	3.054E-01	-2.364E-01	9.224E-01	5.771E-02
1	68	1	3	4	5.240E-02	8.334E-02	9.951E-01	6.221E-02
1	81	1	3	4	9.751E-01	-1.190E-01	1.872E-01	5.692E-02
1	87	1	3	4	8.945E-01	3.049E-01	3.269E-01	5.439E-02
1	88	2	3	4	9.725E-01	2.315E-01	2.358E-02	5.911E-02
1	89	1	3	4	9.980E-01	5.890E-02	2.412E-02	6.066E-02
1	90	2	3	4	9.325E-01	-3.431E-01	1.128E-01	5.668E-02
1	91	2	3	4	9.604E-01	-2.721E-01	-6.021E-02	5.837E-02
1	92	1	3	4	8.681E-01	-3.702E-01	-3.307E-01	5.278E-02
1	97	1	3	4	8.912E-01	-1.148E-01	4.388E-01	4.464E-02
1	98	1	3	4	7.101E-01	-4.217E-01	-5.638E-01	4.322E-02
1	99	1	3	4	9.393E-01	1.063E-01	3.264E-01	4.316E-02
1	106	1	3	4	-3.358E-01	9.417E-01	1.879E-02	3.797E-02
1	107	2	3	4	4.056E-01	9.139E-01	1.385E-02	3.397E-02
1	108	1	3	4	3.111E-01	9.504E-01	-4.114E-03	3.944E-02
1	110	1	3	4	-3.815E-01	7.133E-01	-5.879E-01	6.860E-02
1	111	1	3	4	3.643E-01	-4.552E-01	8.125E-01	6.852E-02
1	116	1	3	4	3.763E-01	8.999E-01	2.202E-01	5.230E-02
1	121	2	3	4	2.096E-01	-4.225E-01	8.818E-01	6.176E-02
1	122	1	3	4	2.791E-02	-6.424E-01	7.659E-01	4.873E-02
1	123	2	3	4	-2.437E-01	-4.468E-01	8.609E-01	6.154E-02
1	131	1	3	4	-6.633E-01	9.192E-02	7.426E-01	4.752E-02
1	132	1	3	4	6.723E-01	7.381E-03	7.402E-01	4.764E-02
1	133	1	3	4	8.802E-01	-9.451E-02	4.651E-01	2.560E-02
1	135	1	3	4	8.710E-01	-1.598E-01	-4.645E-01	2.782E-02
1	140	1	3	4	7.208E-01	-1.759E-01	-6.704E-01	4.910E-02
1	141	1	3	4	9.179E-01	-1.832E-01	-3.520E-01	5.584E-02
1	142	2	3	4	9.200E-01	-2.142E-01	-3.283E-01	5.593E-02
1	143	1	3	4	1.681E-01	-5.791E-01	7.977E-01	5.503E-02
1	144	2	3	4	9.297E-01	2.591E-01	2.616E-01	5.652E-02
1	145	2	3	4	9.131E-01	1.716E-01	3.699E-01	5.555E-02
1	146	1	3	4	7.210E-01	2.614E-01	6.418E-01	5.052E-02
1	153	1	3	4	7.346E-01	-1.504E-01	6.616E-01	4.761E-02
1	154	1	3	4	9.137E-01	-1.907E-01	3.588E-01	5.558E-02
1	155	2	3	4	9.254E-01	-1.981E-01	3.232E-01	5.625E-02
1	156	2	3	4	-4.867E-01	6.802E-01	5.482E-01	4.924E-02
1	157	2	3	4	9.376E-01	2.372E-01	-2.541E-01	5.701E-02
1	158	1	3	4	9.319E-01	1.665E-01	-3.223E-01	5.669E-02
1	159	1	3	4	7.524E-01	2.965E-01	-5.883E-01	4.851E-02
1	164	1	3	4	-4.268E-02	1.012E-01	9.940E-01	4.143E-02
1	165	1	3	4	-7.174E-02	3.850E-02	9.967E-01	4.155E-02
1	199	1	3	4	6.387E-02	-1.613E-02	9.978E-01	4.160E-02
1	200	1	3	4	4.394E-02	-7.570E-02	9.962E-01	4.152E-02
1	201	1	3	4	8.891E-01	3.687E-01	2.713E-01	6.956E-02
1	202	1	3	4	-2.086E-01	2.769E-01	9.380E-01	2.994E-02
1	206	1	3	4	4.098E-01	-2.804E-01	8.680E-01	3.432E-02
1	207	1	3	4	-5.635E-01	4.269E-02	8.250E-01	4.846E-02
1	225	2	3	4	6.932E-02	3.849E-01	9.204E-01	7.610E-02
1	227	1	3	4	-1.397E-01	-3.517E-02	9.896E-01	7.154E-02


	Description:	beam 3d	Unit system:	Metric
	Note:	3d		

MACROELEMENT 1 - CRACK ATTRIBUTES (TBL.1/3)

Element Crack Attributes								
Group	Elem.	N.cracks [-]	Dim [-]	N.attr [-]	N1(1) [m]	N1(2) [m]	N1(3) [m]	Size1 [m]
1	233	1	3	4	3.871E-01	-2.825E-02	9.216E-01	5.937E-02
1	234	1	3	4	4.143E-01	1.731E-01	8.935E-01	6.789E-02
1	236	1	3	4	-1.936E-01	-4.273E-01	8.832E-01	6.160E-02
1	237	1	3	4	-3.171E-01	-1.310E-01	9.393E-01	6.409E-02
1	238	1	3	4	1.815E-01	-4.157E-01	8.912E-01	6.229E-02
1	240	1	3	4	-4.583E-01	1.456E-01	8.768E-01	6.640E-02
1	241	1	3	4	-3.766E-01	8.820E-02	9.222E-01	6.163E-02
1	244	1	3	4	9.852E-01	-6.350E-02	1.590E-01	1.822E-02
1	247	1	3	4	-4.702E-01	-2.534E-01	8.454E-01	3.382E-02
1	248	1	3	4	9.786E-01	7.041E-02	-1.932E-01	4.178E-02
1	256	1	3	4	7.902E-01	4.744E-01	3.879E-01	7.346E-02
1	258	1	3	4	9.124E-01	3.046E-01	-2.734E-01	6.841E-02
1	259	1	3	4	4.121E-01	2.645E-01	8.719E-01	3.260E-02
1	260	1	3	4	2.011E-01	-2.289E-01	9.525E-01	2.844E-02
1	264	1	3	4	-4.628E-01	3.160E-01	8.283E-01	3.514E-02
1	265	1	3	4	6.254E-01	4.578E-02	7.790E-01	4.809E-02
1	275	1	3	4	8.104E-01	4.301E-01	-3.977E-01	7.321E-02
1	276	1	3	4	9.899E-01	-2.224E-02	-1.398E-01	1.944E-02
1	281	1	3	4	2.585E-01	-8.812E-02	9.620E-01	6.637E-02
1	282	1	3	4	-3.170E-01	-1.782E-02	9.482E-01	6.040E-02
1	283	1	3	4	-2.665E-01	-2.272E-01	9.367E-01	7.009E-02
1	284	1	3	4	4.599E-01	1.296E-01	8.784E-01	5.620E-02
1	294	1	3	4	-6.897E-02	5.929E-02	9.959E-01	6.856E-02
1	295	1	3	4	1.197E-01	8.595E-01	4.970E-01	7.184E-02
1	296	1	3	4	8.032E-02	4.089E-02	9.959E-01	6.858E-02
1	305	1	3	4	7.643E-01	-3.990E-02	-6.437E-01	4.650E-02
1	306	1	3	4	9.158E-01	-6.458E-02	-3.964E-01	5.573E-02
1	307	2	3	4	9.268E-01	-5.896E-02	-3.708E-01	5.636E-02
1	309	1	3	4	9.253E-01	1.995E-02	3.788E-01	5.625E-02
1	310	1	3	4	9.083E-01	2.512E-02	4.176E-01	5.526E-02
1	311	1	3	4	7.566E-01	8.651E-02	6.481E-01	4.604E-02
1	325	1	3	4	5.338E-01	-2.000E-01	8.217E-01	5.349E-02
1	330	1	3	4	6.746E-01	2.549E-01	6.928E-01	3.798E-02
1	332	1	3	4	-1.117E-01	9.937E-01	5.141E-03	7.454E-02
1	342	1	3	4	7.124E-01	2.780E-01	-6.444E-01	4.090E-02
1	343	1	3	4	-5.207E-01	2.609E-01	8.129E-01	5.019E-02
1	348	1	3	4	6.736E-01	4.982E-03	7.391E-01	5.841E-02


MACROELEMENT 1 - CRACK ATTRIBUTES (TBL.2/3)

Element Crack Attributes								
Group	Elem.	Cod1 [m]	Sig N1 [MPa]	Sig T1 [MPa]	N2(1) [m]	N2(2) [m]	N2(3) [m]	Size2 [m]
1	1	1.743E-05	1.520E+00	8.554E-01				
1	2	2.307E-05	1.208E+00	6.084E-01				
1	4	3.470E-05	8.399E-01	9.049E-01				
1	9	6.557E-05	4.331E-01	9.047E-01				
1	10	1.254E-04	3.678E-03	4.248E-02	-2.068E-01	7.670E-01	-6.074E-01	6.852E-02
1	11	1.668E-04	3.678E-03	6.424E-02				
1	12	1.400E-04	3.678E-03	1.189E-02				
1	13	1.154E-04	6.250E-02	4.354E-01	1.976E-01	7.495E-01	-6.318E-01	6.740E-02

	Description:	beam 3d	Unit system:	Metric
	Note:	3d		

MACROELEMENT 1 - CRACK ATTRIBUTES (TBL.2/3)								
Element Crack Attributes								
Group	Elem.	Cod1 [m]	Sig N1 [MPa]	Sig T1 [MPa]	N2(1) [m]	N2(2) [m]	N2(3) [m]	Size2 [m]
1	14	4.736E-05	6.298E-01	1.157E+00				
1	32	8.678E-06	2.275E+00	1.973E-01				
1	34	1.258E-04	1.115E-02	1.079E-01				
1	35	6.775E-05	4.191E-01	6.961E-01				
1	38	8.350E-06	2.355E+00	3.472E-01				
1	42	2.254E-05	1.229E+00	1.101E+00				
1	43	9.030E-05	1.987E-01	1.273E+00	1.947E-01	-7.763E-01	5.996E-01	7.830E-02
1	45	9.401E-05	1.938E-01	1.426E+00				
1	46	1.517E-05	1.681E+00	9.505E-01				
1	53	1.105E-05	2.053E+00	1.727E-01				
1	55	1.840E-05	1.457E+00	6.487E-01				
1	56	2.951E-05	9.378E-01	7.628E-01	-1.216E-02	1.152E-01	9.933E-01	6.644E-02
1	57	2.521E-05	1.117E+00	8.457E-01				
1	59	1.627E-05	1.600E+00	1.083E-01				
1	60	2.879E-06	3.148E+00	2.426E-02				
1	65	1.096E-05	2.062E+00	5.164E-01				
1	66	2.151E-05	1.282E+00	5.883E-01				
1	68	3.589E-05	8.152E-01	1.200E+00				
1	81	1.076E-05	2.031E+00	2.820E-01				
1	87	3.996E-05	7.327E-01	1.808E+00				
1	88	1.315E-04	3.678E-03	4.010E-02	-2.098E-01	8.284E-01	5.194E-01	6.333E-02
1	89	1.367E-04	3.678E-03	4.770E-02				
1	90	1.680E-04	3.678E-03	2.723E-02	1.240E-01	5.975E-01	7.922E-01	7.188E-02
1	91	1.445E-04	3.678E-03	4.341E-02	2.649E-01	8.239E-01	5.011E-01	6.196E-02
1	92	3.013E-05	9.438E-01	1.491E+00				
1	97	1.011E-04	1.439E-01	7.257E-01				
1	98	5.668E-05	5.236E-01	6.632E-01				
1	99	7.730E-07	3.527E+00	2.044E-01				
1	106	3.450E-05	8.442E-01	8.129E-01				
1	107	3.989E-05	7.183E-01	8.881E-01	8.734E-03	-1.902E-02	9.998E-01	6.376E-02
1	108	2.350E-05	1.189E+00	8.627E-01				
1	110	5.670E-06	2.711E+00	1.820E-02				
1	111	2.842E-07	3.622E+00	2.345E-02				
1	116	8.281E-06	2.364E+00	3.035E-01				
1	121	6.852E-05	3.888E-01	1.145E+00	1.908E-01	-8.668E-01	-4.607E-01	7.279E-02
1	122	1.912E-05	3.960E-01	5.802E-01				
1	123	1.045E-04	9.899E-02	9.464E-01	-2.161E-01	-8.404E-01	-4.971E-01	7.562E-02
1	131	1.339E-05	1.831E+00	7.129E-01				
1	132	1.607E-05	1.616E+00	3.701E-01				
1	133	6.696E-05	4.266E-01	5.508E-01				
1	135	8.734E-05	2.454E-01	5.612E-01				
1	140	4.204E-05	7.037E-01	1.662E+00				
1	141	1.691E-04	3.678E-03	2.939E-02				
1	142	1.422E-04	3.678E-03	3.009E-02	-1.228E-01	6.380E-01	-7.602E-01	5.120E-02
1	143	2.475E-05	3.466E-01	6.980E-01				
1	144	1.184E-04	2.112E-02	1.034E-01	5.738E-02	5.999E-01	-7.980E-01	5.159E-02
1	145	1.475E-04	3.678E-03	2.684E-02	1.633E-01	6.773E-01	-7.173E-01	4.958E-02
1	146	4.329E-05	6.836E-01	1.760E+00				
1	153	3.819E-05	7.647E-01	1.363E+00				

[Atena - 3D (demo version) | version 1.2.14.01 | (c)Cervenka Consulting 2007 | www.cervenka.cz]

	Description:	beam 3d	Unit system:	Metric
	Note:	3d		

MACROELEMENT 1 - CRACK ATTRIBUTES (TBL.2/3)


Element Crack Attributes								
Group	Elem.	Cod1 [m]	Sig N1 [MPa]	Sig T1 [MPa]	N2(1) [m]	N2(2) [m]	N2(3) [m]	Size2 [m]
1	154	1.401E-04	3.678E-03	8.645E-03				
1	155	1.199E-04	1.417E-02	1.182E-01	1.356E-01	-6.232E-01	-7.702E-01	5.221E-02
1	156	1.313E-06	6.508E-01	9.164E-01	7.463E-01	-2.304E-03	6.656E-01	4.532E-02
1	157	1.456E-04	3.678E-03	2.443E-02	4.941E-02	6.325E-01	7.730E-01	4.981E-02
1	158	1.634E-04	3.678E-03	2.314E-02				
1	159	3.959E-05	7.422E-01	1.449E+00				
1	164	3.379E-05	8.586E-01	1.344E+00				
1	165	3.362E-05	8.631E-01	1.050E+00				
1	199	3.058E-05	9.402E-01	8.363E-01				
1	200	3.075E-05	9.356E-01	1.166E+00				
1	201	4.455E-05	6.724E-01	1.005E+00				
1	202	1.362E-05	1.810E+00	8.472E-02				
1	206	1.668E-05	1.571E+00	1.348E+00				
1	207	1.106E-05	2.053E+00	7.332E-01				
1	225	6.971E-05	4.005E-01	1.451E+00	6.068E-02	-9.225E-01	3.812E-01	6.920E-02
1	227	3.695E-05	7.944E-01	9.685E-01				
1	233	6.583E-06	2.583E+00	8.061E-02				
1	234	4.173E-06	2.937E+00	8.379E-02				
1	236	4.326E-06	2.913E+00	1.071E-01				
1	237	5.489E-05	5.487E-01	2.158E-01				
1	238	1.777E-05	1.498E+00	3.889E-01				
1	240	1.285E-05	1.879E+00	1.620E-01				
1	241	6.464E-06	2.600E+00	5.498E-02				
1	244	2.308E-06	3.246E+00	5.130E-01				
1	247	1.551E-05	1.657E+00	6.841E-01				
1	248	2.559E-06	3.203E+00	5.319E-01				
1	256	3.968E-05	7.459E-01	8.847E-01				
1	258	3.639E-05	8.053E-01	1.089E+00				
1	259	1.193E-05	1.965E+00	6.189E-01				
1	260	1.198E-05	1.960E+00	2.107E-01				
1	264	1.975E-05	1.377E+00	1.722E+00				
1	265	1.415E-05	1.766E+00	3.935E-01				
1	275	2.978E-05	9.629E-01	5.555E-01				
1	276	1.626E-06	3.368E+00	4.715E-01				
1	281	1.885E-05	1.429E+00	1.403E-01				
1	282	5.701E-05	5.262E-01	3.337E-01				
1	283	5.417E-06	2.748E+00	8.875E-02				
1	284	8.033E-06	2.395E+00	8.769E-02				
1	294	4.022E-05	7.369E-01	5.594E-01				
1	295	1.065E-05	2.095E+00	3.488E-01				
1	296	5.925E-05	5.029E-01	9.042E-01				
1	305	4.259E-05	6.946E-01	8.600E-01				
1	306	1.776E-04	3.678E-03	2.943E-02				
1	307	1.472E-04	3.678E-03	9.532E-03	1.126E-01	9.858E-01	1.248E-01	7.394E-02
1	309	1.245E-04	1.642E-02	6.187E-02				
1	310	1.533E-04	3.678E-03	2.086E-02				
1	311	4.186E-05	7.035E-01	7.856E-01				
1	325	4.053E-05	7.319E-01	1.206E+00				
1	330	1.032E-05	2.129E+00	9.075E-01				

[Abaqus - 3D (planovský) | verze 1.2.14.0 | ©Cervenka Consulting 2007 | www.cervenka.cz]

C	Description:	beam 3d	Unit system:	Metric
	Note:	3d		

MACROELEMENT 1 - CRACK ATTRIBUTES (TBL.2/3)								
Element Crack Attributes								
Group	Elem.	Cod1 [m]	Sig N1 [MPa]	Sig T1 [MPa]	N2(1) [m]	N2(2) [m]	N2(3) [m]	Size2 [m]
1	332	5.163E-06	2.785E+00	3.911E-02				
1	342	1.430E-05	1.753E+00	1.433E+00				
1	343	3.081E-05	9.339E-01	1.272E+00				
1	348	2.004E-06	3.300E+00	1.473E-01				

MACROELEMENT 1 - CRACK ATTRIBUTES (TBL.3/3)				
Element Crack Attributes				
Group	Elem.	Cod2 [m]	Sig N2 [MPa]	Sig T2 [MPa]
1	1			
1	2			
1	4			
1	9			
1	10	2.922E-05	1.034E+00	4.130E-02
1	11			
1	12			
1	13	1.383E-05	1.908E+00	5.329E-01
1	14			
1	32			
1	34			
1	35			
1	38			
1	42			
1	43	2.530E-05	1.204E+00	5.643E-01
1	45			
1	46			
1	53			
1	55			
1	56	1.590E-05	1.743E+00	8.101E-01
1	57			
1	59			
1	60			
1	65			
1	66			
1	68			
1	81			
1	87			
1	88	2.396E-05	1.235E+00	1.500E-01
1	89			
1	90	8.024E-06	2.522E+00	1.682E-01
1	91	3.327E-05	9.113E-01	3.911E-01
1	92			
1	97			
1	98			
1	99			
1	106			
1	107	1.582E-05	1.735E+00	9.862E-01
1	108			
1	110			
1	111			

	Description:	beam 3d	Unit system:	Metric
	Note:	3d		
MACROELEMENT 1 - CRACK ATTRIBUTES (TBL.3/3)				
Element Crack Attributes				
Group	Elem.	Cod2 [m]	Sig N2 [MPa]	Sig T2 [MPa]
1	116			
1	121	1.816E-05	1.580E+00	5.753E-01
1	122			
1	123	3.166E-05	9.722E-01	1.219E+00
1	131			
1	132			
1	133			
1	135			
1	140			
1	141			
1	142	1.015E-04	1.517E-01	1.256E-01
1	143			
1	144	5.846E-05	5.272E-01	4.235E-01
1	145	4.324E-08	2.333E+00	2.490E-01
1	146			
1	153			
1	154			
1	155	9.470E-05	2.009E-01	4.302E-01
1	156	1.245E-07	3.268E+00	3.668E-01
1	157	8.633E-05	2.664E-01	6.271E-01
1	158			
1	159			
1	164			
1	165			
1	199			
1	200			
1	201			
1	202			
1	206			
1	207			
1	225	1.095E-06	3.466E+00	1.137E+00
1	227			
1	233			
1	234			
1	236			
1	237			
1	238			
1	240			
1	241			
1	244			
1	247			
1	248			
1	256			
1	258			
1	259			
1	260			
1	264			
1	265			
1	275			

[Alena - 3D (denovon) | version 1.2.14.0 | ©Cervinka Consulting 2007 | www.cervinka.cz]

c	Description:	beam 3d	Unit system:	Metric
	Note:	3d		

MACROELEMENT 1 - CRACK ATTRIBUTES (TBL.3/3)				
Element Crack Attributes				
Group	Elem.	Cod2 [m]	Sig N2 [MPa]	Sig T2 [MPa]
1	276			
1	281			
1	282			
1	283			
1	284			
1	294			
1	295			
1	296			
1	305			
1	306			
1	307	1.276E-05	2.004E+00	6.036E-01
1	309			
1	310			
1	311			
1	325			
1	330			
1	332			
1	342			
1	343			
1	348			

BAR REINFORCEMENT 1 - CRACK ATTRIBUTES				
Element Crack Attributes				
No values have been found.				

BAR REINFORCEMENT 2 - CRACK ATTRIBUTES				
Element Crack Attributes				
No values have been found.				

Appendix D- LIST OF PUBLICATION

Conference

1. A. Kurniawan , N. Shafiq and M. F. Nuruddin, 2008, Optimum Mix Design for Self compacting Concrete Using Fly Ash as Partial Replacement to Cement, International Conference on Construction and Building Technology in Kuala Lumpur, MALAYSIA on 16-20 June 2008.
2. A. Kurniawan , N. Shafiq and M. F. Nuruddin, 2008, Bond Strength Characteristic of Self Compacting Concrete Incorporating Fly Ash, 2nd International Conference on Built Environment in Developing Countries 2008 , to be held in the Universiti Sains Malaysia, Penang , Malaysia on 3rd – 4th December 2008.
3. A. Kurniawan , N. Shafiq and M. F. Nuruddin, 2009, Performance of Fly Ash Self Compacting Concrete (FASCC), 3rd International Conference on Built Environment in Developing Countries 2009 , to be held in the Universiti Sains Malaysia, Penang , Malaysia on 2nd – 3rd December 2009. Won The Best Paper Award.
4. N. Shafiq, M. F. Nuruddin and A.Kurniawan, 2010, 21th International Invention and Technology Exhibition, ITEX 2010, Kuala Lumpur, Malaysia, 14th – 16th May 2010. Won bronze medal.
5. A. Kurniawan , N. Shafiq and M. F. Nuruddin, 2010, Mechanical and Structural Performances of Self Compacting Concrete containing fly ash and MIRHA, 1st International Conference on Sustainable Building and Infrastructure, Universitii Teknologi PETRONAS, Kuala Lumpur, Malaysia, 15th – 17th June 2010.

Journal

1. A. Kurniawan , N. Shafiq and M. F. Nuruddin, 2010, Effects of water to binder ratio on the fresh properties and compressive strength of SCC, Elsevier Science Material Science and Engineering, submitted

2. A. Kurniawan , N. Shafiq and M. F. Nuruddin, 2010, Bond Characteristic and Embedment resistance of steel bars in self compacting concrete, Elseiver Construction and Building Materials, submitted